Development of Sustained Release, Anti-Cytokine Short Interfering RNA (siRNA) Therapy for Equine Osteoarthritis

Thesis submitted in accordance with the requirements of the University of Liverpool for the degree of Doctor in Philosophy

By

Rhiannon Emma Morgan

January 2016

THIS THESIS IS DEDICATED TO MY FATHER WHO INSPIRED MY PASSION FOR SCIENCE, ALWAYS ENCOURAGED AN INQUISITIVE NATURE AND MADE ME BELIEVE IN MYSELF.

Acknowledgements

The work within this thesis was carried out at the Institute of Ageing and Chronic Disease, Department of Musculoskeletal Biology based at the University of Liverpool School of Veterinary Science's Leahurst Campus.

First and foremost I would like to express my sincerest gratitude to my main supervisor Dr Simon Tew, whose profound expertise and continued guidance and support were invaluable in completing this thesis. I would also like to thank my co-supervisors Professor Peter Clegg and Professor John Hunt for their vital guidance and encouragement, particularly in regards to their unwavering support of ideas and in furthering my career. A special mention goes to Professor John Innes for the initial research he completed which lead to this PhD being possible.

One of the biggest pleasures I have had throughout this time was the opportunity to work with our lab group. I am indebted to everyone for their patience and willingness in teaching me the plethora of laboratory-techniques needed for this work. A special thank you goes to Eithne, Alan, Danae, Mandy, Ben, Kate, John, Louise, Eleri, Sumaya and Yalda whose friendship I will always value.

None of this would have been possible without the generous funding of the Horserace Betting Levy Board (HBLB).

Last but not least I would like to thank those who have propped me up throughout this process and kept me smiling, my Leahurst friends, Niamh for being my PhD agony aunt, my dear horse Boris and dog Ella who provided a work life balance, close friends for constantly being there, Tim for coming into my life throughout this time, supporting my endeavours wholeheartedly and being my rock, and my mum Cilla, sister Bethan and brother Owain, for always being there and supporting every crazy idea I have without question. Thanks and love to you all.

List of Abbreviations

3'-UTR	3'-Untranslated Region
ACS	Autologous Conditioned Serum
ADAMTS	A Distintegrin And Metalloproteinase with Thrombospondin Motifs
ADAMTS4_v1	ADAMTS4 Variant
AGE	Advanced Glycation End-products
BSA	Bovine Serum Albumin
Cadherin-1	Calcium-Dependent Adhesion Molecule 1
chABC	Chondroitinase ABC
CIA	Collagen-Induced Arthritis
CM	Conditioned Media
COMP	Cartilage Oligomeric Martix Protein
COX-2	Cyclooxygenase-2
CRP	C-Reactive Protein
CS-2	Second Chondroitin-Sulphate Rich Domain
Ct	Number of Thermal Cycles
Cy-3	Cyanine 3
DAMP	Damage Associated Molecular Patterns
DAPI	4',6-Diamidino-2-Phenylindole
DCM	Denatured Conditioned Media
DDH_2O	Double Distilled Water
DDS	Drug Delivery System
DEPC	Diethylpyrocarbonate
DH82	Canine Macrophage-Monocyte Cell Line
DMEM	Dulbeccos' Modified Eagle Medium
DMM	Destabilisation of the Medial Meniscus
DMMB	1-9 Dimethylmethylene Blue
DMOADs	Disease Modifying Osteoarthritis Drugs
DMSO	Dimethyl Sulfoxide
dNTPs	Deoxynucleotide
dsRNA	Double Stranded Ribonucleic Acid
DTT	Dithiothreitol
ECM	Extracellular Matrix
EDTA	Ethylenediaminetetraacetic Acid
EFLS	Equine Fibroblast-Like Synoviocyte
ELISA	Enzyme-Linked Immunosorbent Assay
EPBMCs	Equine Peripheral Blood Mononuclear Cells
FACS	Fluorescence-Activated Cell Sorting
FBS	Foetal Bovine Serum
FDA	Food and Drugs Administration
FI	Fluorescence Intensity
FITC	Fluoroscein Isothiocyanate

FLS	Fibroblast-Like Synovioyte
FSC	Forward Scatter
GAG	Glycosaminoglycan
GAPDH	Glyceraldehyde-3-Phosphate Dehydrogenase
GCP-2	Granulocyte Chemotactic Protein 2
GRO-β	Growth Regulatory Oncogene-β
H&E	Haematoxylin & Eosin
HCl	Hydrochloric Acid
HRP	Horseradish Peroxidase
IA	Intra-Articular
ICE/Caspase	Interleukin-1β Converting Enzyme
IDCR	Ionic Detergent Compatibility Reagent
IFN	Interferon
IGD	Interglobular Domain
IGF-1	Insulin-Like Growth Factor 1
IL-1	Interleukin-1
IL-1R	Interleukin-1 Receptor
IL-1RA/IRAP	Interleukin-1 Receptor Antagonist
IL-1RAcp	Interleukin-1 Receptor Accessory Protein
IL-1RI	Interleukin-1 Receptor Type I
IL-1RII	Interleukin-1 Receptor Type II
IL-6	Interleukin-6
IL-6Rα	Interleukin-6 alpha Receptor
IRAK	Interleukin-1 Receptor Associated Kinase
KCl	Potassium Chloride
KO	Knockout
LIF	Leukocyte Inhibitory Factor
LPS	Lipopolysaccharide
LRP	Leucine Rich Protein
LRP-1	Low-Density Lipoprotein Receptor-Related Protein 1
M-CSF	Macrophage-Colony Stimulating Factor
M-MLV	Moloney-Murine Leukaemis Virus
mAb	Monoclonal Antibody
MAPK	Mitogen Activated Protein Kinase
MCP-1/CCL-2	Monocyte Chemoattractant Protein-1/Chemokine (C-C Motif) Ligand 2
MCPJ	Metacarpophalangeal Joint
$MgCl_2$	Magnesium Chloride
MIF	Macrophage Migration Inhibitory Factor
MMPi	Matrix Metalloproteinase Inhibitor
MMPs	Matrix Metalloproteinases
MOI	Multiplicity Of Infection
mRNA	Messenger Ribonucleic Acid

MTPJ	Metatarsophalangeal Joint
NaCl	Sodium Chloride
NF-κB	Nuclear Factor-κB
NO	Nitric Oxide
NSAIDs	Non-Steroidal Anti-inflammatory Drugs
OA	Osteoarthritis
OSM	Oncostatin M
PAMP	Pathogen Associated Molcular Pattern
PBS	Phosphate Buffered Saline
PDGF	Platelet Derived Growth Factor
PEG	Polyethylene Glycol
PFA	Paraformaldehyde
PGE_2	Prostaglandin E2
PLEH	Philip Leverhulme Equine Hospital
PLGA	Poly-Lactide Glycolic Acid
PPS	Polypropylene Sulphide
PRR	Pattern Recognition Receptors
PTGS	Post-Transcriptional Gene Silencing
PVA	Polyvinyl Alcohol
qRT-PCR	Quantitative Real-Time Polymerase Chain Reaction
R	Efficiency of Determination
RA	Rheumatoid Arthritis
RAGE	Receptor for Advanced Glycation End-products
ReIL-1β	Recombinant Equine IL-1β
RISC	RNA-induced silencing complex
RNAi	Ribonucleic Acid Interference
ROS	Reactive Oxygen Species
scAAV	Self-complementary Adeno-Associated Virus
SDS	Sodium Dodecyl Sulfate
SF	Synovial Fluid
sGAG	Sulphated Glycosaminoglycan
shRNA	Short Hairpin Ribonucleic Acid
sIL-1RAcp	Soluble Interleukin-1 Receptor Accessory Protein
sIL-1RI	Soluble Interleukin-1 Receptor Type I
sIL-1RII	Soluble Interleukin-1 Receptor Type II
sIL-6Rα	Soluble Interleukin-6 alpha Receptor
SiRNA	Short Interfering RNA
SOX-9	SRY-box-9 gene
SSC	Side Scatter
TBS	Tris-Buffered Saline
TGF-β	Transforming Growth Factor-β
TIMP	Tissue Inhibitor of Metalloproteinase
TIR	Toll-and-Interleukin-1 Receptor

TLR	Toll-Like Receptors
TMB	Tetramethylbenizidine
TNF	Tumour Necrosis Factor
TNF-RI	Tumour Necrosis Factor Receptor Type I
TNF-RII	Tumour Necrosis Factor Receptor Type II
TP	Total Protein
UDPGD	Uridine Diphosphoglucose-Dehydrogenase
VCAM-1	Vascular Cell Adhesion Molecule 1 (CD106)
VEGF	Vascular Endothelial Growth Factor
WBCC	White Blood Cell Count

Abstract

Synovitis is a key mediator of osteoarthritis (OA) and in the perpetuation of cartilage degradation, and approximately 60% of lameness in the horse has previously been attributed to OA. Synovial inflammation is characterised by a mononuclear cell infiltration into the synovial membrane, with concurrent increases in catabolic cytokines predominantly produced by synovial macrophages. These cytokines cause changes in fibroblast-like synoviocyte gene expression, including the up-regulation of damaging cartilage matrix degrading proteinases and further cytokines. It was therefore hypothesised that the synovial membrane may represent a disease-modifying target. When referring to synovial macrophages and fibroblast-like synovioctyes collectively, the term synoviocytes is used.

The general aims of this thesis were to design and test an anti-cytokine therapy; short interfering RNA (siRNA), and to analyse its potential with respect to decreasing target catabolic cytokines produced by synoviocytes. Delivery of this therapy to synoviocytes via biodegradable polymer microspheres was also examined. The effects of the therapy and therapy-delivery system on synoviocyte and cartilage health, were assessed using *in vitro* co-culture systems, which were designed and used to elucidate interactions between the two predominant cell populations present during synovitis; synovial macrophages and fibroblast-like synoviocytes.

Successful equine anti-IL-1β siRNA was designed and tested on equine synovoicytes. These cells were also shown to successfully phagocytose 2-6μm biodegradable polymer microspheres in a highly efficient manner. A novel multi-species *in vitro* model was created to quantify cell-specific responses to inflammatory stimulation, of both macrophages and fibroblast-like synoviocytes in co-culture. This model revealed that macrophages can stimulate fibroblast-like synoviocyte mitosis, and modulate its ADAMTS5 mRNA expression in an inflammatory environment. Using an inflammatory stimulated co-culture model involving a mixed culture of macrophages, fibroblast-like synoviocytes and cartilage explants, it was observed that the mixed synoviocyte culture can also act to moderate the inflammatory response. Synoviocytes were shown to exert a protective mechanism over cartilage glycosaminoglycan release, whilst driving the inflammatory

response through the production of pro-inflammatory cytokines. This thesis has successfully provided the initial design and testing of an equine anti-IL-1β therapy and delivery vehicle *in vitro*, providing a platform for further experimentation to assess the efficiency of delivery and therapeutic potential when used together.

Index of Figures

Index of Tables

Index of Schemas

Chapter 1. Introduction

Exploring the role of Synovitis in Equine Osteoarthritis and its Potential as a Therapeutic Target for Anti-cytokine RNA Interference Delivered by PLGA-Microspheres

1.1 The Equine Joint

1.1.1 The Synovial Joint

A common joint capsule surrounds the articulating surfaces of bones, creating a multi-tissue intra-articular environment known as the synovial joint. Synovial membrane lines the inside of the joint capsule and produces synovial fluid by acting as a macromolecular sieve to filter certain nutrients and small proteins from the plasma into the intra-articular space. Cells within the synovial membrane, known as fibroblast-like synoviocytes (FLS), produce molecules of a larger molecular weight found within synovial fluid, such as glycosaminoglycans (GAGs) and proteoglycans. Synovial fluid fills the intra-articular space, lubricating the articular cartilage-covered surfaces of the long bones to aid frictionless movement between the bone surfaces, providing nutrients to the avascular cartilage and acting as a transport medium for cellular signalling molecules. Extra- and intra-capsular ligamentous and muscular attachments provide joint stability and produce flexion, extension and rotation of the joint (Frisbie 2012).

Diarthrodial joints are the most common type of synovial joint found within the equine skeleton. They are designed to facilitate equine athletic exertions and must withstand high degrees of flexion and extension, and large compressional forces. A traumatic incident, loss of joint stability or joint tissue integrity, or irregularity in joint conformation, can lead to the production of factors which incite the inflammatory process, or can result in abnormal loading patterns which in turn also produces pro-inflammatory factors. These incite the intra-articular inflammatory cascade and potentially result in osteoarthritis (Heinegård and Saxne 2011). The space within the joint capsule is exposed to two tissues, the synovial membrane and articular cartilage.

1.1.2 Synovial Membrane

The synovial membrane is formed from an outer fibrous subintimal layer, which contains the synovial vasculature and nerve innervation, and an inner intima layer in which two main cell populations reside; FLS and synovial macrophages. The intima layer lining consists of overlapping cells around three FLS thick, with no basement membrane or tight cell junctions (Ghadially 1983) and is surrounded by a collagen-free fibrillar matrix (Edwards 1994). The majority of the subintimal layer is made up of collagen fibres interspersed with fibroblasts (Moskalewski, Osiecka-Iwan et al. 2014), areolar and fatty tissue (Frisbie 2012). FLS precursor cells reside within the intimal lining and FLS expand locally (Alwan, Carter et al. 1991). FLS proliferation can be stimulated by factors including macrophage inhibitory factor (MIF) (Edwards 1994, Lacey, Sampey et al. 2003) and interleukin-1

(IL-1) (Lacey, Sampey et al. 2003, Rosengren, Boyle et al. 2007), both of which are produced by synovial macrophages. This may explain why synovial hyperplasia is observed during inflammatory conditions. Synovial macrophages are thought to arise from two origins; from precursors residing within the intimal lining and from a systemic bone-marrow derived lineage (Edwards 1994). The maturation of macrophages descended from intimal lining precursors were found to be dependent on locally produced macrophage colony stimulating factor (M-CSF) (Edwards 1994). Whereas bone marrow derived macrophages may represent those seen during the mononuclear cellular infiltration of the synovial membrane that characterises synovitis.

Synovial fluid is chiefly produced by the intima layer. Proteins and nutrients extravasate from subintimal vasculature before being filtered by the intima layer into synovial fluid. Molecules of <10kDa can move through the intima layer, which is why the synovial fluid is often thought of as an ultrafiltrate of the plasma (Frisbie 2012). Larger molecules found within the synovial fluid, such as the glycosaminoglycan hyaluronan (Yielding, Tomkins et al. 1957) and the proteoglycan lubricin (Jay, Britt et al. 2000), are synthesised by FLS and released directly into the intra-articular space, although chondrocytes also synthesise hyaluronan (Mason, Kimura et al. 1982). These are critical to reduce friction during movement and provide adequate articular cartilage surface lubrication (Jay, Britt et al. 2000, Scanzello and Goldring 2012). The concentration of hyaluronan and lubricin changes, and the molecular weight of hyaluronan reduces, during pathological processes, which contributes to

the initiation of cartilage degradation (Scanzello and Goldring 2012). FLS and macrophages are also capable of producing cytokines, aggrecanases and matrix metalloproteinases (MMPs) which contribute to inflammation and cartilage degradation (Frisbie 2012).

1.1.3 Cartilage

Cartilage is a specialised tissue designed to protect articulating bone surfaces from compressive and shear forces (Poole, Kobayashi et al. 2002), and facilitate pain-free, frictionless movement of the skeleton (Houard, Goldring et al. 2013). Chondrocytes, the only cell-type found within articular cartilage, are embedded within extracellular matrix (ECM) synthesised by the chondrocytes (Goldring and Marcu 2009). Different compositions of ECM are found within particular locations relative to the chondrocyte. Directly enveloping the chondrocyte is the pericellular matrix which mainly consists of hyaluronan and proteoglycan, with some collagen VI. Chondrocytes synthesise hyaluronan which, once released, can bind to the chondrocyte cell membrane through the cell surface receptor CD44, or to the ECM (Cohen, Klein et al. 2003). A fibrillar pericellular capsule encases the pericellular matrix, which is surrounded by the territorial matrix. Within this area, collagen fibrils extend outwards between 5-10μm from the pericellular capsule and provide some resistance to mechanical stress. These components; the chondrocyte, pericelluar matrix and capsule, and territorial matrix, form a unit called the chondron. In-between chondrons lies the inter-territorial matrix, which chiefly contains collagen type II, aggrecan aggregates involving hyaluronan, cartilage oligomeric protein (COMP) and other link

proteins to facilitate cross-linking of the collagen network. This network provides resistance to compressive and shear forces (Goldring and Marcu 2009, Frisbie 2012). See figure 1.1 which has been adapted (McIlwraith 2005, Heinegård and Saxne 2011).

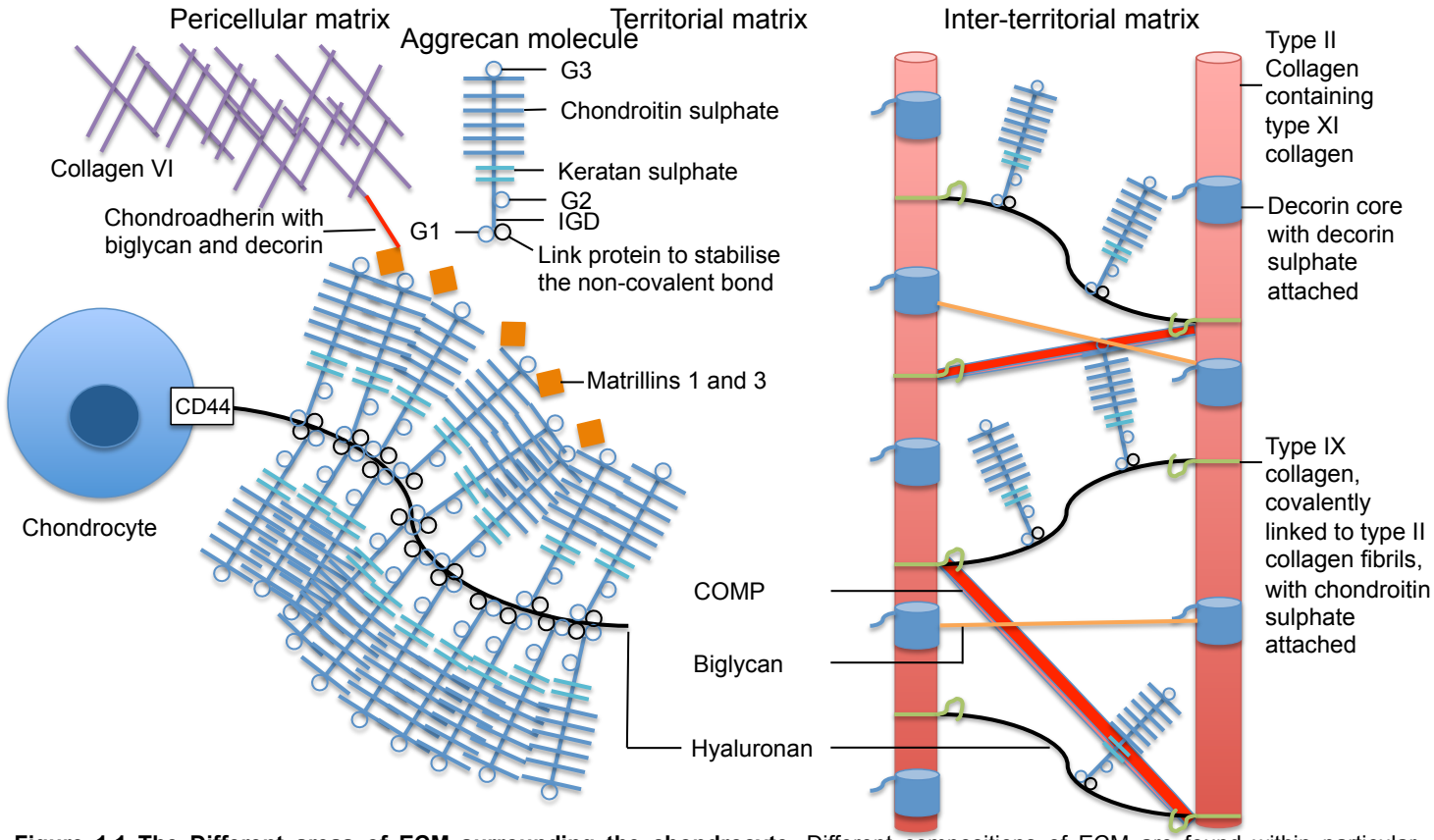

Figure 1.1 The Different areas of ECM surrounding the chondrocyte. Different compositions of ECM are found within particular locations relative to the chondrocyte; the pericellular matrix directly surrounds the chondrocyte and is composed of hylauronan, proteoglycan and collagen VI. The territorial matrix surrounds this and contains collagen fibrils radiating from the pericellular matrix outwards. These areas including the chondrocyte form a unit called the chondron. Between chondrons lies the inter-territorial matrix which chiefly contains collagen type II, aggrecan aggregates involving hyaluronan, COMP and other link proteins. Diagram adapted from McIlwraith *et al.* (2005) and Heinegård and Saxne (2011).

Differences between regions of the cartilage at varying distances from the articular surface also occur. The orientation of collagen fibres, and chondrocyte morphology changes in each region. The area adjacent to the articular surface, the superficial zone, contains tightly packed smaller-diameter (~31nm) collagen fibres that run parallel to the articular surface (Frisbie 2012). The ECM has a high decorin (Goldring and Marcu 2009) and collagen (Frisbie 2012), and low glycosaminoglycan and aggrecan (Goldring and Marcu 2009) content. Chondrocytes lie close together, flattened and elongated with their longitudinal axes lying parallel to the articular surface. This arrangement of densely packed cells and collagen fibres adjacent to the articular surface provides high tensile strength to resist shear forces, and impedes the movement of high molecular weight molecules, such as hyaluronan, from leaving the ECM whilst allowing smaller molecules such as nutrients and cytokines to move freely (Frisbie 2012). The intermediate/transitional zone collagen network, contains larger-diameter collagen fibres (~40-100nm) arranged in a random formation (Frisbie 2012). Chondrocytes are large, round and also randomly spaced apart, and chondrons are formed around each individual chondrocyte. The deep zone contains the largest-diameter collagen fibrils which are anchored in the calcified cartilage and subchondral bone lying beneath this surface (Martel-Pelletier, Boileau et al. 2008, Goldring and Marcu 2009). Fibres are orientated perpendicular to the articular surface. Large chondrocytes align themselves into vertical columns also running perpendicular to the articular surface and the chondrons surrounding them combine. The tidemark separates the deep zone and the calcified cartilage layer which contains

mineralised cells and matrix overlying the subchondral bone (Frisbie 2012). Chondrocytes within the calcified cartilage layer have been shown to express markers of hypertrophy, and with increasing age, evidence of blood vessels and nerves originating from the underlying subchondral bone layer become apparent (Houard, Goldring et al. 2013) (Figure 1.2).

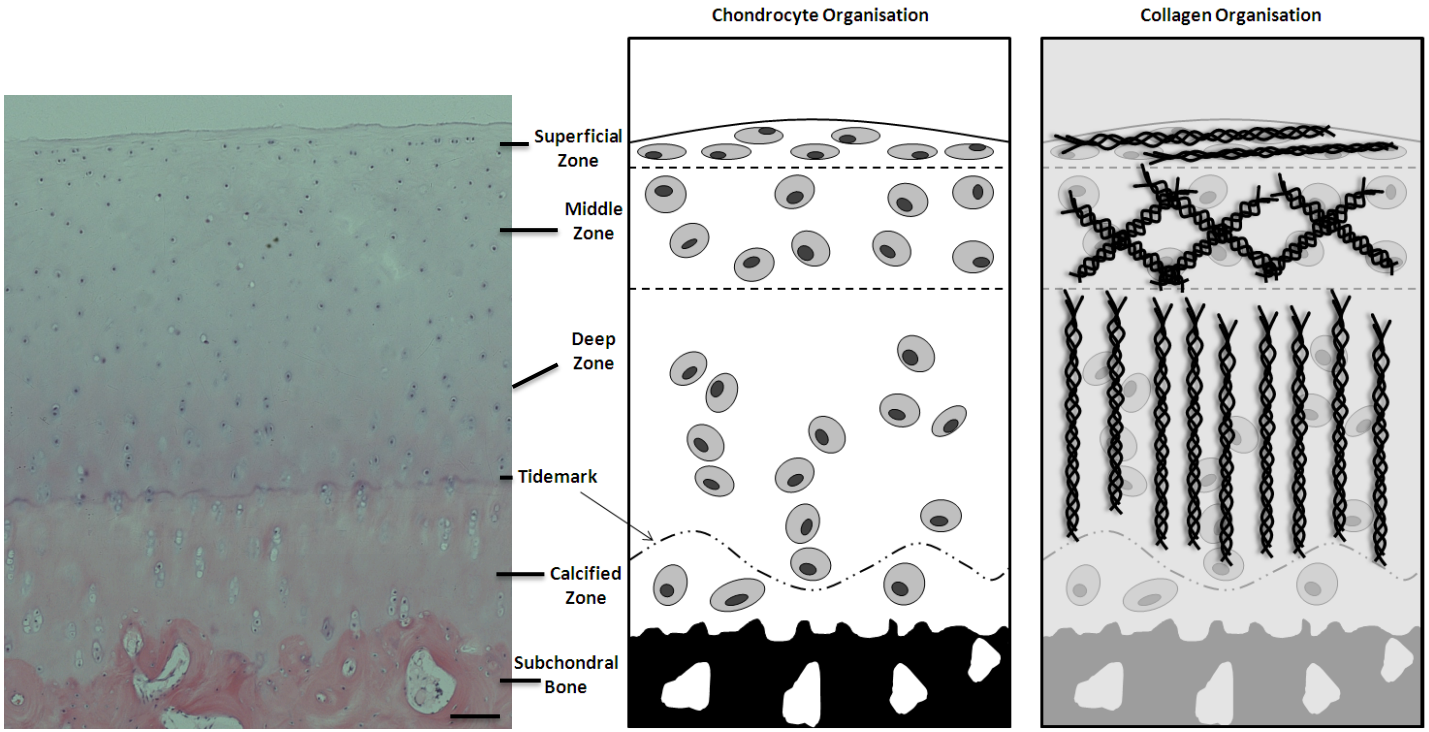

Figure 1.2 Chondrocyte and collagen organization and distribution within different zones of articular cartilage. The superficial zone lies in contact with the synovial fluid and confers tensile properties associated with articulating joint forces. This zone contains few proteoglycans, a thin layer of dense collagen fibrils and flat, elongated chondrocytes orientated parallel to the cartilage surface. The transitional (middle) zone contains fewer chondrocytes which are larger and spherical with a random distribution. Aggrecan is abundant and with thick decussating collagen fibrils, forms layers of tissue that correspond to up to 60% of overall cartilage height. In the deep zone aggrecan content is high (providing resistance to compressive force) and chondrocytes are spherical, arranged in columns and low in density. Collagen fibrils are radially distributed and are structurally largest in this zone. Calcified cartilage anchors the cartilage to the bone via collagen fibrils that penetrate from the deep zone to the calcified cartilage. Chondrocytes are hypertrophic and are physically separated from the deep region by the 'tidemark' (Martell-Pelletier, Boileau et al. 2008).

1.1.4 Cartilage Extracellular Matrix

The majority of mature cartilage is comprised of ECM, and chondrocytes represent between 1-12% of the volume depending on the species. It has been shown that there is an inverse relationship between cell density and thickness of articular cartilage (Stockwell 1971). Approximately 70% of cartilage wet weight is water, however, when analysing the dry weight components, 50% is collagen, 35% proteoglycan, 10% glycoprotein (growth factors, COMP and proteinases), 3% minerals, 1% lipids and 1% miscellaneous substances (Frisbie 2012). Under normal healthy conditions, a fine balance between anabolic and catabolic mechanisms maintains a steady composition of ECM components. Chondrocytes slowly synthesise ECM constituents, maintained by a group of matrix metalloproteinases (MMPs) and aggrecanases (Goldring and Marcu 2009).

1.1.4.1 Collagen

The collagen network within the ECM provides resistance to compressive and shear strains, and also acts as a scaffold around which all other matrix components are situated. Collagen is synthesised by chondrocytes, however turnover is extremely slow which contributes to the poor regenerative capacity of cartilage (Goldring and Marcu 2009). Collagen type II is by far the most abundant form found in articular cartilage, constituting between 90-95% of total collagen content (Vachon, Keeley et al. 1990). Collagen type II is a homotrimer, made up of three identical alpha chains that form collagen fibrils. Within the fibrils each strand is characteristically offset by 25%, otherwise known as a quarter stagger (Frisbie 2012). Type IX and XI are also present

in the inter-territorial matrix of articular cartilage, type IX is found on the surface of the type II collagen fibril, whereas type XI is found both within and on the type II fibril surface (Poole, Kobayashi et al. 2002). Type VI collagen is also found within the territorial region of the chondron (Goldring and Marcu 2009).

1.1.4.2 Proteoglycans

Proteoglycans contain a core protein with covalently attached GAGs, which are made up of linear carbohydrate chains involving repeating disaccharide units with negatively-charged sulphate and carboxylate groups (Stanton, Melrose et al. 2011, Hynes and Naba 2012). The GAG side chains are characteristic for each proteoglycan (Hardingham and Fosang 1992), whereas the protein cores are diverse and unrelated to one another in their structure (Stanton, Melrose et al. 2011). Side chains may comprise chondroitin sulphate, dermatan sulphate, keratan sulphate, heparan sulphate or heparan, and each proteoglycan may have a different combination of these chain types covalently-bound to its core protein (Stanton, Melrose et al. 2011).

Aggrecan is the most abundant and largest aggregating proteoglycan found in cartilage ECM. It has a core protein with three globular domains (G1-3), an interglobular domain (IGD) between G1 and G2, and a large region of covalently-associated GAGs made up of chondroitin sulphate chains and a smaller region of keratan sulphate chains (Hardingham and Fosang 1992). Chondroitin sulphate is comprised of two alternating monosaccharides N-

acetyl-D-galactosamine and D-glucuronic acid, whilst keratan sulphate is made up of repeating disaccharides galactose and N-acetyl-D-galactosamine. The molecule is non-covalently bound to hyaluronan at the G1 domain and stabilised with a link protein (a small glycoprotein) (Goldring and Marcu 2009). The GAGs high negative charge strongly attracts an abundance of water molecules which produces the cartilage swelling pressure providing stiffness and resistance to mechanical compression, whilst also allowing the distribution of load through the tissue (Brew, Clegg et al. 2010, Stanton, Melrose et al. 2011). Cartilage properties therefore depend on the amount of aggrecan and hyaluronan content within the ECM, and their interaction with the collagen network.

Other small proteoglycans, known as leucine-rich proteoglycans (LRPs) exist within the ECM; biglycan, decorin and fibromodulin. They contain low molecular weight (~40kDa) leucine-rich core proteins, which are structurally related to one another (Hardingham and Fosang 1992), and have only one or two GAG chains attached. For example, biglycan has one or two chondroitin/dermatan sulphate GAG chains bound to a core protein of 38kDa (Palmer and Bertone 1994). These proteoglycans contribute to the formation and stabilisation of the ECM (Frisbie 2012). Decorin has been associated with the regulation of fibrillogenesis (including the determination of fibre diameter) and collagen organisation (Palmer and Bertone 1994), and fibromodulin has also been implicated in the organisation of the ECM (Hardingham and Fosang 1992).

1.1.5 Osteoarthritis

Osteoarthritis (OA) is a major cause of disability in the UK and results in the breakdown of the articular cartilage within synovial joints. During OA, chondrocytes fail to maintain the equilibrium between anabolic and catabolic processes which normally preserve the composition of ECM. Anabolic processes are inhibited whilst catabolic processes accelerate, causing the integrity of the ECM to fail which leads to the degradation of cartilage (Goldring and Marcu 2009). This is caused by an increase in chondrocyte and synoviocyte synthesised pro-inflammatory cytokines and proteases, such as MMPs and aggrecanases. Two key cytokines, IL-1β and TNF-α, stimulate a multitude of pro-catabolic activities including the up-regulation of other pro-inflammatory cytokines, aggrecanases and MMPs, whilst inhibiting chondrocyte synthesis of aggrecan and type II collagen. Aggrecanases and MMPs cleave ECM constituents such as collagen, aggrecan and other small matrix proteins, which leads to the ultimate failure of the cartilage matrix. The synovial contribution to this inflammatory cascade is not completely understood and further investigation into its role in the pathogenesis of osteoarthritis is needed. The pathogenesis of osteoarthritis is described in more detail further on.

1.1.6 Proteolysis

The proteolysis of aggrecan is facilitated by two major proteinase families; the MMPs and a disintegrin and metalloproteinase with thrombospondin motifs (ADAMTS) family (these are also referred to as aggrecanases). Both families of proteinases cleave aggrecan at specific sites on the aggrecan

core protein (Durigova, Nagase et al. 2011). Aggrecan degradation facilitated by these families contributes to ECM turnover during normal cartilage homeostasis. However, during pathological conditions levels of these enzymes can increase, additionally MMPs can also degrade collagen, and these factors cause a catabolic state resulting in cartilage breakdown. During the early stages of osteoarthritis, the loss of aggrecan can be reversed, however the degradation and loss of collagen type II from the ECM, that subsequently occurs, is permanent (Loeser, Goldring et al. 2012, Felson and Hodgson 2014). This is discussed in more detail in section 1.4.5 Aggrecanases and Matrix Metalloproteinases.

1.2 Synovitis

1.2.1 Equine Synovitis Plays a Major Role in the Pathophysiology of Osteoarthritis

In 67.6% of racehorses in training, lameness causes the greatest number of lost training days (Rossdale, Hopes et al. 1985), and it is by far the most important factor in the wastage of young racehorses (Jeffcott, Rossdale et al. 1982). Surveys estimate that up to 60% of lameness in the horse is related to OA (McIlwraith 2011). Equine OA is considered a group of disorders with the same outcome: progressive degradation of the tissues within synovial joints (McIlwraith, Frisbie et al. 2012). The metacarpophalangeal joint is the most common site for spontaneous OA in the racehorse, followed by the carpal joints (McIlwraith, Frisbie et al. 2012).

Synovitis clinically manifests as a palpable joint thickening, due to the inflamed synovial membrane, or as synovial fluid effusion (Sellam and Berenbaum 2010). Synovitis can be detected by ultrasound, MRI (with and without contrast enhancement) and through arthroscopic examination. These modalities have diagnosed synovitis in patients where synovitis was clinically unapparent. Synovitis was found in up to 50% of OA patients as confirmed by arthroscopy (Attur, Samuels et al. 2010). Non-contrast imaging modalities grade the joint as a whole-organ including assessment of total synovial fluid volume, or extent of synovial cavity distension. Contrast enhanced MRI and US can now distinguish synovial thickening from effusion; a recent study diagnosed synovitis in 95% and 70% of joints with and without an effusion,

suggesting that synovial thickening and effusion are discrete (Scanzello and Goldring 2012).

In horses, synovitis has long been associated with OA in high motion joints, but inflammation due to capsulitis or synovitis is also believed to be almost always present in equine OA (McIlwraith and Vachon 1988). However, further investigation is required to determine the exact incidence of concomitant synovitis and OA.

OA is characterised by cartilage degeneration, subchondral bone sclerosis, osteophyte formation, varying degrees of synovial inflammation and periarticular tissue fibrosis (Kidd, Fuller et al. 2001). The exact role that synovitis plays is unknown, but it is becoming widely acknowledged as an important mediator of the disease process (Ley, Ekman et al. 2009). Post-traumatic OA occurs after a single traumatic event (Rickey, Cruz et al. 2012) to the joint causing joint degeneration, dysfunction and pain (Buckwalter and Brown 2004). Whereas traumatic osteochondrosis (also known as palmar osteochondral disease) is caused by a focal overloading within the joint, leading to subchondral bone damage, which mainly occurs in racehorses (Rickey, Cruz et al. 2012). OA, once termed a non-inflammatory disease, is now considered a complex condition potentially involving all joint components and should now be considered a whole joint disease (Goldring and Marcu 2009, Goldring and Otero 2011, Goldring, Otero et al.), although the majority of OA research remains focused on cartilage injury (Lee, Kisiday et al. 2013). However, the synovial membrane, subchondral bone, and

associated adipose tissue are under scrutiny in regards to their contribution to the pathophysiology of OA. Synovitis plays a highly influential role in driving the progression of OA and in the perpetuation of cartilage degradation. Equine synovitis alone, without concurrent joint instability or injury, has been found capable of potentiating cartilage degradation (Lee, Kisiday et al. 2013). This organ, the synovium, is therefore an ideal therapeutic target for disease modifying OA drugs (DMOADs), and could reveal the presence of acute OA through the analysis of biomarkers or imaging modalities.

1.2.2 An Introduction to Equine Synovitis Research

Since the 1980s, it has been evident that synovitis plays a role in the pathogenesis of equine OA (McIlwraith and Vachon 1988). Equine OA can be caused by a primary traumatic event or occur naturally, and humans and equids both commonly experience spontaneous OA (McIlwraith, Frisbie et al. 2012). Intra-articular (IA) deleterious agents such as lipopolysaccharide (LPS) and interleukin-1 (IL-1) were, and still continue to be, used to model naturally occurring OA without the influence of joint trauma or instability. Early models produced IA changes similar to those seen in naturally occurring OA, inferring that synovitis is capable of inducing cartilage degradation (McIlwraith and Van Sickle 1981). Equine IL-1β was first characterised in 1990 (May, Hooke et al. 1990), and was quickly identified within synovial fluid (SF) (Morris, McDonald et al. 1990) and serum of horses with OA, alongside a molecule capable of inhibiting this cytokine (Alwan, Carter et al. 1991, May, Hooke et al. 1992). IL-1β secreted from equine

peripheral blood mononuclear cells (EPBMC) was then shown to stimulate prostaglandin E2 (PGE_2) production from synovial cells and chondrocytes *in vitro* (May, Hooke et al. 1992). These characteristics highlighted the value of IL-1β in reproducing naturally occurring OA in the horse. Throughout the 1990s, synovitis models were further refined to elicit a mild to moderate synovitis with associated clinical signs, such as lameness and increased surface skin temperature, but without deleterious systemic effects (Palmer and Bertone 1994). Synovial fluid white blood cell count (WBCC), total protein (TP) and pro-inflammatory mediators were concurrently elevated. Various doses of LPS (Hawkins, MacKay et al. 1993) and recombinant equine IL-1β (ReIL-1β) (Simmons, Bertone et al. 1999) were tested as synovitis-inducing agents, concluding that doses >0.5ng LPS per joint caused systemic endotoxaemia (Palmer and Bertone 1994). Intra-articular LPS (0.2μg/kg bwt) caused enhanced immunoreactivity for IL-1β, TNF-α and TNF-α receptors within synovium and non-calcified cartilage, further reinforcing that the inflammed synovium is an important source of pro-inflammatory mediators in joint disease (Todhunter, Kincaid et al. 1996). IL-1β and TNF-α are considered chief pro-inflammatory drivers of the OA disease process. Extensive research into the equine IL-1β cytokine has revealed an alternatively spliced transcript minus exon 5, which includes the IL-1β converting enzyme (ICE) cleavage site within SF (Kato, Youn et al. 1996); and an IL-1 receptor antagonist (IL-1RA) which was isolated from LPS-stimulated EPBMCs and identified through molecular cloning and functional expression tests (Kato, Ohashi et al. 1997). This receptor antagonist is now one of the most extensively researched proteins with

respect to DMOADs in equids (Frisbie and McIlwraith 2000). The ReIL-1β synovitis model revealed a positive association between IL-1β and SF interleukin-6 (IL-6) levels (Simmons, Bertone et al. 1999) and IL-6 was then discovered to be a sensitive and specific marker for joint disease *in vivo* when lameness is intermittent or difficult to identify (Bertone, Palmer et al. 2001). Both bioactive and normal SF TNF-α levels do not correlate with the degree of articular cartilage damage in a joint, or the SF WBCC. In one study, bioactive TNF-α was significantly induced in joints suffering from degenerative joint disease post-racing, but this did not significantly differ from normal joints. However, these joints contained osteochondral chip fractures; an acute inflammatory response may have been induced by the impact of racing but a concurrent chronic inflammatory response was also present (Billinghurst, Fretz et al. 1995). In a second study, SF TNF-α levels were detected in horses with no signs of active inflammation present which may explain the lack of correlation (Jouglin, Robert et al. 2000). The majority of SF TNF-α was therefore postulated to have been produced by resident articular cells, rather than SF cells, due to the non-linear WBCC, further emphasising the role of synovitis on IA cytokine levels (Billinghurst, Fretz et al. 1995). In a study looking at naturally occurring active disease, there were no correlations found between TNF-α and grade of articular cartilage damage (Ley, Ekman et al. 2007).

Equine articular IL-1β gene expression is constitutive and primarily produced by the synovial membrane (Trumble, Trotter et al. 2001). Aside from being a principal driver of inflammation and cartilage degradation, IL-1β is also a crucial regulator of the balance between anabolism and catabolism required

for normal joint homeostasis. This finding was reinforced by murine studies investigating the complete deletion of the IL-1β gene and the gene encoding ICE, which transforms IL-1β into an active enzyme, which demonstrated that a lack of these genes accelerated development of OA cartilage lesions after undergoing surgery to destabilise the joint of interest (Clements, Price et al. 2003). These lesions were associated with increased levels of MMP, aggrecanase and collagenase-generated cleavage neoepitopes in areas adjacent to the lesion, whilst remote areas showed no evidence of their presence. It may be hypothesised that whilst IL-1β is known to stimulate the production of proteases, it may also moderate the degree of their up-regulation.

1.2.2.1 In Vitro Research

The Effects of IL-1β on Cartilage

When cartilage explants were exposed to IL-1β in vitro, cartilage sulphated GAG (sGAG) content decreased (Pettipher, Higgs et al. 1986, Gregg, Fortier et al. 2006, Gregg, Fortier et al. 2006) whilst sGAG content within the culture media increased (Busschers, Holt et al. 2010). Histological analysis of cartilage explants stimulated with IL-1β revealed decreased levels of sGAG within the extracellular matrix (Pettipher, Higgs et al. 1986, Ley, Svala et al. 2011). More detailed study of gene expression indicated that chondrocyte aggrecan and collagen type II mRNA levels were inhibited by IL-1β (Gregg, Fortier et al. 2006, Gregg, Fortier et al. 2006, Ley, Svala et al. 2011). Furthermore, IL-1β up-regulated chondrocyte MMP gene expression (Busschers, Holt et al. 2010, Ley, Svala et al. 2011), including MMP3 and

MMP13 (Flannery, Little et al. 1999, Gregg, Fortier et al. 2006, Gregg, Fortier et al. 2006), and aggrecanase gene expression (Flannery, Little et al. 1999); ADAMTS4 (by 27 fold) and ADAMTS5 (by 13 fold) (Busschers, Holt et al. 2010). These studies conclude that certain concentrations of IL-1β can promote the degradation of the cartilage ECM, both through the up-regulation of ECM-cleaving enzymes, and the down-regulation of anabolic gene expression.

Chondrocytes and Synoviocytes Can Influence Each Other

However, when cartilage explants were co-cultured with synoviocytes, the influence of IL-1β on cartilage degradation was significantly altered. Cartilage explant sGAG content, chondrocyte aggrecan gene expression and cartilage metachromasia were significantly less reduced under these conditions (Gregg, Fortier et al. 2006). However, the degree of sGAG within explant culture media was unchanged. These findings may reflect a positive anabolic stimulus from synoviocytes on chondrocyte aggrecan synthesis, rather than an anti-catabolic effect.

IL-1β has also been shown to stimulate synoviocyte MMP3 and -13 gene expression, however this was less up-regulated by IL-1β in the presence of cartilage (Gregg, Fortier et al. 2006), which may suggest an anti-catabolic feedback mechanism produced by the cartilage. A similar synoviocyte response was noted in the presence of injured cartilage; FLS ADAMTS4 and -5 gene expression was lower compared to FLS cultured independently and with uninjured cartilage, however expression of MMP-1 was increased and

tissue inhibitor of metalloproteinases (TIMP)-1 was decreased (Lee, Kisiday et al. 2013). However, chondrocyte aggrecan synthesis was lower when injured cartilage was cultured with FLS compared to injured cartilage cultured alone (Lee, Kisiday et al. 2013). Furthermore, when injured bovine cartilage was co-cultured with synovial explants, there was an increase in catabolic chondrocyte gene expression, resulting in a reduction of cartilage aggrecan content (Lee, Fitzgerald et al. 2009). The FLS culture used in Lee *et al* (2013) did not express detectable IL-1β or TNF-α, which are the chief cytokines produced during synovitis and are therefore unrepresentative of the responses occurring within an inflamed joint. Whereas the synovial explants used in Lee *et al.* (2009) contain synovial macrophages and may more closely reflect intra-articular responses to injury. These studies do, however, emphasise the simultaneous catabolic and anabolic responses, and the complex interactions between the different cell populations, occurring during inflammation. Ultimately, it is crucial to fully elucidate inter-cellular communications when evaluating potential disease modifying targets.

1.2.2.2 In Vivo Research

Studies on the *in vivo* cell responses to intra-articular recombinant-equine IL-1β and LPS have shown that they resemble those produced by *in vitro* models. Chondroctye ADAMTS4, ADAMTS5, IL-1β and MMP1 gene expression were all up-regulated compared to normal joints. However it is worth noting that MMP13 and TNF-α were not significantly affected (Ross, Kisiday et al. 2012). These changes in gene expression generally reflect those observed *in vitro*, apart from the disparity in chondrocyte expression of

MMP13. Synoviocyte gene expression of IL-1β, MMP1 and ADAMTS4 were significantly up-regulated, whilst MMP13, ADAMTS5 and TNF-α gene expression did not differ between treated and control joints (Ross, Kisiday et al. 2012).

1.2.2.3 Naturally Occurring Joint Disease

In naturally occurring OA, no increase in synoviocyte IL-1β gene expression was observed, whereas TNF-α was significantly up-regulated in moderate OA compared to non-diseased joints. OA chondrocyte IL-1β and TNF-α gene expression were significantly up-regulated compared to normal chondrocytes. MMP-13 gene expression was significantly up-regulated by both OA synoviocytes and chondrocytes. ADAMTS4 gene expression was not significantly up-regulated by synoviocytes whereas an increase was seen in chondrocyte gene expression between normal and OA conditions. ADAMTS5 synoviocyte gene expression was significantly up-regulated in moderate OA compared to non-diseased joints, whereas chondrocyte gene expression was unchanged (Kamm, Nixon et al. 2010).

There is a degree of disparity when comparing the *in vivo* synoviocyte and chondrocyte mRNA levels of cytokines, aggrecanases and MMPs induced by intra-articular administration of IL-1β, to those observed during naturally occurring OA. When analysing mRNA levels on exposure to intra-articular IL-1β, they reflect the initial cell response to injury. However, mRNA levels observed in cells isolated from osteoarthritic joints, are displaying the

response to injury inflicted over a longer period of time. This may explain the differences in response observed.

Innate Immunity Activates the Intra-Articular Inflammatory Response

Joint structures can be injured either through repetitive cycles of over-loading causing a build up of micro-trauma known as stress-induced fatigue damage, or through a single traumatic event. Damage results in the release of endogenous molecules known as damage-associated molecular patterns (DAMPS), either from cartilage ECM disruption or through cell injury (Li, Shi et al. 2011). DAMPs trigger pattern recognition receptors (PRRs), which activate the inflammatory response (Berenbaum 2013). Two predominant types of PRRs are the toll-like receptors (TLRs) and receptor for advanced glycation end-products (RAGE) (Sellam and Berenbaum 2010, Goldring and Otero 2011). TLRs initiate the major signalling pathways involved in the inflammatory response during the early stages of OA (Berenbaum 2013). They activate the nuclear factor-kappa B (NF-κB) pathway which leads to the production of pro-inflammatory cytokines, chemokines and aggrecanases (Liu-Bryan 2013). TLRs are present on synovioctyes and chondrocytes during OA, and chondrocyte TLRs and RAGE have been found to be up-regulated during OA (Li, Shi et al. 2011, Berenbaum 2013). RAGE activated pathways are triggered when advanced glycation end products (AGEs) bind to receptors on chondrocytes, up-regulating pro-inflammatory cytokines and MMPs (Berenbaum 2013). A second innate immune system; the complement system, also plays an influential part in the inflammatory response during

OA. Complement complex deposits have been found in synovial tissue and correlate with the extent of synovitis present (Haseeb and Haqqi 2013).

1.3 The Role of the Synovium in the Pathophysiology of Osteoarthritis

Inflammation is a key driver in the development and progression of OA, even in the early stages of the disease (Kapoor, Martel-Pelletier et al. 2011). The extent to which synovitis affects the pathogenesis of OA is not completely understood, but it is known to be strongly associated (Scanzello and Goldring 2012). OA tissue and synovial fluid, when compared with 'normal synovial fluid' was found to be highly enriched with plasma proteins, complement components and cytokines (Sokolove and Lepus 2013). Comparison of OA synovium and chondrocyte microarray data, to OA synovial fluid proteomic analysis has recently confirmed that the synovial membrane contributes to this rich soup of inflammatory-associated proteins present in OA synovial fluid. Proteins that play a role in the acute phase response and complement pathways were found, in part, to be produced by the synovium (Ritter, Subbaiah et al. 2013).

Equine synovitis is characterised by an infiltration of mononuclear cells into the synovial membrane and synovial fluid (McIlwraith, Frisbie et al. 2010), with a concurrent associated enzymatic response (Todhunter, Kincaid et al. 1996). This is accompanied by hyperplasia of the intima layer, oedema, vascularisation, and fibrosis of the subintima (Sutton, Clutterbuck et al. 2009, Frisbie 2012). Within this cellular infiltration are T-cells, B-cells and an abundance of macrophages. An up regulation of synoviocyte gene expression, and increased synovial fluid concentration, of pro-inflammatory

cytokines IL-1β and TNF-α, have a major impact on the pathophysiology of equine OA (Kamm, Nixon et al. 2010). These pro-inflammatory cytokines dis-regulate the expression of other cytokines, matrix metalloproteinases and aggrecanases; upsetting the chondrocyte metabolic equilibrium and resulting in an excessive catabolic state. This leads us to recognise pro-inflammatory cytokines produced by the synovium, alongside those produced by chondrocytes, as important drivers of cartilage degradation. However, the temporal relationship between subchondral bone damage, inflammation of the synovial tissue, and cartilage erosion, is still largely unknown (Kapoor, Martel-Pelletier et al. 2011), even though cartilage, bone (Kapoor, Martel-Pelletier et al. 2011), synovium (Ritter, Subbaiah et al. 2013) and adipose tissue (Houard, Goldring et al. 2013) have all been found to contribute to the inflammatory process. Acute synovitis may be one of the first changes to occur in OA; synovial tissue has been shown to over-express inflammatory mediators such as pro-inflammatory cytokines (Benito *et al.* 2005); especially IL-1β and TNF-α (Todhunter *et al.* 1996). In comparison to normal equine joints, OA equine synovium exhibits significantly up-regulated gene expression of TNF-α, ADAMTS5 and MMP13 at all stages of OA, and IL-1β was moderately up-regulated. Whereas chondrocytes in OA cartilage significantly up-regulated the gene expression of IL-1β, TNF-α, ADAMTS4 and MMP13 (Kamm, Nixon et al. 2010).

1.3.1 Fibroblast-Like Synoviocytes and Their Contribution to Synovitis

FLS are cells of mesenchymal stromal lineage found within the synovial membrane (Bartok and Firestein 2010). As explained previously, FLS precursors reside within the synovial membrane, and FLS expand locally (Alwan, Carter et al. 1991). Whilst FLS and subintimal fibroblasts share some similarities such as the expression of collagen, vimentin and CD90, FLS also express specific markers including uridine diphosphoglucose-dehydrogenase (UDPGD), vascular cell adhesion molecule-1 (CD106) (VCAM-1) and calcium-dependent adhesion molecule-11 (Cadherin-11) (Bartok and Firestein 2010). These factors play roles in both normal joint maintenance and in joint disease. Cadherin-11 is crucial for the adhesion and organisation of synoviocytes within the synovial membrane, and cadherin deficient mice have been found to develop a disordered synovial membrane with a defective inflammatory response rendering the mice resistant to inflammatory arthritis (Lee, Kiener et al. 2007). UDPGD is a hyaluronan synthesis-related enzyme which is very specific to the FLS (Edwards 1994, Rosengren, Boyle et al. 2007) whereas VCAM-1 is thought to bind mononuclear cells in the synovial membrane (Bartok and Firestein 2010).

FLS Help Drive the Mononuclear Cellular Infiltration Seen in Synovitis

The chemotaxis of mononuclear cells into the synovial membrane, a process which aids in characterising synovitis, is driven by a number of chemokines (Haringman, Smeets et al. 2006) and growth factors such as transforming growth factor-β (TGF-β) (Allen, Manthey et al. 1990) and platelet derived

growth factors (PDGF) (Deuel, Senior et al. 1982). Pro-inflammatory cytokines such as IL-1β have also been shown to stimulate the production of chemokines in OA chondrocytes (Haseeb and Haqqi 2013). Amongst the key chemotaxis inducing chemokines, is the macrophage chemoattractant protein-1 (MCP-1 or CCL-2). FLS have been found to be an important source of MCP-1, which also contributes to monocyte activation (Villiger, Terkeltaub et al. 1992). The activated synovial membrane is a potent producer of mediators such as IL-1β, TNF-α, TGF-β and PDGF which in turn stimulate further MCP-1 secretion resulting in a positive feedback cycle cultivating the inflammatory response (Villiger, Terkeltaub et al. 1992). Two further chemokines, involved in chemotaxis and the exacerbation of the inflammatory response, found to be expressed by OA FLS are the growth regulatory oncogene-β (GROβ) and the granulocyte chemotactic protein (GCP-2) (Scaife, Brown et al. 2004). Abundant expression of the chemokine receptor CCR-5 has been observed on cells within inflamed synovium (Haringman, Smeets et al. 2006). OA FLS have also been found to express CCR-5 and activation of this receptor with its ligands CCL-19 and CCL-21 has been shown to result in cell migration and increased secretion of vascular endothelial growth factor (VEGF) which promotes angiogenesis (Haseeb and Haqqi 2013).

FLS Help Drive the Inflammatory Reaction

FLS are key mediators of tissue destruction, through the production of MMPs, inflammatory cytokines, chemokines, proteases and indirectly through the regulation of monocytes. During early OA, the soluble CD14

receptor within synovial fluid, has been found to enhance the FLS response to TLR-2 and -4 ligands (Nair, Kanda et al. 2012). Binding of ligands to these receptors promotes pro-inflammatory cytokine gene expression. Cytokines IL-1β and TNF-α, chiefly produced by synovial macrophages (Bondeson, Wainwright et al. 2006) but also by FLS, can increase the secretion of themselves (Fernandes, Martel-Pelletier et al. 2002) and can promote FLS production of IL-6, IL-8, leukocyte inhibitory factor (LIF), proteases and PGE_2 (Pelletier, Martel-Pelletier et al. 2001). A substantial difference was detected when examining differentially expressed genes between FLS from rheumatoid arthritis (RA) and OA, however, a common observation was their increase in IL-6 and MCP-1 protein (Scaife, Brown et al. 2004). IL-6 is significantly elevated in OA synovium and contributes to the development of OA by potentiating the effects of IL-1β when stimulating MMP production and inhibiting proteoglycan production, however it can also promote tissue inhibitor of metalloproteinase (TIMP) (Fernandes, Martel-Pelletier et al. 2002). FLS also have the ability to activate T cells and support B cell survival (Filer, Parsonage et al. 2006, Donlin, Jayatilleke et al. 2014). Furthermore FLS have been found to express MMP10, which is associated with the invasion potential of these cells (Davidson, Waters et al. 2006).

FLS Can Exert Both Protective and Catabolic Effects

Equine FLS co-cultured with mechanically injured equine cartilage explants, down-regulated their gene expression of ADAMTS4 and -5, and TIMP-1, and up-regulated their MMP1 expression, compared to those exposed to non-injured cartilage. The mechanically injured cartilage, in co-culture with

synoviocytes, experienced increased chondrocyte gene expression of collagen type II and ADAMTS5. However on histologic examination, decreased focal cell loss and decreased chondrocyte cluster formation were observed (Lee, Kisiday et al. 2013). These findings suggest cross-talk between synoviocyte and chondrocyte populations influence their gene expression. In a similar experiment, bovine mechanically injured cartilage was co-cultured with bovine synovial explants which contained other cell types alongside FLS. No increase in chondrocyte ADAMTS5 gene expression was observed, but an increase in ADAMTS5 protein was present in relation to both injury and co-culture (Lee, Fitzgerald et al. 2009). Other synovial cells, such as synovial macrophages, may have prevented the FLS-induced increase in chondrocyte ADAMTS5 gene expression observed in the first study, or this could be a species-related difference. As well as promoting the inflammatory response, FLS have also been observed to moderate the synovial macrophage reaction. FLS strongly suppress TNF-mediated induction of an interferon (IFN)-β autocrine loop and downstream expression of IFN-stimulated genes that are classical of macrophage activation (Donlin, Jayatilleke et al. 2014)

1.3.2 Synovial Macrophages and their Contribution to Synovitis

Synovial Macrophages become Activated in Synovitis and Exert a Significant Influence on Cartilage Degradation

As previously described, upon initiation of an inflammatory event the synovium experiences a massive cellular infiltration; mononuclear cells extravasate from blood vessels into the intima layer and synovial fluid (Caron 2011). Equine histopathology grading systems consider small areas of mononuclear cells to reflect a grade 1 synovitis, whereas a marked presence of mononuclear cells in greater than 50% of the section is classified a grade 4 synovitis (McIlwraith, Frisbie et al. 2010). Similar synovitis grading systems are available for the dog, sheep and goat, however they also incorporate the scoring of lymphoid follicles within the synovial membrane (Cook, Kuroki et al. 2010, Little, Smith et al. 2010). Macrophages are abundant within this cellular infiltration (Haseeb and Haqqi 2013) and chemokines responsible for their chemotaxis have been implicated in the development of OA (Blom, van Lent et al. 2004). Whether factors from injured cartilage activate the macrophages, or other stimuli initiate macrophage activation, which subsequently causes them to influence cartilage degradation, is unknown. The predominant roles of activated macrophages include pro-inflammatory cytokine production and phagocytosis of pathogenic material. Macrophages manifest in three distinct activated phenotypes; the classically activated, the alternatively activated and the type II-activated macrophage. The classically activated macrophage is triggered by IFN-γ and TLR signalling; once TLR-ligands are bound endogenous TNF-α production by the macrophage

commences. This induces an up-regulation in the gene expression of pro-inflammatory cytokines IL-1, TNF-α, IL-6 and IL-12, and VEGF (Haywood, McWilliams et al. 2003). VEGF is the principal driver of angiogenesis, also seen in the intimal layer at the onset of synovitis, and a recent study has shown that anti-VEGF antibodies can reduce the onset of OA (Nagai, Sato et al. 2014). The alternatively activated macrophages are activated by IL-4, however they fail to produce nitric oxide which diminishes their ability to kill phagocytosed microbes. The type II-activated macrophages are similarly stimulated to the classically activated macrophages but secrete a large amount of IL-10, suggesting this population have anti-inflammatory properties (Mosser 2003).

Activated synovial macrophages produce significant amounts of the pro-inflammatory cytokines IL-1β and TNF-α, which play a crucial role in the pathogenesis of OA. Bondeson *et al.* (2006) extracted synovial macrophages from digested human synovial membrane using CD14+ beads. The resulting synovial cultures produced significantly less IL-1β and TNF-α than those containing synovial macrophages. Cultures also experienced significantly reduced gene expression of IL-6, IL-8, MMP1 and -3, which are chiefly produced by synovial fibroblasts (Bondeson, Wainwright et al. 2006).

On further investigation using IL-1β and TNF-α inhibitors in synovial cultures, it was noted that the inhibition of both cytokines were necessary to reduce IL-6, IL-8, MCP-1, MMP1, -3, -9, and -13 to the same extent as that of synovial macrophage depleted cultures (Bondeson, Wainwright et al. 2006). Using the

synovial culture model descried above, it was also found that synovial macrophage TNF-α was the main driver of FLS ADAMTS4 gene expression, and that neither IL-1β nor TNF-α had any influence over FLS ADAMTS5 gene expression (Bondeson, Wainwright et al. 2006). This finding was contradicted by Kamm et al. 2010 (Kamm, Nixon et al. 2010) which may highlight differences between human and equine synovium. This will be discussed in more detail further on.

Activated Macrophages Stimulate Osteophyte Formation and MMP-Induced Cartilage Degradation

A murine model of collagenase-induced arthritis (CIA) depleted of synovial macrophages by intra-articular administration of clodronate-liposomes, produced a 66-84% reduction in osteophyte formation (Blom, van Lent et al. 2004). A concurrent decrease in the production of growth factors TGF-β, and bone morphogenetic proteins-2 and -4 in the intima layer were also observed (Blom, van Lent et al. 2004). In a subsequent study using a similar macrophage depleted murine model subjected to intra-articular administered TGF-β, it was observed that macrophages were crucial intermediate factors in osteophyte formation induced by TGF-β (van Lent, Blom et al. 2004). Macrophages obviously play a pivotal role in the degree of bone pathology observed during OA.

Activated synovial macrophages have also been associated with MMP-mediated cartilage damage, and appear to up-regulate MMP production within the synovial membrane (Blom, van Lent et al. 2007). Proteinases such

as MMPs and aggrecanases (ADAMTS family) cleave aggrecan, one of the chief constituents of cartilage ECM, within its interglobular domain but between different amino acid sequences. Neoepitope antibodies designed for specific N or C terminal amino acid sequences, can identify the origin of these aggrecan fragments, and subsequently determine whether they were produced through MMP or aggrecanase proteolysis (Stanton, Golub et al. 2011). These antibodies will only bind to protein degradation products and not intact protein (Fosang, Last et al. 2010), allowing measurable changes in ECM degradation. Mice depleted of macrophages and subjected to the CIA model, were found to have generated fewer MMP-induced neoepitope fragments than those of control mice (Blom, van Lent et al. 2007). Furthermore a significant reduction in macrophage-depleted synovial membrane MMP3 and MMP9 gene expression was observed, which did not occur in cartilage, implying that synovial macrophages mediate MMP production in the synovial membrane.

Highlights

1. Activated synovial macrophages play a major role in osteophyte formation and cartilage degradation, through the production of growth factors (VEGF and TGF-β), and proteases (MMP3 and -9).
2. Synovial macrophages are significant producers of IL-1β and TNF-α which drive the inflammatory pathway.
3. During inflammation synovial macrophages influence FLS through signalling mediators and IL-1β and TNF-α.

1.4 The Role of Pro-inflammatory Cytokines in Osteoarthritis

1.4.1 Interleukin-1

The complex pathway of interleukin-1 instigated cellular activation, involves many factors including membrane bound and soluble receptors, receptor accessory proteins, soluble forms of both interleukin isoforms and receptor antagonist proteins (Figure 1.3). This multifactorial cascade makes it ideal for therapeutic intervention.

IL-1β is a pro-inflammatory cytokine, produced within the joint by FLS, synovial macrophages, chondrocytes and osteoblasts. It is a key driver of cartilage degeneration within OA, however it also plays a complex role in joint homeostasis (Kapoor, Martel-Pelletier et al. 2011). IL-1β knock out mice experienced accelerated cartilage lesion formation after joint destabilisation compared to control mice (Clements, Price et al. 2003). However IL-1β also has catabolic influences, decreasing chondrocyte gene expression of type II collagen, aggrecan, and proteoglycans (Gregg, Fortier et al. 2006), and increasing chondrocyte gene expression of MMP1, -3 and -13, all key mediators of cartilage destruction (Kapoor, Martel-Pelletier et al. 2011). Blocking IL-1 action with recombinant IL-1 receptor antagonist (IL-1RA) was found to significantly reduce MMP-derived aggrecan neoepitopes (van Meurs, van Lent et al. 1998), directly linking IL-1 to MMP-mediated cartilage degradation. There is a fine balance between inhibiting the catabolic effects

of IL-1β and disrupting joint homeostasis, which needs to be considered when targeting IL-1β .

IL-1 is produced in two isoforms α and β; around 26% of their amino-acid sequences are homologous, and each is transcribed from a separate gene, however IL-1β mRNA predominates (Dinarello 1988). Both isoforms are first synthesised as precursor proteins (31kDa), before being activated (proteolytically cleaved to 17.5kDa forms) by intracellular ICE (Caspase I) enabling them to bind to receptors (Clements, Price et al. 2003). Both bind to the same specific cell membrane bound receptors (Dower, Kronheim et al. 1986); IL-1 receptor type I (IL-1RI) and type II (IL-1RII). IL-1RI is an 80kDa member of the immunoglobulin superfamily, and contains a 20kDa cytoplasmic element crucial for the transduction of IL-1β intracellular signalling (Saklatvala, Davis et al. 1996, Murray, Parry-Jones et al. 2015). IL-1RII is commonly termed a decoy receptor (around 67kDa), as it contains a short cytoplasmic element which is unable to transduce a signal (Kapoor, Martel-Pelletier et al. 2011). An increase in IL-1Rs have been observed in both OA synoviocytes and chondrocytes (Kapoor, Martel-Pelletier et al. 2011), and within areas surrounding cartilage lesions. Equine IL-1 was first characterised at The University of Liverpool in 1990 by Stephen May (May, Hooke et al. 1990).

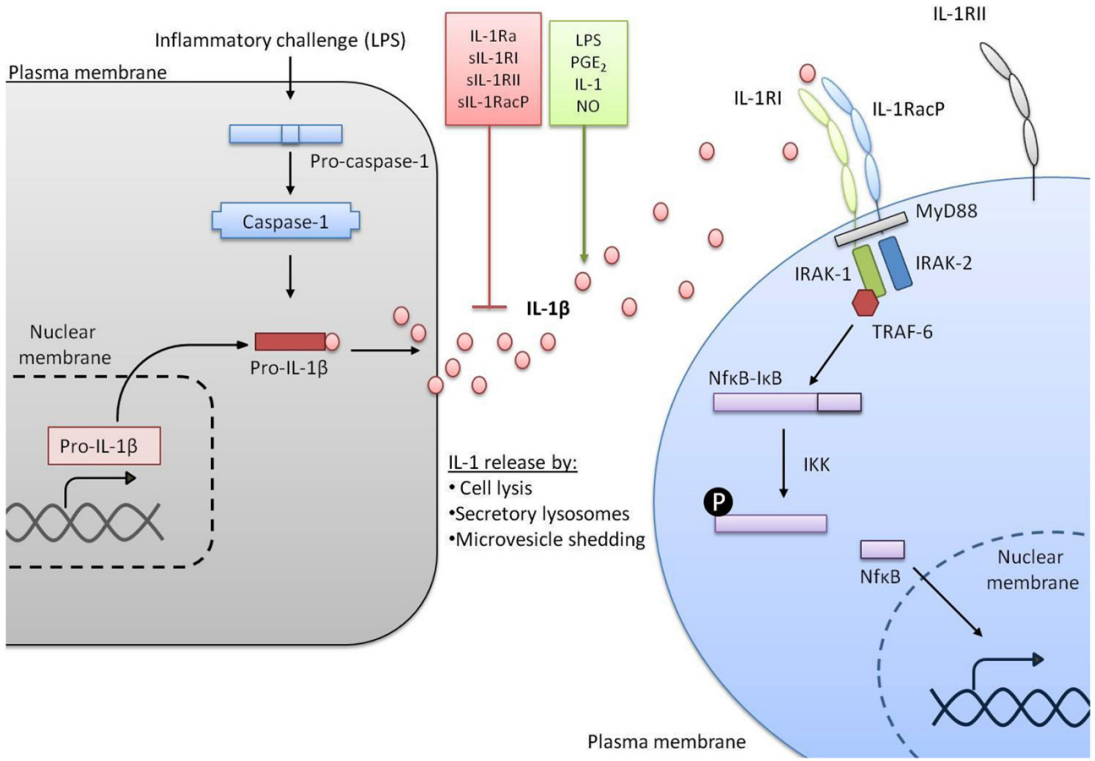

Figure 1.3 IL-1 Signaling Pathways. In response to a stimulus such as LPS, transcription of the gene encoding IL-1β is initiated. IL-1β ismade as an inactive precursor protein and caspase-1 cleaves this pro-IL-1β to make the active IL-1β. A variety of factors can promote or inhibit the release of active IL-1β. Once released, IL-1β binds to IL-1RI alongside IL-1 receptor accessory protein (IL-1RAcp) and signal transduction is triggered, including co-localisation of myeloid differentiation primary response protein 88 (MyD88), IL-1 receptor associated kinase (IRAK-1) and IRAK-2, recruitment of TNF receptor associated factor 6 (TRAF-6) and activation of nuclear factor kappa B (NFκB) from complex with IκB. Conversely IL-1RII does not induce signal transduction (Murray, Parry-Jones et al. 2015)

1.4.1.1 Soluble Interleukin-1 Receptors Act as Interleukin-1 Scavengers

Proteases lyse and release both membrane bound IL-1Rs to produce soluble forms; sIL-1RI and sIL-1RII. These act as scavengers of both interleukin isoforms and IL-1RA; sIL-1RI preferentially binds to IL-1RA, whereas sIL-1RII preferentially binds to IL-1β (Svenson, Hansen et al. 1993, Dinarello 1996, Jotanovic, Mihelic et al. 2012).

1.4.1.2 Soluble Interleukin-1 Receptor Accessory Protein Scavenges Interleukin-1β

IL-1 receptor accessory protein also exists in both membrane bound (IL-1RAcp) and soluble (sIL-1RAcp) forms. Once IL-1β has bound to IL-1RI, the IL-1RAcp is required to initiate intracellular signalling (Svenson, Hansen et al. 1993), sIL-1RAcp is unable to carry out this function. sIL-1RAcp scavenges IL-1β using 2 methods (1) sIL-1RAcp competes with membrane bound IL-1RAcp to bind IL-1β to IL-1RI. sIL-1RAcp will inhibit the cytokine's function. (2) sIL-1RAcp and sIL-1RII preferentially bind to IL-1β, acting as a soluble sIL-1RII scavenger. Once IL-1β is bound to the sIL-1RII with the accompanying receptor accessory protein no signal transduction will occur and the cytokine's function will be inhibited. When sIL-1RAcp and sIL-1RII interact, it increases the IL-1 binding affinity of the receptor by 100-fold, whilst maintaining a low binding affinity to IL-1RA (Smith, Hanna et al. 2003).

1.4.1.3 Interleukin 1 Receptor Antagonist Protein

This protein binds to the 80kDa membrane bound IL-1RI on fibroblasts and T cells with high affinity, and with lower affinity to IL-1RII on neutrophils and B cells. Once bound it does not initiate any IL-1 mediated protein kinase signal transduction (Dripps, Brandhuber et al. 1991). A 10-1000 fold increase of IL-1RA to IL-1 must occur to block all of the available IL-1 receptors that are up-regulated during OA (Wehling, Moser et al.). Recombinant IL-1RA has previously been reported to reduce the severity of disease in animal models, suggesting that this recombinant protein may hold therapeutic qualities. A group in Tokyo successfully produced a non-glycosylated recombinant version of equine IL-1RA protein. E.Coli were transformed with a recombinant equine IL-1RA containing plasmid and expanded. Recombinant equine IL-1RA protein was then extracted from these cells, and used to successfully inhibit cytotoxic activity of IL-1. They hypothesised that, as in human medicine, this recombinant protein could be used in a therapeutic manner (Kato, Ohashi et al. 1997). After a thorough literature search, no further investigation into this therapeutic pathway could be found. There are two IL-1RA protein preparations currently licensed for humans, Anakinra (Kineret), which is a recombinant human IL-1RA, and Orthokine, which is an autologous IL-1RA injection. They elicit certain clinical and biological responses and have been shown to produce statistically significant improvements in pain scores in knee OA as assessed by the KOOS (knee injury and osteoarthritis outcome score) (Jotanovic, Mihelic et al. 2012).

1.4.1.4 Interleukin-1β Signal Transduction

The intracellular portion of IL-1R1 is very similar to that of the TLR, and is termed the Toll-and-IL-1 receptor (TIR) region (Kapoor, Martel-Pelletier et al. 2011). TLRs are important PRRs; recognising pathogen associated molecular patterns (PAMPS) such as LPS (Bobacz, Sunk et al. 2007, Kwon, Vandenplas et al. 2010), and DAMPs such as cartilage degradation fragments (Nair, Kanda et al. 2012). These receptors activate many pathways including two major pathways, the NF-κB pathway (Kwon, Vandenplas et al. 2010), and IL-1R Associated kinase (IRAK) (Janssens and Beyaert 2003). These pathways play a major role in the regulation of inflammatory cytokine and MMP gene expression. IRAK partly controls the mitogen-activated protein kinases (MAPK); ERK, JNK and p38. Protein kinases are enzymes, which add phosphate groups (phosphorylation) to other proteins, causing them to functionally change; this can be reversed by specific protein phosphatases, which remove phosphate groups. These pathways regulate signal transduction and eventually transcriptional factors of specific genes.

1.4.2 Tumour Necrosis Factor-α

TNF-α is the second major pro-inflammatory cytokine responsible for the pathophysiology of OA, but it is also involved in maintaining joint homeostasis. This cytokine is produced in two isoforms; TNF-α is primarily produced by monocytes and macrophages but all joint cells are capable of producing this cytokine, whereas TNF-β is produced by activated T lymphocytes (Saklatvala, Davis et al. 1996). Both isoforms bind to two

specific cell membrane receptors TNFRI (p55) and TNFRII (p75) (Saklatvala, Davis et al. 1996, Russo and Polosa 2005); TNFRI is responsible for driving the inflammatory response (Nophar, Kemper et al. 1990) (Figure 1.4). TNFRI is up-regulated in OA chondrocytes (Westacott, Atkins et al. 1994) and synovial fibroblasts (Alaaeddine, DiBattista et al. 1997), and is the more dominant receptor for mediating TNF activity in articular tissues. TNF activates a number of protein kinases, similar to IL-1 (Saklatvala, Davis et al. 1996). Since the 1980s it has been known that TNF-α suppresses proteoglycan synthesis and degrades proteoglycan through proteolysis (Saklatvala 1986).

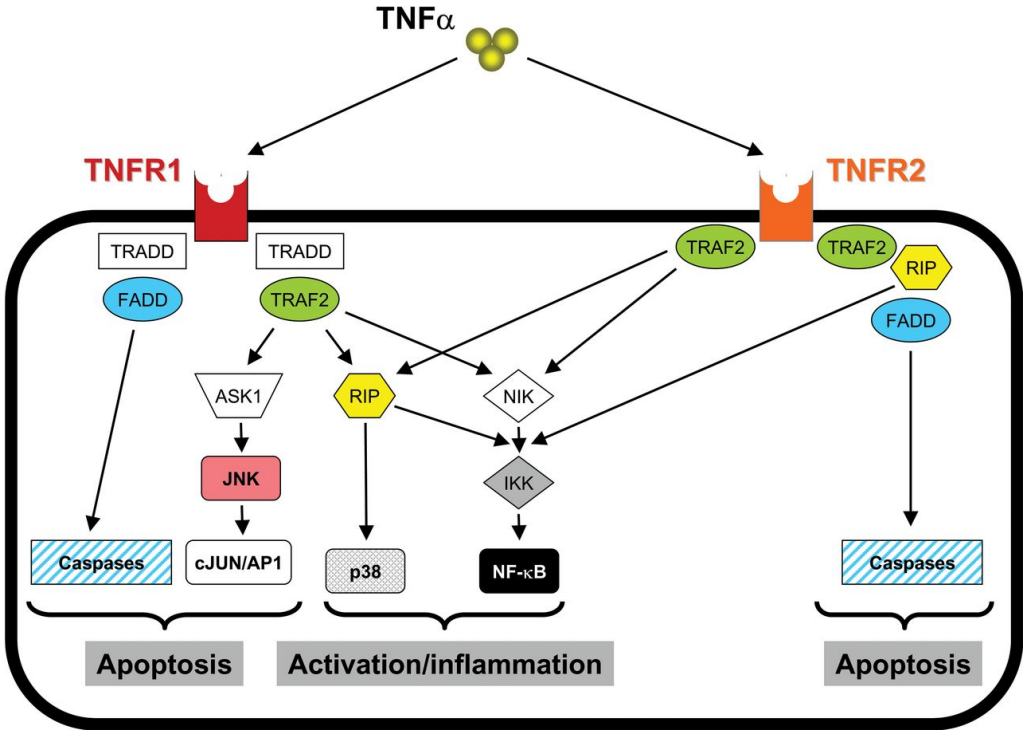

Figure 1.4 TNF-α Signalling Pathways. Binding of TNF-α to TNFRI results in the configuration of TRADD (TNFR-associated death domain) and FADD (Fas-associated death domain). TRADD complex recruits the adapter protein TRAF-2 (TNFR-associated factor 2), whereas FADD stimulates the caspase cascade. Known downstream signalling molecules that interact with TRAF-2 and NIK (NF-κB-inducing kinase), RIP (receptor-interacting protein) and ASKI (apoptosis signal-regulating kinase I) and these are capable of chanelling signals towards cell death and inflammation. Binding of TNF-α to TNFR2 recruits the adapter protein TRAF-2, which directly activates the inflammatory cascade via the generation of NF-κB or p38 MAPK (mitogen-activated protein kinase) and activates caspase-mediated cell death through recruitment of FADD and RIP (Russo and Polosa 2005).

1.4.3 Interleukin-1β and Tumour Necrosis Factor-α

Both IL-1β and TNF-α potentiate similar responses. Chondrocyte gene expression of MMPs, nitric oxide (NO) and PGE_2 are stimulated whilst synthesis of link protein and type II collagen is inhibited by both IL-1β and TNF-α (Lefebvre, Peeters-Joris et al. 1990, Frisbie 2012). These cytokines also increase chondrocyte gene expression of IL-6 (Guerne, Carson et al. 1990), IL-8 (Lotz, Terkeltaub et al. 1992), and synoviocyte MCP-1 (Villiger, Terkeltaub et al. 1992). They also induce reactive oxygen species (ROS) which contribute to cartilage degeneration, and down-regulate expression of antioxidants (Kapoor, Martel-Pelletier et al. 2011).

1.4.4 Interleukin-6

The IL-6 subfamily of cytokines share the signal transducing receptor-β subunit gp130 (Rose-John, Scheller et al. 2006); IL-6 and IL-6 alpha receptor (IL-6Rα) bind together to form a signalling complex (Boulanger, Chow et al. 2003). Soluble IL-6Rα (sIL-6Rα) can bind to IL-6 to induce IL-6 effects on cells that don't express the receptor. However, soluble gp130 also exists and can bind to IL-6/sIL-6Rα and inhibit their actions (Narazaki, Yasukawa et al. 1993).

IL-6 is produced by equine synoviocytes and chondrocytes in both normal and diseased joints (Ishimi, Miyaura et al. 1990, Ley, Ekman et al. 2009), and this has been reproduced in equine models such as LPS-induced arthritis (Hawkins, MacKay et al. 1993), and synovectomy-induced synovitis. IL-6 has been associated with bone resorption (Ishimi, Miyaura et al. 1990),

equine subchondral bone cysts (Rechenberg, Leutenegger et al. 2001) and equine chip fractures (Ley, Ekman et al. 2007). This is interesting as synovitis is always a concurrent finding in joints suffering from chip fractures (Ley, Ekman et al. 2007). Whether cytokines produced from an inflamed synovial membrane predispose the bone to a chip fracture, or the chip fracture itself produces cytokines causing synovitis, is so far unknown. Significant correlation between synovial fluid IL-6 and TP concentrations were associated with chip fractures, yet no correlation to WBCC occurred. IL-6 is therefore most likely produced by resident joint cells rather than infiltrating synovial fluid cells (Ley, Ekman et al. 2007). Both IL-1β and TNF-α can directly stimulate IL-6 production (David, Farley et al. 2007). Whether IL-6 exerts a predominantly anabolic or catabolic effect upon cartilage in OA is so far unknown. IL-6 reduces cartilage loss in murine models (de Hooge, van de Loo et al. 2005) and IL-1 induced PGE_2 production in chondrocytes and synoviocytes (Hauptmann, Van Damme et al. 1991). IL-6 can also up-regulate chondrocyte SOX-9 (SRY-box-9 gene) (Ley, Svala et al. 2011) and TIMP production (Lotz and Guerne 1991). However, IL-6 can also up-regulate MMP-1, MMP-13 and C-reactive protein (CRP) levels. CRP has been linked to OA in humans; high baseline levels of IL-6 and CRP were associated with an increased risk of cartilage damage visualised through magnetic resonance imaging (Kapoor, Martel-Pelletier et al. 2011). Some studies suggest the effects of IL-6 are determined by the presence of the soluble IL-6Rα (sIL-6Rα) as IL-6 has been found to inhibit proteoglycan synthesis (Guerne, Desgeorges et al. 1999) and induce aggrecanase-

mediated proteoglycan catabolism (Flannery, Little et al. 2000) in the presence of sIL-6Rα.

1.4.5 Aggrecanases and Matrix Metalloproteinases

1.4.5.1 Matrix Metalloproteinases

MMPs are capable of degrading cartilage ECM proteins which is essential for normal ECM turnover. However in pathological conditions, catabolic processes outweigh anabolic chondrocyte metabolism resulting in the degradation of cartilage (Vincenti and Brinckerhoff 2002, Fosang, Last et al. 2010). Key members of this large family of proteinases, in regards to cartilage degradation during OA, are the interstitial collagenases MMP1 and -13 (Goldring, Otero et al. 2011), the gelatinases MMP2 and MMP9 (Clegg and Carter 1999) and the stromelysin MMP3 (Peffers, Thornton et al. 2015). MMPs are produced as latent proteins; most are secreted in a pro-form and are activated in the extracellular environment (Clegg and Carter 1999). A small percent undergo intracellular furin-like activation before being secreted. Interstitial collagenases (MMP1 and MMP13) are able to unwind the type II collagen triple helix, making it vulnerable to MMP9 proteolysis. MMP3 is the most highly expressed MMP in cartilage, and capable of degrading proteoglycans including aggrecan, and activating pro-collagenases (Peffers, Thornton et al. 2015). MMPs are also capable of degrading other ECM proteins including decorin, biglycan, fibromodulin and COMP (Peffers, Thornton et al. 2015). MMPs are induced by cytokines, predominantly IL-1β

and TNF-α, which activate the MAPK downstream signalling. Once MAPKs have translocated to the nucleus, they activate JNKs and ERKs which phosphorylate and activate C-Jun to induce expression of MMP genes, and ERK which activates transcription factors and drives MMP promotors (Vincenti and Brinckerhoff 2002). NF-κB is the second pathway to activate MMP genes and drive expression.

MMPs cleave aggrecan within the IGD at two sites; $DIPEN_{341}\downarrow_{342}FFGVG$ and $SED_{441}\downarrow_{442}LVV$. Proteinases including MMP1, -2, -3, -9, and -13 preferentially cleave at the $DIPEN_{341}\downarrow_{342}FFGVG$ site. Neoepitope antibodies, recognising unique specific newly formed N- or C- termini of the degradation products, allow identification of specific proteinase activity on aggrecan (Fosang, Last et al. 2010). These proteinases cleave matrix proteins at a later stage of OA than aggrecanases, possibly due to the delayed activation of the latent proteases (Durigova, Nagase et al. 2011).

1.4.5.2 Aggrecanases

There are over 28 different members of the ADAMTS family (**A D**isintegrin **A**nd **M**etalloproteinase with **T**hrombo**S**pondin motif), and of these, a subgroup are aggrecanases with significant catabolic activity. These aggrecanases cleave aggrecan in particular, but can also degrade smaller ECM proteins. The ADAMTS family mainly cleave the aggrecan core protein within the IGD between the two globular domains G1 and G2. Here they cleave at the specific Glu^{373}-Ala^{374} bond, giving rise to the N-terminal neoepitope $_{374}ARGSV$ and the C-terminal neoepitope $NITEGE_{373}$ (Fosang,

Last et al. 2010). However, they can also cleave aggrecan at four sites within the second chondroitin-sulphate rich domain (CS-2) (East, Stanton et al. 2007, Fosang, Last et al. 2010). ADAMTS5 is thought to be responsible for cleavage within the IGD, whereas other aggrecanases cleave within the CS-2 domain (East, Stanton et al. 2007). Aggrecanases can also effect other proteoglycans within the ECM such as biglycan, brevican, decorin and fibromodulin, and glycoproteins fibronectin and carboxymethylated transferrin (Gendron, Kashiwagi et al. 2007). Aggrecanases are now considered the principle proteases responsible for cartilage ECM proteolysis during OA rather than MMPs (Durigova, Nagase et al. 2011, Zhang, Yan et al. 2013). This conclusion was reflected in a study which reported 90% reduction in IL-1 induced aggrecanase activity after ADAMTS4 and -5 were immunodepleted from bovine cartilage explants (Tortorella, Malfait et al. 2001). Lower MMP proteolytic activity, in comparison to aggrecanase activity, is thought to be due to the delayed activation of pro-MMPs, and the relatively low cleavage efficiency of these enzymes (Bakali, Gras-Masse et al. 2014). There are also certain members of the ADAMTS family which can cleave aggrecan but it is not their preferred substrate, these include ADAMTS 1, 8, 9 and 15 (Kataoka, Ariyoshi et al. 2013). However, the key mediators of OA within this family, are ADAMTS4 (aggrecanase-1) and ADAMTS5 (aggrecanase-2), and ADAMTS5 is thought to have 1000 times more aggrecanase activity than ADAMTS4 (Gendron, Kashiwagi et al. 2007). ADAMTS4 and -5 are produced as zymogens, and undergo intracellular activation by furin enzymes through cleavage of their pro-domain. Whether other pro-protein convertases have the same effect, or whether activation is

necessary for secretion from the cell, is so far unknown (Bondeson, Wainwright et al. 2013).

The exact mechanisms of aggrecanase expression in chondrocytes and synoviocytes are yet to be determined in the horse. ADAMTS5 is thought to be the predominant mediator of aggrecanolysis in mice, whereas it is constitutively expressed by human synovium and chondrocytes (Bondeson 2015). Human synoviocyte and chondrocyte ADAMTS4 gene expression was found to be significantly up-regulated by TNF-α and IL-1β in an NF-κB dependent manner (Bondeson, Wainwright et al. 2006), which may indicate ADAMTS4 is predominantly activated during OA. However when short interfering RNA (siRNA) was used to block both ADAMTS4 and ADAMTS5 gene expression in human cartilage explants, both were found to facilitate aggrecanolysis either independently or concurrently (Song, Hua et al. 2007). These species-variations in gene expression cause us to ponder the question of whether the murine model should be used to investigate human OA. Much research has, so far, been carried out using murine models of OA, and as previously stated, ADAMTS5 has been found to cause the majority of aggrecanolysis and is therefore considered the pathologically inducing aggrecanase during murine OA (Bondeson, Wainwright et al. 2013). This has been proved through many different experimental studies, including those involving ADAMTS4 knock-out (KO) mice subjected to destabilisation of the medial meniscus (DMM) which developed instability-induced OA joint changes comparable to wild-type mice (Glasson, Askew et al. 2004). Whereas, ADAMTS5 KO mice experienced significantly less cartilage

degradation than wild-type mice. The role of ADAMTS5 aggrecanolysis was further supported by the lack of aggrecan fragments specific to ADAMTS5 aggrecan cleavage sites found (Glasson, Askew et al. 2005).

A variant of ADAMTS4 mRNA (ADAMTS4_v1) has been identified in human OA synovium. The protein it translates is identical to ADAMTS4 apart from the spacer domain, which is replaced with a non-homologous C-terminal domain. Both forms are produced as inactive pro-domain proteins, which are activated by furin-cleavage. ADAMTS4 is activated before being secreted, however ADAMTS4_v1 is secreted in its inactive form and associates with the cell membrane. It may then be activated by extracellular enzymes, by self-activation, or by an unknown mechanism (Wainwright, Bondeson et al. 2013).

Equine ADAMTS5 gene expression appears to contrast that of humans. Synoviocyte ADAMTS5 gene expression was found to be significantly up-regulated during equine OA, whereas expression of ADAMTS4 remained unchanged. However equine chondrocytes significantly increased their ADAMTS4 gene expression during OA, but there was no increase in ADAMTS5 mRNA observed (Kamm, Nixon et al. 2010). This may indicate that equine synovium is the chief producer of ADAMTS5, however more insight into the regulation of ADAMTS5 is needed to confirm this. As previously mentioned, human synoviocyte ADAMTS4 gene expression has been found to be significantly up-regulated by both IL-1β and TNF-α cytokines, however ADAMTS5 expression remained unchanged (Bondeson,

Wainwright et al. 2006). A similar pattern of expression was observed in human chondrocytes, although a slight increase in ADAMTS5 occurred (Song, Hua et al. 2007). However, one study reported that human ADAMTS5 mRNA was more abundant in both normal and OA cartilage compared to that of ADAMTS4 mRNA (Bau, Gebhard et al. 2002), although levels of ADAMTS4 mRNA and protein correlated with OA progression whereas ADAMTS5 levels did not. ADAMTS5 protein is rapidly cleared by endocytosis and degraded by low-density lipoprotein receptor-related protein (LRP-1) in cartilage, however this pathway is disrupted in OA as LRP-1 is lost (Yamamoto, Troeberg et al. 2013). These findings suggest that increased ADAMTS5 aggrecanolytic activity may result from a build up of extracellular ADAMTS5 protein rather than an increase in mRNA levels stimulated by the onset of OA and concurrent increases in cytokine levels.

Table 1.1 Aggrecanase gene expression levels observed in healthy joint cells exposed to inflammatory inducing agents.

Gene	Cell	Reason	Species	Expression	Study
ADAMTS4	Synoviocytes	TGF-β	Human	Up-regulated	(Yamanishi, Boyle et al. 2002)
		LPS or IL-1β	Equine	Up-regulated (13-fold)	(Ross, Kisiday et al. 2012)
	Chondrocytes	IL-1	Human	Was induced by IL-1 but low level of expression.	(Bau, Gebhard et al. 2002)
		IL-1, TNF, OSM	Human	All induced expression	(Song, Hua et al. 2007)
		TNF-α, OSM	Murine	Up-regulated expression but not aggrecanase activity.	(Rogerson, Chung et al. 2010)
		IL-1β, TNF-α	Bovine	Up-regulated, but undetected without induction	(Tortorella, Malfait et al. 2001)
		IL-1 induces aggrecanase activity	Bovine	Constitutively expressed	(Pratta, Scherle et al. 2003)
		IL-1β	Equine	Up-regulated (27-fold)	(Busschers, Holt et al. 2010)
		LPS or IL-1β	Equine	Up-regulated (20-fold)	(Ross, Kisiday et al. 2012)
ADAMTS5	Synovium	Not affected by IL-1, TNF-α, or TGF-β	Human	Constitutively expressed	(Yamanishi, Boyle et al. 2002)
		LPS or IL-1β	Equine	Unaffected	(Ross, Kisiday et al. 2012)

Chondrocytes	IL-1	Human	Not influenced by IL-1. Overall expression was much stronger than ADAMTS4.	(Bau, Gebhard et al. 2002)
	IL-1β, TNF-α, OSM	Human	All induced expression	(Song, Hua et al. 2007)
		Human	Constitutively expressed	(Naito, Shiomi et al. 2007)
	TNF-α, OSM, IL-6	Murine	Up-regulated	(Rogerson, Chung et al. 2010)
	Not induced by IL-1β or TNF-α	Bovine	Constitutively expressed	(Tortorella, Malfait et al. 2001)
	IL-1β	Equine	Up-regulated (13-fold)	(Busschers, Holt et al. 2010)
	LPS or IL-1β	Equine	Up-regulated (3-fold)	(Ross, Kisiday et al. 2012)

Table 1.2 Aggrecanase gene expression levels observed in cells extracted from osteoarthritic joints.

Gene	Cell	Reason	Species	Expression	Study
ADAMTS4	Synoviocytes	Driven by synovial macrophage-produced TNF-α and IL-1β	Human	Up-regulated	(Bondeson, Wainwright et al. 2006)
			Human	Constitutively expressed	(Yamanishi, Boyle et al. 2002)
			Equine	Unchanged	(Kamm, Nixon et al. 2010)
	Chondrocytes		Human	Four-fold higher than normal cartilage	(Bau, Gebhard et al. 2002, Song, Hua et al. 2007)
			Human	Increased with progression of OA	(Bau, Gebhard et al. 2002)
			Human	Increased with progression of OA	(Naito, Shiomi et al. 2007)
			Equine	Up-regulated	(Kamm, Nixon et al. 2010)
ADAMTS5	Synoviocytes	Not driven by synovial TNF-α and IL-1β expression	Human	Constitutively expressed in OA synovium	(Bondeson, Wainwright et al. 2006)
			Human	Constitutively expressed	(Yamanishi, Boyle et al. 2002)
			Equine	Up-regulated in OA	(Kamm, Nixon et al. 2010)

Chondrocytes	Human	Constitutively expressed	(Bau, Gebhard et al. 2002) (slight but significant increase found in late stage OA).
	Human	Constitutively expressed	(Naito, Shiomi et al. 2007)
	Human	Two-fold higher than normal cartilage	(Song, Hua et al. 2007)
	Equine	Unchanged	(Kamm, Nixon et al. 2010)

1.5 Disease Modifying Osteoarthritis Therapy

1.5.1 Anti-Interleukin-1 Therapy

Numerous targets are available to facilitate the inhibition of IL-1 activity.

1.5.1.1 Interleukin-1 Receptor Antagonist

Of the numerous IL-1β receptors expressed by each cell, only a low number require ligand binding to initiate the downstream signalling process, and potentiate IL-1β effects. IL-1RA binds to IL-1 membrane-bound receptors (IL-1RI) to block the initiation of IL-1β activity. IL-1RA and IL-1β are produced at similar times and have equal affinity for IL-1RI . A high ratio of IL-1RA to IL-1β is therefore required to have any therapeutic effect. Supplementing the intra-articular environment with IL-1RA may reinforce antagonistic actions. This can be performed using two methods; delivery of autologous IL-1RA protein (IRAP) into the joint space, or through gene therapy to up-regulate expression of the IL-1RA gene. The administration of IRAP is widely used in veterinary medicine. Autologous conditioned serum (ACS) is commonly termed IRAP in veterinary practice. The description IRAP, however, is incorrect; ACS is a mixture of many different anti- and pro-inflammatory mediators whereas IRAP refers to a single protein. ACS is produced through the incubation of whole blood with borosilicate glass beads for 24 hours. Interaction with the glass beads are believed to stimulate monocytes to produce cytokines and growth factors. Using human blood, ACS was first reported in 2003, to produce a 140-fold increase in IL-1RA, and a 2-fold increase in IL-4 and IL-10. No significant elevations of IL-1β or TNF-α were noted (Meijer, Reinecke et al. 2003). Positive symptom and disease

modifying effects on an equine OA model were observed through applied gene therapy designed to up-regulate the IL-1RA protein (Frisbie, Ghivizzani et al. 2002), validating the therapeutic effects of IL-1RA in equine OA. The clinical effects of ACS were then trialled on an equine osteochondral fragment model situated within the middle carpal joint. By day 70 post-surgery, ACS-treatment of OA affected joints was associated with a lower lameness grade than those treated with a placebo (approximately 1 and 2 out of 5 respectively; 0 represents normal gait, 5 represents severe lameness). However, there were no changes in carpal joint effusion or response to joint flexion, or difference seen in radiographic joint changes. A lower degree of cartilage erosion, synovial haemorrhage and subintimal hyperplasia within the synovial membrane was noted when treated with ACS. However, there were no changes in synovial membrane cellular infiltration, subintimal oedema, cartilage histopathology scores or GAG content evident (Frisbie, Kawcak et al. 2007). Similar observations were made when equine articular chondrocytes were exposed to recombinant human IL-1β. ACS had no significant beneficial effects on cartilage proteoglycan matrix metabolism (Carlson, Stewart et al. 2013). A second ACS preparation technique, called IRAP II (Arthrex Ltd, FL, USA), uses a similar system to that used to produce IRAP. IL-1RA levels in IRAP II ACS produced from human blood were reported to be 7x higher than levels in IRAP (Dechant, Baxter et al. 2003). ACS from both systems contained significantly elevated levels of IL-1RA, however IRAP II produced significantly higher levels of IL-1RA (approximately 350pg/ml) compared to IRAP. IRAP II, IRAP and 24h incubated control samples contained significantly higher levels of IL-1β

(approximately 150-200pg/ml) compared to 1h control samples (approximately 50pg/ml) (Hraha, Doremus et al. 2011). Levels of IL-1β in the three preparations other than the 1h control, were significantly higher than mean synovial fluid IL-1β concentrations reported in naturally occurring mild and advanced osteoarthritis (35.3pg/ml and 47.4pg/ml respectively) (Ehrle, Lischer et al. 2015). A 100-1000 fold increase of IL-1RA compared to IL-1β is required to effectively block the IL-1 receptors and prevent the activation of IL-1 signalling (Wehling, Moser et al. 2007). The ratio of IL-1RA:IL-1β was significantly better with IRAP II, than IRAP and control samples (approximately 6 and 2.5 respectively). IRAP II also produced significantly higher levels of growth factors (TGF-β and insulin-like growth factor (IGF)-1) and IL-10 than 1h control samples (Hraha, Doremus et al. 2011). A recent study of IRAP and IRAP II preparations has reported levels of IL-1RA (both approximately 180ng/ml) and IL-1β (approximately 10ng/ml and 12ng/ml) respectively (Fjordbakk, Johansen et al. 2015). An estimated 10 fold difference between IL-1RA and IL-1β would therefore be present, and concentrations of pro-inflammatory cytokine IL-1β within ACS would be around 100 times higher than those found in naturally occurring OA. To conclude, most evidence for the use of ACS in equine OA is anecdotal (Moreira, Moraes et al. 2015), however, many veterinary clinicians recommend its use once corticosteroids fail to induce positive clinical effects (Textor 2011). Large variations in ACS IL-1RA concentrations have been reported, and ratios of IL-1RA:IL-1β required to block the effect of pro-inflammatory IL-1β have not been produced. This may explain the lack of

substantial clinical evidence in favour of ACS; could favourable results have been influenced by a different mediator other than IL-1RA in ACS?

Up-regulation of IL-1RA gene expression is the mainstay of equine anti-IL-1 gene therapy research. Self-complementary adeno-associated virus (scAAV) IL-1RA equine serotype 2 is capable of markedly protecting a joint from developing surgically induced osteoarthritic pathology (Watson, Broome et al. 2014). This form of gene therapy proves promising, however it may be problematic to gain approval of its use in species which could potentially enter the food-chain.

A recombinant form of IL-1RA, Anakinra (Kinaret, Sweden), is now a licensed product used for rheumatoid arthritis in humans and provides good anti-inflammatory action. However, intra-articular therapeutic concentrations are not achieved (Watson, Broome et al. 2013). In a double-blinded, placebo controlled, randomised trial in human patients suffering from knee OA, no differences were found between treatment groups (Chevalier, Goupille et al. 2009).

1.5.1.2 IL-1 Monoclonal Antibodies

Monoclonal antibody (mAb) therapies designed to block IL-1 action include the monoclonal anti-IL-1β antibody Canakinumab (ACZ885, Ilaris, Novartis, Switzerland) which binds to and neutralizes IL-1β, and AMG108, a monoclonal antibody designed to bind to the IL-1RI. Canakinumab is licensed for use in cryopyrin-associated periodic syndrome and systemic juvenile idiopathic arthritis in humans. AMG108 has so far failed to improve

pain associated with knee OA in humans (Yu and Hunter 2015). Other monoclonal antibodies (gevokizumab and ABT-981) are presently in phase II clinical trials (Yu and Hunter 2015).

1.5.1.3 Other Anti-Interleukin-1 Therapies

The soluble decoy receptor Rilonacept (Regeneron pharmaceuticals, New York, USA) is a fusion protein consisting of the extracellular portion of the IL-1 receptor and the Fc domain of human IgG1. This binds IL-1β preventing its interaction with IL-1RI (Kapoor, Martel-Pelletier et al. 2011). This is also licensed to treat cryopyrin-associated periodic syndrome in humans. Other alternative therapies include the overexpression of the IL-1RII (decoy receptor) to scavenge IL-1β (Kapoor, Martel-Pelletier et al. 2011). Diacerin, an anthraquinone derivative, inhibits the production of IL-1β and has generated a modest symptomatic benefit when used to treat OA. However it has been associated with higher rates of gastrointestinal toxicity when used long term (Panova and Jones 2015). ICE inhibitors, to prevent the activation of IL-1β, and MAPK inhibitors, to prevent the downstream signalling events that occur upon IL-1β binding to the receptor, are also being investigated.

1.5.2 Anti-Tumour Necrosis Factor Therapy

TNF-inhibitors have been used to treat rheumatoid arthritis, amongst other conditions, with great success. Monoclonal antibodies designed to bind to and neutralise TNF-α activity include infliximab (Remicade), adalimumab (Humira) and etanercept (Enbrel). However, in phase III clinical trials using adalimumab to treat hand OA, a lack of improvement in clinical symptoms

was observed (Verbruggen, Wittoek et al. 2012). Infliximab has been shown to offer a reduction in anatomical lesion radiographic score in patients with erosive hand OA, after 12 months (Fioravanti, Fabbroni et al. 2009). A fourth antibody, ESBA105, has been trialled *in vivo* in animals, and has been shown to have similar clinical efficacy to infliximab, but is able to penetrate joint tissues (Urech, Feige et al. 2010, Yu and Hunter 2015).

1.5.3 Anti-Aggrecanase Therapy

Several theoretical strategies to prevent aggrecanase activity exist; (1) introduce a molecule (mAb or small inhibitor) to bind to and block the aggrecanase, (2) block aggrecanase cleavage sites on aggrecan, mutate aggrecan therefore preventing aggrecanase binding, or (3) introduce a null-aggrecanase to bind to and block aggrecan cleavage sites (Bondeson, Wainwright et al. 2015). A chimeric murine/human IgG4 monoclonal antibody (mAb, CRB0017), with high affinity for the ADAMTS5 spacer domain, and highly selective to the ADAMTS5 antigen, was created using intracellular antigen capture technology. This anti-ADAMTS5 mAb, administered into STR/ort mice (mice which develop spontaneous OA) joints, delayed cartilage breakdown (Chiusaroli, Visentini et al. 2013), and also reduced surgically induced OA histopatholoy in STR/ort mice (Caselli, Chiusaroli et al. 2015). This monoclonal antibody will enter phase I clinical trials in 2016. A second anti-ADAMTS5 mAb (GSK2394002) has been trialled systemically in mice subjected to DMM, it was administered after the onset of cartilage degeneration reflecting a therapeutic model. Mice were protected from cartilage degeneration and osteophyte formation, and were alleviated from

pain whilst still experiencing subchondral bone changes (Miller, Tran et al. 2014). However, this mAb can cause prolonged cardiovascular side effects (Larkin, Lohr et al. 2014). Short interfering RNAs (siRNA) that have been chemically modified to enable access to the cell without requiring a transfection process, have been successfully used *in vivo* to target MMP13 and ADAMTS5 expression in a murine model of surgically induced OA, resulting in decreased cartilage breakdown (Hoshi, Sasho et al. 2014). Engineered and synthetic small-molecule inhibitors of ADAMTS4 and ADAMTS5 are being designed to selectively and potently inhibit aggrecanase activity (Dancevic and McCulloch 2014). One in particular, AGG-523 (Wyeth/Pfizer, New York, USA), a reversible, non-hydroxamate, zinc-binding selective inhibitor, is currently under-going phase I clinical trials in patients with mild-moderate OA. It can reduce the release of aggrecanase generated aggrecan fragments in rat joints (Chockalingam, Sun et al. 2011). However, concerns over systemic effects of aggrecanase inhibition remain (Bondeson, Wainwright et al. 2015).

MMP inhibitors (MMPi) were initially investigated for use as anti-tumour agents, due to their association with tissue remodelling and carcinogenesis. However, major systemic side effects halted this avenue of research. For use in locally contained diseases, such as OA, selectivity of MMPi poses a concern. Broader non-selective inhibitors have undergone clinical trials, but also produced adverse side effects (Li, Shi et al. 2011). There is new hope, however for the treatment of OA through selective MMP13 inhibition (Li, Shi et al. 2011).

1.6 Short Interfering RNA

1.6.1 Introduction to Short Interfering RNA

Short interfering RNA (siRNA) molecules are capable of inhibiting gene expression by cleaving mRNA at a specific site. These molecules are double-stranded RNA duplexes, which are 20-25 nucleotide base pairs in length with two nucleotide 3' overhangs (Elbashir, Harborth et al. 2001). They are designed to complement target gene mRNA, and are synthetically produced. Several techniques facilitate introduction of the siRNA into the cell, known as transfection. Within the cytoplasm, the siRNA duplex is incorporated into the RNA-induced silencing complex (RISC). This contains an argonaute family protein with a Paz domain enabling interaction with the siRNA 3' overhang, and a binding pocket which associates with the 5' overhang (Deleavey and Damha 2012). The siRNA double helix is unwound, the sense strand released, and the now active RISC complex seeks out complementary 3'-untranslated regions (3'UTR) of mRNA. The ability of the RISC complex to differentiate between strands is crucial when selecting which strand to release, as incorrect selection can lead to reduced target gene silencing and the initiation of off-target gene silencing (Kanasty, Whitehead et al. 2012). Strand selection is determined by thermodynamic stability; the antisense strand is selected due to its low hybridisation stability at the 5' end. Other characteristics, designed to increase strand asymmetry, such as A-U base pair content, also contribute to correct strand selection (Kanasty, Whitehead et al. 2012). The antisense strand anneals to the complementary sequence via Watson-crick base pairing, the phosphodiester

bonds between base pairs 10 and 11 are positioned within an RNase-H-like active site (Elbashir, Harborth et al. 2001, Deleavey and Damha 2012). RNase-H is an endogenous endonuclease which catalyses the enzymatic reaction that cleaves target mRNA and releases the RISC (Deleavey and Damha 2012). This prevents translation of the complementary mRNA into amino acid sequences, effectively silencing the gene.

1.6.2 Use of Short Interfering RNA in Osteoarthritis

SiRNA therapy has successfully decreased the expression of target pro-inflammatory mediators in experimental OA models. Collagen-induced arthritis (CIA) in mice and rats has been ameliorated by anti-TNF-α and anti-IL-1β siRNA delivered to cells via intra-articular electroporation (Inoue, Takahashi et al. 2005, Inoue, Takahashi et al. 2009), one study demonstrated siRNA localised to the synovium rather than the cartilage (Inoue, Takahashi et al. 2005). Intra-articular poly-lactide glycolic acid (PLGA) microspheres loaded with anti-TNF-α siRNA, used in a murine CIA model, have also successfully inhibited synovial TNF-α expression, as assessed by immunohistochemistry and intracellular staining of mononuclear cells (Présumey, Salzano et al. 2012). Treated joints had significantly lower joint swelling up to 15-28 days after induction of CIA, and radiographic and histological arthritis scores were significantly lower at 28 days (Inoue, Takahashi et al. 2009). Similar results were achieved with anti-TNF-α siRNA loaded PLGA microspheres in a murine CIA model at 10 days post-OA induction (te Boekhorst, Jensen et al. 2012).

LPS-stimulated (100μg/ml) equine primary chondrocytes transfected with anti-IL-1β siRNA via electroporation, experienced a significantly lower level of IL-1β gene expression than untreated cells. These siRNAs also decreased gene expression levels of MMP13, IL-1α and stromelysin (Nixon and Strassheim 2006). However, IGF-I and aggrecan gene expression significantly decreased through LPS exposure, were unaffected by IL-1β RNA interference (RNAi). Synovial cells, transfected with anti-IL1 siRNA and exposed to LPS in a similar manner, showed comparable gene expression levels to treated chondrocytes (Nixon, Goodrich et al. 2007). Using a polycistronic plasmid for *ex vivo* transduction of equine chondrocytes, simultaneous overexpression of IGF-1 and transcriptional silencing of IL-1 using short hairpin RNA (shRNA) was achieved. This method maybe useful for a multi-targeting technique (Nixon, Strassheim et al. 2007). IGF-1 is a crucial mediator of anabolic chondrocyte metabolism, resulting in increased expression of aggrecan and collagen type II (Ortved, Begum et al. 2014). *Ex vivo* transduction of equine chondrocytes using a self-complementary adeno-associated 5 vector overexpressing IGF-1, were implanted into full-thickness femoral chondral defects using a fibrin vehicle. After 8 months, histological scores were improved compared to contra-lateral defects filed with naïve chondrocyte-fibrin implants; increased chondrocyte numbers and collagen type II content were present (Ortved, Begum et al. 2014). The mechanical properties of cartilage produced by chondrocytes over-expressing IGF-1 were also superior to naïve chondrocytes (Griffin, Ortved et al. 2015). These recombinant AAV vectors have been shown to be minimally immunogenic within equine joints, making them a potentially useful tool to target intra-

articular tissues during OA (Ortved, Wagner et al. 2015).

Vectors, including lentivirus and adeno-associated virus vectors, to transfect cells with shRNA for TNF knockdown, have successfully targeted dendritic cells, and FLS and synovial macrophages respectively. However, safety concerns reside over the use of viral vectors (Apparailly and Jorgensen 2013).

Delivery of siRNA to target cells has been a major limiting factors with regards to their clinical use. Successful results in OA models using viral vectors, electroporation and PLGA microspheres have already been described. Chemically modulated siRNA has been designed to enable siRNA transfection without the need of an agent. Studies investigating intra-articular administration of chemically modulated anti-MMP13 and anti-ADAMTS5 siRNAs in a murine OA model, have shown successful inhibition of cartilage degradation in early OA (Hoshi, Sasho et al. 2014).

1.7 Biodegradable Polymer Microsphere as Drug Delivery Vehicles

Intra-articular DMOADs to counteract pain and slow joint degradation driven by OA, are of major interest. Intra-articular therapies prevent systemic side effects, and optimise bioavailability and therapeutic efficacy to target cells. However, further optimisation is required to prevent drug clearance, by producing a delivery system providing targeted sustained release of the drug in order to generate a clinical effect.

Targeted intra-articular OA therapies have been historically hindered by the lack of an effective drug delivery system (DDS). Interest in PLGA microspheres as DDS has been substantial since the 1980s (Janssen, Mihov et al. 2014). More specifically, investigating the use of this system to target intra-articular disease processes has been on going since the 1990s. Microspheres taken up by synovial macrophages offer a DDS which not only delivers the drug directly to the target inflammatory cell, but also provides sustained controlled release (Edwards 2011). Many obstacles have impeded the use of microspheres as DDS within the intra-articular environment; such as rapid hydrolysis of the drug by serum nucleases or failure of delivery/entry to the target cell. The following factors influence successful targeted drug delivery; microsphere size, resistance to intra-articular degradation, ability to retain the drug during delivery, sustained release of a therapeutic dose of the drug once at the target cell, and biocompatibility. Microspheres enter target cells through phagocytosis. PLGA microsphere phagocytosis appears to be size dependent; where 1-10μm was found to be optimal for synoviocyte

phagocytosis (Butoescu, Seemayer et al. 2009). PLGA microspheres have excellent biocompatibility, especially when used in horses and are degraded within the cell by both surface and bulk erosion (Bragdon, Bertone et al. 2001, Larsen, Ostergaard et al. 2008). SiRNAs are high molecular weight hydrophilic molecules, unable to enter cells by passive diffusion, and rapidly degradable by nucleases. Consequently they have a short half-life in biological fluids (Khanna, Balgir et al. 2007). Their partnership with PLGA microspheres has been proposed to protect them from nuclease degradation, eliminate the need for a transfection agents, abolish their negatively charged hydrophilic nature preventing entry to the cell, and prolong their half life through sustained release. The arrangement of PLGA molecules around the drugs core due to ionic interactions between the basic amino acids of the siRNA and the terminal carboxylic anions of the PLGA, results in a rigid structure. This produces high encapsulation efficiency when PLGA is combined with a negatively charged drug such as siRNA (Murata, Takashima et al. 2008). The PLGA microsphere successfully releases the siRNA into the cytosol (Jensen, Cun et al. 2010), where the mechanisms for RNA interference are positioned (te Boekhorst, Jensen et al. 2012). There have been some successful reports of the use of siRNA-loaded PLGA microspheres, such as the down-regulation of TNF-α in experimental murine RA (Présumey, Salzano et al. 2012) and OA (Mountziaris, Sing et al. 2011).

There have also been varying reports of success in using siRNA-PLGA nano/microsphere as DDS. One report suggests that carriers such as arginine or polyethylenimine (PEI) promote siRNA encapsulation efficiency to

64.3% and 80%, respectively from 48.6% using only PLGA (Murata, Takashima et al. 2008). These reported capsulation efficiencies are highly incomparable to the efficiencies found using solely PLGA in this study 70%. This previous study also found that both siRNA-PLGA microspheres with and without carriers significantly reduced tumour growth using VEGF-siRNA, with PEI-carriers being slightly more effective (Murata, Takashima et al. 2008). However, these carriers are associated with toxic effects and can delay the release of siRNA (Cun, Jensen et al. 2011).

1.8 Hypotheses and Aims

1.8.1 General Hypotheses

The experimental work described in this thesis aimed to design and test a novel therapy and therapy-delivery system intended to provide a sustained release, anti-cytokine therapy for equine OA. Interactions between the predominant cell populations present during synovitis were examined to help assess the effects of the therapy and therapy-delivery system on synoviocyte and cartilage health. It was hypothesised that an anti-cytokine therapy delivered to target synoviocytes would help prevent cartilage degradation driven by inflammatory stimulation.

1.8.2 Aims

To answer our hypotheses, this thesis aimed to:

- Create a co-culture model to determine equine FLS gene expression profiles following exposure to an inflammatory stimulus and in the presence or absence of macrophages, and determine to what extent IL-1β and NF-κB signalling pathways were involved.
- Optimise the extent of IL-1β gene knockdown in equine FLS and macrophages using an siRNA approach.
- Determine the capacity of equine macrophages to phagocytose biodegradable polymer microspheres.
- Determine the influence of synovitis on cartilage health, and subsequently investigate whether anti-IL-1β siRNA-loaded biodegradable polymer microspheres could effect synoviocyte gene expression and alter the effect of synovitis on cartilage health.

Chapter 2. Materials and Methods

2.1 Cell Culture

2.1.1 Equine Distal Limb Collection, Preparation and Scoring

Equine distal limbs, disarticulated at the middle carpal joint or tarsus, were collected from abattoirs (Nantwich, Cheshire, and Swindon, Wiltshire) and processed within 6-8 hours. Each limb was secured in a table vice, positioning the dorsal aspect of the metacarpo/tarsophalangeal joint (MCPJ/MTPJ) upwards. Skin was removed with a no. 22 scalpel blade, the leg scrubbed with dilute chlorhexidine gluconate (Hibiscrub, Regent Medical Limited, Manchester, UK), and sprayed with surgical spirit. Using sterile gloves, rat-toothed tissue forceps, and a sterile no.10 scalpel blade, subcutaneous tissues overlying the dorsal aspect of the MCPJ/MTPJ were dissected and removed. The joint capsule, collateral ligaments and common digital extensor tendon were transected providing full access to the joint cavity. Gross macroscopic scoring of the MCPJ/MTPJ was recorded, and tissues were harvested from joints scoring 0 – 1 (Table 2.1).

Table 2.1 Macroscopic scoring system to describe gross changes located on the condyles of the equine third metacarpal bone (McIlwraith, Frisbie et al. 2010).

Lesion	Grade	Description
Wear lines	0	None
	1	1 or 2 partial-thickness wear lines/joint surface.
	2	3-5 partial-thickness or 1-2 full-thickness wear lines/joint surface.
	3	>5 partial thickness or >2 full-thickness wear lines/joint surface.
Erosions	0	None
	1	Partial-thickness erosion, <5mm in diameter.
	2	Partial-thickness erosion, >5mm in diameter.
	3	Full-thickness erosion.
Palmar arthrosis (osteochondral lesions distal palmar aspect of metacarpus)	0	None
	1	Partial-thickness erosion, <5mm in diameter.
	2	Partial-thickness erosion, purple discoloration, >5mm in diameter.
	3	Full-thickness erosion, purple discoloration, 5mm in diameter.

2.1.2 Tissue Harvesting

2.1.2.1 Synovial Membrane Harvesting

Synovial membrane from the dorsal and palmar/plantar pouches of the MCPJ/MTPJ was used. The synovial membrane was elevated using fine tissue forceps before being dissected with a no.11 scalpel blade, taking care to avoid the adjacent fibrous joint capsule (Figure 2.1 A and B). Dissected synovial membrane was placed in sterile 1 x phosphate buffered saline (PBS). A number of synovial membrane sections, approximately <5mm^2, were placed in sterile 1 x PBS to be used as synovial membrane explants.

2.1.2.2 Equine Cartilage Explant Harvesting

Under sterile conditions, articular cartilage explants were harvested using fine smooth forceps and a no.10 scalpel blade. Explants were taken from the distal condyles of the third metacarpal bone, taking care not to include the underlying subchondral bone. Explants were approximately 5mm x 10mm, and were immediately placed into sterile PBS.

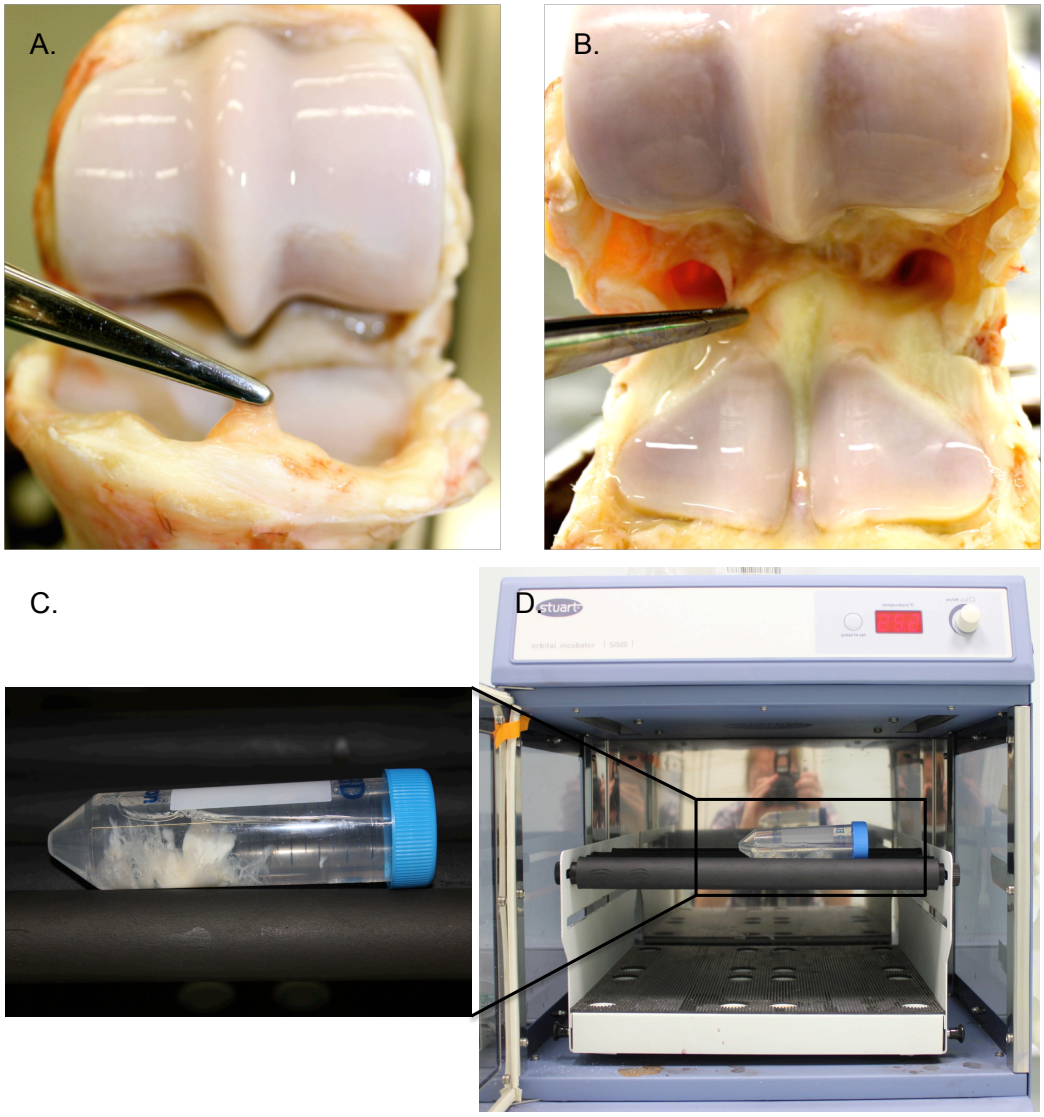

Figure 2.1 Synovial membrane harvesting and digestion. Synovial membrane was dissected from the dorsal (A) and palmar/plantar (B) pouches of the equine metacarpo/tarsophalangeal joints. Synovial membrane was finely diced and digested first in 0.25% (w/v) trypsin/0.1% (w/v) EDTA, and secondly in 2mg/ml collagenase type 2 solutions (C), whilst incubated at 37°C under continuous agitation (D).

2.1.3 Isolation and Culture of Equine Fibroblast-like Synoviocytes

In a cell culture hood, the synovium was finely diced, immersed in 25ml sterile PBS, thoroughly mixed and centrifuged at 453 – 805g for 10 minutes. The PBS was removed without disturbing the synovium pellet, before the process was repeated to wash the tissue. Synovium was then mixed with 12ml 0.25% (w/v) trypsin/0.1% (w/v) ethylenediaminetetraacetic acid (EDTA) in PBS, and agitated at 250rpm at 37°C for one hour. One and a half millilitres of foetal bovine serum (FBS, Gibco, Thermofisher Scientific, Massachusetts, USA) was added to the trypsin/EDTA solution to deactivate it. The contents were thoroughly mixed and centrifuged at 805g for 10 minutes. The trypsin/EDTA solution was discarded and the synovium re-suspended in 10ml sterile 2mg/ml collagenase type 2 (Worthington Biochemicals, Berkshire, UK) in Dulbeccos' Modified Eagle Medium (DMEM, Life Technologies, California, USA) with 10% FBS, 100U/ml penicillin/streptomycin (Penstrep, Life Technologies, California, USA) and 500ng/ml amphotericin B (Life Technologies, California, USA). This media will be referred to as standard culture media. Overnight, the suspension was agitated and incubated at 37°C, at which point the majority of the tissue had been digested (Figure 2.1). The suspension was centrifuged, media discarded and cells re-suspended in standard culture media. The cell suspension was strained through a 70μm cell strainer (SLS, Yorkshire, UK) to remove any remaining tissue. Cells were then washed, suspended in 25ml fresh standard culture media and seeded at approximately 1 x 10^6 cells per cell culture flask (175cm^2). Flasks were incubated at 37°C, in 5% CO_2. Standard culture media was changed every 3 days, and cells were passaged

when 80-90% confluent. Cultures were considered predominantly equine fibroblast-like synoviocytes (EFLS) by passage 3 (Rosengren, Boyle et al. 2007).

2.1.4 Canine Macrophage-Monocyte (DH82) Cell Line Culture

DH82 cells (Sigma-Aldrich, Missouri, USA), a macrophage-monocyte cell line isolated from a dog with malignant histiocytosis, were suspended in 25ml standard culture media and seeded at approximately 1 x 10^6 cells per cell culture flask (175cm^2). They were incubated at 37°C in 5% CO_2. The standard culture media was changed every 3 days, and cells were passaged when 80-90% confluent.

2.1.5 DH82 and EFLS Passage

Used standard culture media was discarded before the cell layer was gently washed twice with PBS to remove any traces of FBS. Cells were then covered with 0.05% trypsin-EDTA (Lonza, Slough, UK), 5ml for a 175cm^2 cell culture flask, and incubated at 37°C in 5% CO_2. After 5-10 minutes, the flasks were vigorously agitated before an equal volume of standard culture media containing FBS was added to the suspension to deactivate the trypsin. The cell suspension was centrifuged at 290g for 4 minutes, and the cell pellet re-suspended in fresh standard culture media. Cells were seeded at 1 x 10^6 cells in 25ml standard culture media in a 175cm^2 cell culture flask.

2.1.6 Equine Venous Blood Collection

Equine venous blood was collected from inpatients at the University of Liverpool's Philip Leverhulme Equine Hospital (PLEH) and from an abattoir (Swindon, Wiltshire). The University of Liverpool Veterinary Research Ethics Committee granted ethical approval (VREC91) based on the following stipulations. Excess blood collection from PLEH inpatients only occurred if the owner had given informed consent, the horse had an intravenous catheter *in situ*, blood was being collected for diagnostic or therapeutic reasons, the horse was free from systemic illness, the horse was over 6 months old, or if the horse was euthanised under general anaesthesia and used for blood bank purposes. Blood was collected in lithium heparin vacutainer tubes. At the abattoir blood was free caught at the time of exsanguination. Half a litre was collected in a glass-jar containing 100ml acid-citrate dextrose solution (7.35g glucose, 2.2g sodium citrate and 730mg citric acid). The blood and acid-citrate dextrose solution were thoroughly mixed and processed within 24 hours.

2.1.7 Density Gradient Separation to Isolate Equine Mononuclear Cells

A solution of polysucrose (57g/L) and sodium diatrizoate (90g/L) adjusted to an approximate density of 1.077g/ml (Histopaque-1077, Sigma-Aldrich, Missouri, USA) was used to isolate mononuclear cells from equine blood. PBS and Histopaque-1077 were used at room temperature. In a cell culture hood, the blood was thoroughly re-mixed following separation into blood cell and plasma layers during transit. Blood was distributed between Falcon 50ml

conical centrifuge tubes, and spun at 1200g for 15 minutes at room temperature, with no brake. Whole blood separates into 3 distinct fractions (bottom to top); the darkly coloured red blood cell layer, a white layer lying on top of this called the buffy coat containing white blood cells and platelets, and the plasma layer above this (Figure 2.2A). The buffy coat was removed from all tubes using a glass pipette, without disturbing the red blood cell layer, and combined. Twenty-five millilitres buffy coat was diluted with 25ml PBS, and half of the suspension was carefully layered onto 15ml Histopaque-1077 in a falcon 50ml conical centrifuge tube; this was repeated in duplicate (Figure 2.2B). Tubes were centrifuged at 1811g for 25 minutes with the brake off. The density gradient media separated the buffy coat into 3 layers (bottom to top); any red blood cells that were contaminating the buffy coat, a white cloudy mononuclear cell layer, and a clear layer of histopaque (Figure 2.2C). Using a pipette, the mononuclear cell layer was transferred into a clean 50ml centrifuge tube and diluted with PBS (50ml total). Tubes were centrifuged at 600g for 15 minutes at 4°C with the brake on. The supernatant was discarded and the white cell pellet re-suspend in fresh PBS. The tubes were centrifuged at 400g with the brake on. The supernatant was discarded and the cells were re-suspended in a known volume of fresh culture media. Cells were then counted using a haemocytometer. Cells were either cultured (see below), or frozen at -80°C in RPMI-1640 culture media with 20% FBS, containing 10% dimethyl sulfoxide (DMSO, Sigma-Aldrich, Missouri, USA). These cells were known as equine peripheral blood mononuclear cells (EPBMCs).

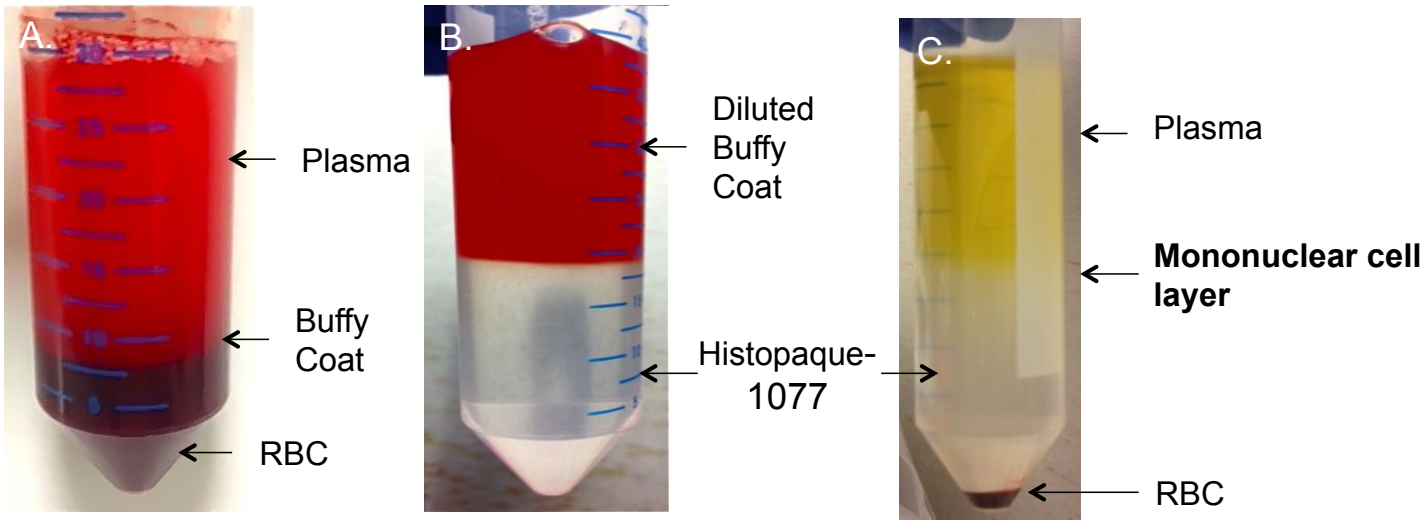

Figure 2.2 Density gradient separation of equine blood to isolate equine mononuclear cells. (A) Equine whole blood mixed with acid-citrate dextrose solution, the red blood cells (RBC) were in the process of settling at the bottom of the centrifuge tube. (B) Once the whole blood was centrifuged, the buffy coat was removed, diluted with PBS and layered onto Histopaque-1077. This sample had a large degree of RBC contamination which was unusual. (C) The buffy coat and Histopaque-1077 are centrifuged for 25 minutes to isolate the mononuclear cell layer.

2.1.8 Equine Peripheral Blood Mononuclear Cell Culture

EPBMCs were seeded in 24-well cell culture plates at 5 x 10^4 cells per well in 1ml RPMI-1640 medium with L-alanyl-L-glutamine (RPMI 1640 Medium, GlutaMAX™ Supplement, Life Technologies, California, USA). This was supplemented with 10% horse serum (New Zealand origin, Life Technologies, California, USA), 100U/ml penicillin/streptomycin (Penstrep, Life Technologies, California, USA), 500ng/ml amphotericin B (Life Technologies, California, USA) and 50ng/ml recombinant human granulocyte-macrophage colony stimulating factor (rhGMCSF 300-03, Peprotech, New Jersey, USA). This media will be referred to as standard EPBMC culture media. Half of the standard EPBMC culture media (500µl) was replenished every 3 days, to avoid wasting non-adherent cells. Within 7 days to 2 weeks cells adhered to the cell culture plate.

2.1.9 Stimulating a Cellular Inflammatory Response *In Vitro*

To stimulate a cellular response *in vitro* comparable to that found in an inflammatory environment *in vivo*, 10µg/ml LPS from *Escherichia coli* (026:B6) (Sigma-Aldrich, Missouri, USA) was added to culture media. The addition of LPS represented day 0 in all experiments.

2.2 Cell Labelling and Analysis

2.2.1 Fluorescent Labelling of EFLS Cells

Cell Proliferation Dye eFluor® 670 (eBioscience Inc., San Diego, USA) is a fluorescent dye which binds to all cellular proteins containing primary amines. The dye is detectable in cells for up to 6 cells divisions. This fluorescent dye was used to label EFLS. The dye was dissolved at a concentration of 5mM in anhydrous DMSO, aliquoted for storage at -20°C and protected from light. A suspension of EFLS cells at double the desired cell number/ml were washed twice with PBS to remove any serum present, and re-suspended in PBS. To optimise the concentration of dye required to produce maximum fluorescence, six different dye concentrations were trialled; 10, 9, 8, 7, 6 and 5μM. All concentrations produced very similar fluorescence intensities, however the 8μM dye solution produced optimum labelling. An equal volume of the 8μM dye solution was mixed with the cell suspension, and vortexed thoroughly. It was incubated for 10 minutes at 37°C in the dark. Approximately four to five times the final volume of cold complete standard culture media was added, and the cells were incubated on ice to stop the labelling process. Cells were washed three times with standard culture media (at room temperature) and cultured as normal.

2.2.2 Lentiviral-Mediated Generation of GFP Expressing DH82 Cells

A multiplicity of infection (MOI) optimisation experiment determined the ideal number of particles required to produce effective transfection; for example a MOI of 1 represents 40,000 lentiviral particles used to transfect 40,000 cells. DH82 cells were seeded into 24-well plates at a density of 2.1 x 10^4/cm^2 in 1ml standard culture media. Each well received 1µl of sterile filtered 8mg/ml hexadimethrine bromide 1000x (Sigma-Aldrich, Missouri, USA), which was then mixed thoroughly, taking care not to spill contents. Lentiviral particles expressing a constitutively active green fluorescent protein gene (CMV promoter) and a puromycin resistance cassette (Sigma, Missouri, USA) were added to the DH82 cells at MOI 0.5, 1, 2 and 4. Wells were incubated at 37°C for 24 hours, after which the standard culture media was replaced with fresh standard culture media and transfection was assessed using fluorescent microscopy. Standard culture media was replenished every 3-4 days and wells were incubated for a further 10 days. Cells successfully transfected with the GFP-expressing plasmid were selected using 2µg/ml puromycin (Life Technologies, California, USA) for ten days with standard culture media changes every three days. Following selection it was evident that wells using a MOI of 0.5 and 1 had not been effectively transfected with the GFP-expressing lentivirus. Wells containing cells exposed to an MOI of 2 and 4 were 70-80% confluent, and were 90-100% GFP positive. These cells were passaged, expanded in cell culture flasks and frozen for later use.

2.2.3 Fluorescence-Activated Cell Sorting

To determine the proportion of each cell population within a mixed co-culture, EFLS labelled with the cell proliferation dye eFluor® 670 or DH82 cells expressing GFP were analysed using a BD Accuri C6 Flow Cytometer (BD-Biosciences, New Jersey, USA). The Cell Proliferation Dye eFluor® 670 has a peak excitation of 647nm, excited by the red laser line (633nm), and a peak emission wavelength of 670nm which is detected using a 675/25 interference filter. GFP has a peak emission wavelength of 507nm and is detected by a 533/30nm interference filter. Peak emission wavelengths of these fluorophores were sufficiently different to ensure no overlap in detection between the interference filters occurred (Figure 2.3). Fluorescence-Activated Cell Sorting (FACS) analysis was performed by the BD Accuri^{Tm} C6 Analysis Software 1.0.264.21.

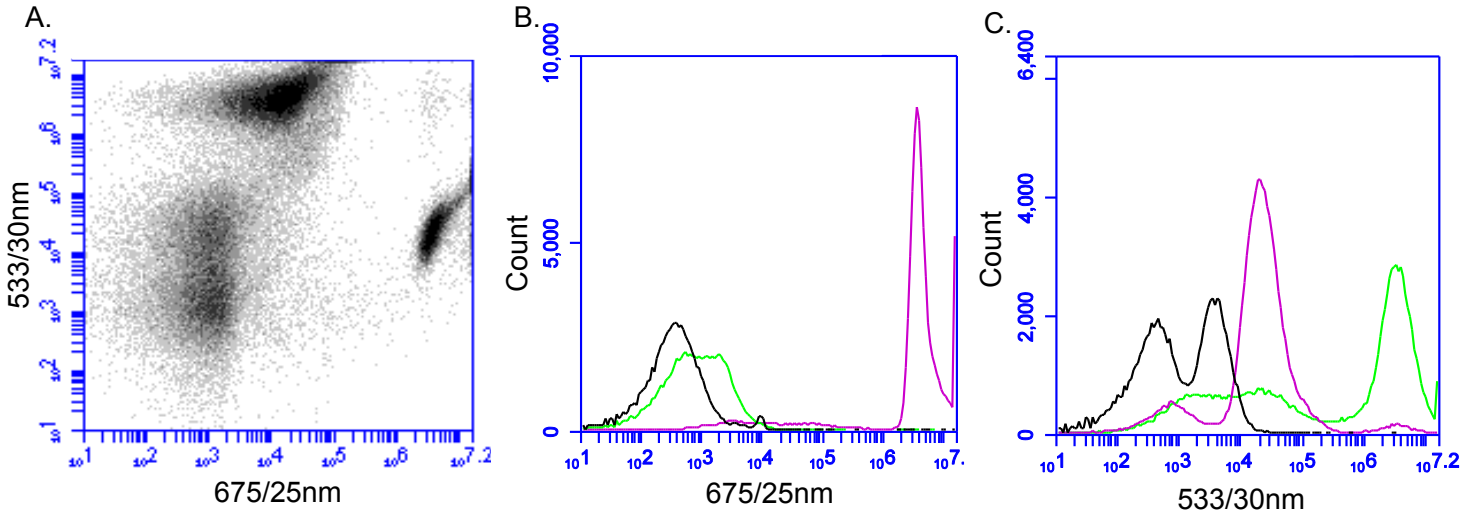

Figure 2.3 FACS analysis demonstrates two separate fluorophores present within a mixed culture of DH82 and EFLS cells. (A) Density plot graph displaying two discernable plots, consistent with the two fluorophores used. The plot with maximum fluorescence intensity detected by the 533/30nm and 675/25nm interference filter represents the GFP-DH82 cells and efluor-labelled EFLS respectively. The third, less dense area, represents background fluorescence. (B) Peak fluorescence intensity detected by the 675/25nm filter is consistent with efluor-labelled EFLS (purple line). The GFP-DH82 cells (green line) and unlabelled EFLS cells (black line) only emit fluorescence at a wavelength consistent with background fluorescence, as detected by this filter. (C) Peak fluorescence intensity detected by the 533/30nm filter is consistent with GFP-DH82 cells (green line). The efluor-labelled EFLS (purple line) and unlabelled EFLS (black line) only emit fluorescence at a wavelength consistent with background fluorescence, as detected by this filter.

2.3 Short Interfering RNA Transfection

Short interfering RNA (siRNA) duplexes and transfection reagents were purchased from Life Technologies (California, USA); Silencer Cyanine (Cy3) labelled negative control siRNA (Life technologies, California, USA), and Silencer Select Custom Designed siRNA to target certain cytokines. SiRNA was reconstituted to 100μM (100pmol/μl) concentration using nuclease-free water, then aliquoted and frozen at -20°C as stock solution.

Cells were transfected in 6-well plates once they had reached 60-80% confluence. For each well, 9μl lipofectamine RNAiMAX reagent was mixed with 150μl Opti-MEM medium. A working stock solution of 10μM siRNA (10pmol/μl) was made for immediate use; 3μl was mixed with 150μl Opti-MEM. The diluted siRNA suspension was then added to the diluted lipofectamine RNAiMAX solution (at a 1:1 ratio), mixed thoroughly and incubated for 5 minutes at 37°C. SiRNA-lipid solution (250μl) containing a final quantity of 25pmol siRNA and 7.5μl lipofectamine, was added to the well, and contents were thoroughly mixed. Cells were exposed to the siRNA-lipid complex for 6-12 hours, before it was removed and cells were replenished with fresh culture media.

The ability of each synthetic siRNA sequence, to silence the target gene was measured through gene expression analysis via qRT-PCR, and protein expression analysis via western blotting.

2.4 ELISA Analysis

2.4.1 Equine IL-1β ELISA

An equine IL-1β ELISA kit (Bethyl Laboratories, Texas, USA) was used to measure the IL-1β protein concentration within culture media. A standard curve was produced using recombinant equine IL-1β ranging from 3.125 – 200ng/ml as a standard. Media sample or standard of 100µl were added, in duplicate, to a 96-well microplate, coated with anti-equine IL-1β capture antibody. The plate was sealed and incubated for 2 hours at room temperature. All contents were discarded and the plate washed four times, before blotting thoroughly to remove waste fluid. Detection antibody was then added, 100µl per well, to all wells before sealing and incubating the plate for one hour at room temperature. Contents were once again discarded and washing steps repeated preceding the addition of 100µl horseradish peroxidase (HRP) solution to each well. The plate was sealed and incubated for 30 minutes at room temperature. Contents were once again discarded and washing steps repeated preceding the addition of 100µl tetramethylbenizidine (TMB) substrate to each well. The plate was incubated for 30 minutes in the dark at room temperature, before the addition of 100µl of stop solution to each well. The plate was agitated and absorbance's immediately read at a wavelength of 450nm (Figure 2.4).

2.4.2 Equine TNF-α ELISA

An equine TNF-α ELISA kit (R&D Systems, Minneapolis, USA) was used to measure the TNF-α protein concentration within culture media. A standard curve was produced using 31.3 - 2000pg/ml recombinant equine TNF-α. The goat anti-equine TNF-α capture antibody was diluted with PBS; 100µl per well was used to coat a 96-well microplate before sealing and incubating the plate overnight. The plate was washed twice with wash buffer (0.05% Tween® 20 in PBS, pH 7.2-7.4) before blocking the plates with 300µl per well of reagent diluent (1% bovine serum albumin (BSA) in PBS, pH 7.2-7.4, 0.2um filtered) for 1 hour. The contents of all wells were aspirated and the wells were washed twice, before 100µl media sample and standard were added, in triplicate, into individual wells of the 96-well microplate previously coated with anti-equine TNF-α capture antibody. The microplate was sealed and incubated for 2 hours at room temperature. The plate was aspirated and washed as previously described before detection antibody was added at 100µl per well, to all wells before sealing and incubating the plate for two hours at room temperature. Contents of all wells were then aspirated and the plate washed twice with wash buffer before 100µl diluted streptavidin-HRP was added to all wells, the plate sealed and incubated in darkness at room temperature for 20 minutes. Wells were once again aspirated and washed before 100µl substrate solution (1:1 mixture of H_2O_2 and TMB) was added to each well. The plate was sealed, incubated in darkness at room temperature for 20 minutes before 50µl stop solution ($2NH_2SO_4$) was added to each well. After ensuring the contents were thoroughly mixed, absorbances were read spectrophotometrically at a wavelength of 450nm (Figure 2.4).

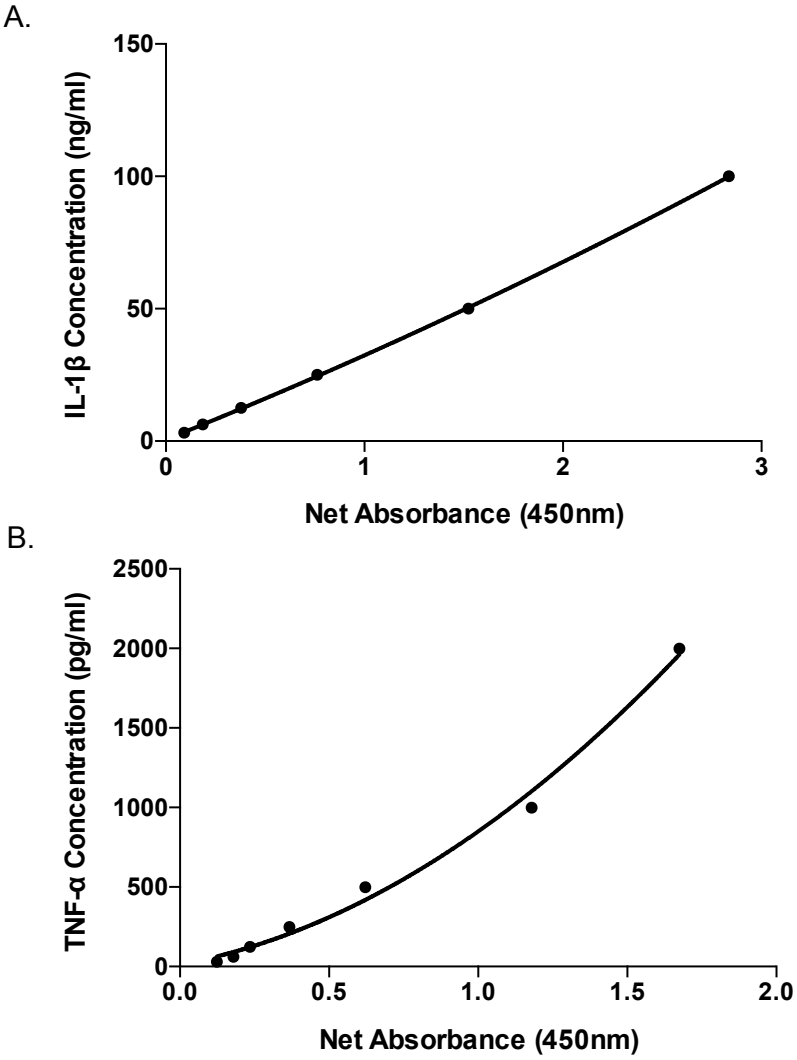

Figure 2.4 Typical ELISA standard curve for extracellular equine (A) IL-1β and (B) TNF-α protein quantification in culture media. Concentrations of recombinant equine (A) IL-1β and (B) TNF-α ranging from 3.125 – 200ng/ml and 31.3 - 2000pg/ml respectively, were used as known standard concentrations, in duplicate and triplicate respectively. Absorbance was read spectrophotometrically at a wavelength of 450nm. Lines of best fit, in both cases a polynomial curve, were applied to the readings.

2.5 Glycosaminoglycan Assay

Sulphated glycosaminoglycan (sGAG) concentrations within culture media were measured using the 1-9 dimethylmethylene blue (DMMB) assay (Farndale, Buttle et al. 1986). DMMB is a thiazine chromotrope agent which, when bound to sGAG, induces metachromasia which causes a change in its absorption spectrum. Samples were diluted 10-fold using nuclease-free water and 40µl of each sample was added, in duplicate, to wells of a flat-bottomed transparent 96-well plate. DMMB dye (16mg 1-9 dimethylmethylene blue, 2g sodium formate, 2ml formic acid, 1L water, pH 3.5) was added to each well at 200µl per well. Absorbance was immediately measured spectrophotometrically at a wavelength of 570nm, and unknown sGAG concentrations were calculated using a standard curve. Standard concentrations ranging from 0-70µg/ml were made using chondroitin sulphate (shark cartilage, C-4384, Sigma-Aldrich, Missouri, USA) dissolved in ultrapure water using a stock solution of 5mg/ml (Figure 2.5).

A.

Standard Concentration (µg/ml)	Stock solution (µl)	H_2O (µl)
0	0	1000
10	2	998
20	4	996
30	6	994
40	8	992
50	10	990
60	12	988
70	14	986

B.

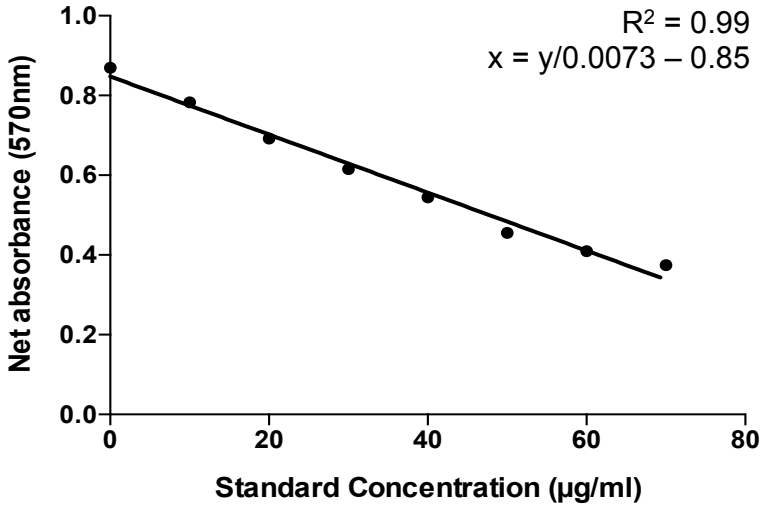

Figure 2.5 Constituents of the standard concentrations (A), and typical standard curve (B) used for the GAG Assay. (A) Table displaying relative volumes of chondroitin sulphate stock solution (5mg/ ml) and water combined to produce known standard concentrations ranging from 0-70µg/ml. (B) Standard curve using absorbance measurements for standard concentrations. A linear line of best fit was used to calculate unknown GAG concentrations.

2.6 Intra- and Extracellular Protein Analysis Through Western Blotting

2.6.1 Sample Collection and Processing

Intracellular proteins were analysed within cell lysates, and extracellular proteins within cell culture media. For cell lysate protein extraction, the media was removed and the cell layers were gently washed with PBS before 200µl Novex tris-glycine sodium dodecyl sulfate (SDS) sample buffer 1X (Life Technologies, California, USA) was added to each well of a 6-well plate and the cell layer was detached using a cell scraper. Samples were sonicated (10Hz, 50% power) on ice three times for 10 seconds, a process that was repeated three times with >1 minute intervals for each sample. Following sonication, samples were then centrifuged at 20817g at 4°C for 10 minutes. The supernatant was transferred to a clean microcentrifuge tube, taking care not to disturb the pellet of cell debris. Samples were stored at -20°C.

2.6.2 Pierce^{Tm} 660 Protein Assay

This colorimetric assay spectrophotometrically measures absorbance at a wavelength of 660nm, allowing the quantitation of total protein within a sample. The protein assay reagent is a dye-metal complex in an acidic buffer. At an acidic pH, the dye undergoes deprotonation becoming negatively charged and binding to positively charged amino acids. These protein-binding interactions aid in a stable colour change, due to deprotonation of the dye, from a reddish-brown to green. A series of known BSA dilutions (0-2000µg/ml) were produced from a BSA stock solution

(2mg/ml), and were assayed and measured alongside unknown samples, providing a standard curve of absorbance and protein concentrations, with which to reference unknown protein concentrations (Figure 2.6). Protein sample and protein standards (10µl) were entered, in duplicate, into a transparent flat-bottomed 96-well plate. The Pierce^{Tm} 660 protein assay is compatible with most detergents and reducing agents. However, the concentration of SDS in the cell lysate samples (>0.0125%) required the addition of an ionic detergent compatibility reagent (IDCR, Life Technologies, California, USA) to treat the protein assay reagent prior to use. One gram of IDCR was diluted in 20ml of the Pierce^{Tm} 660 protein assay reagent before performing the assay. Each well received 150µl of protein assay reagent (Thermo Fisher Scientific, Maryland, USA), with or without the IDCR depending on the samples assayed. The plate was covered, agitated for 1 minute and incubated at room temperature for 5 minutes. Absorbance was immediately measured by a plate reader at a wavelength of 660nm.

A.

Vial	Final BSA concentration (µg/ml)	BSA (µl)	Diluent (µl)
A	2000	300 stock solution	0
B	1500	375 stock solution	125
C	1000	325 stock solution	325
D	750	175 of vial B	175
E	500	325 of vial C	325
F	250	325 of vial E	325
G	125	325 of vial F	325
H	25	100 of vial G	400
I	0	0	400

B.

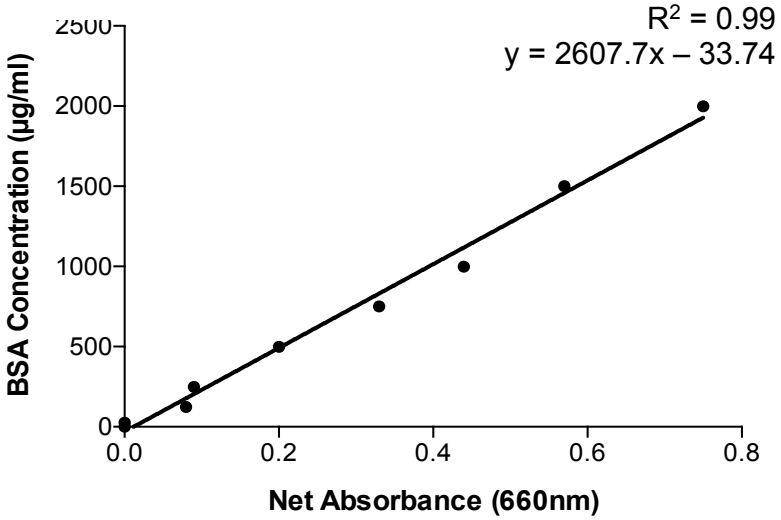

Figure 2.6 Constituents of the standard concentrations (A), and standard curve (B) used for the Pierce 660 Protein Assay. (A) Table displaying relative volumes of BSA stock solution (2mg/ml) and water combined to produce known standard concentrations ranging from 0-2000µg/ml. (B) Standard curve using absorbance measurements for standard concentrations. A linear line of best fit was used to calculate unknown protein concentrations.

2.6.3 Deglycosylation of aggrecan in media with Chondroitinase ABC

The anti-aggrecan ARG antibody (BC-3) recognises the N-terminal neoepitope of aggrecan formed through aggrecanase cleavage between amino acids Glu^{373}-Ala^{374} within the interglobular domain. The antibody is specific for aggrecanase cleaved (ARG) neoepitopes and will not bind to ARG sequences within the intact aggrecan protein core. Media samples were treated with proteinase inhibitors 1 tablet/10ml media (Complete ULTRA tablets, EDTA-free, Roche, Basel, Switzerland) to remove soluble degradation products of varying lengths from protein breakdown, which would contaminate the protein preparation. Media samples were mixed with a solution containing 250mM Tris HCl and 300mM Sodium Acetate Buffer with 0.05% (w/v) BSA, ph 8.0, with chondroitinase ABC (from proteus vulgaris; c2905, Sigma-Aldrich, Missouri, USA) at 0.001U chABC/10µg sGAG, and incubated at 37°C overnight. This de-glycosylates the samples for optimal neoepitope recognition by the antibody.

2.6.4 Extraction of Protein from Cell Media using Protein-Resin Binding

StrataClean^{Tm} Resin was used to concentrate protein secreted into cell culture media. The protein concentration of each sample was determined using the Pierce^{Tm} 660 Protein Assay; the volume of sample containing the desired protein content (40µg) was transferred to a new eppendorph tube. Ten µl StrataClean^{Tm} Resin was added to each sample, vortexed and centrifuged at 805g for 1 minute. The silica-based solid phase resin binds to

proteins through its hydroxyl groups. The supernatant above the resin pellet was discarded, and the pellet washed with 1ml double distilled water (DDH_2O). The vortex and centrifuge stages were repeated, the supernatant removed and the pellet re-suspend in 15µl diluted (1X) Novex tris-glycine SDS sample buffer (Life Technologies, California, USA).

2.6.5 Sodium Dodecyl Sulfate Polyacrylamide Gel Electrophoresis (SDS PAGE)

Samples of equal protein content (40µg) were prepared as described above and suspended in 15µl diluted (1X) Novex tris-glycine SDS sample buffer (Life Technologies, California, USA). Samples were reduced by adding 1µl 2-mercaptoethanol (Sigma-Aldrich, Missouri, USA) to each, following which they were mixed thoroughly by vortexing and then the proteins denatured by heating at 100°C for 5 minutes.

A NuPAGE 4-12% Bis-Tris Gel cassette (Novex Life Technologies, California, USA), was rinsed with water, before the spacer comb and adhesive strip protecting the exposed gel, were removed. The gel cassette was locked in place within the gel tank, by a gel tension wedge. Running buffer (1x) (NuPAGE MES SDS Running Buffer, Novex Life Technologies, California, USA) filled the upper and lower buffer chambers of the gel tank, ensuring exposed gel at the top and bottom of the gel cassette were covered. Ten µl Novex Sharp Pre-Stained Protein Standard (Life Technologies, California, USA) was loaded into the first well in the gel cassette, to allow identification of molecular weight in unknown samples. The

samples were centrifuged and 15µl of each sample (total amount) was loaded individually into their assigned well using loose gel tips. The gel tank lid was fixed into position, ensuring that the connections were correctly aligned, and connected to an electrical power source (Powerpac 300, Biorad, Hertfordshire, UK). The SDS detergent attaches to the proteins, resulting in a negative charge proportional to the protein size being produced. Once electrophoresis begins, the proteins migrate through the gel towards the positive cathode. Larger proteins will move more slowly through the polyacrylamide gel. For cell lysate samples, the gel was subjected to 100V for approximately 10 minutes, then 150V for approximately 50 minutes, or until the samples had moved sufficiently distal to separate proteins of different molecular weights, without allowing them to contact the exposed gel strip. Cell culture media samples were subjected to 200V for 50 minutes.

2.6.6 Western Blotting

Once electrophoresis was complete the gel was removed from its plastic cassette and laid against a similarly sized piece of nitrocellulose transfer membrane which had been pre-soaked in NuPAGE Transfer Buffer (Novex Life Technologies, California, USA). The gel/membrane were sandwiched between pieces of filter paper which had also been pre-soaked with Transfer Buffer. Care was taken to remove any bubbles between the gel and nitrocellulose transfer membrane, as these inhibit protein transfer. This was then packed into an X-Cell II blot module (Invitrogen, California, USA) amongst foam pads (which had also been pre-soaked in Transfer Buffer) with the nitrocellulose membrane positioned closest to the anode. The tank

was filled with NuPAGE Transfer Buffer (Novex Life Technologies, California, USA), and the unit connected to an electrical power source (Powerpac 300, Biorad, Hertfordshire, UK). The module was subjected to 35V for 90 minutes, after which the nitrocellulose membrane was carefully removed. The side which had been in contact with the gel, was placed upwards in a tray filled with a blocking buffer appropriate for the antibody of intended use. The blocking buffers used within this thesis were non-fat milk blocking buffers (see Table 2.2), prepared with 1g or 2g non-fat milk powder diluted in 100ml (1x) tris-buffered saline (TBS) respectively. The membrane submerged in blocking buffer was agitated at room temperature for 1 hour.

2.6.7 Antibody Detection

TBS stock solution (10x) was prepared using a 0.2M trizma base (Sigma-Aldrich, Missouri, USA) and 1.37M sodium chloride (NaCl) solution; pH 7.6. TBS working solution (1x) was prepared using 50ml TBS (10x) mixed with 450ml ultrapure water, and in a second batch, 500µl Tween® (Sigma-Aldrich, Missouri, USA) was added to make TBS (1x) with 0.1% Tween®. As previously stated, nitrocellulose transfer membranes were submerged in an appropriate blocking buffer, depending on the specific protein of interest and antibody used (see Table 2.2). The primary antibody was then added to the blocking buffer at the recommended concentration, making sure it was thoroughly diluted, and the membrane was incubated overnight at 4°C under gentle agitation. The following day, the membrane was washed four times with; TBS (1x), TBS (1x) with 0.1% Tween® (twice) and TBS (1x), each wash lasting 5 minutes. The membrane was then incubated for 1 hour at

room temperature, in a suitable blocking buffer containing the secondary HRP-conjugated antibody at an appropriate concentration (see Table 2.2). The four-step washing process was repeated before the membrane was exposed to a 1:1 combination of Oxidising Reagent Plus and Enhanced Luminal Reagent Plus (Western Lightening-Plus ECL Enhanced chemiluminescence substrate, Perkin Elmer, Massachusetts, USA) for one minute under gentle agitation. Excess fluid was blotted from the membrane before it was placed in a plastic cover, with the protein ladder situated on the left hand side. Membranes were exposed to chemiluminescence using a UVP ChemiDoc-it imaging system. Trial images were taken and exposure time adjusted as required to produce optimal band intensity. Images were assessed and modified using VisionWorksLS image acquisition and analysis software. Images were superimposed using Microsoft Powerpoint, to enable the molecular weight ladder to be observed on the same blot as the bands.

2.6.8 Stripping of Blots and Reprobing with Loading Control Antibody

Control antibodies were used on membranes analysing intracellular proteins extracted from cell lysates. The primary antibody was stripped from the membrane by immersing it in stripping buffer (7.6g/L Tris hydrochloric adid (HCl), 7ml 2-mercaptoethanol, 2-g/l SDS, pH 6.7) for 30 minutes at 50°C under gentle agitation. After repeated washing (3x) of the membrane in TBS (1x) with 0.1% Tween®, the membrane was incubated in 2% (w/v) milk blocking buffer for 1 hour at room temperature. It was re-probed with an HRP-conjugated glyceraldehyde-3-phosphate dehydrogenase (GAPDH)

antibody, and incubated at 4°C overnight under gentle agitation. The four-wash procedure was carried out, and the membrane was exposed to the 1:1 combination of Oxidising Reagent Plus and Enhanced Luminal Reagent Plus and imaged as detailed above.

Table 2.2 Primary and secondary antibody concentrations used in western blot.

Primary Antibody	Manufacturer (Cat. No.)	Conc.	Blocking buffer	Secondary Antibody	Manufacturer (Cat. no.)	Conc.
Aggrecan interglobular doman (IGD) aggrecanase site-specific neoepitope monoclonal (BC-3)	Kind gift from Prof. B Caterson, Cardiff University.	1:200	1% non-fat milk blocking buffer	Anti-mouse IgG-peroxidase monoclonal	Sigma-Aldrich (A4416)	1:2000
Sheep anti-mouse ADAMTS5 monoclonal	Kind gift from Prof. A Fosang, Melbourne, AUS.	1:500	2% non-fat milk blocking buffer	Anti-goat/sheep IgG-peroxidase conjugated monoclonal	Sigma-Aldrich (A9452)	1:1000
Equine IL-1 beta/IL-1F2 monoclonal (Clone 424823)	R&D Systems (MAB3340)	1:500	2% non-fat milk blocking buffer	Anti-rat IgG peroxidase conjugated monoclonal	Sigma-Aidrich (A9037)	1:1000
Anti-GAPDH peroxidase monoclonal	Sigma-Aldrich (G9295)	1:5000	2% non-fat milk blocking buffer			

2.7 Gene Expression Analysis Through qRT-PCR

2.7.1 The Design, Validation and Testing of Species-Specific Primers

The mRNA sequences associated with the equine and canine genes listed in table 2.3 alongside their gene accession numbers, were acquired from the NCBI Genebank database. Equine and canine mRNA sequences were directly compared for similarity through the NCBI BLAST facility (http://blast.ncbi.nlm.nih.gov/Blast.cgi). Species-specific primers were designed using Primer Express 2.0 (Applied Biosystems, California, USA) against non conserved sequences.

Equine and canine primers were validated using serial doubling dilutions (0 = undiluted, (1) 1:2 dilution, (2) 1:4 dilution, (3) 1:8 dilution, (4) 1:16 dilution, (5) 1:32 dilution) of EFLS and DH82 cDNA respectively, from cells that had been cultured individually and exposed to 10µg/ml LPS (Figures 2.7 and 2.8).

Table 2.3 Equine and Canine primers.

***Equus Caballus* Primers**

Gene	Gene Accession No.	Sequence	R	Effici-ency
GAPDH	NM_001163856.1	F:TGACCCCCTAACATATTGAGAGTCT R: GCCCCTCCCCTTCTTCCTG	1	108%
IL-1β	NM_001082526.1	F: GAGCCCAATCTTCAACATCTATGG R: ATACCAAGTCCTTTTACCAAGCCTG	0.99	91%
IL-6	NM_001082496.1	F: CCTGGTGATGGCTACTGCTTTC R: GGATGTACTTAATGTGCTGTTTGGTT	0.99	92%
ADAMTS4	NM_001111299.1	F: CAGCCTGGCTCCTTCAAAAA R: ATGTGGTCACTATTCCTGCGG	0.99	106%
ADAMTS5	XM_003364218.2	F: ACCGATCCTGCAGTGTCACA R: AAATCTTTTCGCCATGAGCAG	1	101%
MMP3	NM_001082495.1	F: TCTTGCCGGTCAGCTTCATATAT R: CCTATGGAAGGTGACTCCATGTG	0.99	97%
MMP13	NM_001081804.1	F: CTGGAGCTGGGCACCTACTG R: ATTTGCCTGAGTCATTATGAACAAGAT		>90%

***Canis Lupus* Primers**

Gene	Gene Accession No.	Sequence	R	Effici-ency
GAPDH	NM_001003142.1	F: AACTGCTTGGCTCCTCTAGCC R: CCACGATGCCGAAGTGGT	0.99	123%
IL-1β	NM_001037971.1	F: CTATCATCTGCAAAACAGATGCG R: GCATGGCTGCATCACTCATAAA	1	94%
IL-6	NM_001003301.1	F: CCTGGTGATGGCTACTGCTTTC R: TGGCATCATCCTTGGAATCTC	1	95%

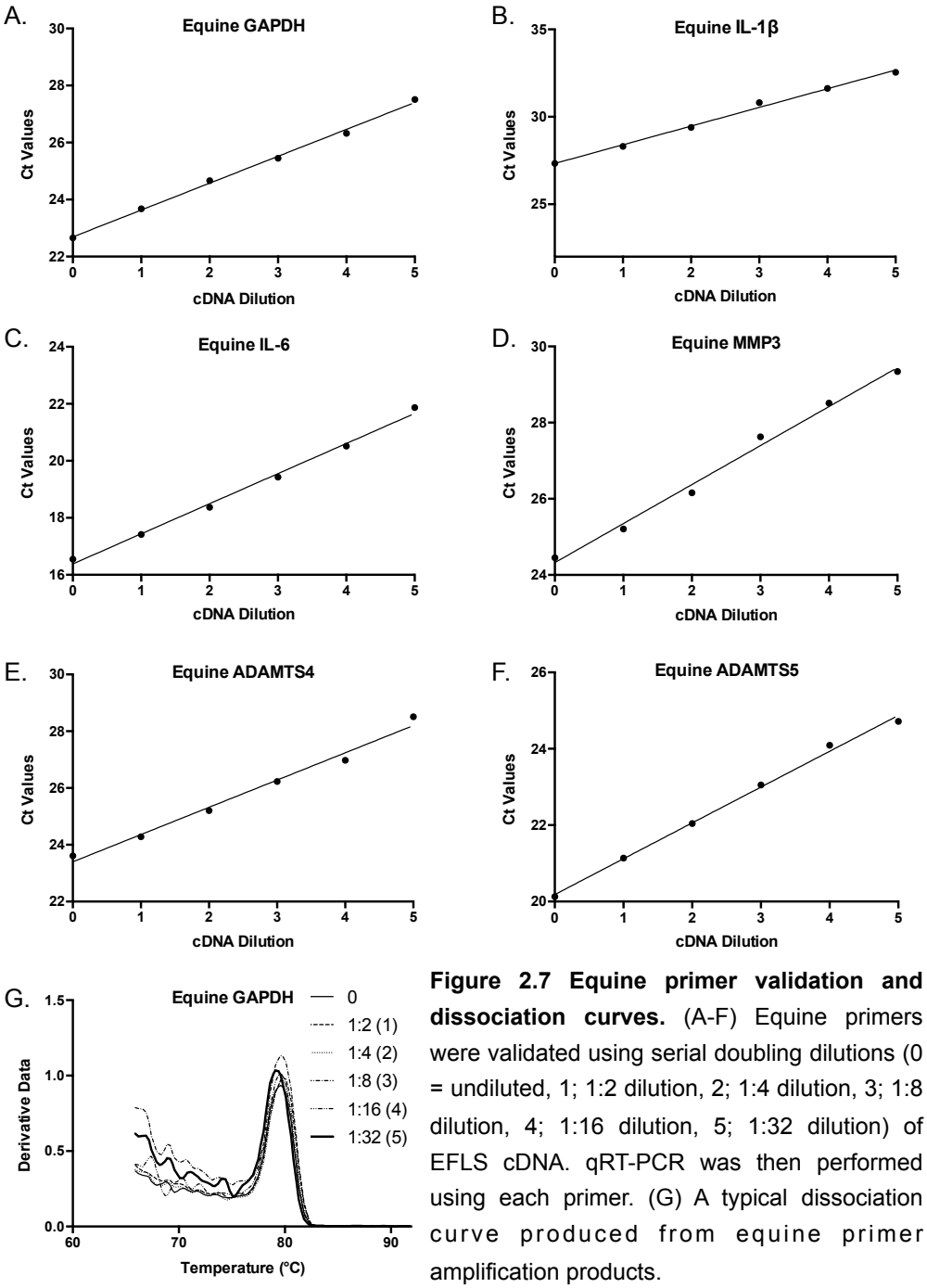

Figure 2.7 Equine primer validation and dissociation curves. (A-F) Equine primers were validated using serial doubling dilutions (0 = undiluted, 1; 1:2 dilution, 2; 1:4 dilution, 3; 1:8 dilution, 4; 1:16 dilution, 5; 1:32 dilution) of EFLS cDNA. qRT-PCR was then performed using each primer. (G) A typical dissociation curve produced from equine primer amplification products.

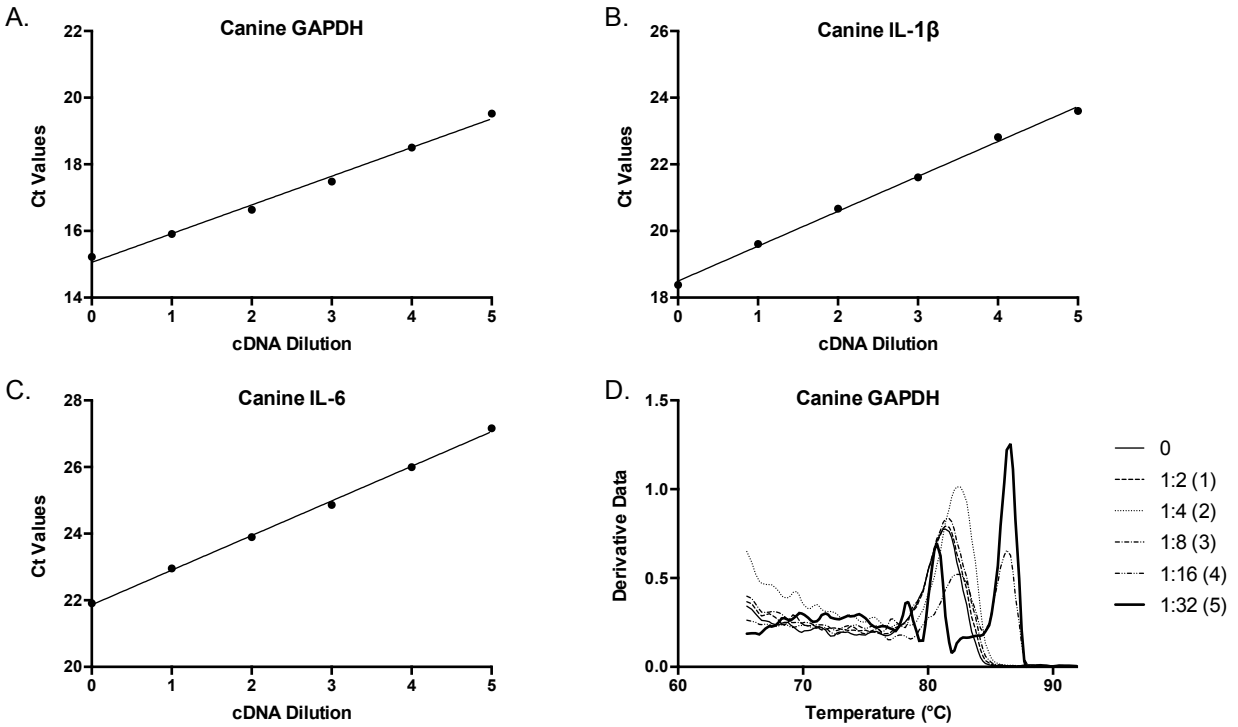

Figure 2.8 Canine primer validation and dissociation curves. (A-C**)** Canine primers were validated using serial doubling dilutions (0 = undiluted, 1; 1:2 dilution, 2; 1:4 dilution, 3; 1:8 dilution, 4; 1:16 dilution, 5; 1:32 dilution) of DH82 cDNA. qRT-PCR was then performed using each primer. (D) A typical dissociation curve produced from canine primer amplification products.

2.7.2 RNA Extraction

For each well of a 6 well plate culture media was transferred to a 1.5ml centrifuge tube for storage at -20°C, and then 1ml Tri-reagent (Ambion, Warrington, UK) was added to the cell layers. Cells were exposed to the Tri-reagent for 1-2 minutes before being pipetted vigorously to ensure complete homogenisation. Suspensions were transferred to RNAse-free centrifuge tubes and stored at -80°C. The guanidinium-thiocyanate-phenol-chloroform technique (Chomczynski and Sacchi 1987) with ethanol was used to extract RNA from Tri Reagent lysates. Each sample had 100µl chloroform (Sigma-Aldrich, Missouri, USA) added to it, and samples were thoroughly mixed. Samples were rested for 5 minutes, allowing the suspension to separate into a pink-coloured bottom layer and a clear upper layer. Samples were then centrifuged at 20817g for 15 minutes at 4°C. This process separates the suspension further into three distinct layers; the bottom pink-coloured layer contains protein, the white layer overlying this contains DNA, and the clear layer above these contains RNA. The upper clear aqueous layer was transferred to a new centrifuge tube, taking care not to disturb the other layers. The aqueous layer, approximately 400µl, was mixed with an equal volume of 2-propanol (Sigma-Aldrich, Missouri, USA) to precipitate the RNA and the suspension was centrifuged at 20817g, for 10 minutes at 4°C. The suspension was discarded and the centrifuge tube carefully blotted to remove as much of the 2-propanol-chloroform mixture as possible, taking care not to disturb the RNA pellet. The pellet was then washed with 1ml 70% ethanol (prepared using diethylpyrocarbonate(DEPC)-water). Samples were centrifuged again at 20817g for 5 minutes before the 70% ethanol solution

was discarded, the tube blotted and the samples allowed to air dry for 20 minutes. The RNA pellet was then dissolved in 20µl 0.1% DEPC-water and stored at -80°C.

2.7.3 Reverse Transcription

The RNA content of each sample was quantified using a Nanodrop ND-100 spectrophotometer (Labtech, East Sussex, UK). One µl (0.5µg) random hexadeoxynucleotides (Random Primers, Promega, Wisconsin, USA) were added to 1µg RNA of each sample. 0.1% DEPC-water was also added to the samples to equalise sample volumes to 13.4µl. Samples were then subjected to 70°C heat for 5 minutes, to uncoil the RNA secondary structure. Samples were immediately rested on ice for >1 minute. A volume containing 100µM nucleotide triphosphates (dNTP mix, Promega, Wisconsin, USA) which includes 25µM of each dATP, dCTP, dGTP, and dUTP, was combined with 200U moloney-murine leukaemis virus (M-MLV) reverse transcriptase (200U/µl), 5µl M-MLV reverse transcriptase 5x reaction buffer (50mM Tris-HCl, 75mM potassium chloride (KCl), 3mM magnesium chloride ($MgCl_2$) and 10mM Dithiothreitol (DTT)), and 24U rRNasin Plus ribonuclease inhibitor (40U/µl) (Promega, Wisconsin, USA). This mixture was added to each 13.4µl sample to result in a total volume of 25µl. Complementary DNA was then synthesised under standard reverse transcription conditions.

2.7.4 Quantitative Real-Time Polymerase Chain Reaction

Quantitative real-time polymerase chain reaction (qRT-PCR) was performed using 160ng cDNA in a total volume of 20µl containing SYBR Green master mix (GoTaq qPCR Master Mix, Promega, WI, USA) at 1X, 300µM forward primer and 300µM reverse primer. Reactions were performed on a ABI 7300 Real Time PCR system (Applied Biosystems, California, USA), under the following standard amplification conditions; 2 minutes at 50°C, 10 minutes at 95°C, followed by 40 cycles of 15 seconds at 95°C and 1 minute at 60°C. Using the Sequence Detection Systems (SDS) software system (Applied Biosystems, California, USA), PCR products were quantified using the number of thermal cycles (Ct) required for each PCR product to produce the amount of fluorescence needed to reach a defined threshold. The relative quantification of each gene normalised to the GAPDH reference gene was calculated using the $2^{-\Delta Ct}$ method (Livak and Schmittgen 2001).

2.8 Poly Lactic-co-Glycolic Acid Microspheres

PLGA microspheres were created by Dr Rui Chen and Professor John Hunt, at the Centre for Materials and Structures within the Institute of Ageing and Chronic Disease, University of Liverpool, using the technique outlined below,

2.8.1 Emulsion Solvent Evaporation Technique; Water-in-Oil-in-Water (W1/O/W2)

PLGA microspheres were constructed from the biodegradable polymers; lactide and glycolide. The emulsion solvent evaporation technique; water-in-oil-in-water (W1/O/W2) method was used to create the PLGA microspheres (Chen, Curran et al. 2006). The polymeric coat material (PLGA) is dissolved in a volatile organic solvent; dichloromethane. Fluorescein isothiocyanate-dextran or equine anti-IL-1β siRNA were dissolved in pure water and added to the polymer solution as an inner-water phase (10%w/w). The water in oil emulsion (W1/O) was prepared with a micro-homogenizer in a 25ml flask at 20W for 30 seconds at 4°C. The prepared emulsion was then added to 100ml 1% polyvinyl alcohol (PVA) solution. The emulsion was stirred at 1000rpm for 30 minutes to obtain the water-in-oil-in-water emulsion (W1/O/W2). This was added to 100ml 0.1% PVA solution to prevent coagulation, and to evaporate the solvent (dichloromethane). Microspheres were suspended in 0.1M PBS (pH 7.4) at 10mg/ml for use in cell culture experiments, and frozen at -20°C.

2.9 Histology

2.9.1 Tissue Explant Preparation

Synovial explants, which had been cultured with fluorescein isothiocyanate-dextran-loaded microspheres, were embedded in Tissue-TEK OCT (Sakura Finetek, CA, USA) on a cork disc. A plastic vessel containing 2-propanol (Isopentane, Sigma-Aldrich, Missouri, USA) floating above liquid nitrogen within a dewer, was used to snap freeze the explants. Both embedded synovial explants and cartilage explants were immersed within the 2-propanol for approximately 30 seconds, before being transferred to a labelled conical falcon tube or eppendorph tube and frozen at -80°C. Synovial explants were sectioned using a cryostat (Leica CM 1900). Sections 10μm thick were adhered to glass slides, dried, and labelled. Sections were stored at -20°C. Synovial sections were incubated with 4',6-diamidino-2-phenylindole (DAPI) (1:1000 diluted in PBS) (Invitrogen, Massachusetts, USA) and mounted under coverslips using Vecatshield mounting media (Vector laboratories, California, USA).

2.9.2 Cartilage Explant Preparation and Sectioning

Cartilage explants were fixed in 4% neutral buffered paraformaldehyde (PFA) for 48 hours, before being immersed in 70% ethanol. Explants were embedded in paraffin wax, cut into 10μm sections and mounted onto glass slides.

2.9.3 Osteochondral Wedge Biopsy Preparation

Osteochondral wedge biopsies were fixed in 4% neutral buffered PFA for at least 24 hours. Samples were then de-calcified in 7.4% EDTA for one month. Water within the sample was first replaced with alcohol by dehydrating the samples; the tissue was passed through increasing concentrations of ethyl alcohol (0 to 100%). The alcohol was then replaced by xylene, which is miscible with paraffin wax, in the clearing step. Finally, the tissue was impregnated with, and embedded in, paraffin wax. Explants were cut into 10µm sections using a microtome, and mounted onto glass slides.

2.9.4 Tissue Staining and Histological Scoring

All histological cartilage, synovial membrane and osteochondral sections were stained with either Haematoxylin and Eosin (H&E), or celestine blue, 0.5% fast green and 1% Safranin-O stains. Sections were visualised using a Nikon Eclipse 80i microscope, and images were acquired using a Nikon DS-L2 standalone control unit. Cartilage explant sections were scored using a modified version of the cartilage histopathologic scoring system (McIlwraith, Frisbie et al. 2010). Osteochondral sections and synovial sections were scored using unmodified scoring systems (McIlwraith, Frisbie et al. 2010). Sections were scored twice by two users blinded to section identity. Inter- and intra- variability was assessed using Cohen' kappa coefficient (Cohen 1960). Cartilage explant depth was measured at three different locations on each explant, using lines drawn perpendicular to the long axis of the explant.

2.9.5 Cell Mounting and Staining

Cells (EFLS, DH82 or EPBMCs) were cultured on sterile poly-l-lysine (Sigma-Aldrich, Missouri, USA) coated glass coverslips within 6-well plates, and non-adherent cells were cyto-spun onto glass slides.

2.9.5.1 Adherent Cells

Glass coverslips were soaked in 70% ethanol, placed into wells of a 6-well tissue culture plate and allowed to air dry within a cell culture hood. Coverslips were then covered with 400µl 0.01% poly-l-lysine solution (Sigma-Aldrich, Missouri, USA) and incubated at room temperature for 15 minutes. Excess poly-l-lysine was removed and wells air dried within a cell culture hood. Adherent cells on coverslips were gently washed with PBS before being fixed with 500µl 4% PFA. Plates were incubated at room temperature for 20 minutes. Coverslips were then washed twice with PBS and once with wash buffer (0.1% BSA in PBS) before being air dried within a cell culture hood. Vectashield mounting medium containing DAPI was dispersed over the coverslip which was then mounted onto a slide. Coverslips were permanently sealed around the perimeter with nail polish.

2.9.5.2 Non-adherent Cells

Non-adherent cells and culture media were transferred to 1.5ml eppendorphs, spun in a microfuge at 20817g for 30 seconds, and the supernatant discarded. Cells were fixed in a solution containing 250µl PBS and 250µl 4% paraformaldehyde, and incubated for 20 minutes at room temperature. Cells were then washed twice with PBS and once with wash

buffer (0.1% BSA in PBS) before finally being re-suspended in 50µl PBS. A volume of cell suspension, 25µl, was transferred onto each slide. Slides were placed at the bottom of whatmann paper-lined centrifuge buckets. Slides were spun at 1811g for 2 minutes and allowed to air dry. Vectashield mounting medium containing DAPI (Vector laboratories, California, USA) was dispersed over the cells and covered with a coverslip. Coverslips were permanently sealed around the perimeter with nail polish.

2.9.6 Fluorescence Microscopy

Cells and tissue sections were imaged using a three channel confocal microscope (Zeiss LSM510 Meta Confocal microscope, Axioplan 2 stand); the fluorescein isothiocyanate-dextran microspheres were imaged using the Cy3-fluorescein isothiocyanate (FITC) filter (488-532nm), and the DAPI stained nuclear material with the blue filter (364nm).

Chapter 3.

Testing Short-Interfering RNA Mediated Gene Silencing and Biodegradable Polymer Microspheres As Delivery Vehicles on Equine Synoviocytes

3.1 Introduction

Synovial inflammation, or synovitis, has been reported to play a major role in both the structural and symptomatic progression of osteoarthritis (OA). Whether it predisposes the joint to OA or is a secondary result of OA is so far unknown. It is characterised by an increase in catabolic cytokines such as TNF−α and IL-1β, both of which are produced by FLS and synovial macrophages.

A joint capsule surrounds every diarthrodial joint. It consists of 3 layers and the synovial membrane (intima) is the innermost layer overlying the subsynovium. This membrane is one to four FLS thick and acts as a macromolecular sieve (Caron 2011) allowing molecules, such as glucose, oxygen, carbon dioxide, and small proteins, to move from plasma into the synovial fluid (Frisbie 2012), whereas larger components of synovial fluid are directly secreted by FLS into the joint (Yielding, Tomkins et al. 1957, Jay, Britt et al. 2000). When the synovial membrane becomes inflamed, this highly regulated process is compromised. Changes to synovial fluid protein content, cell numbers and subsequent fluid consistency occur. Two major cell populations reside within the synovial membrane: FLS and synovial macrophages. Characterisation of each population has determined these populations to be mutually exclusive (Edwards 1994) although some reports

suggest the presence of an intermediate cell population (Caron 2011). Resident synovial macrophages are produced by precursors within the synovial membrane, whereas infiltrating mononuclear cells present in the synovium during synovitis originate from bone marrow (Edwards 1994). FLS produce collagen, hyaluronan, lubricin and various cytokines including TNF-α and IL-1β. Resident synovial macrophages, which comprise between 10 - 20% of the synoviocyte population, carry out phagocytosis, and also produce cytokines, eicosanoids (PGE_2) and proteinases (Caron 2011). They are the chief producers of both TNF-α and IL-1β, and expression of these cytokines increases in all degrees of equine OA (Kamm, Nixon et al. 2010).

TNF-α and IL-1β, play a substantial role in the pathogenesis of OA (Sellam and Berenbaum 2010). Alongside other cytokines, such as IL-6 and IL-18, they stimulate the NF-κB and MAPK intracellular signalling pathways, which in turn cause an increase in the transcription of several different MMPs, cycloxygenase (COX-2) and inducible nitric oxide (Kamm, Nixon et al. 2010). These cause joint pain and inflammation. IL-1β can also stimulate an increase in aggrecanases which cause cartilage matrix destruction through proteolysis (Kamm, Nixon et al. 2010).

Synovitis has many causes including bacterial infection and systemic autoimmune inflammatory disorders. However, the condition referred to in this thesis, is synovitis triggered by an initial trauma to the joint. Events predisposing the joint to OA and/or synovitis are comparable. Much like the chicken and egg argument, whether innate immunity responses from synoviocytes cause deleterious effects on articular cartilage, or primary cartilage damage releases matrix fragments and pro-inflammatory mediators,

stimulating an inflammatory response by synoviocytes, is yet to be determined. Initial trauma could reflect an acute episode of excessive force, or frequent episodes of recurrent low-grade excessive force experienced by the joint. Alternatively, it can arise from normal forces exerted on an abnormal joint; be it through incorrect conformation or developmental orthopaedic disease resulting in disproportionate forces experienced by the joint, or from defects in joint tissue integrity. Whichever way synovitis is initiated, it has the potential to progress to OA. Synovial inflammation is characterised by a mononuclear cell infiltration of neutrophils, T lymphocytes and monocytes; as well as vascularisation and hyperplasia of the synovium (Sutton, Clutterbuck et al. 2009). In osteoarthritis, acute synovitis may be one of the first changes to occur during which synovial tissue has been shown to over-express inflammatory mediators such as pro-inflammatory cytokines (Benito, Veale et al. 2005); especially IL-1β and TNF-α (Todhunter, Kincaid et al. 1996). Reducing the action of IL-1β and TNF-α has been shown to be therapeutically beneficial for inflammatory joint disease in humans.

RNA interference (RNAi) facilitates manipulation of target gene expression, resulting in post-transcriptional gene silencing (PTGS). Double stranded synthetic siRNA molecules are between 20-25 nucleotide base pairs long, and are incorporated into a RISC once inside the cell. The siRNA sense strand is released from the complex, and the anti-sense strand binds to complementary mRNA. Cleavage of mRNA at this site inhibits its translation to a protein, effectively silencing the gene. However, *in vivo* delivery of this molecule to the target cell is problematic. Optimal PTGS requires (1) siRNA

protection from nuclease degradation, (2) an efficient method of siRNA transportation into the cells cytoplasm (siRNA duplex is negatively charged and can therefore not move across the cell membrane), and (3) sustained siRNA release from the delivery vehicle, at an appropriate dose to ensure an effective therapeutic response. The delivery vehicle must also be biodegradable, non-toxic and able to be loaded with an siRNA concentration sufficient to permit sustained release over the required period.

Interest in PLGA microspheres as drug delivery systems has been substantial since the 1980s (Janssen, Mihov et al. 2014). More specifically, investigating the use of this system to target intra-articular disease processes has been on-going since the 1990s. It has previously been proved that the DH82 cell line (a canine macrophage-like cell line) can phagocytose PLGA microspheres (Wasserman, Diese et al. 2012). Unpublished data from our laboratory has demonstrated the effective use of PLGA (65:35 lactide: glycolic acid) microspheres for the delivery of siRNA molecules to DH82 cells. PLGA microspheres were shown to encapsulate siRNA with 70% efficiency and this was uniformly distributed throughout a <20μm microsphere. Degradation of the microsphere occurred over 6 weeks, releasing the siRNA in a controlled manner, resulting in 30-40% remaining in the microsphere at 6 weeks. IL-1β and TNF-α siRNA-loaded microspheres were successfully phagocytosed by DH82 cells. When challenged with LPS, a decrease in the release of IL-1β and TNF-α, as analysed by ELISA assays, occurred at 8 days and 2 weeks of culture.

Building on our laboratory's findings, this chapter describes a series of investigations into RNAi of catabolic cytokines produced by equine fibroblast-like synoviocyte (EFLS) and equine peripheral blood mononuclear cells (EPBMC), using siRNA and siRNA-loaded PLGA microspheres.

3.1.1 Aims

- Determine EFLS and EPBMC gene expression profiles following exposure to an inflammatory stimulus.
- Optimise the extent of IL-1β gene knockdown in EFLS and EPBMC using an siRNA approach.
- Determine the capacity of EPBMCs to phagocytose PLGA microspheres.
- Determine the *in vitro* effectiveness of siRNA-loaded microspheres on reducing synoviocyte IL-1β gene expression.

3.2 Study Design

An overview of the experimental design can be found in Schema 3.1.

3.2.1 Synoviocyte Gene Expression in Response to Inflammatory Stimulation

EFLS and EPBMCs were isolated from equine synovium and peripheral equine venous blood respectively, as described in Chapter 2 Materials and Methods, section 2.1.

3.2.1.1 LPS Concentration Optimisation

The responses of EFLS (n=3) and EPBMCs (n=3) to LPS (*Escherichia coli* 026:B6, Sigma-Aldrich, Missouri, USA) exposure were tested using 0-100µg/ml and 0-10µg/ml LPS respectively. EFLS were seeded in 6-well plates at 3.3 x 10^5 cells per well in 2ml standard culture media. Once cells had adhered, media was replaced with fresh media containing either 0, 0.1, 0.5, 1, 5, 10, 50 or 100µg/ml LPS. EPBMCs were seeded in 96-well plates at 7 x 10^4 cells per well in 300µl standard EPBMC culture media. Once adhered, media was removed and replaced with fresh media containing 0, 0.1, 1 or 10µg/ml LPS. In each case cells were exposed to LPS for 24 hours. EFLS were harvested in tri-reagent and underwent RNA extraction, reverse transcription and qRT-PCR. Cytokine mRNA levels were normalised to GAPDH, and calculated using the $2^{-\Delta Ct}$ method (Livak and Schmittgen 2001) (Figure 3.2). EPBMC culture media was analysed for secreted TNF−α and IL-1β protein concentrations using TNF−α and IL-1β ELISA assays

respectively (Figure 3.3). A curve of best fit was positioned among the optical density readings produced by the standards (of known concentrations) for both equine IL-1β and TNF−α assays, yielding a linear regression equation from which unknown sample IL-1β and TNF−α protein concentrations could be deduced respectively.

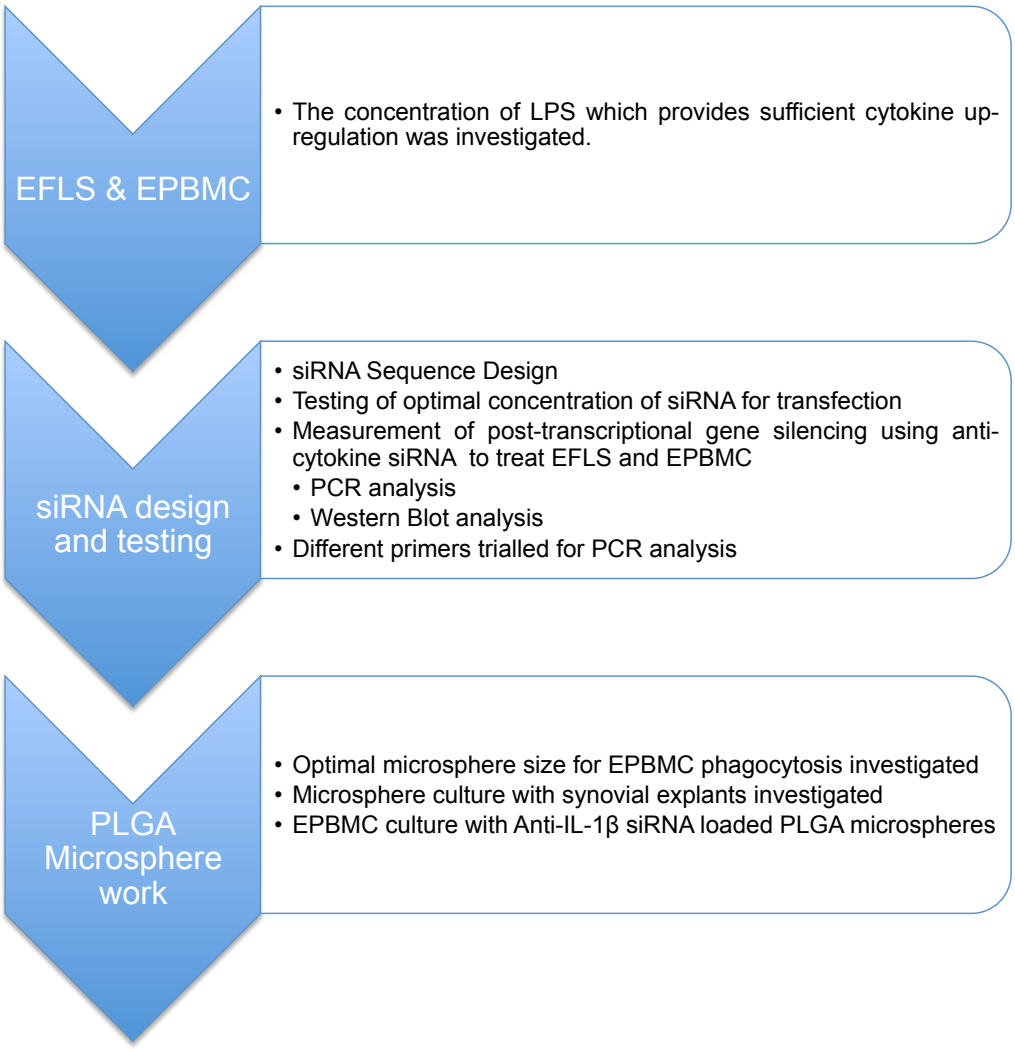

Schema 3.1 Experimental strategy for work within Chapter 3. An overview of order of experimental investigations included in Chapter 3.

3.2.2 RNA Interference Optimisation

3.2.2.1 Short Interfering RNA Sequence Design

As described in Chapter 2 Materials and Methods, section 2.7, equine IL-1β and TNF−α mRNA sequences were acquired from the NCBI Genbank database. Custom made synthetic siRNA duplexes were designed by Ambion (Life technologies, California, USA) to complement these mRNA sequences (Table 3.1). BLAST searches were performed on all siRNA sequences to determine their compatibility with the equine genome, and to detect any compatibility to non-target genes.

Gene	siRNA sequence (‘5 to 3’)	
Equine anti-IL-1β (1)	*Sense*	CGACAUUUGUAACAUAUUAtt
	Antisense	UAAUAUGUUACAAAUGUCGat
Equine anti-IL-1β (2)	*Sense*	Sequence not disclosed in the interest of intellectual property protection
	Antisense	
Equine anti-TNF−α (1)	*Sense*	GCAUGAUCCGAGAUGUGGAtt
	Antisense	UCCACAUCUCGGAUCAUGCtt
Equine anti-TNF−α (2)	*Sense*	GGAUGUCUGGUACAUGGAAtt
	Antisense	UUCCAUGUACCAGACAUCCta

Table 3.1 SiRNA sequences used to target equine IL-1β and TNF-α mRNA sequences. The antisense strand anneals to the complementary fragment of the target mRNA sequence.

3.2.2.2 Determining what Concentration of SiRNA will Produce Optimal Post-Transfection Intracellular SiRNA Levels

Initial optimisation experiments were conducted to ensure maximal intracellular post-transfection siRNA levels. EPBMCs (n=4 horses, 2 bioloigcal replicates) were seeded in 96-well plates at 7 x 10^4 cells per well in 300µl standard EPBMC culture media. Cells were incubated overnight and allowed to adhere. Cells were then transfected with 0, 0.2 or 1pmol/µl silencer Cy3 labelled negative control siRNA (Life technologies, California, USA). To create the transfection reagents, 2µl Lipofectamine 2000 (Thermo Fisher Scientific, California, USA) reagent was diluted in 50µl serum free OPTI-MEM medium (Life Technologies, California, USA). Separately, Cy3 labelled negative control siRNA (Life technologies, California, USA) was diluted at either 0.2pmol/µl or 1pmol/µl in OPTI-MEM media. The lipofectamine and siRNA dilutions were combined at a 1:1 ratio, and incubated for 25 minutes to allow the formation of siRNA-lipid complexes. Cell culture media was replenished with standard EPBMC culture media and the siRNA-lipid complexes added. An equivalent volume of OPTI-MEM was added to wells which did not receive siRNA-lipid complexes. Four hours later, wells were analysed microscopically using the FITC filter, as the fluorescein derivative Cy3 has a peak excitation and emission at wavelengths of 547nm and 563nm respectively. The percentages of fluorescent cells were calculated in four different areas of each well, and the average value used to determine the optimum siRNA concentration to be used during transfection.

3.2.2.3 Measurement of Post-Transcriptional Gene Silencing Produced by SiRNA

Gene and protein levels of target cytokines, from both EFLS and EPBMCs, were analysed. The majority of experiments compared the effects of custom designed anti-cytokine siRNA (Ambion, Thermofisher Scientific, UK) to that of control cells transfected with silencer select negative control no.1 siRNA (Ambion, Thermofisher Scientific, UK), and all cells were stimulated with 10µg/ml LPS. Messenger RNA expression and extracellular secreted protein levels were analysed through qRT-PCR, and western blot and ELISA assays of culture media, respectively.

3.2.2.4 The Effects of Anti-cytokine SiRNA on Extracellular Secreted Protein

EPBMCs (n=3 horses) and EFLS (n=3 horses) were seeded separately into 96-well plates in 300µl standard EPBMC culture media, and standard culture media respectively, and cultured until 80% confluent. Cells were either transfected with 1pmol/µl silencer select negative control no.1 siRNA (Ambion, Thermofisher Scientific, UK), anti-IL-1β (1) or anti-IL-1β (2) siRNA, or anti-TNF−α (1) or anti-TNF−α (2) siRNA (Ambion, Thermofisher Scientific, UK). Lipofectamine-siRNA complexes were diluted in OPTI-MEM before being added to wells for 6 hours. Culture media was then replenished with normal media containing 10µg/ml LPS for 12 hours. Media was stored at -20°C before being analysed using an equine IL-1β and TNF−α ELISA assay.

3.2.2.5 EFLS IL-1β mRNA Interference by Anti-IL-1β (2) SiRNA

EFLS (n=3 horses, 2 biological replicates) were seeded in 12 well plates at 1.5 x 10^5 cells per well in 1ml standard culture media and incubated overnight. When cells were 80% confluent, media was replaced with serum-free standard culture media. Cells were transfected with 1pmol/µl siRNA in 8µl lipofectamine 2000 reagent for 6 hours. Cells were either transfected with silencer select negative control no.1 siRNA or anti-IL-1β (2) siRNA. Media was then exchanged for serum-free standard culture media containing 10µg/ml LPS. Cells were incubated for 3 hours before being harvested. Media was stored at -20°C. Cells layers were exposed to 0.5ml Tri-reagent (Sigma-Aldrich, Missouri, USA) for two minutes before cell lysates were thoroughly pipetted and collected.

3.2.2.6 EFLS IL-1β Gene Expression After Treatment with Anti-IL-1β SiRNA

Cell lysates underwent RNA extraction using the Guanidinium-thiocyanate-phenol-chloroform technique (Chomczynski and Sacchi 1987), reverse transcription, and qRT-PCR using two different equine IL-1β primers. Equine IL-1β gene expression was normalised to GAPDH.

Two equine IL-1β primer pairs were used to analyse post-siRNA IL-1β mRNA expression. The first pair was designed to anneal to sequences towards the 5' end of reverse transcribed IL-1β cDNA, whilst the second pair annealed towards the 3' end. Figure 3.1. shows the relative complementary primer positions on the IL-1β mRNA sequence in comparison to the anti-IL-1β siRNA antisense strand binding site.

A.

	Forward	Reverse
Primer 1	5'-GCAGTACCCGACACCAGTGA-3'	5'-TTTGGGCCATCCTCCTCA-3'
Primer 2	5'-GAGCCCAATCTTCAACATCTATGG-3'	5'-ATACCAAGTCCTTTTACCAAGCCTG-3'

B.

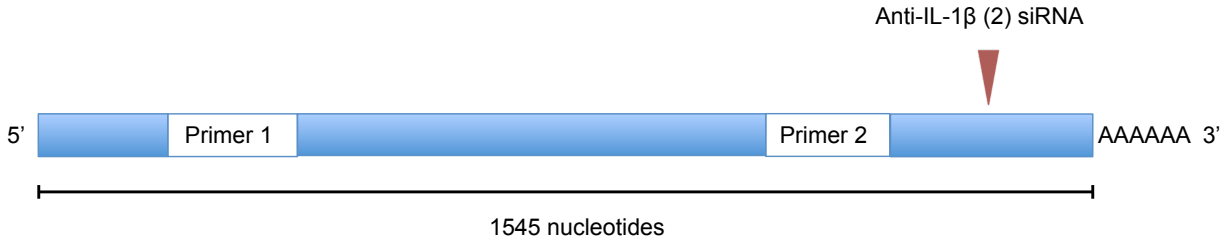

Figure 3.1 Locations of primer and siRNA complementary binding sites on the Equine IL-1β mRNA sequence.
(A) Two equine IL-1β primer sequences. (B) The relative locations of primer and siRNA binding sites on the equine IL-1β mRNA sequence.

3.2.2.7 Western Blot Analysis of Protein Secreted by Anti-IL-1β EFLS

Protein concentrations within culture media samples were measured using the Pierce^{Tm} 660 protein assay kit. Protein was then extracted from the culture media using StrataClean resin (Agilent, California, USA) and re-suspended in 20µl of (1X) Novex tris-glycine sodium dodecyl sulfate (SDS) sample buffer (Life Technologies, California, USA). Each sample was loaded onto a 4-12% Bis-tris gel and proteins were separated under reducing conditions using electrophoresis. Proteins were transferred to a nitrocellulose membrane, which was stained with ponseau stain to test for the presence of protein. Membranes were probed with equine IL-1beta/IL-1F2 MAb (Clone 424823) 1:500 (R&D Systems, Minnesota, USA) and anti-rat peroxidase conjugated anti-immunoglobulin antibody 1:1000 (Sigma-Aldrich, Missouri, USA). Membranes were exposed to chemiluminescence using a UVP ChemiDoc-it imaging system.

A Pierce^{Tm} 660 protein assay was performed on three samples at three points; (1) media post-incubation with StrataClean resin, (2) SDS supernatant post-boiling, (3) resin-SDS suspension loaded into the gel.

3.2.3 Phagocytosis of PLGA Microspheres

3.2.3.1 Investigating the Optimal Microsphere Size for EPBMC Phagocytosis

EPBMCs (n=2 horses, 2 biological replicates) were seeded onto poly-l-lysine coated glass coverslips at 3 x 10^6 cells per well of a 6-well tissue culture plate, and in 2ml standard EPBMC culture media. Cells were cultured for one week; 1ml standard EPBMC culture media was replenished every 3 days. Small (2-6μm diameter) or medium (6-20μm diameter) fluorescein isothiocyanate-dextran microspheres were added to the media at 1mg/ml in 0.1M PBS (pH 7.4), and cultured for a further week. Again, 1ml standard EPBMC culture media was replenished every 3 days, taking care not to disturb the cells or microspheres.

Non-adherent EPBMCs were cyto-spun onto glass slides, and all slides and coverslips were processed, and permanently sealed to enable imaging. Cells were imaged using a three channel confocal microscope (Zeiss LSM510 Meta Confocal microscope, Axioplan 2 stand); the fluorescein isothiocyanate-dextran microspheres were imaged using the Cy3-FITC filter (488-532nm), and the DAPI stained nuclear material with the blue filter (364nm).

3.2.3.2 Culture of Microspheres with Synovial Explants

Synovial explants, approximately 5mm^2 were cultured in 6 well-plates, in 2ml standard culture media containing 1mg/ml fluorescein isothiocyanate-dextran microspheres (2-100µm diameter). Explants were incubated with the microspheres for 3 days before being washed with PBS three times. Explants were processed for cryosectioning. Sections 10-30µm thick were stained with DAPI and imaged using a three channel confocal microscope (Zeiss LSM510 Meta Confocal microscope, Axioplan 2 stand).

3.2.4 RNA Interference of EPBMC Gene Expression using Anti-IL-1β-siRNA Loaded PLGA Microspheres

EPBMCs (n=2 horses, 2 biological replicates) were seeded in 24-well plates at 1 x 10^5 cells per well in 500µl standard EPBMC culture media. Cells were cultured for 7 days during which 50% of the media was replenished every 3 days. One pmol/µl of either anti-IL-1β microspheres or anti-IL-1β siRNA was added to the media bathing the cells. The microspheres were incubated with the EPBMCs for 48 hours prior to LPS (10µg/ml) exposure. EPBMC were transfected with anti-IL-1β siRNA for 6 hours before exposure to LPS (10µg/ml). Cells were harvested in tri-reagent at 4 and 8 days post-LPS exposure. Half the media was replenished every 3 days. EPBMC IL-1β mRNA expression was analysed through RT-qPCR.

3.2.5 Statistical Analysis

A minitab general linear model was used to perform comparisons between EFLS mRNA levels produced by different concentrations of LPS. Paired two-tailed t tests were used to investigate the EPBMC transfection efficiency using fluorescent siRNA between paired groups, and to investigate EFLS IL-1β gene expression when treated with anti-IL-1β (2) siRNA. One-tailed t tests with bonferroni post hoc corrections were used to investigate the difference in secreted protein concentrations of EPBMCs and EFLS when transfected with anti-cytokine siRNA

3.3 Results

3.3.1 Synoviocyte response to LPS Stimulation

3.3.1.1 EFLS mRNA Expression in Response to LPS Exposure

EFLS IL-1β and TNF−α mRNA expressions in response to LPS concentrations ranging 0 - 100μg/ml varied (Figure 3.2A & B respectively). Exposure to all concentrations of LPS increased the level of IL-1β and TNF−α mRNA expression compared to EFLS unexposed to LPS. Whilst direct comparisons cannot be performed quantitatively between different genes, it was clear from the scale of the $2^{-\Delta Ct}$ values that TNF−α mRNA expression was approximately 100-fold lower than IL-1β mRNA expression. It was also clear that 10μg/ml LPS stimulated the largest increase in EFLS IL-1β mRNA expression compared to unexposed cells. This concentration also stimulated a moderate to high level of increased TNF−α mRNA expression. Two outliers of both TNF−α and IL-1β EFLS mRNA expression were removed due their values being between 3×10^3 – 9×10^3 fold lower than the mean values at 10 and 50μg/ml LPS. Using a Multitab general linear model, a statistically significant increase in TNF−α mRNA expression ($p<0.0005$) was stimulated by LPS, whereas the increase in IL-1β mRNA expression was not statistically significant.

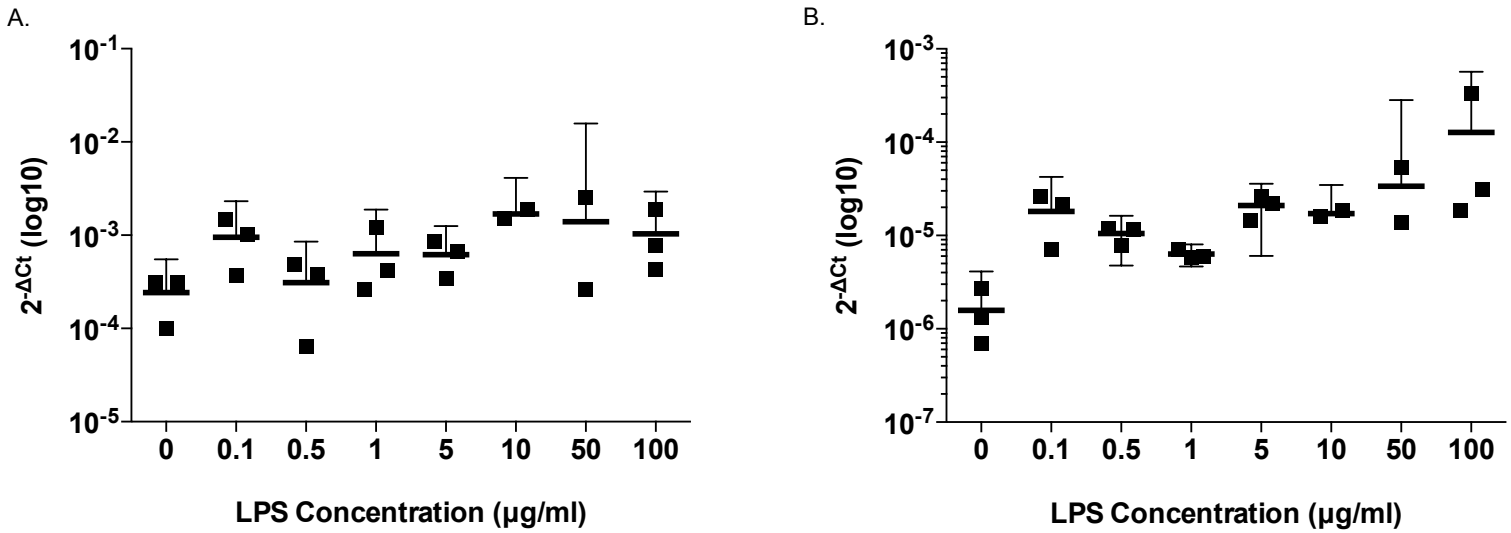

Figure 3.2 EFLS gene expression levels when exposed to different concentrations of LPS. Individual EFLS donor (n=3) IL-1β (A) and TNF-α (B) mRNA expression levels when exposed to a range of LPS concentrations for 24 hours, are displayed. Cytokine gene expression was normalised to GAPDH. The horizontal band represents the mean expression level, and error bars represent 95% confidence intervals. 10µg/ml LPS produced a good degree of IL-1β and TNF-α mRNA expression in EFLS compared to cells unexposed to LPS.

3.3.1.2 EPBMC Protein Secretion in Response to LPS

The levels of cytokine protein secreted by EPBMCs into culture media when exposed to different LPS concentrations varied between samples (Figure 3.3). Levels of both cytokines tended to increase upon exposure to increasing concentrations of LPS. Secreted IL-1β protein ranged from 0.17 – 0.46ng/ml to 0.23 – 1.1ng/ml, when cells were exposed to 0 or 10μg/ml LPS respectively. Secreted TNF-α protein ranged from 47.55 – 52.6pg/ml to 67.5 – 308.9pg/ml, when cells were exposed to 0 or 10μg/ml LPS respectively. The mean cytokine response when cells were exposed to each LPS concentration (Figure 3.3C & D) clearly shows a general trend of increased extracellular secreted cytokine protein on exposure to increased LPS concentrations. Levels of both secreted cytokines are significantly greater when EPBMCs are exposed to 10μg/ml LPS compared to EPBMCs unexposed to LPS.

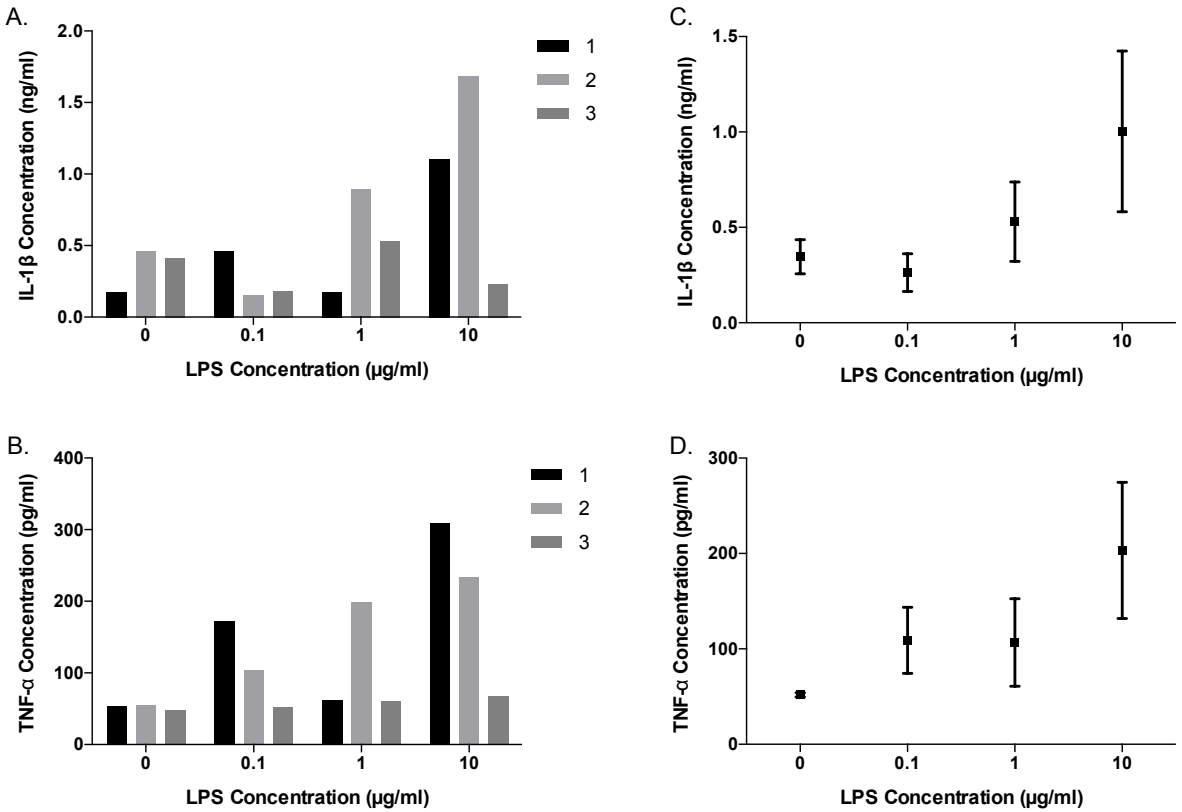

Figure 3.3 EPBMC extracellular secreted protein levels released on exposure to different LPS concentrations. Individual EPBMC (n=3) IL-1β (A) and TNF-α (B) protein concentration profiles display the degree of variation between each donor (n = 3) on exposure to each LPS concentration. The mean IL-1β (C) and TNF-α (D) concentration clearly shows a general trend of increased extracellular cytokine protein on exposure to increased LPS concentrations. When taking into consideration the wide margin of error, secreted protein levels of both cytokines are greater at 10µg/ml LPS compared to those unexposed to LPS. Error bars represent SEM.

Based on the responses of EPBMC at the mRNA and protein level, it was decided that 10μg/ml *Escherichia coli* LPS provided adequate simulation to investigate RNA interference of equine IL-1β within these cell populations. Due to the relatively low degree of EFLS TNF-α gene expression, and EPBMC TNF-α secreted protein, further analyses concentrated on IL-1β post-transcriptional gene silencing.

3.3.2 RNA Interference Optimisation

3.3.2.1 A Higher Concentration of SiRNA Produces Higher Transfection Efficiency

To optimise the intracellular delivery of our siRNA molecules to EPBMCs, we investigated the effects of different siRNA concentrations on transfection efficiency by using a non-targeting Cy3 labelled siRNA (Figure 3.4). Significantly more EPBMCs were transfected with this siRNA when using a concentration of 1pmol/μl (69.5-79.0%, mean ± SD: 72.1±6.7%) compared to 0.2pmol/μl (24.5-50.0%, mean ± SD: 39.4±14.0%) ($p<0.005$, paired two tailed t-test).

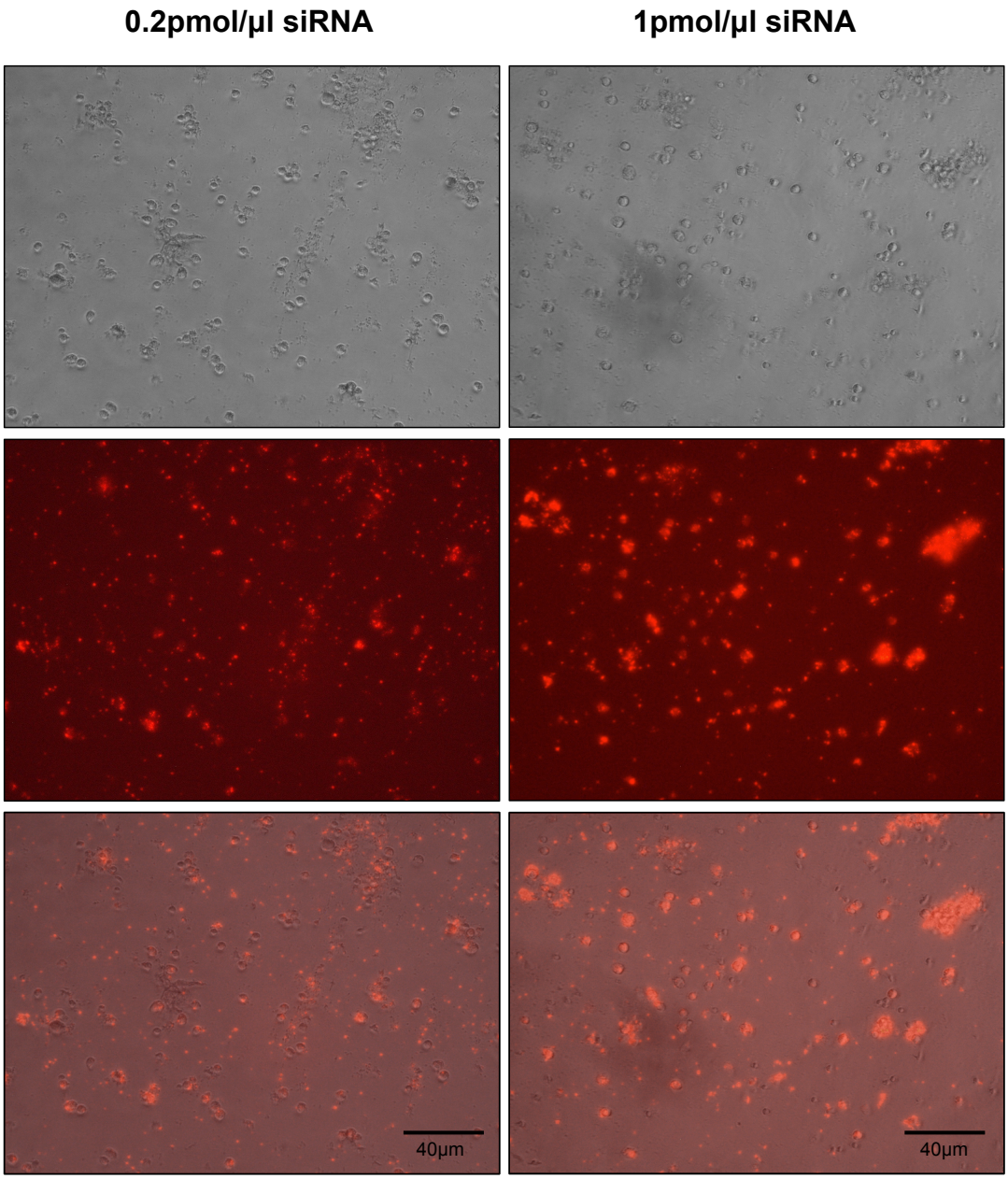

Figure 3.4 EPBMCs transfected with two concentrations of Cy3 labelled negative control siRNA. Microscopy images; phase contrast images (top), FITC filter (middle), two images overlaid (bottom). Using 1pmol/µl fluorescent siRNA 72.1±6.7% (mean ± SD) cells were transfected compared to 39.4±14.0% (mean ± SD) of cells when using 0.2pmol/µl fluorescent siRNA ($p<0.005$, paired two tailed t-test).

3.3.3 Measurement of Post-Transcriptional Gene Silencing Produced by SiRNA

3.3.3.1 EPBMCs and EFLS Secrete More IL-1β than TNF−α Protein in Response to LPS

After transfection with control or anti-IL-1β siRNA, EPBMCs secreted 5.6 and 5.0ng/ml, and EFLS secreted 4.42 and 3.5ng/ml IL-1β protein respectively. After transfection with control or anti-TNF−α siRNA, EPBMCs secreted 100.5 and 68.5pg/ml, and EFLS secreted 31.9 and 20.0pg/ml TNF−α protein respectively.

Extracellular secreted IL-1β and TNF−α protein levels are shown as fold differences in comparison to those of cells transfected with negative control siRNA (Figure 3.5). Knockdown of secreted proteins was observed in both cell types for each siRNA, although the extent of knockdown was greater in the EFLS. Both EPBMCs and EFLS transfected with anti-IL-1β (2) siRNA demonstrated a trend toward reduced levels of secreted IL-1β protein. EFLS transfected with anti-IL-1β (1) siRNA secreted less IL-1β protein than control cells, however, EPBMCs showed a slight increase in secreted protein (Figure 3.5A). EFLS transfected with either anti-TNF−α (1) or (2) siRNA displayed lower concentrations of secreted TNF−α within the media, compared to those of control cells. Whereas the concentration of TNF−α within anti- TNF−α EPBMC media was comparable to those of control cells, leading to the conclusion that treatment with anti-TNF−α (2) siRNA had minimal effect on the level of TNF−α protein translation and secretion (Figure 3.5B). One-tailed

t tests with bonferroni post hoc corrections did not show statistically significant reduction in gene expression using the anti-cytokine siRNA compared to control siRNA.

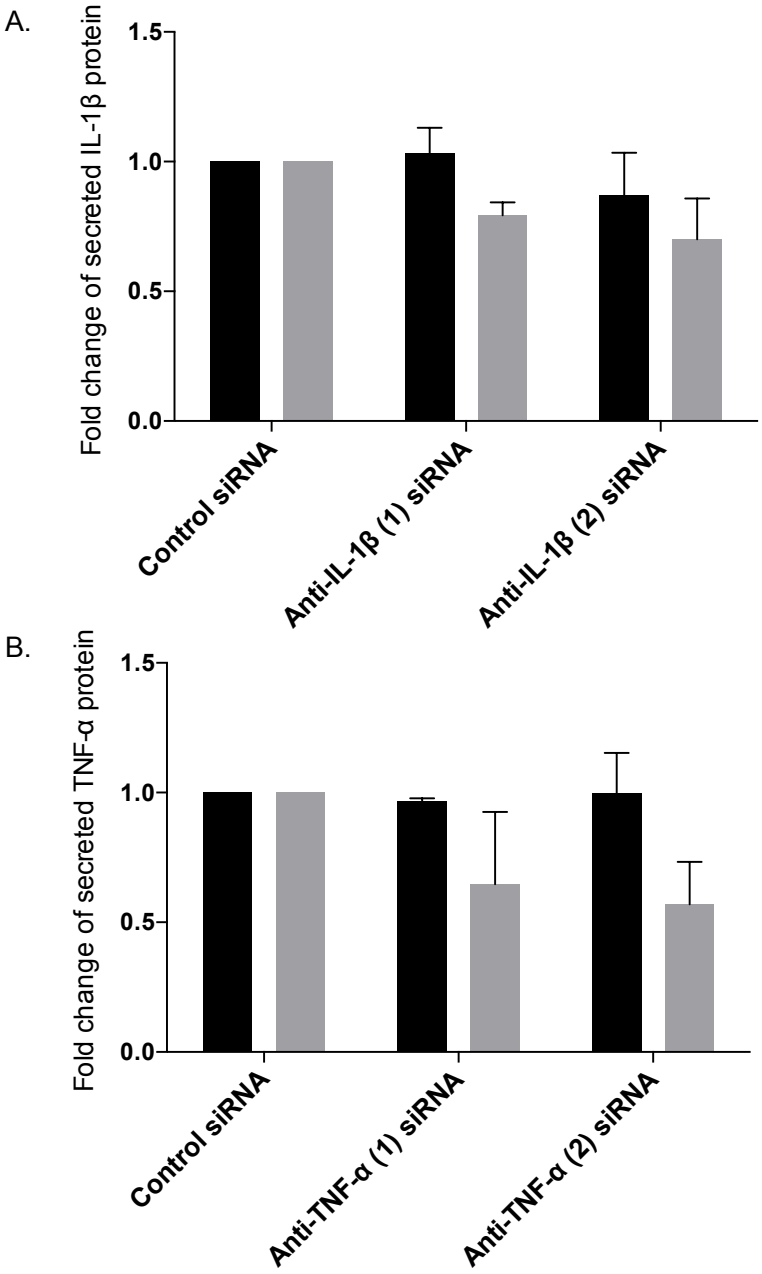

Figure 3.5 EPBMC and EFLS secreted protein concentrations after RNA interference with different siRNA sequences. Fold changes of secreted IL-1β (A) and TNF-α (B) protein by EPBMCs (black bars; n=3) and EFLS (grey bars; n=3) treated with two different anti-IL-1β and anti-TNF-α siRNA sequences, when compared to cells treated with negative control siRNA. All cells were exposed to 10μg/ml LPS for 12 hours. No statistically significant reductions in gene expression found. Error bars represent SEM.

3.3.3.2 SiRNA Sequence Comparison to Equine mRNA Sequences

BLAST searches between all siRNA sequences and the *Equus Caballus* genome only detected 100% similarity between the anti-IL-1β (2) siRNA sequence and the genome. The other siRNA sequences were less optimally matched. All further investigation was therefore carried out using the equine anti-IL-1β (2) siRNA.

3.3.4 EFLS IL-1β mRNA Interference by Anti-IL-1β (2) siRNA

3.3.4.1 Anti-IL-1β (2) SiRNA Significantly Reduced EFLS IL-1β mRNA Levels

The IL-1β gene expression of EFLS treated with negative control siRNA was compared to those treated with anti-IL-1β (2) siRNA, exposed to 10μg/ml LPS for 3 hours. Significantly different $2^{-\Delta Ct}$ values were produced when using equine IL-1β primer 1 and primer 2 ($p = 0.01$). EFLS IL-1β mRNA expression was normalised to EFLS GAPDH mRNA expression. EFLS treated with negative control siRNA and anti-IL-1β (2) siRNA, produced 0.008 and 0.003, and 0.018 and 0.019 $2^{-\Delta Ct}$ values respectively, when primer 1 and 2 were used respectively. Primer 1 demonstrated a large reduction in IL-1β mRNA expression when EFLS were treated by anti-IL-1β (2) siRNA in comparison to cells treated with negative control siRNA. The change in IL-1β mRNA expression did not represent a statistically significant decrease, however it did represent a 65.7% reduction, which is considered a good reduction (Figure 3.6).

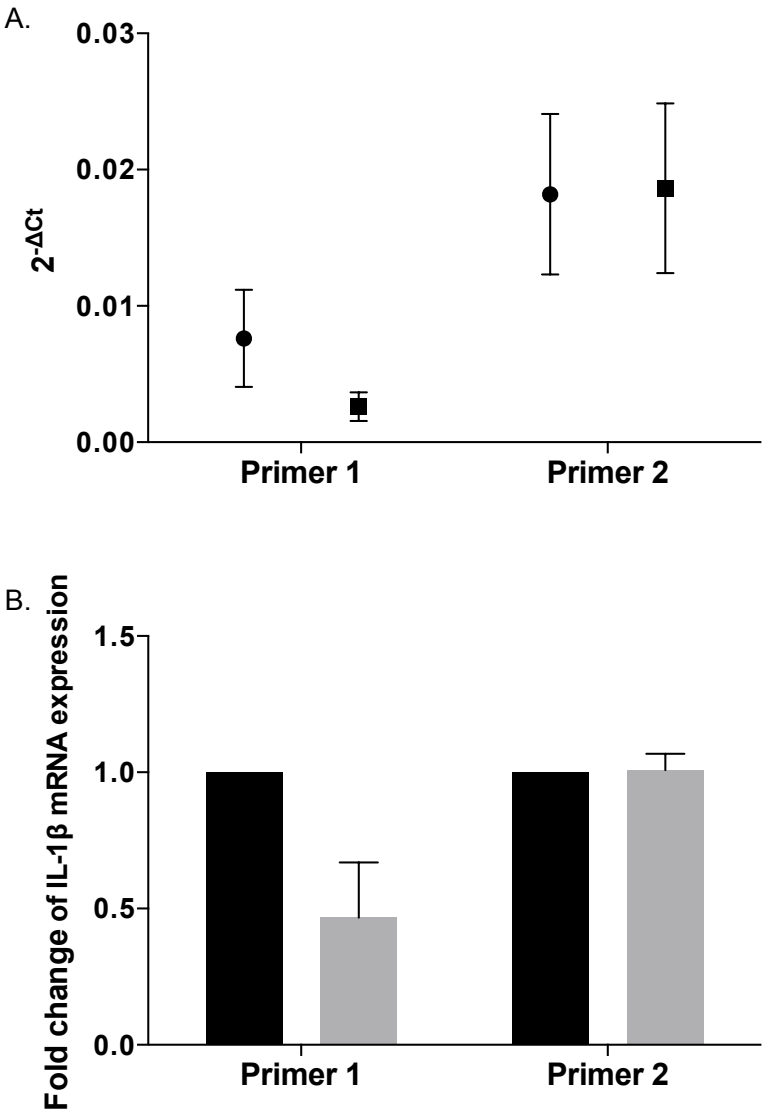

Figure 3.6 EFLS IL-1β gene expression after treatment with either negative control siRNA or anti-IL-1β (2) siRNA. Two different IL-1β primers were used to analyse the IL-1β gene expression of EFLS (n = 3) treated with negative control siRNA (circle and black bars) compared to those treated with anti-IL-1β (2) siRNA (square and grey bars). IL-1β gene expression is displayed as $2^{-\Delta Ct}$ values (A) and as fold changes (B) in comparison to EFLS gene expression after treatment with negative control siRNA. A 65.7% reduction in IL-1β gene expression was found using primer 1, however there was no statistically significant difference found. Error bars represent SEM.

3.3.5 Analysis of Protein Secreted by EFLS

3.3.5.1 Successful Protein Extraction from Culture Media

Average protein concentrations within the serum-free culture media of EFLS treated with negative control siRNA or anti-IL-1β siRNA, were 533 and 508μg/ml respectively. Following incubation with Strataclean resin, the average culture media protein concentration decreased to 198μg/ml. Once protein-bound resin was reconstituted in SDS loading buffer, the average protein concentration was >2000μg/ml which reflected successful extraction of protein from the culture media.

3.3.5.2 Presence of Culture Media Protein on the Nitrocellulose Membrane

The nitrocellulose membrane stained positive for ponseau stain, which inferred that protein had been successfully transferred onto the membrane. Two bands are evident for each sample of EFLS treated with both negative control siRNA and anti-IL-1β siRNA. These bands reflect the presence of protein of approximately 57 and 65kDa (Figure 3.7). It was hypothesised that a much bigger range of proteins, with different molecular weights, would be extracted from the culture media.

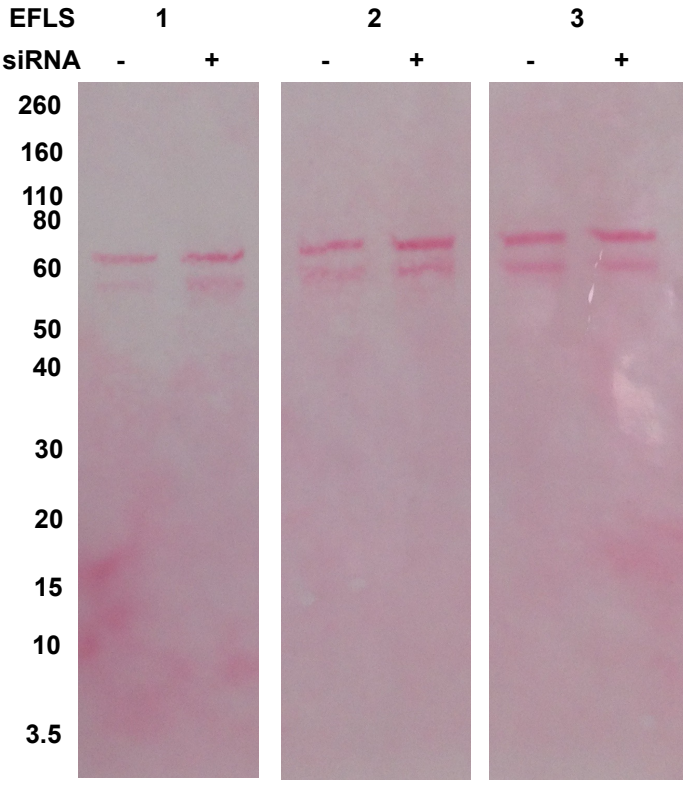

Figure 3.7 Protein secreted from EFLS transfected with either negative control (-) or anti-IL-1β (+) siRNA. EFLS (n=3) were transfected with siRNA for 6 hours before being exposed to 10μg/ml LPS for 3 hours. Secreted protein was extracted from serum-free culture media and run on an SDS-PAGE gel. Successful protein transfer to a nitrocellulose membrane is evident by positive Ponseau staining at 57 and 65kDa.

3.3.5.3 Equine IL-1β Protein was Undetected within EFLS Culture Media

Using an equine IL-1β mAb the nitrocellulose membrane was probed. There was no evidence of protein consistent with either pro-IL-1β (33kDa) or active secreted IL-1β (17.5kDa) protein within the culture media of EFLS transfected with either negative control or anti-IL-1β siRNA.

3.3.6 EPBMCs Successfully Phagocytose Microspheres

EPBMCs carried out successful phagocytosis of fluorescein isothiocyanate-dextran microspheres, between 2-6μm diameter. This was displayed using multichannel scanning confocal laser microscopy to create a colour composite z-stack series of transverse images spanning the entire cell volume (Figure 3.8). A close association between intracellular fluorescent microsphere particles and the cell nucleus was evident. Intracellular co-localisation of phagocytosed microsphere particles and the cell nucleus was further demonstrated by three channel confocal imaging (Figure 3.9). Between one and seven fluorescent particles were present within 71% of EPBMCs, reflecting positive intracellular presence of the microspheres. Microspheres larger than 6μm failed to be phagocytosed by the EPBMCs.

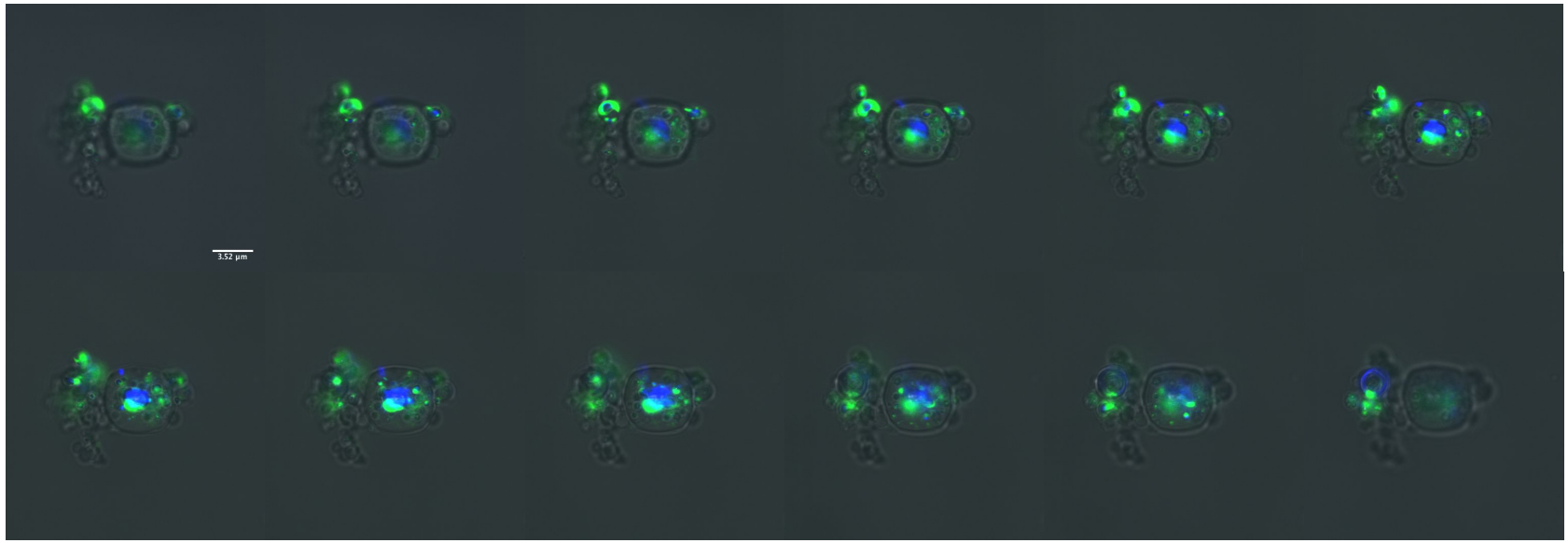

Figure 3.8 A series of z-sections demonstrating extensive phagocytic uptake of fluorescein isothiocyanate-dextran microspheres by an equine macrophage, imaged using multichannel scanning confocal laser microscopy. Three channels were merged to create a colour composite z-stack series (100x); 488nm (green) to visualise the microsphere, 364nm (blue) to visualise the nucleus, and a transmitted light channel (grey) to visualise the macrophage. The series of images (top left to bottom right) represent transverse sections from the bottom to the top of the cell, allowing visualisation of intracellular components throughout the entire cell.

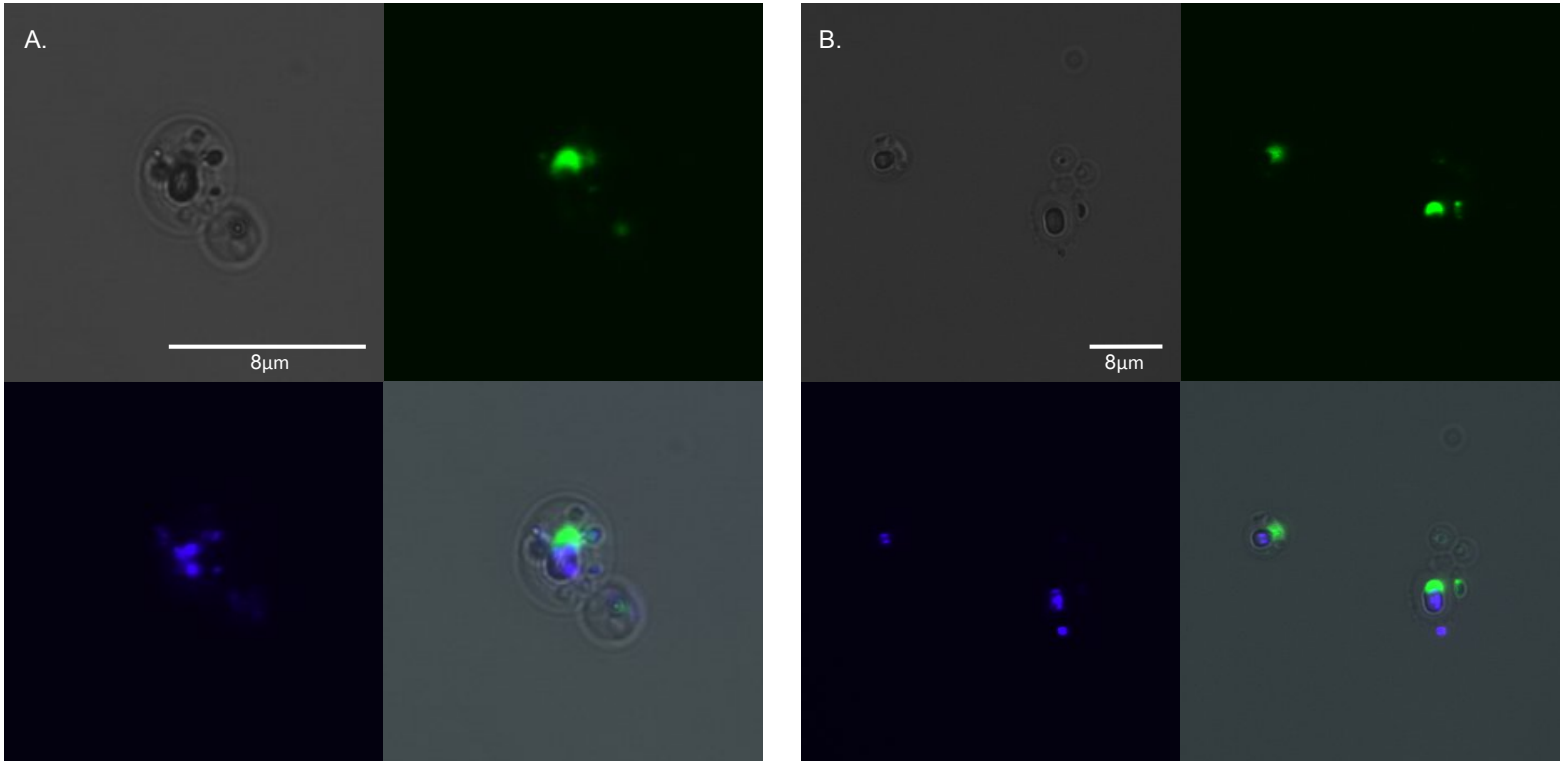

Figure 3.9 Confocal microscopy images of EPBMCs phagocytosis of 2-6µm fluorescein isothiocyanate-dextran microspheres (A-D). Transmitted light image (top left), 488nm channel detects the fluorescein isothiocyanate-dextran microsphere (top right), 364nm channel detects the DAPI stained cell nucleus (bottom left), and all three images overlaid (bottom right). A. x100, B. x63, C. x63, D. x63. Images C and D are on the next page.

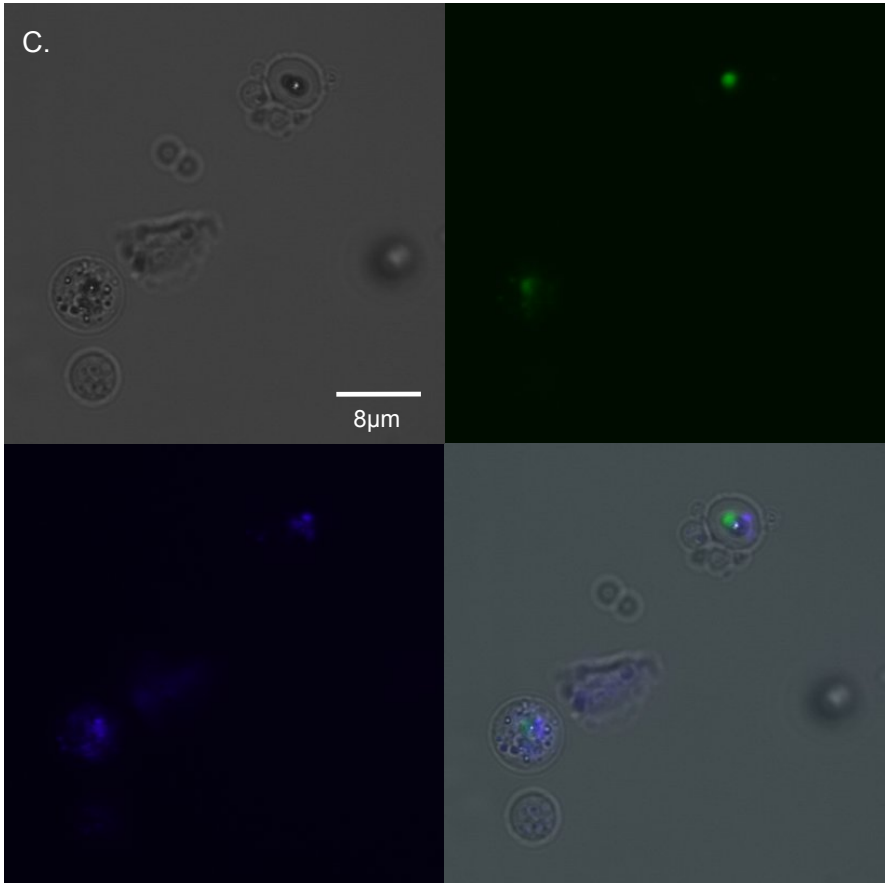
C.
8µm

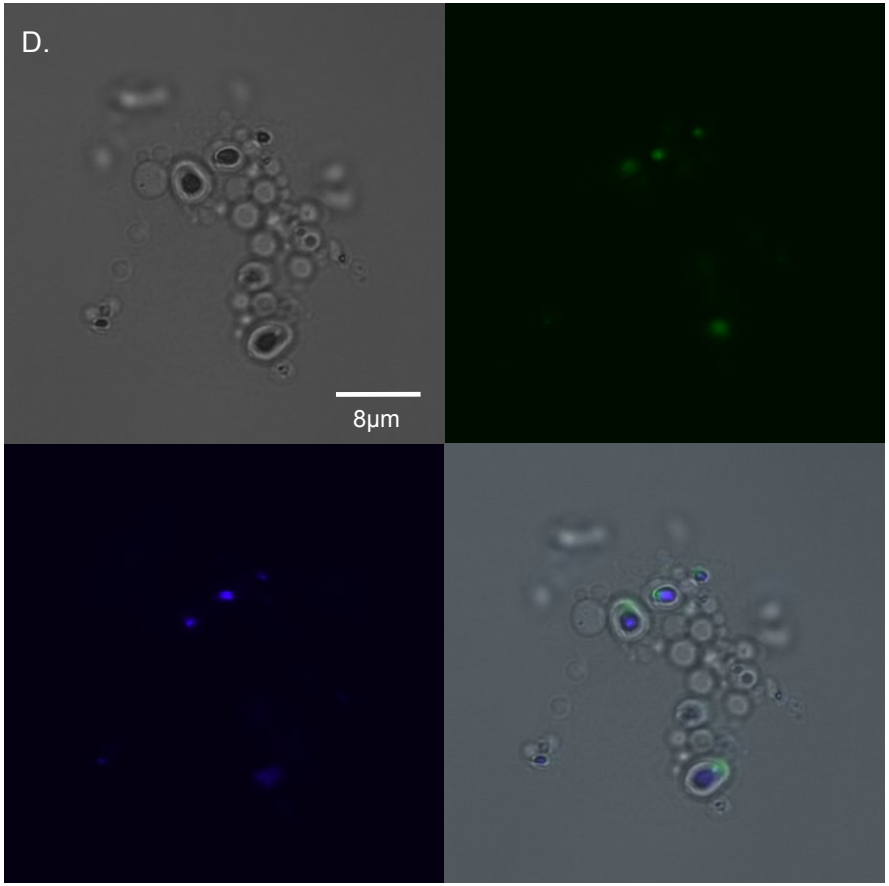
D.
8µm

3.3.7 Microspheres Cultured with Synovial Explants were Associated with Synovicoytes

Close association of the microspheres and synovial explants, after a vigorous washing procedure and histological sample preparation, was evident when samples were visualised through confocal microscopy (Figure 3.10). This supports the presence of successful phagocytic activity within the explant. Additionally, multiple fluorescent particles, smaller than the microspheres that were originally added to the culture, were detected within the explant. These are consistent with small digested particles of the fluorescent microsphere within multiple intracellular phagosomes (Figure 3.10).

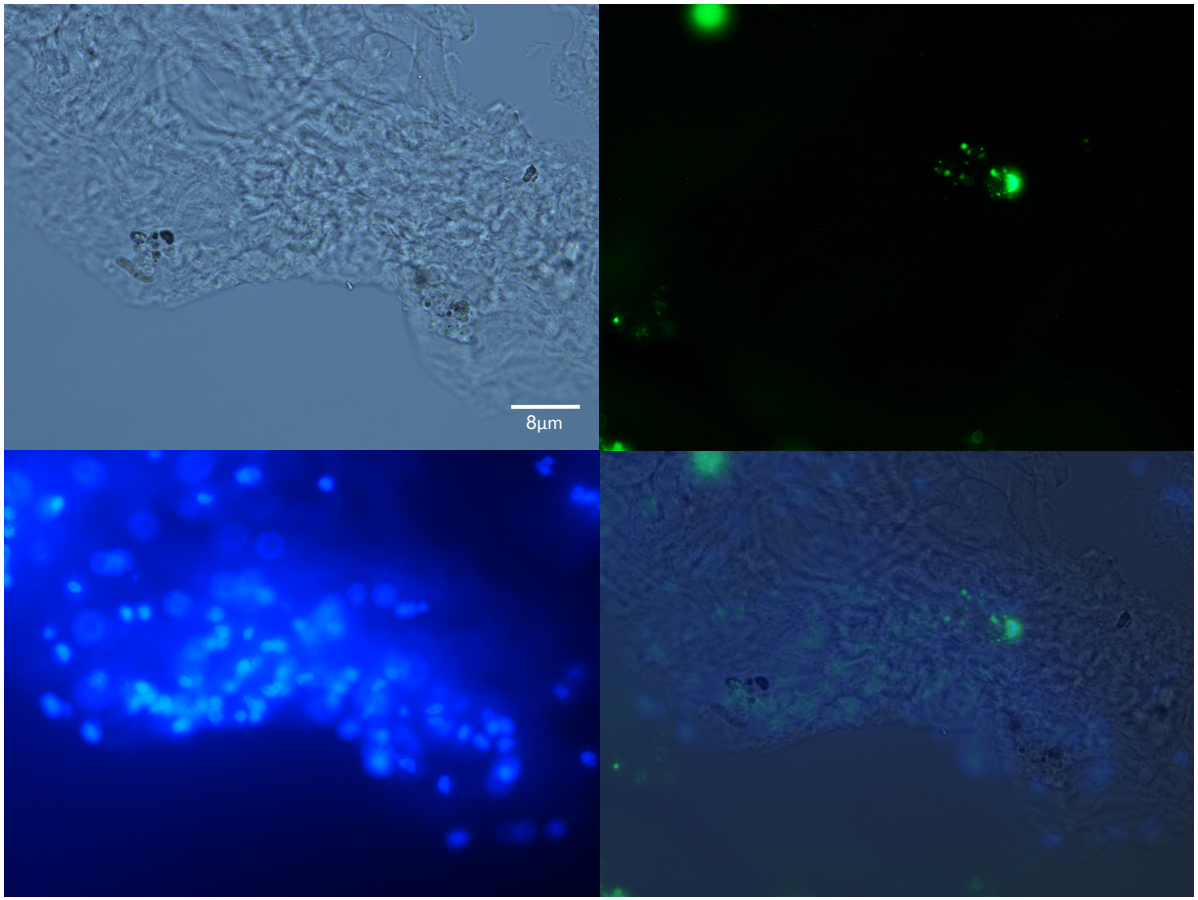

Figure 3.10 Synovial explant section associated with fluorescein isothiocyanate-dextran microspheres. Transmitted light image (top left), 488nm channel detects the fluorescein isothiocyanate-dextran microsphere (top right), 364nm channel detects the DAPI stained cell nucleus (bottom left), and all three images overlaid (bottom right).

3.4 Discussion

Severe synovitis is characterised by the presence of a marked mononuclear cell infiltration, marked increase in vascularity, subintimal oedema and fibrosis, and intimal hyperplasia (McIlwraith, Frisbie et al. 2010). When cells from the synovium are isolated and cultured, the proliferation of FLS quickly exceeds that of synovial macrophages. Previous reports have suggested by passage 3-4, cultures contain solely FLS (Rosengren, Boyle et al. 2007). This study incorporated both cell types to investigate the cellular interactions that would arise within synovial membrane during synovitis.

LPS was chosen to stimulate synoviocytes because it activates the same cell signalling pathways as those which initiate the inflammatory response during early OA. LPS binds to the cell surface TLR-4, which is the same receptor that DAMPs (Scanzello and Goldring 2012, Houard, Goldring et al. 2013), such as extracellular matrix components (Nair, Kanda et al. 2012), bind to. This activates the NF-κB pathway, subsequently up-regulating transcription of cytokines and chemokines responsible for the mononuclear cell infiltration characterising synovitis (Scanzello and Goldring 2012, Houard, Goldring et al. 2013). Up-regulation of TLR-4 and DAMPs have been observed in OA synovial tissue (Goldring, Otero et al. 2011).

To allow testing of cytokine RNAi in synoviocytes, cytokine expression had to be sufficiently up-regulated. The optimal LPS concentration for the stimulation of both IL-1β and TNF−α production in EFLS and EPBMCs was 10μg/ml. This was a high concentration compared to previous reports. However, this concentration stimulated good expression of EFLS IL-1β and

TNF−α mRNA expression respectively, when compared to LPS concentrations ranging from 0-100μg/ml. Exposing EFLS to 100μg/ml LPS produced the highest level of TNF−α mRNA expression, however this concentration has been reported to cause a decrease in cell viability (Sharifi, Hoda et al. 2010). Ten μg/ml LPS also produced the highest concentration of secreted IL-1β (1.1ng/ml) and TNF−α (203.3pg/ml) protein from EPBMCs when compared to concentrations between 0 - 10μg/ml LPS. The equine IL-1β ELISA kit (Bethyl Laboratories, TX, USA) and equine TNF−α ELISA kit (R&D Systems, MN, USA) used standard concentrations of recombinant equine IL-1β and TNF−α between 3.125–200ng/ml and 31.3–2000pg/ml respectively. The IL-1β protein concentrations are below the lower threshold of this assay, therefore there maybe a larger degree of error in the quantitation of IL-1β protein. Using a lower concentration (<10μg/ml) of LPS may have led to undetectable IL-1β protein concentrations. For future investigations, proteins within culture media would be extracted and concentrated if intended to be used with ELISA kits.

A slight increase in EPBMC secreted IL-1β protein was observed when cells were transfected with anti-IL-1β (1) siRNA using the lipofectamine transfection reagent. Lipofectamine, a cationic lipid carrier, is required to facilitate intracellular delivery of the large anionic hydrophilic siRNA molecules, due to the negative hydrophilic extracellular surface of the cell membrane. Lipid-delivered siRNAs bind to the cell membrane, and are internalised through endosomal formation (Dominska and Dykxhoorn 2010). During this process the innate immune system can be activated through endosomal TLRs and intracellular cytoplasmic receptors, which can detect

and react to siRNA in a sequence independent manner (Kanasty, Whitehead et al. 2012). TLR3 has been identified in macrophages (Rehli 2002, Kawai and Akira 2008) and is expressed on cell membranes in endosomes. This receptor can activate pathways leading to the production of inflammatory cytokines. This may explain the small increase in secreted IL-1 protein.

Of the two IL-1β siRNA molecules examined, the anti-IL-1β (2) siRNA sequence provided the strongest degree of gene expression knockdown, causing a 65.7% reduction in EFLS IL-1β transcript abundance. EPBMCs showed a moderate decrease in the secretion of IL-1β protein when transfected with anti-IL-1β (2) siRNA, as analysed via ELISA. These assays were performed on cells which had been exposed to LPS for different lengths of time; EFLS and EPBMCs were exposed to LPS for 3 and 12 hours respectively. Once cells were stimulated, IL-1β intracellular signalling mechanisms caused a rapid increase in IL-1β mRNA and secreted IL-1β protein within 1-3 hours (Wang, Olschowka et al. 1997) and >3 hours respectively (Lee, Yuk et al. 2012). It has been reported that IL-1β mRNA has a half life of 4-5 hours in monocytes and macrophages (Herzyk, Allen et al. 1992), however many factors can affect this. A period of $\leq$3 hours of exposure to LPS facilitated detection of a true positive decrease in mRNA expression. However, exposure to LPS for 12 hours may have resulted in a false negative decrease in secreted IL-1β protein concentration. IL-1β protein is produced as an inactive precursor protein (31-33kDa) which accumulates within the cell cytosol and has a half life of 2.5 hours (Moors and Mizel 2000). The intracellular converting enzyme (ICE) cleaves this protein to produce the 17.5kDa active form (Lopez-Castejon, Brough et al. 2011). Both the

precursor and active forms of IL-1β protein are released by human monocytes (Moors and Mizel 2000), and both forms are detected by the ELISA. The active IL-1β protein has a half life of 2 - 2.5 hours in plasma (Kudo, Mizuno et al. 1990). IL-1β protein release is unusual as it bypasses the endoplasmic reticulum and golgi apparatus (Lopez-Castejon, Brough et al. 2011), and is released approximately 2 hours after synthesis (Moors and Mizel 2000). To detect a strong decrease in EBMC secreted IL-1β protein caused by anti-IL-1β siRNA, a sampling time of 6 hours post-LPS exposure may have provided a more sensitive reflection of the siRNA effects on protein translation. Interestingly, previous studies have demonstrated that LPS is capable of inducing IL-1β transcription without effecting translation (Sung and Walters 1991), contrasting other reports suggesting that LPS can stabilise IL-1β mRNA, resulting in increased translation (Caput, Beutler et al. 1986).

The siRNA used within this study fulfilled design criteria recommended to ensure optimal RNA interference. Low G/C content (24%), A/U base pairs within nucleotide positions 15-19, and certain sense strand base preferences at positions 3 (A), 10 (U), and 19 (A, no G or C). A/U base pair content is a simple measure of local internal stability of the siRNA molecule. Presence of these base pairs towards the 3’ end of the duplex correlates well with functionality of the siRNA (Reynolds, Leake et al. 2004). Specific sequence-related determinants, such as the inclusion or exclusion of certain nucleotides at specific positions along the sense strand, also correlates with siRNA functionality (Reynolds, Leake et al. 2004).

When analysing gene silencing via qRT-PCR, it was noted that the relative siRNA and primer positions on the target mRNA sequence were highly important. Messenger RNA fragments produced through siRNA-mediated cleavage are usually cleared through normal cellular mRNA degradation pathways. However the 5' and 3' mRNA fragments do not share the same routes of degradation (Valencia-Sanchez, Liu et al. 2006). One study has suggested that the 3' mRNA fragments may fail to be effectively degraded by these cellular mechanisms, and can subsequently act as a template for cDNA synthesis. Primers designed to complement cDNA towards the 3' end of the gene, will detect these transcripts during qRT-PCR and false negative reductions in gene expression will occur (Holmes, Williams et al. 2010). It is hypothesised that this failure of degradation may occur due to the presence of particular RNA binding proteins, to the secondary structure of the mRNA, or to the accumulation of 3' mRNA cleavage products reported during siRNA treatment (Holmes, Williams et al. 2010). The difference between $2^{-\Delta Ct}$ values produced by anti-IL-1β (2) siRNA using primer 1 compared to primer 2 were significant. Primer 1 demonstrated a 65.7% reduction in EFLS IL-1β mRNA transcripts compared to those treated with control siRNA, whereas primer 2 demonstrated no reduction. Primer pair 1, which is complimentary to a region toward the 5' end of the IL-1β mRNA, was able to detect a significant effect of the siRNA mediated knockdown whereas primer pair 2 which is located towards the 3' end, could not detect the knockdown. These results would suggest the presence of un-degraded 3' mRNA fragments within EFLS.

EPBMCs were also cultured with anti-IL-1β siRNA loaded microspheres, and exposed to LPS. The RNA derived from these cultures was highly

contaminated and qRT-PCR produced no Ct results. Further work is required to investigate whether presence of the PLGA microspheres hinders the extraction of good quality pure RNA.

To provide gold-standard proof of effective silencing by siRNA, analysis of intracellular and secreted protein via western blot analysis is required. However this was not achieved. Each stage of the culture media protein extraction process was tested by performing serial Pierce^{Tm} 660 protein assays. This verified successful protein-resin binding. Protein transfer to the nitrocellulose membrane also tested positive using the Ponseau staining. However, ponseau staining revealed only two protein bands of around 57 and 65kDa, it was hypothesised that a far greater dispersity in protein size would be present. Once the membranes had been probed with the anti-IL-1β monoclonal antibody and appropriate secondary antibody, there was no evidence of either the pro- or active forms of IL-1β protein within the culture media. This may be due to unsuccessful binding of the primary anti-IL-1β monoclonal antibody, the absence of secreted IL-1β in the cell culture media, or the concentration of secreted IL-1β protein may be undetectable. To investigate this further, a sample of recombinant equine IL-1β would have been probed with the anti-IL-1β monoclonal antibody, to test for compatibility.

The most popular vector to potentiate gene-therapy under current investigation is the adeno-associated virus (Goodrich, Phillips et al. 2013, Hemphill, McIlwraith et al. 2014). This has been extensively tested in equine arthritis models, using the IL-1 receptor antagonist gene (Goodrich, Phillips et al. 2013). Whether IL-1β is the target of choice to aid in the reduction of clinical symptoms and pathology caused by osteoarthritis, is ambiguous. It is

well known that IL-1β plays a major causative role, however, the deletion of this gene has also been found to accelerate osteoarthritis (Clements, Price et al. 2003). It may be yet another factor involved in the modulation, rather than solely inciting, osteoarthritis.

Further identification of the macrophages, using macrophage-specific surface receptors, would have been preferred. Attempts to label this population using primary antibodies to the macrophage markers CD14 and CD68 (Bartok and Firestein 2010) were unsuccessful due to a lack of equine cross-reactive antibodies to these proteins. The lack of such reagents thus continues to make the examination of equine monocytes extremely challenging. However, the highly efficient manner in which the EPBMCs phagocytosed the 2-6μm fluorescein isothiocyanate-dextran microspheres provides convincing evidence supporting their nature. This agreed with previous studies which found that 1-10μm microspheres were optimal for synoviocyte phagocytosis (Butoescu, Seemayer et al. 2009).

3.4.1 Conclusion

To conclude, we have demonstrated successful siRNA-mediated reduction of EFLS IL-1β transcripts, and a moderate decrease in the levels of IL-1β protein secreted from equine synoviocytes. Successful equine macrophage phagocytosis of PLGA microspheres is a positive step towards the provision of a drug-delivery vehicle. Further investigation into the effects of siRNA-loaded microspheres on equine synoviocyte cultures is required to advance this synoviocyte-targeted anti-OA therapy.

Chapter 4.

Species-Specific Co-Culture Synovitis Model to Investigate Intercellular Signalling Between Cellular Populations: Macrophages Attenuate Fibroblast-Like Synoviocyte ADAMTS5 Gene Expression.

4.1 Introduction

Synovitis is a key mediator of osteoarthritis (Goldring, Otero et al.), and of the perpetuation of cartilage degradation (Sellam and Berenbaum 2010). Synovial inflammation is characterised by increases in catabolic cytokines, especially IL-1β and TNF-α, which are predominantly produced by synovial macrophages. These cytokines cause changes in FLS gene expression, including up regulation of damaging cartilage matrix degrading proteinases and further cytokines (Bondeson, Wainwright et al. 2006). In 1991 it was reported that the major aggrecan fragment detected in synovial fluid of arthritic joints, had been cleaved between the Glu373 - Ala374 peptide bond, within the interglobular domain of the aggrecan core protein (Sandy, Flannery et al. 1992). This differed from the cleavage site of MMPs, which had initially been thought to be primarily responsible for aggrecan breakdown. This new group of proteases were termed aggrecanases, and are the principle proteinases of aggrecan degradation during articular cartilage destruction (Zhang, Yan et al. 2013). The ADAMTS family (A Disintegrin And Metalloproteinase with ThromboSpondin motif) have aggrecanase activity and mainly cleave between the Glu373-Ala374 peptide bond; ADAMTS4 (aggrecanase-1) and ADAMTS5 (aggrecanase-2) are key players in cartilage destruction (Bondeson, Wainwright et al. 2013). A recent

study has identified the transcription factor RelA/p65 as a potent activator of ADAMTS5 in chondrocytes during osteoarthritis. It binds to the promoter region, and influences expression in the NF-κB pathway (Kobayashi, Hirata et al. 2013). The ADAMTS-5 full-length protein has a predicted mass of 101kDa. Once secreted, it is cleaved in a furin-dependent manner and becomes proteolytically activated, although it can exist in two isoforms, active and inactive (Bondeson, Wainwright et al. 2013). Increased proteoglycan breakdown in articular cartilage was associated with increased immunohistochemical staining of PACE4 and furin, suggesting that the post-transcriptional activation of these factors may be important in the pathophysiology of arthritis (Wylie, Ho et al. 2012). Extracellular ADAMTS5 proteolytic activity is predominantly inhibited by TIMP-3 through its N-terminal inhibitory domain (Bondeson, Wainwright et al. 2013, Bakali, Gras-Masse et al. 2014). Extracellular active ADAMTS5 protein is also reduced by lipoprotein receptor-related protein 1 (LRP-1) mediated endocytic clearance (Yamamoto, Troeberg et al. 2013, Bakali, Gras-Masse et al. 2014). ADAMTS5 gene expression is thought to be constitutively expressed by both normal and OA human chondrocytes (Bau, Gebhard et al. 2002, Naito, Shiomi et al. 2007) and synovial cells (Yamanishi, Boyle et al. 2002, Bondeson, Wainwright et al. 2006), however one study reports induction of chondrocyte expression by IL-1, TNF-α and oncostatin-M (OSM) (Song, Hua et al. 2007). However, normal bovine (Patwari, Gao et al. 2005) and murine chondrocyte (Rogerson, Chung et al. 2010) ADAMTS5 mRNA levels respond to IL-1 and TNF-α (Bondeson, Wainwright et al. 2013). One report does contradict these findings, suggesting bovine chondrocyte ADAMTS5 mRNA

expression is constitutive (Tortorella, Malfait et al. 2001). Human synoviocyte (Yamanishi, Boyle et al. 2002) and chondrocyte (Bau, Gebhard et al. 2002, Song, Hua et al. 2007) ADAMTS4 gene expression is up-regulated by IL-1β and TGF-β (Bondeson, Wainwright et al. 2006) and during OA (Bau, Gebhard et al. 2002, Bondeson, Wainwright et al. 2006, Naito, Shiomi et al. 2007, Song, Hua et al. 2007). Previous reports suggest ADAMTS5 is the central aggrecanase responsible for cartilage degradation in the murine model; ADAMTS5 KO, and normal mice treated with a potent anti-ADAMTS5 monoclonal antibody, subjected to DMM experienced significantly less cartilage destruction than wild type mice (Glasson, Askew et al. 2005, Chiusaroli, Visentini et al. 2013, Miller, Tran et al. 2014). In addition to cartilage, equine synovium also expresses both ADAMTS4 and -5 (Ross, Kisiday et al. 2012); normal synoviocytes co-cultured with injured cartilage were found to express significantly lower levels of ADAMTS5 mRNA compared to synovium in co-culture with normal cartilage (Lee, Kisiday et al. 2013). Normal equine synoviocyte ADAMSTS5 mRNA expression was found to be unaffected by IL-1 or LPS (Ross, Kisiday et al. 2012), whereas chondrocyte expression was up-regulated by these mediators (Busschers, Holt et al. 2010, Ross, Kisiday et al. 2012). However equine OA synoviocyte ADAMTS5 gene expression was found to be up-regulated, whereas chondrocyte expression was unchanged (Kamm, Nixon et al. 2010). These factors suggest a central role for this aggrecanase in equine cartilage degeneration, with a possible synovial protective component. ADAMTS5 presents a potential disease-modifying target for OA, however further insight into the regulation of this aggrecanase is needed.

A co-culture system modelling synovitis was designed to allow cell-specific responses to an inflammatory environment to be identified. The EFLS response to LPS stimulation, and to direct macrophage contact, and indirect contact through macrophage conditioned-media, were analysed. The signalling pathway responsible for macrophage-mediated regulation of EFLS ADAMTS5 gene expression was found to be NF-κB-independent, and non-responsive to macrophage-secreted IL-1β.

4.1.1 Aims

- To investigate the EFLS response to inflammatory stimulation.
- To analyse how EFLS cytokine and aggrecanase gene expression is affected by macrophages in an inflammatory environment, in a temporal and quantitative manner.
- To examine the influence of IL-1β and NF-κB signalling pathways on macrophage and EFLS gene expression.

4.2 Study Design

4.2.1 Isolation of Equine Fibroblast-like Synoviocytes

As described in Chapter 2 Materials and Methods, section 2.1. EFLS from three horses were used (passage number <4) from metacarpo/tarsophalangeal joints without orthopaedic disease.

4.2.2 Western Blot Analysis; Response of EFLS ADAMTS5 Protein to LPS Exposure

EFLS cells were cultured in 6-well plates at 3.3 x 10^5 cells per well in 2ml standard culture media for 24 hours to allow cells to adhere. Media was replaced with fresh media, with and without serum, and with and without 10µg/ml LPS (E. Coli 026:B6, Sigma-Aldrich, Missouri, USA). Cells were harvested at 6 or 16 hours post-LPS exposure. Media was collected and stored at -20°C. The cell layer was washed using 1x PBS, before being lysed with 200µl 1x SDS sample-loading buffer (62.5mM Tris-HCl, pH 6.8 at 25°C, 2% w/v SDS, 10% glycerol, 50mM DTT, 0.01% w/v bromophenol blue or phenol red). Samples were processed to remove cell debris and sonicated as described in Chapter 2 Materials and Methods, section 2.6. Cell layer and culture media protein concentrations were measured using the Pierce^{Tm} 660 Protein Assay (Life Technologies, Carlsbad, USA). Protein (40µg) was extracted from each media sample using StrataClean^{Tm} Resin according to the manufacturer's protocol and eluted by boiling in 15 µl 1x SDS sample buffer. Cell layer and culture media protein samples were analysed by SDS-PAGE and western blotting using primary sheep anti-mouse ADAMTS5 mAb

1:500 (a kind gift from Prof. A Fosang, Melbourne, Australia) and monoclonal anti-goat/sheep IgG-peroxidase antibody 1:1000 (A9452, Sigma-Aldrich, Missouri, USA). Visualisation of the antibody was achieved using a 1:1 combination of Oxidising Reagent Plus and Enhanced Luminal Reagent Plus (Western Lightening-Plus ECL Enhanced chemiluminescence substrate, Perkin Elmer, Massachusetts, USA), and a UVP ChemiDoc-it imaging system. The primary antibody was stripped from the cell layer membrane by immersing it in stripping buffer before being re-probed with an HRP-conjugated GAPDH antibody 1:5000 (Sigma-Aldrich, Missouri, USA) to serve as a control.

4.2.3 Design of the Inter-species Co-culture Model

4.2.3.1 EFLS Cells were Labelled with Cell Proliferation Dye Efluor® 670

As described in Chapter 2 Materials and Methods, section 2.2, EFLS cells were labelled with the cell proliferation dye eFluor® 670 (eBioscience Inc., San Diego, USA). To determine the concentration of dye with maximum EFLS labelling efficiency, concentrations ranging from 5 - 10μM were tested. Once labelled, cells were cultured in 6-well plates at 3.3 x 10^5 cells per well in 2ml standard culture media, for 24 and 48 hours. Cell layers were then washed with PBS, before being exposed to 0.05% trypsin-EDTA (Lonza, Basel, Switzerland) and incubated at 37°C in 5% CO_2. After 5-10 minutes, the wells were vigorously agitated before an equal volume of standard culture media containing FBS was added to the suspension to deactivate the

trypsin. The cell suspension was centrifuged at 290 x g for 4 minutes, and the cell pellet re-suspended in fresh media. Fluorescence emission at each concentration was analysed using an Accuri^{Tm} C6 flow cytometer (BD Biosciences, California, USA).

4.2.3.2 Lentiviral-Mediated Generation of GFP Expressing DH82 Cells

The canine macrophage derived cell line DH82 was obtained from American Tissue Culture Collection (ATCC, Virginia, USA) and cultured under the same conditions as EFLS. These cells were exposed to 8mg/ml hexadimethrine bromide (1000x) before being mixed with four different multiplicity of infections (MOI) of lentiviral particles expressing a constitutively active green fluorescent protein gene (CMV promoter) and a puromycin resistance cassette (Sigma, Missouri, USA). Successfully transfected cells containing the GFP-expressing plasmid were selected using 2µg/ml puromycin (Life Technologies, Carlsbad, USA) and expanded in culture.

4.2.3.3 Determining Cell-proliferation Characteristics within a Co-Culture Environment

After seeding cells, cultures were incubated for 24 hours to allow cells to attach. When using mixed co-cultures in experiments, it is imperative to know the relative proportions of each population within the culture, to fully elucidate cellular interactions. EFLS cells labelled with 8µM cell proliferation dye eFluor® 670 (eBioscience Inc., California, USA) and GFP-expressing DH82

cells were cultured together at different proportions for 24 hours. Cell numbers and proliferation characteristics were determined by flow cytometry. Cells were seeded in 6-well plates at 3.3 x 10^5 per well in 2ml standard culture media at the following proportions: (1) EFLS, (2) DH82 cells, (3) 33% EFLS and 67% DH82 cells, (4) 50% EFLS and 50% DH82 cells, (5) 67% EFLS and 33% DH82 cells. Cells were incubated at 37°C in 5% CO_2. Proliferation characteristics of each population were analysed using an Accuri™ C6 flow cytometer (BD Biosciences, California, USA). The fluorescence emission intensities of the GFP-expressing DH82 cells and efluor-EFLS were measured by the 533/30nm interference filter (FL-1/GFP-filter) and the 675/25nm interference filter (FL-4/Efluor-filter) respectively. Fluorescence emission wavelengths of these fluorophores were sufficiently different to ensure that no overlap in detection between the interference filters occurred.

Fluorescent microscopy was conducted using a Nikon eclipse 80i microscope to visualise GFP-expressing DH82 cells using a GFP-filter. GFP-expressing DH82 cell confluence within the mixed co-cultures was recorded. Both populations were imaged simultaneously using a three channel confocal microscope (Zeiss LSM510 Meta Confocal microscope, Axioplan 2 stand); the GFP-expressing DH82 cells were excited using a green (488/532nm) laser line and detected with a FITC band pass filter. Efluor-labelled EFLS were excited using a far red (633nm) laser line and detected with a 660/20nm band pass filter. Confluence of both populations were observed and recorded.

4.2.3.4 Design, Validation and Testing of Species-Specific qPCR Assays

Equine and canine mRNA sequences for the following genes; GAPDH, IL-1β, TNF-α, IL-6, ADAMTS4, ADAMTS5, were located from the NCBI Genbank database (Table 4.2). Equine and canine mRNA sequences, for the genes of interest, were directly compared using an NCBI BLAST search to find areas of dissimilarity, which were then used for primer design. All primers were designed using Primer Express 2.0 software (Applied Biosystems, California, USA) and obtained from Eurogentec (Liege, Belgium). BLAST searches, using the entire Equus caballus genome and Canis lupus genome, were performed with all primer sequences to establish gene specificity. Primer pairs were validated using serial 2-fold dilutions of either EFLS or DH82 cDNA, extracted from cells which had been cultured individually (Figures 4.8 and 4.9). Primers were also tested on cDNA from EFLS, DH82, and mixed EFLS and DH82 cultures (n=3) at 0, 1, 3, 6, 12 and 24 hours to investigate their species-specificity (Figures 4.6 and 4.7). QRT-PCR analysis was performed for both the validation and species-specificity tests. Dissociation curves for all PCR reactions were analysed to ensure primers were producing one single amplicon (Figures 4.6 and 4.7).

4.2.3.5 EFLS and DH82 Co-cultured With Direct Contact

EFLS (n=3 horses, 2 biological replicates) and DH82 cells were seeded either independently, or as co-cultures within the same well, in 6-well plates at 1.5 x 10^5 cells per well in 2ml standard culture media (Figure 4.1). Cells were cultured overnight. Cells were then exposed to 10µg/ml LPS and

harvested at 0 (no LPS exposure), 1, 3, 6, 12, and 24 hours post-LPS exposure. Media was removed and stored at -20°C. Cell layers were exposed to Tri-reagent (Ambion, Warrington, UK) for 1-2 minutes then pipetted vigorously to ensure all cells had detached. Samples were transferred to RNA-free eppendorphs and stored at -80°C. Where necessary prior to co-culture, DH82 cells were transfected with 25pmol custom designed anti-canine IL-1β siRNA (Life technologies, California, USA) or silencer Cy3 labelled negative control siRNA (csiRNA) (Life technologies, California, USA). DH82 cells were first seeded at 150,000 cells per well of a 6-well plate, before undergoing transfection using the lipofectamine 2000 transfection reagent (Life Technologies, Carlsbad, USA). Alternatively EFLS in co-culture were pre-treated with either 0.8μM Bay 11-7082 (B5556, Sigma-Aldrich, Missouri, USA) or 200μM Pyrrolidinedithiocarbamic acid (PDTC) (Enzo Life Sciences, New York, USA) for 1 hour prior to LPS exposure.

4.2.3.6 EFLS and DH82 Co-cultured Without Direct Contact

The influence of DH82 cells on EFLS in the absence of direct cell contact was examined in experiments using conditioned medium from DH82 cells or by compartmentalised co-culture of the cells. For the former, DH82 cells were stimulated with 10μg/ml LPS for 24h and conditioned media was collected (CM). To examine the effect of protein denaturation on conditioned media activity, aliquots were heated to 100°C for 10 mins prior to further use. This was referred to as denatured conditioned medium (DCM). EFLS cells were seeded at 5 x 10^4 cells per well in 24-well plates for 24h hours before

being exposed to either unconditioned media, CM or DCM, with and without 10μg/ml LPS. Compartmentalised culture was performed by seeding 20,000 DH82 cells into a 0.45μm cell culture insert (Merck Millipore, Darmstadt, Germany) for 24 hours to attach. Inserts were then transferred to a well containing a monolayer of EFLS (Schema 4.1). The co-cultures were stimulated with 10μg/ml LPS. EFLS cell layers from indirect co-culture experiments were harvested using Tri-reagent (Ambion, Warrington, UK) at 6 and 12 hours post-LPS exposure.

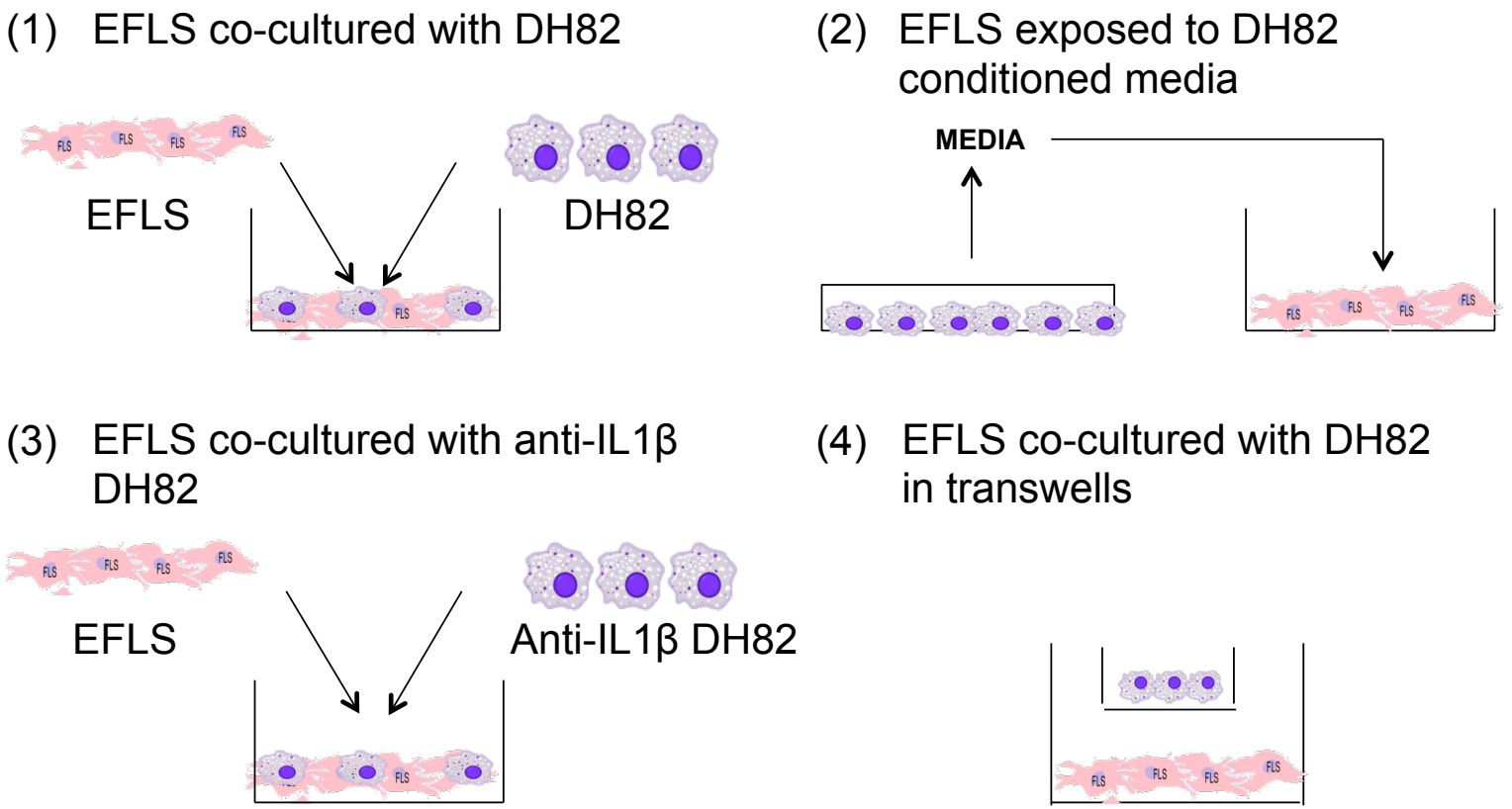

Schema 4.1 Different co-culture conditions. EFLS (n = 3 horses, 2 technical replicates) were co-cultured with DH82 cells using a variety or direct and indirect co-culture conditions.

4.2.4 Reverse Transcription and Quantitative Real-time PCR

Total RNA was purified from tri-reagent extracts using the Guanidinium-thiocyanate-phenol-chloroform technique (Chomczynski and Sacchi 1987), and measured using a Nanodrop ND-100 spectrophotometer (Labtech, Florida, USA). Reverse transcription was carried out on 1µg RNA using M-MLV reverse transcriptase (Promega, Wisconsin, USA) primed with random hexadeoxynucleotides (Random Primers, Promega, Wisconsin, USA). The qRT-PCR was performed with 160ng cDNA using SYBR Green master mix (GoTaq qPCR Master Mix, Promega, Wisconson, USA) and each primer at 300nM concentration on an ABI 7300 Real Time PCR system (Applied Biosystems, California, USA). The relative quantification of each gene normalised to the GAPDH reference gene was calculated using the $2^{-\Delta Ct}$ method (Livak, Schmittgen et al. 2001).

4.2.5 Statistical Analysis

Two tailed t-tests were used to compare fold changes in EFLS mRNA expression when cultured independently in standard culture media, compared to those cultured with DH82, in conditioned media, in denatured conditioned media, and with DH82 cells in well-inserts, and also to compare the gene expression of DH82 cells cultured alone and in co-culture with EFLS. One-tailed t tests with bonferroni post hoc corrections were used to compare DH82 gene expression when treated with control siRNA compared to anti-IL-1β siRNA, and EFLS ADAMTS5 gene expression when cultured with DH82 cells either treated with control siRNA or anti-IL-1β siRNA, or when pre-treated with NF-κB inhibitors.

4.3 Results

4.3.1 LPS Stimulated EFLS Secreted Increased Levels of ADAMTS5 Protein

We were initially interested in the levels of ADAMTS5 protein in the cell layer and media of EFLS exposed to inflammatory stimulation. We therefore cultured EFLS in the presence or absence of LPS for 6 or 16 hours. We analysed proteins in the cell layer and culture media by western blotting using an antibody raised to murine ADAMTS5. Preliminary analysis (not shown) had established that this antibody also recognised the human ADAMTS5 protein, and these experiments demonstrate that it also cross-reacts with equine ADAMTS5 protein. The predominant form of ADAMTS5 in cell layers, had a molecular weight of 75kDa, however different forms of the protein (55-60kDa and 100kDa) were also present. No notable induction of ADAMTS5 protein was observed in cell layers following exposure to LPS. We detected ADAMTS5 protein secreted in to the culture media with a molecular weight of approximately 55kDa. Its levels were increased upon exposure of the cells to LPS and appeared to accumulate with time (Figure 4.1).

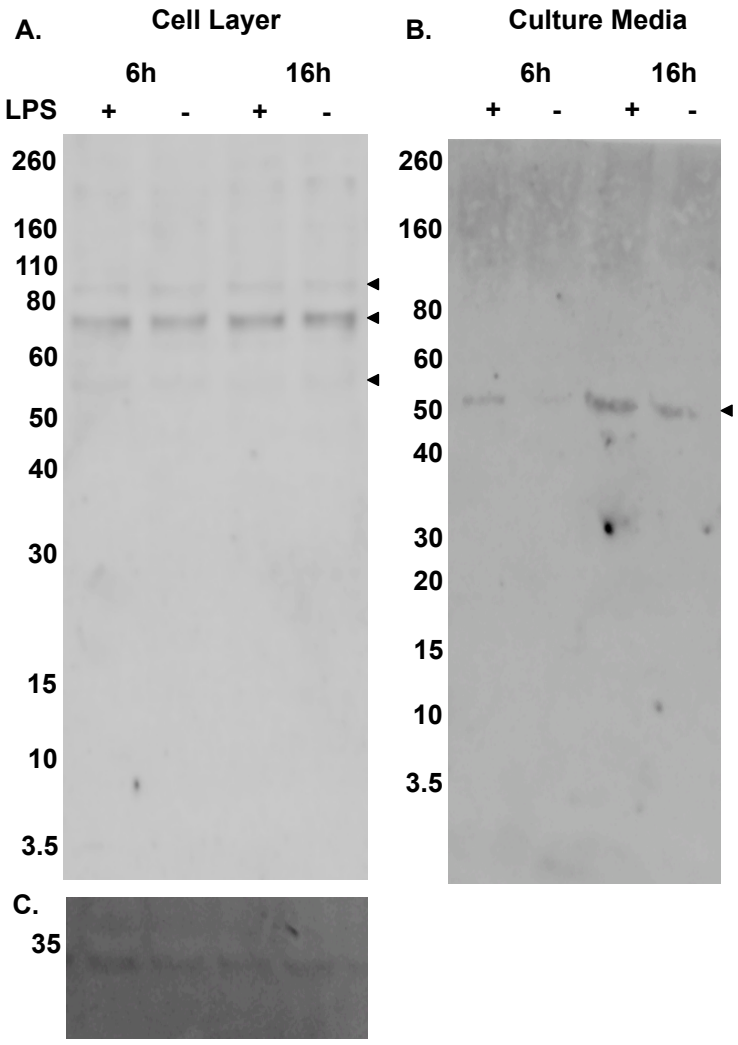

Figure 4.1 Expression of ADAMTS5 in cell layer and culture media. EFLS were cultured in the presence or absence of 10µg/ml LPS. Western blotting was performed on (A) cell layers and (B) culture media harvested at 6 and 16 hours post-LPS exposure, using an antibody which recognises ADAMTS5. (C) GAPDH was used as a loading control.

4.3.2 Design of the Inter-Species Co-Culture Model

We were interested in how the ADAMTS5 response of EFLS was affected by interactions with inflammatory cells that they might encounter in vivo. We therefore generated a multi-species co-culture model to allow us to investigate cell interactions whilst being able to specifically measure the response of the EFLS at the mRNA expression level. We fluorescently labelled EFLS with the Cell Proliferation Dye eFluor® 670 (eBioscience Inc., California, USA), and generated canine DH82 macrophage cells that expressed GFP so that we could examine their proliferation characteristics when cultured together.

4.3.2.1 Optimal Fluorescent Labelling of EFLS for a 24 Hour Experiment

All concentrations of cell proliferation dye eFluor® 670 (eBioscience Inc., California, USA) successfully labelled EFLS, producing fluorescence intensity (FI) $>10^5$ from peak cell numbers after 24 and 48 hours of culture. EFLS labelled with 8μM and 9μM cell proliferation dye eFluor® 670 concentrations, produced the highest number of cells emitting optimal FI after 24 and 48 hours of culture respectively (Figure 4.2). After 24 hours of culture, the highest number of cells were emitting at a FI of approximately 10^6, whereas after 48 hours culture this had decreased to approximately $10^{5.}$ This is consistent with a decrease in the amount of dye contained in each cell due to cell division. On analysis of EFLS gene expression profiles (Figure 4.10), it was noted that peak expression of the cytokines and aggrecanases of interest occurred within 12 hours of LPS-exposure. Co-

culture models were therefore designed to extend a 24 hour time course and 8μM proliferation dye was used to label EFLS.

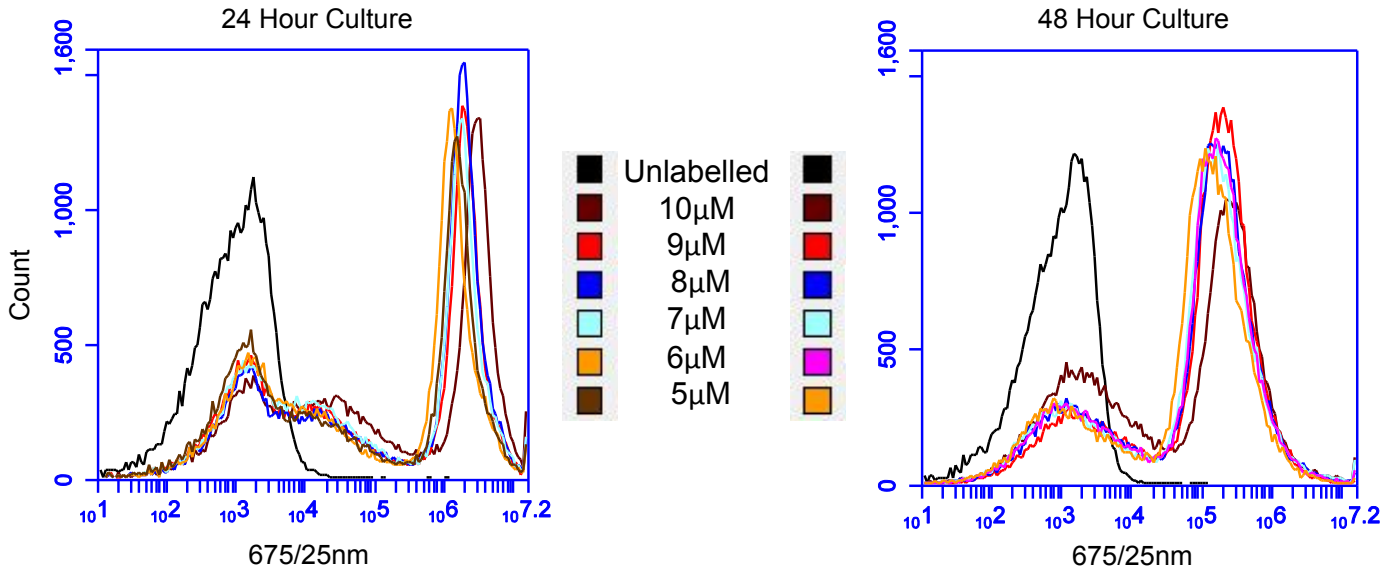

Figure 4.2 Flow cytometric analysis of EFLS labelled with different µM concentrations of Cell Proliferation Dye eFluor® 670. Fluorescence intensity (x-axis) detected using a 675/25nm interference filter (FL4-A) against cell count (y-axis); unlabelled EFLS (black line) demonstrate background fluorescence intensity (<10^5). Labelled EFLS emit a higher fluorescence intensity (>10^5) at a wavelength detected by the 675/25nm interference filter. Cells harvested at 24 hours emit at a higher intensity (approx. 10^6) than those harvested at 48 hours (approx. 10^5). The coloured lines represent different µM concentrations of the cell proliferation dye, used to label EFLS, as shown in the legend.

4.3.2.2 GFP-Expressing DH82 Cells

DH82 cells were infected with four different multiplicities of infection (MOI) conditions; an MOI of 2 and 4 were found to produce the most effective lentiviral transfection (Figure 4.3). Populations of GFP expressing DH82 cells were then selected through exposure to puromycin, and successfully expanded in culture.

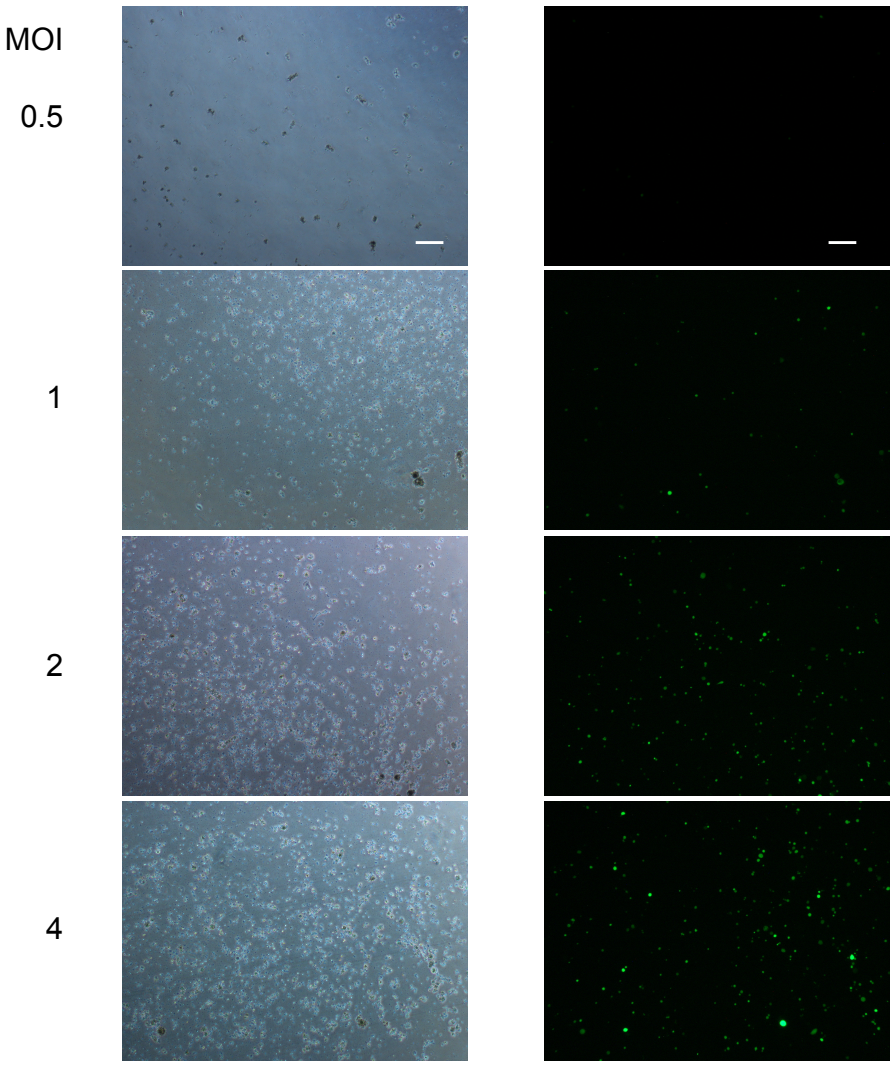

Figure 4.3 DH82 cells infected with different MOIs of lentiviral particles expressing an active GFP gene at. DH82 cells were transfected with differing ratios of lentiviral particle numbers compared to number of cells, otherwise known as multiplicity of infection (MOI). MOI 2 and 4 cultures produced a sufficient number of GFP-expressing DH82 cells and were expanded. Phase contrast image (left), fluorescent microscopy using the green fluorescence filter (right), scale bar = 100µm, x10 .

4.3.2.3 Visualising Fluorescence Emission from Labelled EFLS and DH82

When analysing co-culture samples using a confocal microscope, it was clear that both labelling techniques had been successful. However, the cell proliferation dye produced less discernable EFLS borders, possibly due to the large cell area and subsequent low intracellular concentration of proteins (Figure 4.4). After 24 hours of culture, it was clear that neither cell population had expanded to full confluence, EFLS and DH82 cell populations appeared approximately equal at all co-culture proportions. Flow cytometric analysis enabled specific comparisons of cell proliferation rates to be made.

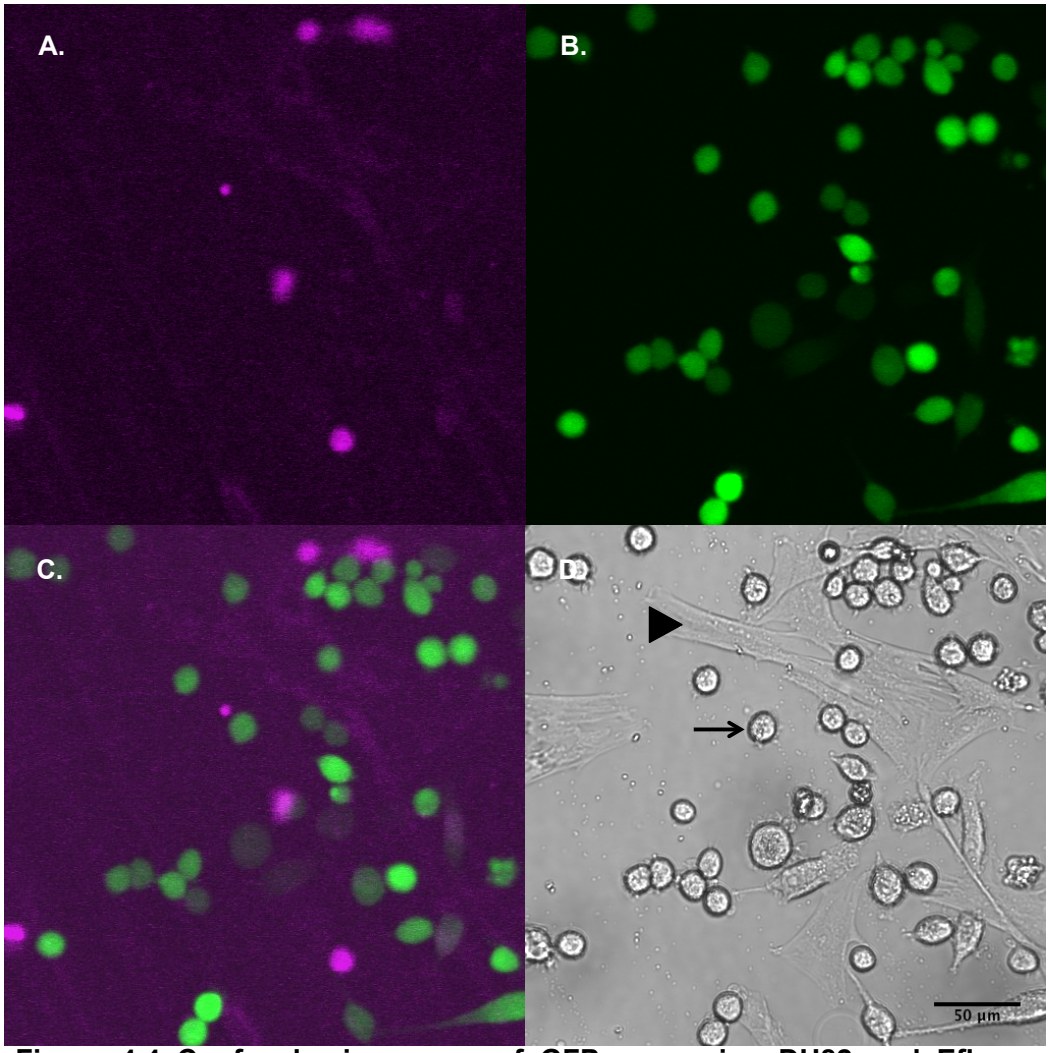

Figure 4.4 Confocal microscopy of GFP-expressing DH82 and Efluor-labelled EFLS cells in 1:1 Co-Culture. (A) Efluor-labelled EFLS (purple) excited using a far red (633nm) laser line and detected with a 660/20nm band pass filter. (B) GFP-expressing DH82 (green) were excited using a green (488/532nm) laser line and detected with a FITC band pass filter. (C) An overlay image of A and B. (D) Plain contrast image of DH82 (arrow) and EFLS (arrowhead) cells in co-culture.

4.3.2.4 Seeding Density of Equal Proportions of DH82 and EFLS Resulted in a Co-Culture Containing 40% DH82 and 60% EFLS after 24 Hours

During flow cytometry, side scatter (SSC) and forward scatter (FSC) describe the direction of light refracted by cells obstructing the path of the laser beam. SSC and FSC are consistent with intracellular complexity, sometimes referred to as granularity, and cell size respectively. SSC versus FSC density plots identified two groups of cells with differing morphological characteristics within the mixed culture. After analysis of individual cultures, EFLS were identified to be smaller and less granular than DH82 cells (Figure 4.5A & B). Once populations were identified, the two populations within the mixed culture were gated on the SSC vs FSC density plot (G1 = EFLS, G2 = DH82) (Figure 4.5C). The majority of cells within the G1 gated area emitted at a FI $>10^5$, detected by the 675/25nm interference filter, consistent with efluor-labelled EFLS (Figure 4.5D). The majority of cells within the G2 gated area emitted at a FI $>10^5$, detected by the 533/30nm interference filter, consistent with GFP-expressing DH82 cells (Figure 4.5E).

Once populations were identified, proliferation rates of each population in co-culture were analysed. A slightly higher rate of EFLS proliferation compared to DH82 proliferation, when co-cultured over 24 hours was observed, and EFLS mitosis was stimulated by co-culture with DH82 cells (Figure 4.5F & G, and Table 4.1). When efluor-labelled EFLS were cultured independently, the majority of cells (67%) emitted at a FI of $10^{5.3}$ – $10^{6.7}$. The efluor cell proliferation dye 670 therefore has a binding efficiency of 67% after 24 hours of culture, when applied to EFLS. The remainder of the cells emitted at a FI

consistent with background fluorescence. Background fluorescence can be due to the auto-fluorescence of the sample, vessel or media. When structures within the cell, such as mitochondria or lysosomes absorb light, it is also emitted at a low FI, otherwise known as auto-fluorescence.

The efluor cell proliferation dye binds to primary amine side chains, found on polypeptides. As the cell undergoes mitosis, the dye is distributed equally between the two daughter cells, and this can be measured by the FI halving. Within mixed co-cultures, fluorescence detected by the 675/25nm interference filter identified two sub-populations of EFLS consistent with the two peaks in cell numbers. Sub-populations emitting FI at $10^{5.3}$-$10^{6.7}$ and $10^{3.3}$-$10^{5.3}$ FI, are consistent with the primary and secondary generation of EFLS respectively (Figure 4.5F). The sum of both populations is equal to the total EFLS cell number. On comparison of EFLS cultured independently and co-cultured with DH82 cells, a secondary EFLS population was only identified upon co-culture. This could indicate that the addition of DH82 cells stimulates EFLS mitosis.

The number of labelled DH82 and EFLS cells within each co-culture was analysed to calculate the proportion of each population after 24 hours. Fluorescence intensities corresponding to peaks in cell numbers were gated; the primary (G3) and secondary (G4) generations of EFLS, and DH82 cells (G5) (Figure 4.5F&G). Cell numbers can be found in Table 4.1. The initial seeding ratio of 50% EFLS and 50% DH82, produced a culture of 60% EFLS and 40% DH82 after 24 hours. An infiltration of cells into the synovial membrane, resulting in 25-50% of the synovial cell population consisting of mononuclear cell, has been classified as a moderate (grade 3 out of 4)

synovitis (McIlwraith, Frisbie et al. 2010). This proportion of cells was therefore deemed appropriate to replicate a moderate synovitis after 24 hours in culture.

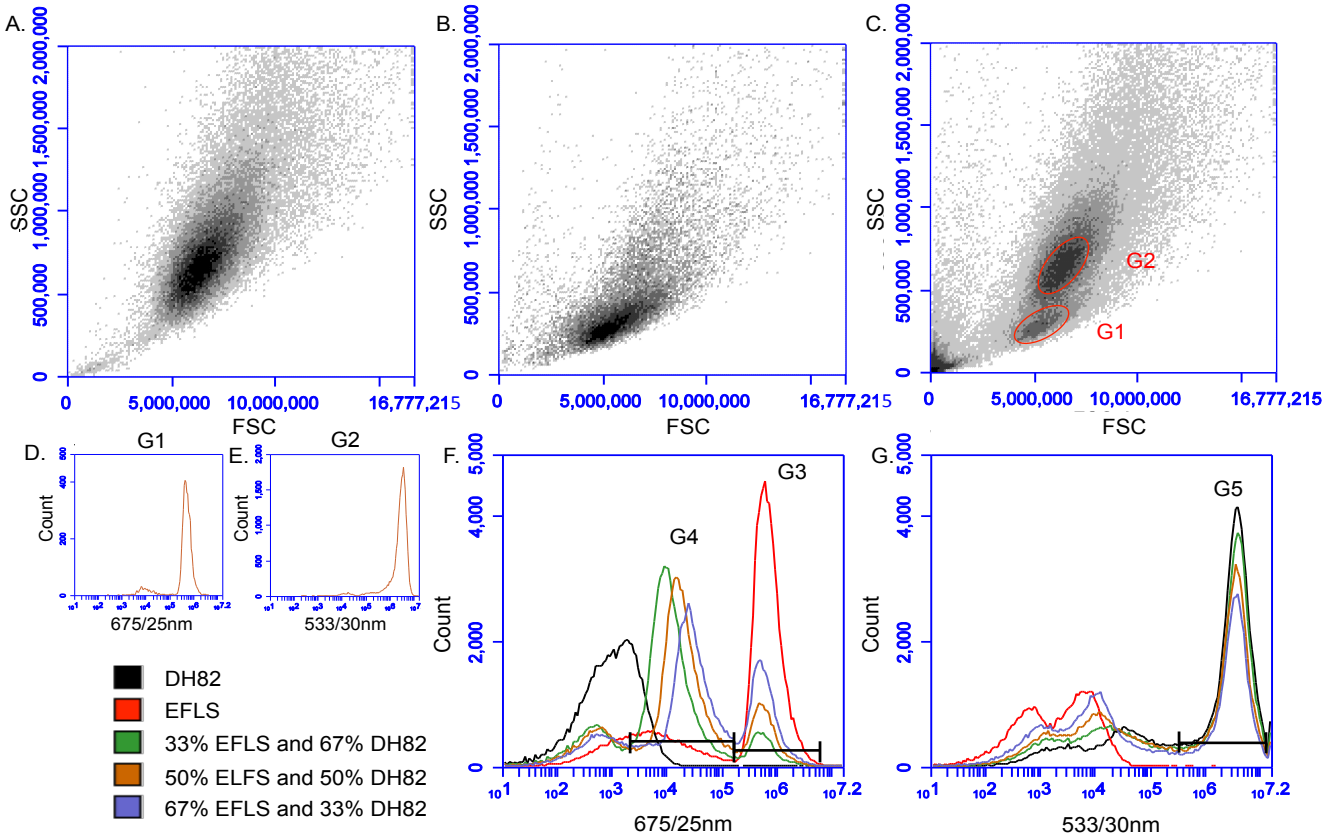

Figure 4.5 Graphs displaying GFP-expressing DH82 and efluor-labelled EFLS cellular characteristics and fluorescence intensities emitted in co-culture. A-C. Density plot diagrams of DH82 (A) and EFLS (B) cultured individually and in co-culture (C); EFLS (G1) and DH82 (G2) populations were gated. D & E. Fluorescence intensity emitted from cells within the gated areas (D = G1, E = G2). F & G. Fluorescence intensity emitted by labelled DH82 and EFLS after 24 hours in co-culture at different proportions, detected by two different interference filters, 675/25nm and 533/30nm respectively. Gates corresponding to EFLS primary (G3) and secondary (G4) generations, and DH82 cells (G5) were applied to enable cell numbers within each co-culture to be determined.

Table 4.1 Cell numbers of DH82 and EFLS within gated regions.

	EFLS			DH82	
Proportion of each population in co-culture	**Cell number emitting FI at $10^{3.3}$ – $10^{5.3}$ (G4)**	**Cell number emitting FI at $10^{5.3}$ – $10^{6.7}$ (G3)**	**Total EFLS cell number emitting FI >$10^{3.3}$**	**Cell number emitting FI at $10^{5.6}$ – $10^{7.2}$ (G5)**	**Relative proportion of each population (EFLS:DH82)**
EFLS	-	66,750	66,750	-	100%
DH82	-	-	-	68,312	100%
33% EFLS and 67% DH82	66,150	8,448	74,598	59,260	55.7:44.3%
50% EFLS and 50% DH82	59,926	15,255	75,181	51,191	59.5:40.5%
67% EFLS and 33% DH82	52,068	15,255	78,096	43,051	64.5:35.5%

4.3.2.5 Production of Species-Specific qRT-PCR Assay

To allow us to specifically measure expression of genes in each cell type when they were cultured together we designed species-specific qRT-PCR assays. To analyse primer performance, cycle threshold (Ct) values from samples (n=3) harvested at each time point (0, 1, 3, 6, 12, and 24 hours) were amalgamated to produce total Ct values for each condition. The mean total Ct values produced by EFLS, DH82 and co-culture cDNA are displayed using histograms in figures 4.6 and 4.7. Primers met the following criteria and were thus deemed to be species-specific.

4.3.2.6 Testing the Species Specificity of each Primer

Firstly, all primers measured robust expression, reflected by low Ct values when used on cultures of the same species (equine and canine primer Ct values were 18.0-25.2 and 15.8-23.6 respectively) which was conserved when analysing the co-cultures (equine and canine primer Ct values were 16.7-25.6 and 15.6-26.9 respectively) (Figure 4.6A-E & 4.7A-C). Low expression of genes, reflected by high Ct values (equine and canine primer Ct values were 32.8-36.1 and 32.2-38.9 respectively) or undetected Ct values (producing a Ct value of 0), were evident when primers were used on mRNA of a different species. However the canine GAPDH primer did produce a Ct value of 26.2, which is consistent with good gene expression, when it was used on equine cDNA.

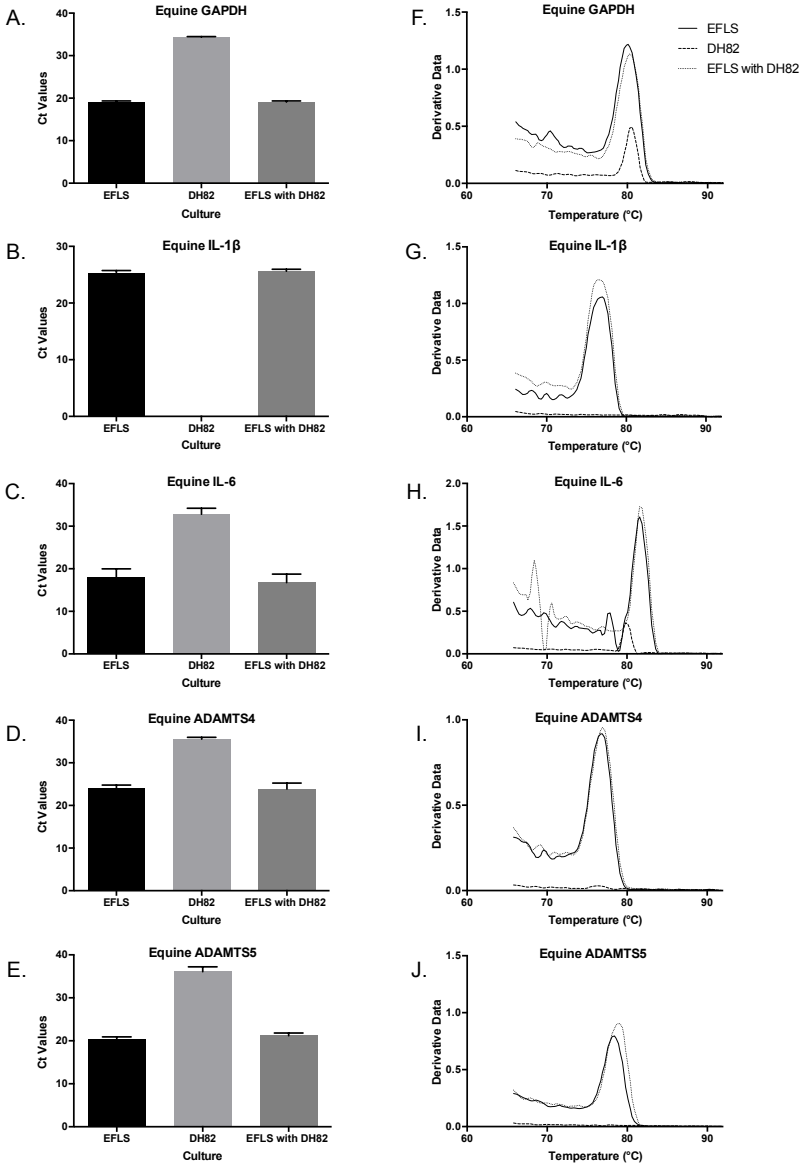

Figure 4.6 Equine primer species-specificity testing. A – E. Histograms display the mean sum of Ct values produced when equine primers were used on EFLS, DH82 or co-culture cDNA samples (n=3) harvested at 0, 1, 3, 6, 12 and 24 hours. Error bars represent SEM. F – J. Dissociation curves of amplicon products produced when equine primers were used on EFLS, DH82 and co-culture cDNA samples (n=3) harvested at 0, 1, 3, 6, 12 and 24 hours.

Secondly, dissociation curves of PCR products displayed a single peak when analysing both cells of the correct species, and co-cultures. Single peaks are often considered to reflect specific binding of the primer, resulting in the production of a single amplicon product. However, it has been shown that peaks at two different temperature can also be produced by the same amplicon product. Peaks were either not evident (Figure 4.6G & J), or very small (Figure 4.6F, H & I. Figure 4.7D-F) and peaking at the same temperature as those produced by cDNA of the same species, when primers were used on cultures of solely the opposite species. Small peaks at the same temperature are consistent with a low level of amplicon product from one species produced by the primer of a different species, however levels were insignificant. Canine GAPDH (Figure 4.7D) and to a much lesser degree IL-1β (Figure 4.7E) primers, also revealed some annealing to equine cDNA. The dissociation curve produced by the canine GAPDH primer used on EFLS cDNA had two peaks, one large peak at a higher temperature (>80°C) than the peak produced by DH82 and co-culture cDNA, and a second smaller peak at the same temperature as the large peak produced by the other cDNA (<80°C). The peak at >80°C may represent the same amplicon as the peaks <80°C, or a second amplicon may have been produced by non-specific binding of the canine GAPDH primer to equine cDNA. Canine GAPDH was used as a housekeeping gene, however, relative quantification of canine genes normalised to this housekeeping gene, may be underestimated. Analysis of canine specific ADAMTS4 and ADAMTS5 in DH82 cells was eventually omitted from the study as repeated iterations of primer design failed to identify a specific assay.

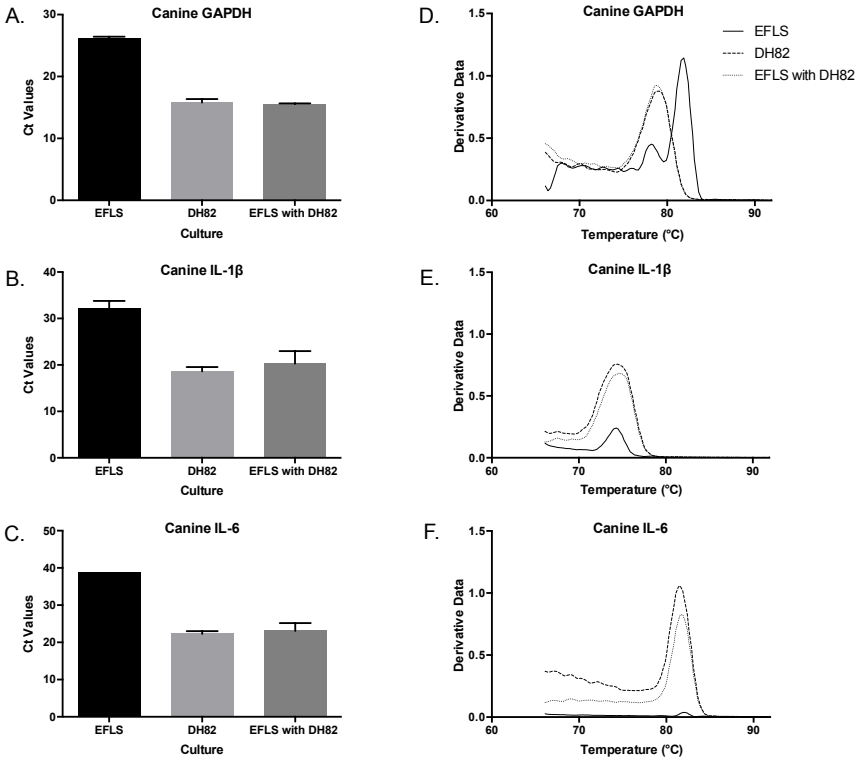

Figure 4.7 Canine primer species-specificity testing. A – C. Histograms display the mean sum of Ct values produced when canine primers were used on EFLS, DH82 or co-culture cDNA samples (n=3) harvested at 0, 1, 3, 6, 12 and 24 hours. Error bars represent SEM. D – F. Dissociation curves of amplicon products produced when canine primers were used on EFLS, DH82 and co-culture cDNA samples (n=3) harvested at 0, 1, 3, 6, 12 and 24 hours.

4.3.2.7 Primer Validation

Primer pairs were validated using serial 2-fold dilutions of cDNA from the same species (either EFLS or DH82 cDNA), extracted from cells which had been cultured individually. Standard curves were created for all primers (Figure 4.8A-E & Figure 4.9A-C). Using the linear regression equation produced by the standard curve, the primer amplification efficiency was calculated. The co-efficiency of determination (R) value produced by the standard curve was also recorded (Table 4.2). All equine primers, canine IL-1β and canine IL-6 annealed to cDNA from the same species (equine and canine cDNA respectively) with excellent amplification efficiency (91-108%). The canine GAPDH primer was less efficient (123%) at amplifying the target gene. Dissociation curves of cDNA at each dilution were produced. Equine primer dissociation curves displayed comparable peaks at all dilutions (Figure 4.8F-J). However dissociation curves produced by canine primer were variable (Figure 4.9D-F). Canine GAPDH and IL-1β primers produced a second dissociation peak from the more dilute canine cDNA samples (1:16 and 1:32 dilutions). The canine IL-6 primer produced a second peak from all dilutions of cDNA; the less dilute canine cDNA samples (0, 1:2, 1:4 and 1:8 dilutions) had a second peak at a higher temperature than more dilute cDNA samples (1:16 and 1:32 dilutions).

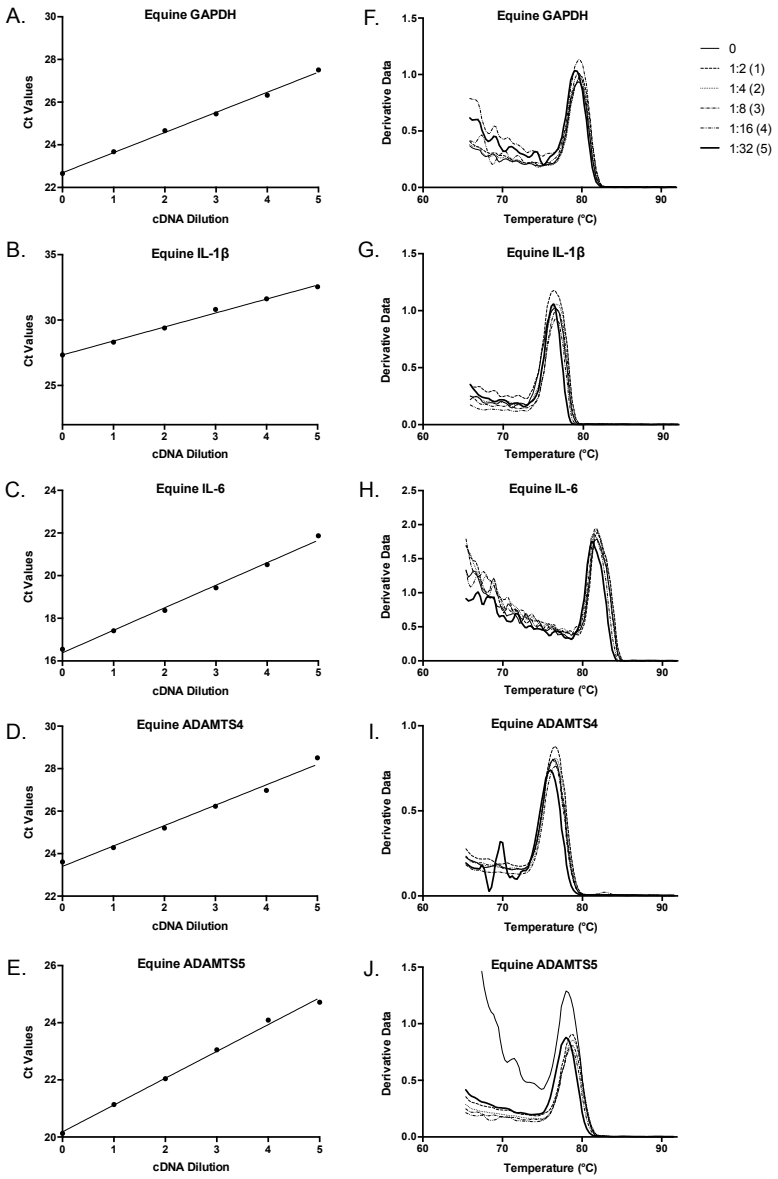

Figure 4.8 Standard curves and dissociation curves for all equine primers tested on EFLS cDNA. A-E. EFLS cDNA (n=3) was diluted in serial 2-fold dilutions and mixed with equine primers. The standard curves are presented as Ct values (y-axis) against the dilution of cDNA (x-axis); concentrated cDNA (0), 1:2 dilution (1), 1:4 dilution (2), 1:8 dilution (3), 1:16 dilution (4), 1:32 (5). F-J. Dissociation curves produced by each primer mixed with cDNA at all dilutions are displayed.

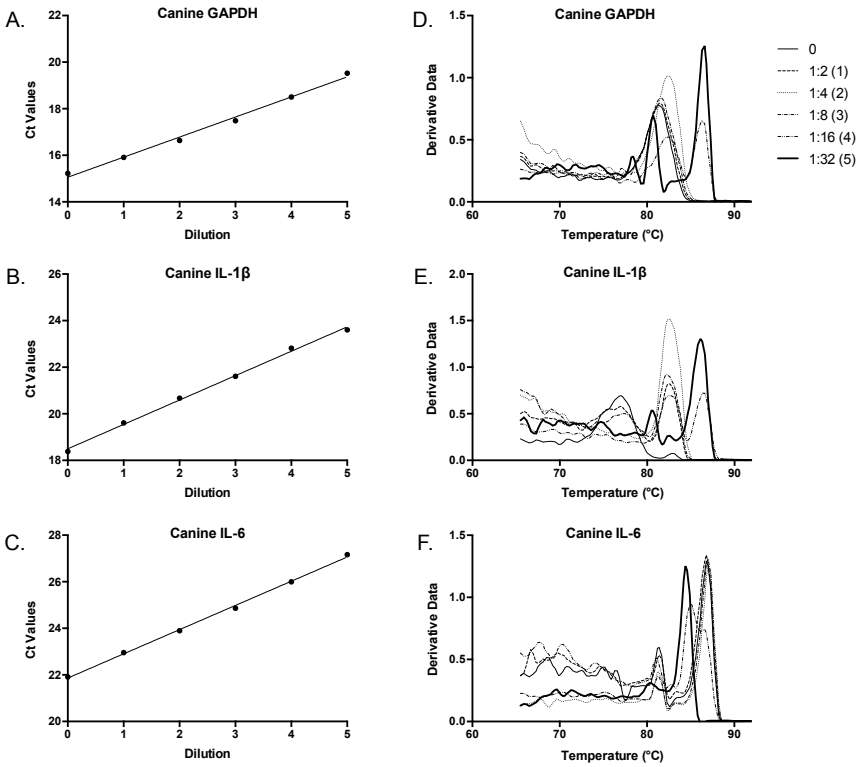

Figure 4.9 Standard curves and dissociation curves for all canine primers tested on DH82 cDNA. A-C. DH82 cDNA was diluted in serial 2-fold dilutions and mixed with canine primers. The standard curves are presented as Ct values (y-axis) against the dilution of cDNA (x-axis); concentrated cDNA (0), 1:2 dilution (1), 1:4 dilution (2), 1:8 dilution (3), 1:16 dilution (4), 1:32 (5). D-F. Dissociation curves produced by each primer mixed with cDNA at all dilutions are displayed.

Equine Primers

Gene	Gene Accession No.	Sequence	R	Efficiency
GAPDH	NM_001163856.1	F:TGACCCCCTAACATATTGAGAGTCT R: GCCCCTCCCCTTCTTCCTG	1	108%
IL-1β	NM_001082526.1	F: GAGCCCAATCTTCAACATCTATGG R: ATACCAAGTCCTTTTACCAAGCCTG	0.99	91%
IL-6	NM_001082496.1	F: CCTGGTGATGGCTACTGCTTTC R: GGATGTACTTAATGTGCTGTTTGGTT	0.99	92%
ADAMTS4	NM_001111299.1	F: CAGCCTGGCTCCTTCAAAAA R: ATGTGGTCACTATTCCTGCGG	0.99	106%
ADAMTS5	XM_003364218.2	F: ACCGATCCTGCAGTGTCACA R: AAATCTTTTCGCCATGAGCAG	1	101%

Canine Primers

Gene	Gene Accession No.	Sequence	R	Efficiency
GAPDH	NM_001003142.1	F: AACTGCTTGGCTCCTCTAGCC R: CCACGATGCCGAAGTGGT	0.99	123%
IL-1β	NM_001037971.1	F: CTATCATCTGCAAAACAGATGCG R: GCATGGCTGCATCACTCATAAA	1	94%
IL-6	NM_001003301.1	F: CCTGGTGATGGCTACTGCTTTC R: TGGCATCATCCTTGGAATCTC	1	95%

Table 4.2 Equine and Canine primers. Equine and canine gene sequences, corresponding to the accession numbers displayed, were located within the NCBI Genbank database. The nucleotide sequences for the primer pairs designed are displayed. The efficiencies and co-efficiencies of determination (R) of all primer pairs were calculated using serial 2-fold dilutions of either EFLS or DH82 cDNA, extracted from cells which had been cultured individually.

4.3.3 Comparative Gene Expression of EFLS and DH82 Cells when Cultured in the Co-Culture Model

4.3.3.1 Macrophages Attenuate EFLS ADAMTS5 Gene Expression.

EFLS cultured independently demonstrated rapid increases in IL-1β, IL-6, ADAMTS4 and ADAMTS5 mRNAs in response to 10μg/ml LPS (Figure 4.10A-D). Peak expression of each mRNA occurred 3 to 6 hours post-LPS exposure. Fold changes in EFLS gene expression were normalised to the gene expression of independently cultured EFLS at 0 hours with no LPS exposure. Maximum fold changes in mRNA levels of EFLS cultured independently and with DH82 cells respectively, were 10 x (at 6 hours) and 14 x (at 3 hours) for IL-1β mRNA, 50 x (at 6 hours) and 27 x (at 6 hours) for IL-6 mRNA, 18 x (at 3 hours) and 16 x (at 3 hours) for ADAMTS4 mRNA, and 4 x (at 6 hours) and 1.4 x (at 6 hours) for ADAMTS5 mRNA. Interestingly, the increased expression of ADAMTS5 mRNA over this time period was significantly ($p < 0.05$) lower in EFLS that were co-cultured with DH82 cells (Figure 4.10D). Although ADAMTS4 and IL-6 mRNA levels tended to be lower when EFLS were in co-culture, lack of a consistent effect across the three biological replicates prevented us from concluding that they were also stastically significantly affected (Figure 4.10B & C).

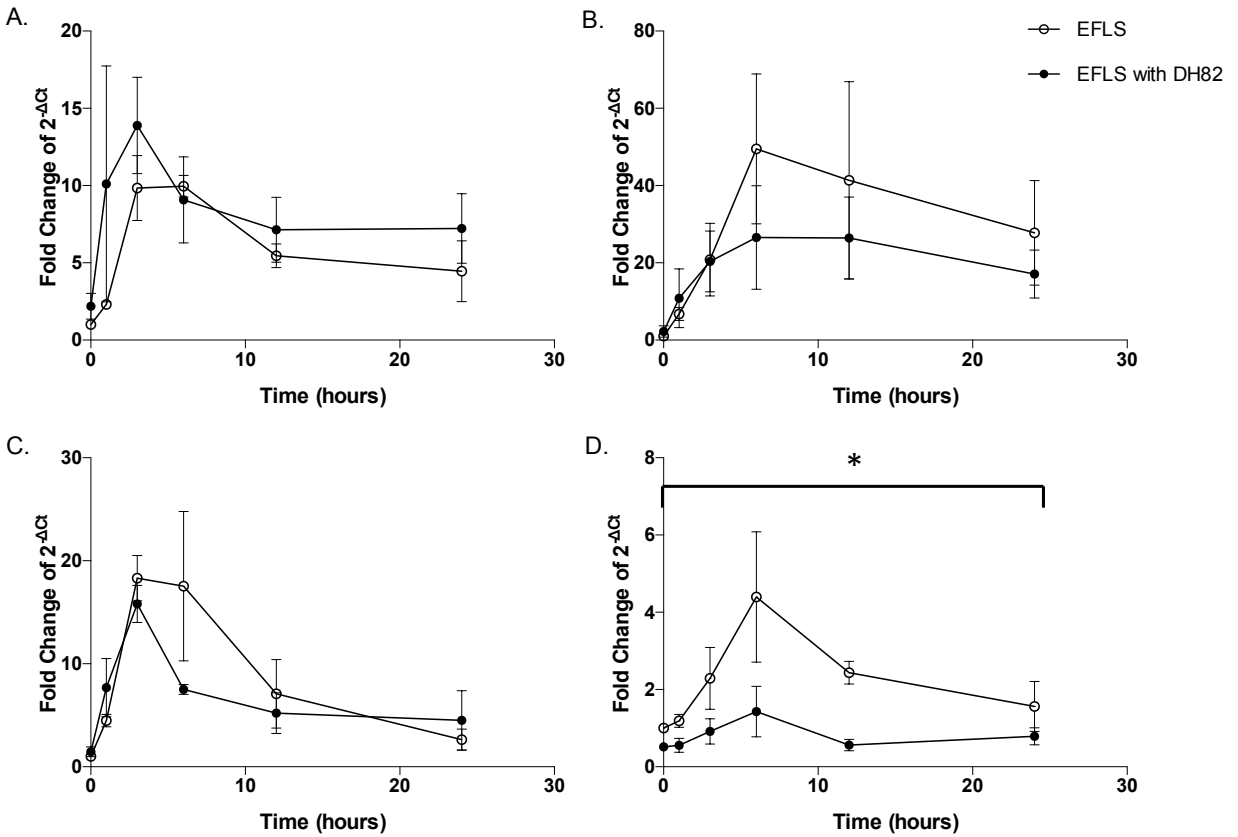

Figure 4.10 Fold changes of EFLS gene expression when cultured independently or in co-culture with DH82 macrophages. EFLS (A) IL-1β, (B) IL-6, (C) ADAMTS4 and (D) ADAMTS5 gene expression when cultured independently (clear circles) or in co-culture with DH82 (black circles) is displayed as fold changes (n=3) compared to the gene expression of independently cultured EFLS at 0 hours with no LPS exposure. Gene expression was measured at 1, 3, 6, 12 and 24 hours post-LPS exposure. Error bars represent SEM. Increased expression of ADAMTS5 mRNA over the 24 hour period was significantly (* $p<0.05$) lower when EFLS were cultured with DH82.

4.3.3.2 DH82 Cell Gene Expression when Co-Cultured with EFLS

DH82 cells cultured independently or in co-culture with EFLS, experienced a repeatable and rapid increase in their gene expression of the cytokines IL-1β and IL-6 upon exposure to LPS (Figure 4.11A-B). Fold changes in DH82 gene expression were normalised to the gene expression of independently cultured DH82 cells at 0 hours with no LPS exposure. Peak fold change in IL-6 gene expression occurred earlier than IL-1β (3 hours and 12 hours respectively), and the mean expression of both cytokines were higher when co-cultured with EFLS, although this was not statistically significant using two-tailed t tests. Maximum fold changes in DH82 mRNA expression when cultured independently and in co-culture, were 103 x (at 12 hours) and 175 x (at 12 hours) for IL-1β mRNA, and 129 x (at 3 hours) and 182 x (at 3 hours) for IL-6 mRNA.

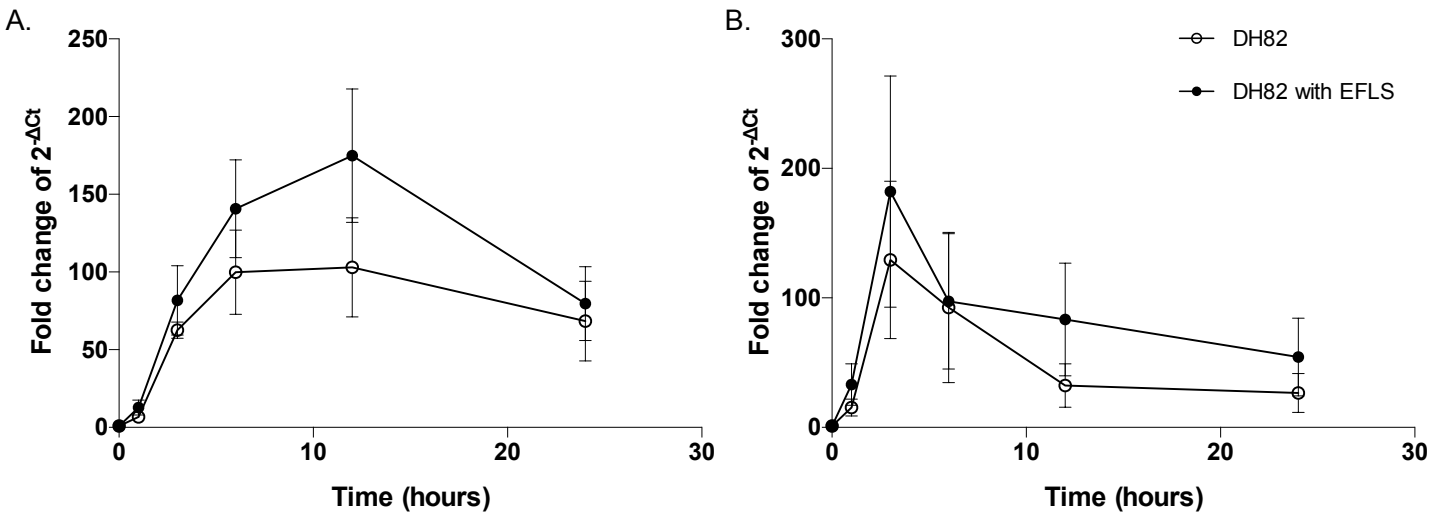

Figure 4.11 Fold changes of DH82 gene expression when cultured independently or in co-culture with EFLS. DH82 (A) IL-1β and (B) IL-6 gene expression when cultured independently (clear circles) or in co-culture with EFLS (n=3) (black circles) is displayed as fold changes (n=3) compared to the gene expression of independently cultured DH82 cells at 0 hours with no LPS exposure. Gene expression was measured at 1, 3, 6, 12 and 24 hours post-LPS exposure. Error bars represent SEM. Fold changes of the different conditions were not statistically different.

4.3.3.3 Macrophage Attenuation of EFLS ADAMTS5 is Not Driven by Macrophage IL-1β expression

When IL-1β binds to the IL-1 membrane bound receptor, it activates several pathways including the NF-κB pathway. RelA/p65, an NF-κB family member, is a strong transcriptional activator of ADAMTS5 in chondrocytes (Kobayashi, Hirata et al. 2013). It was hypothesised that DH82 IL-1β gene expression may influence EFLS ADAMTS5 gene expression. Statistically significant down-regulation of macrophage IL-1β gene expression was achieved at 6h ($p<0.05$) and 12h ($p<0.01$) post-LPS exposure, using anti-IL-1β siRNA compared to control siRNA (csiRNA) (Figure 4.12A). When anti-IL-1β DH82 cells were co-cultured with EFLS, EFLS ADAMTS5 gene expression was similar to that of EFLS cultured with normal DH82 cells (Figure 4.12B).

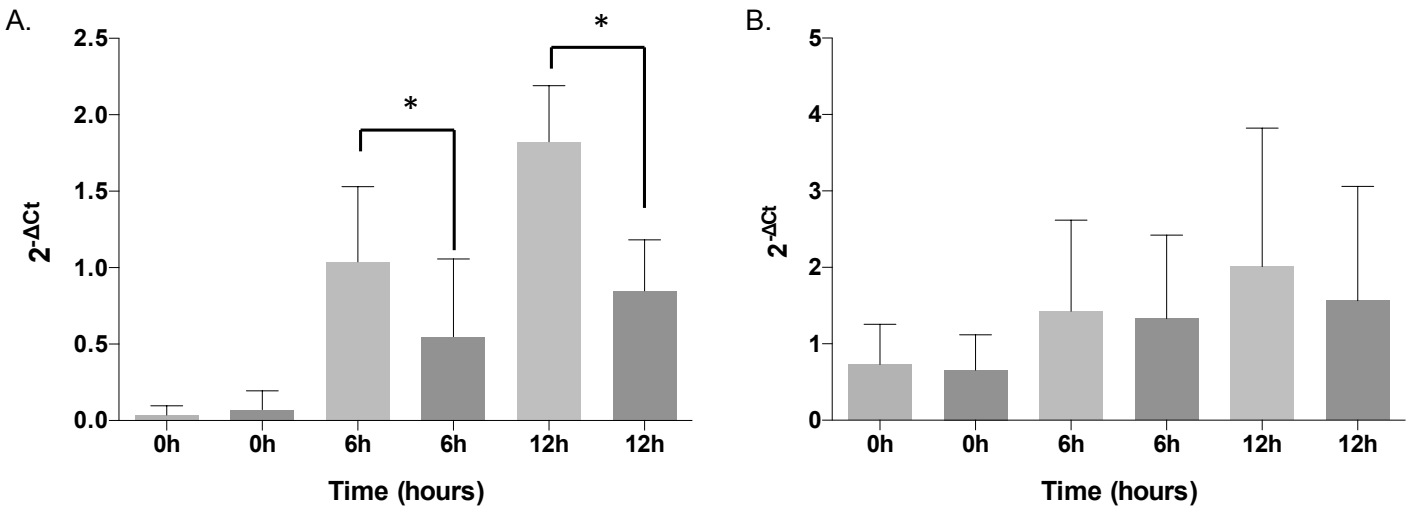

Figure 4.12 Histograms demonstrating DH82 and EFLS gene expression when in direct co-culture. DH82 were transfected with either csiRNA (light grey bars), or with canine anti-IL-1β siRNA (dark grey bars), and co-cultured with EFLS (n=3) in the presence of 10μg/ml LPS. Cultures were harvested at 0, 6 and 12 hours post-LPS exposure. Histograms display (A) DH82 IL-1β gene expression and (B) EFLS ADAMST5 gene expression. Error bars represent SEM. Statistically significant down-regulation of macrophage IL-1β gene expression was achieved at 6h (*$p<0.05$) and 12h (*$p<0.01$) post-LPS exposure, using anti-IL-1β siRNA compared to control siRNA (csiRNA), calculated using one-tailed t tests with bonferroni post hoc corrections.

4.3.3.4 A Soluble Mediator Produced by Macrophages is Responsible for the Attenuation of ELFS ADAMTS5 Gene Expression

Experiments were conducted to investigate whether the EFLS ADAMTS5 gene expression attenuation caused by DH82 cells was mediated through direct contact, or through a soluble mediator. EFLS gene expression is described as fold changes compared to the gene expression of EFLS cultured in standard culture media containing LPS for 12 hours. EFLS cultured in DH82 conditioned media (CM) expressed lower levels of ADAMTS5 mRNA following LPS exposure for 12 hours (Figure 4.13) compared with those cultured in LPS-containing unconditioned media (NM). This suggests that the attenuation of ADAMTS5 in the co-culture system is mediated by a soluble factor. Interestingly, EFLS expression of ADAMTS5 mRNA was also lower when the cells were cultured in denatured conditioned media (DCM) ($p < 0.01$), indicating that this soluble factor is thermally stable (Figure 4.13). Consistent with these findings, indirect co-culture culture of EFLS with DH82 using well inserts, also led to repressed ADAMTS5 mRNAs ($p < 0.01$) (Figure 4.13).

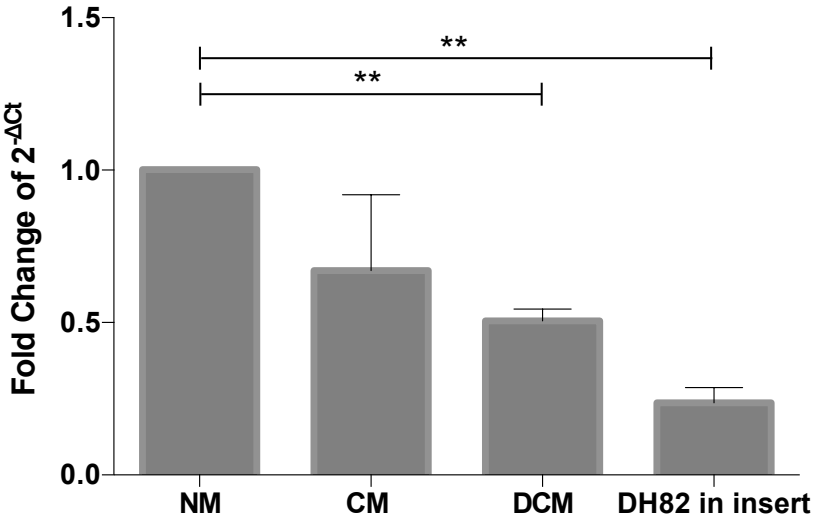

Figure 4.13 Histograms demonstrating EFLS ADAMTS5 gene expression when cultured in DH82 conditioned media, or with DH82 cells within well-inserts. Fold changes in EFLS ADAMTS5 gene expression are compared to EFLS cells cultured in LPS-containing normal media (NM). EFLS expression when cultured with DH82 conditioned media (CM) and DH82 denatured conditioned media (DCM) (** = $p < 0.01$), and with DH82 cultured in well inserts (** = $p < 0.01$) is displayed. Cells (n = 3) were harvested at 12 hours post-LPS exposure. All conditions were exposed to 10ug/ml LPS. Error bars represent SEM.

4.3.3.5 Co-Culture Does Not Influence EFLS ADAMTS5 Gene Expression Through NF-κB Signalling

To investigate the influence of the NF-κB signalling pathway on EFLS ADAMTS5 gene expression, EFLS in co-culture with DH82 cells were pre-treated with NF-κB inhibitors before being exposed to LPS (Figure 4.14). EFLS gene expression was compared to non-NF-κB inhibitor treated EFLS gene expression at 0h, and expressed as fold changes. Neither inhibitor prevented the suppression of ADAMTS5 induction in co-cultures. The presence of the inhibitor PDTC led to an overall suppression of EFLS ADAMTS5 gene expression levels, whilst the inhibitor Bay 11-7082 led to similar levels of ADAMTS5 mRNA compared to non-treated EFLS in co-culture, however these changes were not statistically significant.

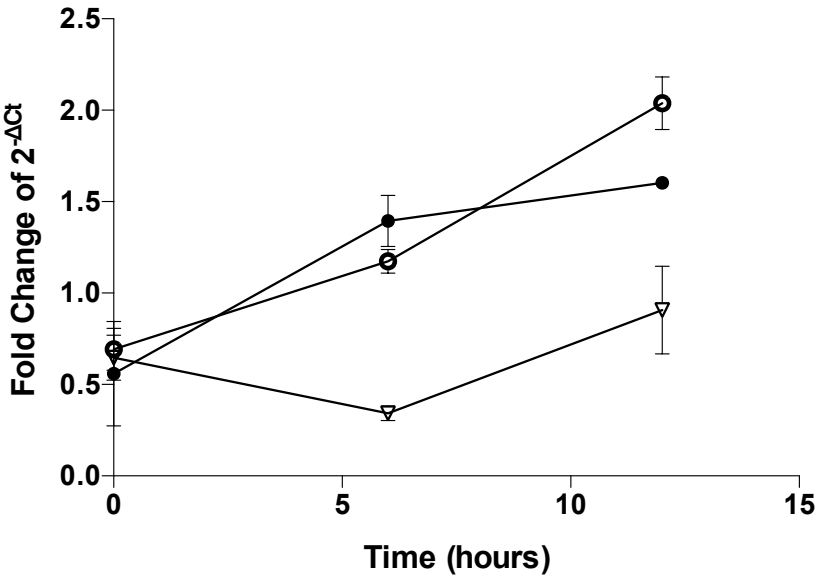

Figure 4.14 Fold changes in EFLS ADAMTS5 gene expression after pre-treatment with NF-κB inhibitors. EFLS (n =3) in direct co-culture with DH82 cells were pre-treated with NF-κB inhibitors; Bay 11-7082 (clear circle) and PDTC (triangle), before being exposed to 10μg/ml LPS. Cells were harvested at 0, 6 and 12 hours post-LPS exposure. Fold changes in EFLS ADAMTS5 gene expression were compared to the gene expression of EFLS cells in co-culture at 0h. EFLS without NF-κB inhibitor treatment are represented by the black circles. Error bars represent SEM.

4.4 Discussion

The synovial membrane is an important source of pro-inflammatory and catabolic mediators that contribute to the pathophysiology of osteoarthritis. Aggrecanases, such as ADAMTS4 and -5, are produced by synoviocytes and chondrocytes. We were particularly interested to observe an increase in the secretion of ADAMTS5 protein by FLS on exposure to LPS. Upon secretion from the cell, the ADAMTS5 zymogen (101.7kDa) is cleaved at furin cleavage sites, becoming activated (Fosang, Rogerson et al. 2008). The active form of ADAMTS5 (73kDa) is further cleaved into smaller breakdown products (40-50kDa) (Vankemmelbeke, Holen et al. 2001). Using western blotting, three variants of the ADAMTS5 protein were identified within the FLS cell layer; a major band (75kDa) consistent with the active form of the aggrecanase protein, and minor bands (55-60kDa and 100kDa) consistent with ADAMTS5 breakdown products and the ADAMTS5 zymogen respectively. The density of the major band (75kDa) increased in proportion to culture time, which reflects a higher degree of FLS activation with increasing time of exposure to LPS. Western blot analysis of cell media revealed extracellular ADAMTS5 protein (55kDa) present; levels increased with the addition of LPS and with increasing time of exposure to LPS. The LPS-induced increase in concentration of small ADAMTS5 fragments within the cell media may be caused by a combination of the following factors; the stimulation of EFLS ADAMTS5 secretion, the suppression of LRP-mediated endocytic clearance of ADAMTS5 from the media, or an increase in furin cleavage of ADAMTS5. The presence of LPS-induced extracellular

ADAMTS5 consistent with the active form, suggests that FLS may respond to inflammatory conditions by secreting active ADAMTS5.

Our co-culture model design was based on the inflammatory response observed in the synovial membrane. Normal synovium contains negligible numbers of lymphocytes. A moderate (grade 3 out of 4) synovitis has been classified, through microscopic histological examination, as having an infiltration of mononuclear cells in greater than 25 - 50% of the synovial membrane (McIlwraith, Frisbie et al. 2010). Macrophages are abundant within this cellular infiltration (Haseeb and Haqqi 2013) and are significant producers of IL-1β and TNF-α (Haywood, McWilliams et al. 2003, Bondeson, Wainwright et al. 2006) which drive the inflammatory pathway. Factors including TGF-β, platelet derived growth factor (PDGF) and macrophage chemoattractant protein-1 (MCP-1) are responsible for the chemotaxis of macrophages into the synovium. MCP-1 is produced by inflamed synoviocytes and this can be induced by IL-1β, TNF-α and LPS (Villiger, Terkeltaub et al. 1992). Cultures of synoviocytes isolated from digested synovium contain FLS and synovial macrophages. However, by passage 3, these cultures contain >95% FLS (Rosengren, Boyle et al. 2007). In this study we developed a co-culture model incorporating FLS from the horse, alongside canine macrophages, to create a model that closely resembled the cellular populations present in the inflammed synovium. This allows us to improve our understanding of intercellular signaling within the synovium during synovitis.

During initial experiments, EFLS isolated from one horse were used at passage 9. However, mRNA levels produced by this sample were vastly

different to those generated by EFLS at passage 3-4. It is thought that cell senescence occurs by passage 9 (Rosengren, Boyle et al. 2007), and that this may have caused the difference in results. This indicates that, when approaching senescence, FLS differ considerably in their responses to inflammatory stimulation. When comparing EFLS isolated from different horses, those used prior to passage 4 experienced similar changes in mRNA expression upon LPS-stimulation, therefore all EFLS used in this experiment are < passage 4.

To identify both EFLS and DH82 cells within co-cultures, we labeled both populations with fluorophores which emitted light at wavelengths which did not overlap. The concentration of efluor cell proliferation dye capable of labelling and subsequently producing good FI ($>10^5$) from the highest of proportion of EFLS cultured for 24 hours, was 8μM. Average FI detected by the 675/25nm interference filter, emitted by EFLS after 24 and 48 hours in culture was 1 x $10^{6.1}$ and 1 x $10^{5.1}$ respectively. This is consistent with a halving of FI between 24 and 48 hours in culture, which occurs when primary cells divide to produce two daughter cells. When EFLS were cultured with DH82 cells, this halving of FI occurred earlier, within the first 24 hours of culture. Interestingly, this indicates that EFLS mitosis was stimulated by the co-culture of DH82 cells, and the rate of EFLS mitosis was proportional to the percentage of DH82 cells present in the co-culture. Synovial hyperplasia is an important gross pathological change that occurs during osteoarthritis. Macrophage migration inhibitory factor (MIF) has been shown to significantly stimulate the proliferation of rheumatoid arthritis FLS, with indirect IL-1β and TNF-α involvement (Lacey, Sampey et al. 2003). IL-1 is also known to

increase FLS proliferation (Alvaro-Gracia, Zvaifler et al. 1990). As macrophages are majors producers of both IL-1 and MIF, these factors may explain the increase in rates of EFLS proliferation when in co-culture with DH82 cells.

As previously stated, the co-culture model was designed to culture macrophages and FLS, in proportions comparable to those in the synovial membrane when experiencing a moderate synovitis. Based upon initial experiments, we had hypothesised that EFLS would proliferate faster than DH82 cells. When analysing rates of proliferation over a 24 hour time course, EFLS proliferated slightly faster than DH82 cells. Equal numbers of EFLS and DH82 cells were therefore used to generate a 60% EFLS and 40% DH82 co-culture model after 24 hours, ready to undergo experimentation

Successful equine GAPDH, IL-1β, IL-6, ADAMTS4 and -5, and canine IL-1β and IL-6 species-specific primer designs were supported by their associated dissociation curves; comparable single peaks were produced by double stranded (ds)DNA of the same species and from the co-culture. A single peak at the same temperature may reflect production of the same amplicon product from both samples of dsDNA, consistent with robust species-specificity of the primer. This was further supported by the generation of Ct values reflecting low gene expression when primers designed for one species, were mixed with cDNA from the second species, supporting low or absent cross-species primer annealing. Areas of dissimilarity between equine and canine genes, to enable species-specific primer design, were not found for equine TNF-α, or canine ADAMTS4 and -5 genes. The canine GAPDH primer was not considered fully species-specific, producing a small

degree of equine GAPDH dsDNA. As the genes of interest are normalised to GAPDH in this study, changes in canine mRNA expression may be underestimated using this canine GAPDH primer. However, canine IL-1β and IL-6 gene expression are both normalised to canine GAPDH and are therefore comparable.

All equine primers, and canine IL-1β and IL-6 primers, proved to have excellent amplification efficiency, and efficiency of determination (R) values when used on cDNA of the same species. Ideally, the amount of cDNA of the gene of interest, within the sample, should equal the amount of dsDNA produced by the PCR. This would reflect 100% amplification efficiency achieved by the primer. When analysing gene expression using the $2^{-\Delta Ct}$ method, primer efficiency is not taken into account, which may lead to small errors in gene expression quantification. In this study error was minimised by using primers with similar efficiencies. R values indicate the accuracy of the standard curve and associated linear equation to calculate for example, the y value using a known x value. Ideally the R value should be 1, which reflects 100% accuracy, however, 0.99 is also accepted. Dissociation curves produced by equine dsDNA at all serial dilutions, produced highly comparable single peaked curves, consistent with robust primer design. The dissociation curves produced by canine dsDNA at serial dilutions were highly variable; each primer produced several peaks at different dilutions, reflecting sub-optimal primer design. However, the amplification efficiency and R values produced by canine IL-1β and IL-6 are excellent. As was their species-specificity when used with co-culture cDNA. Canine GAPDH has sub-optimal amplification efficiency.

EFLS ADAMTS5 gene expression was significantly attenuated when cells were co-cultured with DH82 macrophages ($p<0.05$). Macrophage expression of IL-1β tended to be higher when they were co-cultured with EFLS. However, siRNA-mediated knockdown of the elevated DH82 cell IL-1β expression did not effect the attenuation of EFLS ADAMTS5 expression that we observed in co-culture. This finding is consistent with previous reports of equine synoviocyte ADAMTS5 gene expression being unresponsive to IL-1β (Ross, Kisiday et al. 2012). EFLS ADAMTS5 gene expression was also suppressed when cells were exposed to macrophage-conditioned medium, and even more strongly when EFLS cells were cultured with macrophages indirectly using well inserts. This suppressive effect of DH82 conditioned medium was also evident when it had been heat denatured. A soluble factor released by macrophages is likely to be responsible for these findings, and it is either thermally stable or able to denature reversibly upon heating. A reduced expression of equine synoviocyte ADAMTS5 mRNA was found when normal synoviocytes were cultured with injured cartilage, compared to normal cartilage (Lee, Kisiday et al. 2013). This was proposed to be a protective synoviocyte mechanism to protect injured cartilage. The role of macrophages within the inflammatory response to joint injury has been investigated using murine macrophage depleted experimental OA models. A reduction in osteophyte formation, fibrosis, synovial activation, synovial lining growth factor production, MMP-induced neoepitope formation, and synovial MMP3 and -9 mRNA expression, were observed in macrophage-depleted subjects, suggesting that synovial macrophages are principal moderators of OA joint pathology (Blom, van Lent et al. 2004). However, macrophage-

depletion in OA models, have also been linked to increased acute joint inflammation involving significantly higher synovitis scores, increased cellular density, and a reduction in bone mineral density (Bailey 2014, Bailey 2015). Macrophages are obviously pivotal in the synovial response to joint injury, and provide essential moderation of joint inflammation.

It is interesting that we have observed regulation of FLS ADAMTS5 mRNA levels. Earlier work demonstrated that OA equine chondrocyte ADAMTS5 mRNA levels were similar to normal chondrocyte levels (Fushimi, Troeberg et al. 2008). Yet normal chondrocyte ADAMTS5 mRNA levels were mildly up-regulated by LPS and IL-1β (Busschers, Holt et al. 2010, Ross, Kisiday et al. 2012). Gene expression levels do not always correlate with protein levels. Chondrocyte ADAMST5 protein production can also be influenced by factors such as endocytic clearance mediated by chondrocyte LRP-1 receptors (Yamamoto, Troeberg et al. 2013). This may represent a means for increased levels of ADAMTS5 activity in the joint without any change in mRNA levels. FLS regulation of ADAMTS5 mRNA may indicate an additional source of this matrix-degrading factor.

Given the key role that the NF-κB pathway has been shown to have in the regulation of ADAMTS5 transcription, we were interested to examine how the inhibition of this pathway would affect ADAMTS5 expression in our co-culture system. When treating EFLS with Bay 11-7086, ADAMTS5 gene expression was similar to that of untreated EFLS in co-culture with macrophages. However, co-cultured EFLS ADAMTS5 gene expression was further attenuated when using a broad NF-κB inhibitor (PDTC). The proximal aspect of the 5'-end-flanking region, containing the ADAMTS5 promoter is highly

conserved between species (Kobayashi, Hirata et al. 2013) and RelA/p65, an NF-κB family member, is a strong transcriptional activator of ADAMTS5 in chondrocytes (Kobayashi, Hirata et al. 2013). PDTC is a broad potent inhibitor of NF-κB activity; inhibiting NF-κB-DNA-binding activity, IκB phosphorylation, and expression of nuclear p65 protein (Zhang, Xu et al. 2011), can specifically block LPS-induced NF-κB mobilisation (Ziegler-Heitbrock, Sternsdorf et al. 1993), and can attenuate acute and chronic arthritis inflammation (Cuzzocrea, Chatterjee et al. 2002). Bay 11-7086 inhibits phosphorylation of IκB-α, leading to sequestration of free NF-κB within the cytoplasm, unable to translocate to the nucleus. The attenuation of EFLS ADAMTS5 mRNA using PDTC further supports the theory that NF-κB is a transcriptional activator of EFLS ADAMTS5.

4.4.1 Conclusion

To summarise, we have developed a novel, multi-species co-culture model of synovial cell interaction to enable cell-specific responses to be examined in response to inflammatory stimulation. We have found that macrophages stimulate FLS mitosis, and modulate its ADAMTS5 mRNA expression in an inflammatory environment. Future work will be required to identify the mechanism by which this attenuation occurs, as this may present a means of modulating the expression of this enzyme to prevent the progression of joint diseases in clinical and veterinary medicine.

Chapter 5.

The Effect of Anti-Equine IL-1β siRNA Loaded PLGA-Microspheres on an Equine Co-Culture Model Incorporating Synoviocytes and Cartilage

5.1 Introduction

5.1.1 Intra-Articular Drug Delivery Systems

Intra-articular (IA) disease modifying osteoarthritis drugs (DMOADs) to counteract pain and joint degradation driven by OA are of major interest. These therapies decrease the risk of adverse systemic effects, and optimise bioavailability and therapeutic efficacy directly for the target cells. However factors within the IA environment can impede the efficacy of such therapeutics. For example synovial fluid serum nucleases can hydrolyse certain therapeutic molecules, rendering them useless (Mountziaris, Sing et al. 2011, Jensen, Griger et al. 2012, Présumey, Salzano et al. 2012), whilst rapid drug clearance is facilitated by the dense vascular and highly active lymphatic systems within the synovial membrane (Allen, Adams et al. 2010, Edwards 2011). Delivery systems to facilitate sufficient targeted sustained release of a drug at the target cell, are being designed to overcome these issues (Patil, Panyam et al. 2009, Janssen, Mihov et al. 2014). A number of drug delivery system are used in both clinical and laboratory settings (Janssen, Mihov et al. 2014, Bodick, Lufkin et al. 2015), however this study concentrates on biodegradable polymer microspheres which contain a homogenous mixture of the polymer and encapsulated drug (Janssen, Mihov

et al. 2014). When designing a DDS a number of technical and practical issues have to be considered. These include:

- Size of the vehicle (Caldorera-Moore, Guimard et al. 2010, Mitragotri, Burke et al. 2014).
- Resistance of the microsphere to IA degradation (Présumey, Salzano et al. 2012).
- Ability to retain the drug during delivery (Présumey, Salzano et al. 2012).
- Sustained release of the drug at a therapeutic dose within the target cell (Présumey, Salzano et al. 2012, Zhang and Huang 2012).
- Biocompatibility within the intra-articular environment (no toxicity) (Zhang and Huang 2012).

Targeted intra-articular DMOADs have been historically hindered by the lack of an effective drug delivery system. Research into the use of PLGA microspheres as a drug delivery agent started in the 1980s (Janssen, Mihov et al. 2014) and specific investigation into its use in targetting IA disease processes has been on-going since 1985 (Tice, Lewis et al. 1985, Tice, Lewis et al. 1985). PLGA-microspheres phagocytosed by synovial macrophages offer a system which not only delivers the drug directly to the target inflammatory cell, but also provides sustained controlled release (Edwards 2011). Phagocytosis of these particles appears to be size dependent, and particles 1-10μm in diameter were found to be optimal for synoviocyte phagocytosis (Butoescu, Seemayer et al. 2009). PLGA microspheres have excellent biocompatibility within IA environments

(Mitragotri, Burke et al. 2014), especially when used in horses (Bragdon, Bertone et al. 2001), and do not stimulate an immune response (Janssen, Mihov et al. 2014). They are degraded within the cell by both surface and bulk erosion (Bragdon, Bertone et al. 2001, Larsen, Ostergaard et al. 2008), into the fully resorbable natural metabolites lactic and glycolic acid (Kavanaugh, Werfel et al. 2015). PLGA microspheres experience an initial burst release which may cause local toxic effects (Janssen, Mihov et al. 2014) as high levels of lactic acid can be toxic (Kavanaugh, Werfel et al. 2015). Efforts are being made to reduce this initial burst release with additives such as polyethylene glycol (PEG), however these can also antagonise macrophage phagocytosis, therefore it would depend on the intended application of the microspheres (Kavanaugh, Werfel et al. 2015).

PLGA microspheres are approved by the Food and Drug Administration (FDA) (Janssen, Mihov et al. 2014, Kavanaugh, Werfel et al. 2015) and their use in OA-targeted treatment is currently in phase 3 development, testing the provision of IA sustained steroid release to treat patients with moderate to severe OA pain (Kumar, Bendele et al. 2012, Bodick, Lufkin et al. 2015). Flexion therapeutics (Massachusetts, USA) also have two other PLGA encapsulated products in development; a TrkA receptor antagonist intended for post-operative pain, and a p38 MAP kinase inhibitor intended for end-stage OA patients (Kumar, Boehm et al. 2003, Kavanaugh, Werfel et al. 2015).

Natural polymers, such as chitosan and gelatin, have been used as drug delivery systems in OA models, incorporating non-steroidal anti-inflammatory drugs (NSAIDs) and anti-TNF proteins (Janssen, Mihov et al. 2014,

Kavanaugh, Werfel et al. 2015). However, these natural formulations are more immunogenic which is an undesirable characteristic when treating OA.

Synthetic polymer microspheres have been extensively modified to enable sustained drug release, specific targeting properties and improved cellular uptake. For example, a polypropylene sulphide (PPS) particle preparation can become hydrophilic in response to reactive oxygen species, triggering the release of hydrophobic encapsulated drugs, providing an 'on demand' release when needed (Poole, Nelson et al. 2015). Other particles incorporate a tethering moiety to attach the therapeutic protein, in this case IL-1RA, to the particle, decreasing rate of release and therefore extending the retention of IL-1RA within the joint (Whitmire, Wilson et al. 2012). Nanoparticles are also capable of targeting specific molecular structures, such as collagen I, using a surface peptide as a ligand. This has allowed nanoparticles to infiltrate cartilage *in vivo,* targetting chondrocytes, and maintaining their presence within the ECM for extended periods (Rothenfluh, Bermudez et al. 2008).

5.1.2 Gene Therapy

Gene therapy either facilitates an increase or decrease in gene expression, depending on the desired outcome. Viral vectors enable plasmid cDNA comprising the required gene, to either be incorporated into the target cell chromosomal cDNA, or remain in the cytoplasm, and subsequently be translated into a protein (Casal and Haskins 2006). Viral vectors can be used *in vivo* or *ex vivo*. Retroviral-based vectors that integrate into host DNA and stably modify target cells are often used for *ex vivo* modification (Robbins,

Evans et al. 2003). This process modifies tissues *in vitro* before injecting the cells back into the target area *in vivo*. Studies using autologous synoviocytes modified by a retroviral vector to constitutively express IL-1RA have been shown to be safe and effective (Robbins, Evans et al. 2003). *In vivo* gene therapy involves IA injection of the vector, directly at the site where expression is required, such as the synovium during OA. For this purpose vectors must have high transduction efficiency and sustained gene expression, and cause minimal immunogenic stimulation. ScAAV IL-1RA equine gene serotype 2, has good transduction efficiency in both equine synoviocytes and chondrocytes (Goodrich, Choi et al. 2009, Ishihara, Bartlett et al. 2012, Watson, Broome et al. 2013) in an inflammatory environment (Kay, Gouze et al. 2009), and are safe for IA use (Ishihara, Bartlett et al. 2012). IA therapeutic levels of IL-1RA have been attained over substantial periods (Goodrich, Phillips et al. 2013). During a 'proof of concept' study, this increased expression of IL-1RA provided marked protection from the progression of joint pathologies developed in an equine osteochondral fragment model (Watson, Broome et al. 2014).

Post-transcriptional gene silencing (PTGS) reduces translation of a target gene by decreasing mRNA levels through RNA interference (RNAi). Using synthetic siRNA loaded biodegradable polymer particles as non-viral vectors, safe, non-toxic, non-immunogenic gene silencing has been carried out *in vitro* and *in vivo* (Murata, Takashima et al. 2008, Lee, Yang et al. 2009, Patil, Panyam et al. 2009). This method has suppressed tumour growth in mice using anti-VEGF siRNA (Murata, Takashima et al. 2008), induced potent

silencing of anti-TNF-α secretion in murine peritoneal-residing macrophages (Brunner, Cohen et al. 2010) and PLGA microspheres encapsulating anti-TNF-α siRNA inhibited IA TNF-α expression by 40-50% over 11 days and reduced synovial inflammation in a murine model (Présumey, Salzano et al. 2012).

We have previously described the successful reduction of EFLS IL-1β gene expression using RNA interference, and demonstrated the ability of equine peripheral blood mononuclear cells (EPBMCs) to phagocytose PLGA microspheres. This study incorporates EFLS and EPBMCs which, when cultured together, will be referred to by the umbrella term “synoviocytes”. Synoviocytes will be cultured with cartilage explants to investigate the success of PLGA microspheres in the capacity of therapy delivery vehicles loaded with anti-IL-1β siRNA. The influence of synoviocytes with and without anti-IL-1β siRNA loaded PLGA-microsphere treatment, on cartilage health, will be investigated.

5.1.3 Aims

- To determine the influence of synovitis on cartilage health.
- To investigate whether anti-IL-1β siRNA loaded PLGA-microspheres can effect synoviocyte gene expression.
- To investigate whether anti-IL-1β siRNA loaded PLGA-microsphere treatment alters the effect of synovitis on cartilage health.

5.2 Study Design

An overview of the experimental design can be found in Schema 5.1.

5.2.1 Co-Culture Model Design

5.2.1.1 Metacarpophalangeal Joint Scoring

Equine distal limbs from 12 horses, disarticulated at the carpus, were collected from an abattoir. Limbs were prepared and MCPJ exposed under sterile conditions, using techniques described in Chapter 2. Materials and Methods, section 2.1. Cartilage of the distal condyles of the third metacarpal bone, and proximal aspect of the first phalanx (P1), were grossly scored using a macroscopic cartilage scoring system encompassing pathology such as cartilage wear lines, cartilage erosion and palmar arthroses (McIlwraith, Frisbie et al. 2010). Other abnormalities, such as remodelling of the dorsoproximal aspect of the P1 were noted, and the condition of the synovial membrane and synovial fluid were also taken into consideration when grading the joint (Table 5.1). Nine joints with an overall score of $\leq$1 were used in the study, others with additional pathology such as remodelling of the dorsoproximal aspect of the P1 were disregarded (Figure 5.1).

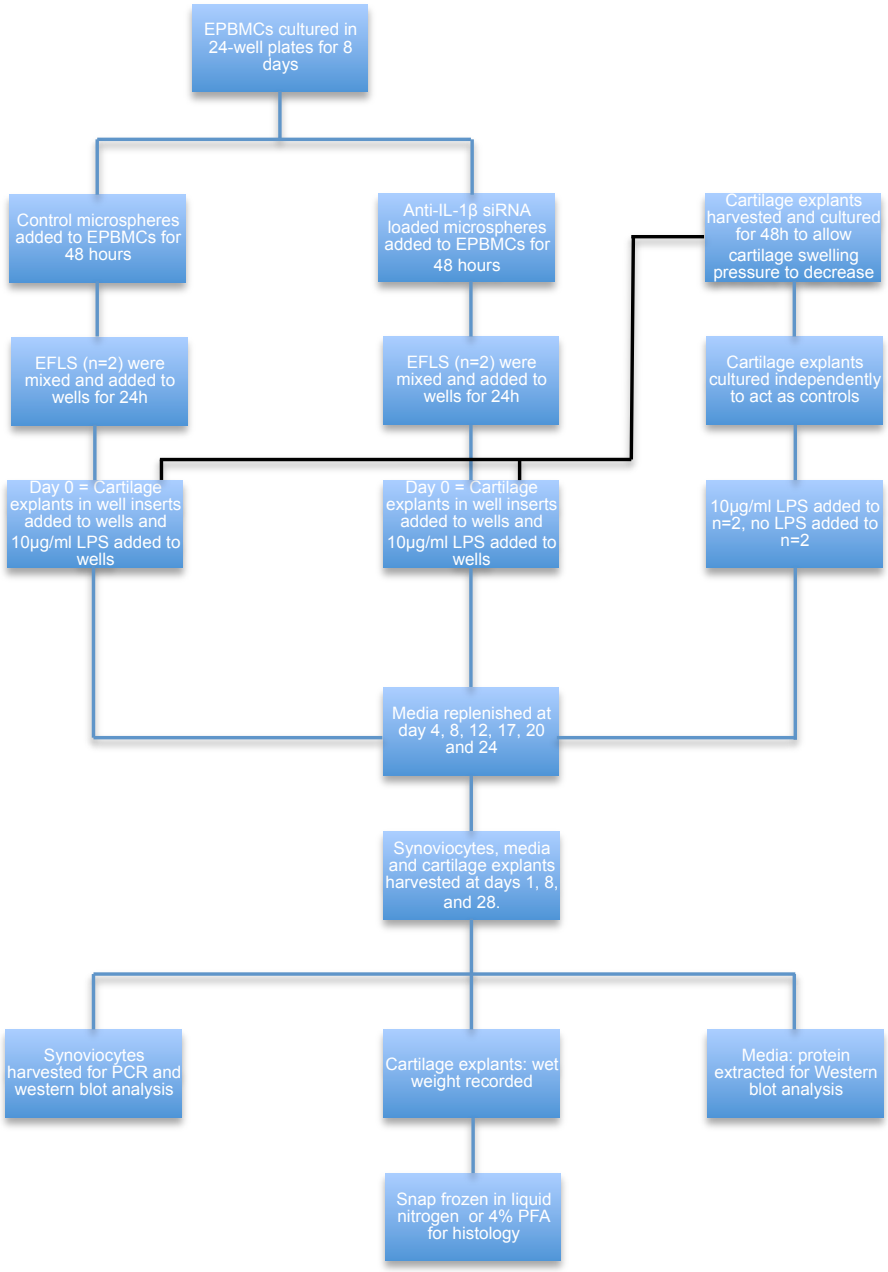

Schmema 5.1 Experimental strategy for work within Chapter 5.

Table 5.1 Cartilage, synovial membrane and synovial fluid macroscopic grading scores.

		Macroscopic cartilage score						Synovial membrane				
		Wear lines		Erosion		Palmar Arthroses						
Horse	Limb	Grade	Position	Grade	Position	Grade	Position	Inflammation	Synovial Fluid	Other	Used in study	Total score
1	Right	0	-	1	Medial	0	-	0	0	No	**Yes**	**1**
2	Left	0	-	0	-	1	Medial	0	0	Yes*	No	1
3	Right	0	-	1	Medial	0	-	0	0	No	**Yes**	**1**
				1	Lateral							
4	Left	1	Medial	0	-	0	-	0	0	No	**Yes**	**1**
	Right	1	Medial	0	-	0	-	Moderate	Haemorrhagic	No	No	1
5	Left	0	-	1	Medial	0	-	0	0	Yes**	No	1
	Right	0	-	0	-	0	-	0	0	Yes**	**Yes**	**0**
6	Left	0	-	1	Lateral	0	-	0	0	No	**Yes**	**1**
7	Left	0	-	0	-	0	-	0	0	No	**Yes**	**0**
8	Left	0	-	0	-	0	-	0	0	No	**Yes**	**0**
9	Right	0	-	0	-	0	-	Mild	0	No	No	0
10	Left	0	-	1	Lateral	0	-	Mild	0	No	No	1
11	Left	0	-	0	-	0	-	0	0	No	**Yes**	**0**
12	Right	0	-	0	-	0	-	0	0	No	**Yes**	**0**

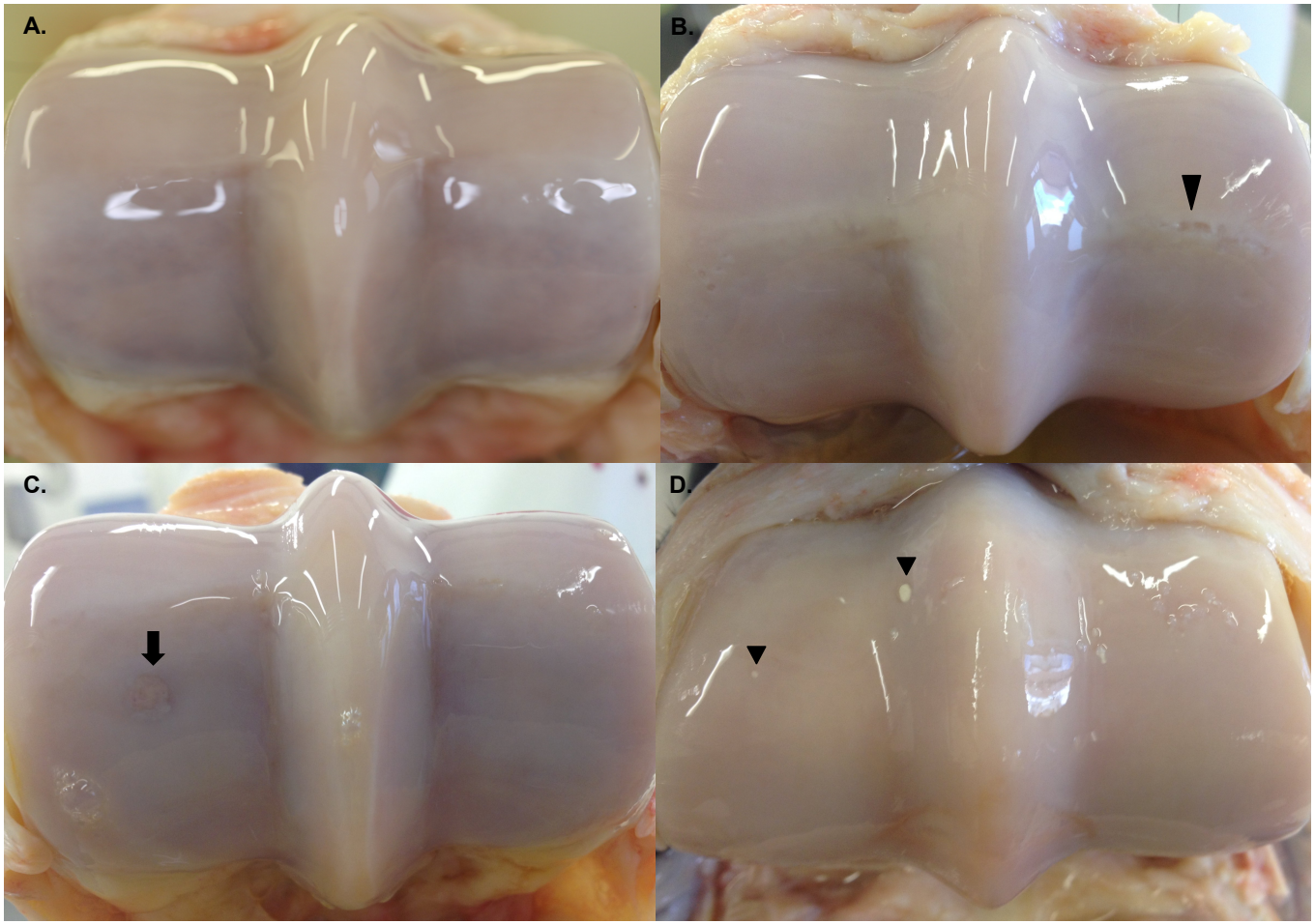

Figure 5.1 Distal condyles of the third metacarpal bone. A. Normal (horse 11). B. Grade 1 Erosion (Arrowhead, horse 6, left forelimb). C. Grade 1 Palmar arthroses (Arrow, horse 2, left forelimb). D. Hard white deposits within the HAC (Small arrowheads, horse 5, right forelimb).

5.2.1.2 Tissue Harvesting

Cartilage explants, approximately 5mm^2 and <1mm thick, were harvested from nine MCPJs, as described in Chapter 2 Materials and Methods, section 2.1, and pooled in PBS. Three cartilage explants were chosen at random and inserted in each cell culture well-insert (0.45µm, Merck Millipore, Hertfordshire UK). Explants were immersed in 1ml Dulbecco's Modified Eagle Medium (DMEM, Life Technologies, Maryland, USA) with 10% foetal bovine serum (FBS, Gibco, Paisley, UK), 100U/ml penicillin/streptomycin (Penstrep, Life Technologies, Paisley, UK), 500ng/ml amphotericin B (Life Technologies, Paisley, UK), this will be referred to as 'standard culture media' when associated with cartilage explants and EFLS. Explants were incubated for 48 hours at 37°C in 5% CO_2, to allow the cartilage swelling pressure to decrease.

Synovium was harvested from two MCPJs and digested using a trypsin/EDTA and type 2 collagenase (Worthington, UK) protocol as described in Chapter 2 Materials and Methods, section 2.1. Isolated EFLS were cultured in normal media and cultures were expanded. All EFLS used within this study had undergone less than 4 passages.

Osteochondral wedge biopsies incorporating cartilage and subchondral bone, and synovial explants were taken from joints which had scored 0 when using the macroscopic cartilage scoring system. Osteochondral wedge biopsies (5mm thick) were extracted using a bone saw. The osteochondral

wedge biopsies and synovial explants were immediately placed in 4% PFA and were processed for histopathology sections.

5.2.1.3 EPBMC Isolation and Culture

EPBMCs (n=1, passage 1) were isolated as described in Chapter 2. Materials and Methods, section 2.1, and cultured in 24 well plates at a seeding density of 1 x 10^5 cells per well in 1ml RPMI-1640 medium with L-alanyl-L-glutamine (RPMI 1640 Medium, GlutaMAX™ Supplement, Life Technologies, UK). This was supplemented with 10% horse serum (New Zealand origin, Life Technologies, UK), 100U/ml penicillin/streptomycin (Penstrep, Life Technologies, Paisley, UK), 500ng/ml amphotericin B (Life Technologies, Paisley, UK) and 50ng/ml recombinant human granulocyte-macrophage colony stimulating factor (rhGMCSF 300-03, Peprotech, NJ, USA). This will be referred to as 'standard EPBMC culture media'. Half the media was replenished every 3 days for 8 days.

5.2.1.4 Anti-IL-1β Microspheres Cultured with EPBMCs

PLGA microspheres, 2-6μm in diameter, were loaded with anti-IL-1β siRNA at 0.2nM/mg, and suspended in PBS at 50mg/ml. Five pM siRNA (0.125mg microspheres) were added to half of the wells containing EPBMCs. Fluorescein isothiocyanate-dextran (FD4, FD10s) microspheres, acting as control microspheres, were suspended in PBS at 16.7mg/ml; 0.125mg control microspheres were added to the remainder of the wells. Cells were incubated with the microspheres for 48 hours.

5.2.1.5 Synoviocyte Co-Culture

Once the EPBMCs had been cultured with the microspheres for 48 hours, EFLS were seeded in the same wells as the EPBMCs, at a seeding density of 1 x 10^5 cells per well. Cells were immersed in 1ml of media consisting of 500µl standard culture media, and 500µl standard EPBMC culture media. Cells were incubated at 37°C in 5% CO_2 for 24 hours.

5.2.1.6 Cartilage and synoviocyte Co-Culture

Synoviocyte (EFLS and EPBMC) media was discarded and replenished with 700µl fresh culture media at the same ratio (50% standard culture media and 50% standard EPBMC culture media) containing 10µg/ml LPS. Cartilage explant media was removed and the well-inserts (containing cartilage explants) were placed into the wells containing the synoviocyte cultures. Cartilage explants were then immersed in 200µl standard culture media. Co-culture of synoviocytes, cartilage explants and LPS within the same well, was considered the start of the experiment (day 0) (Figure 5.2).

5.2.1.7 Control Cartilage Explants

Three cartilage explants per well were cultured in a 24-well plate, that did not contain synoviocyte cultures. These explants were cultured in 1ml standard culture media, with (n=2) and without (n=2) 10 µg/ml LPS. Media, with and without LPS, was replenished at the same time points as described below, and stored at -20°C.

5.2.1.8 Media Changes Across the Course of the Experiment

Synoviocyte culture media was replenished with 700µl fresh media at the same ratio of standard culture:standard EPBMC culture media containing 10µg/ml LPS approximately every four days (day 4, 8, 12, 17, 20 and 24). The cartilage explants also received 200µl fresh standard culture media placed within the well-insert, at these time points. Synoviocyte and cartilage media samples were combined and stored at -20°C.

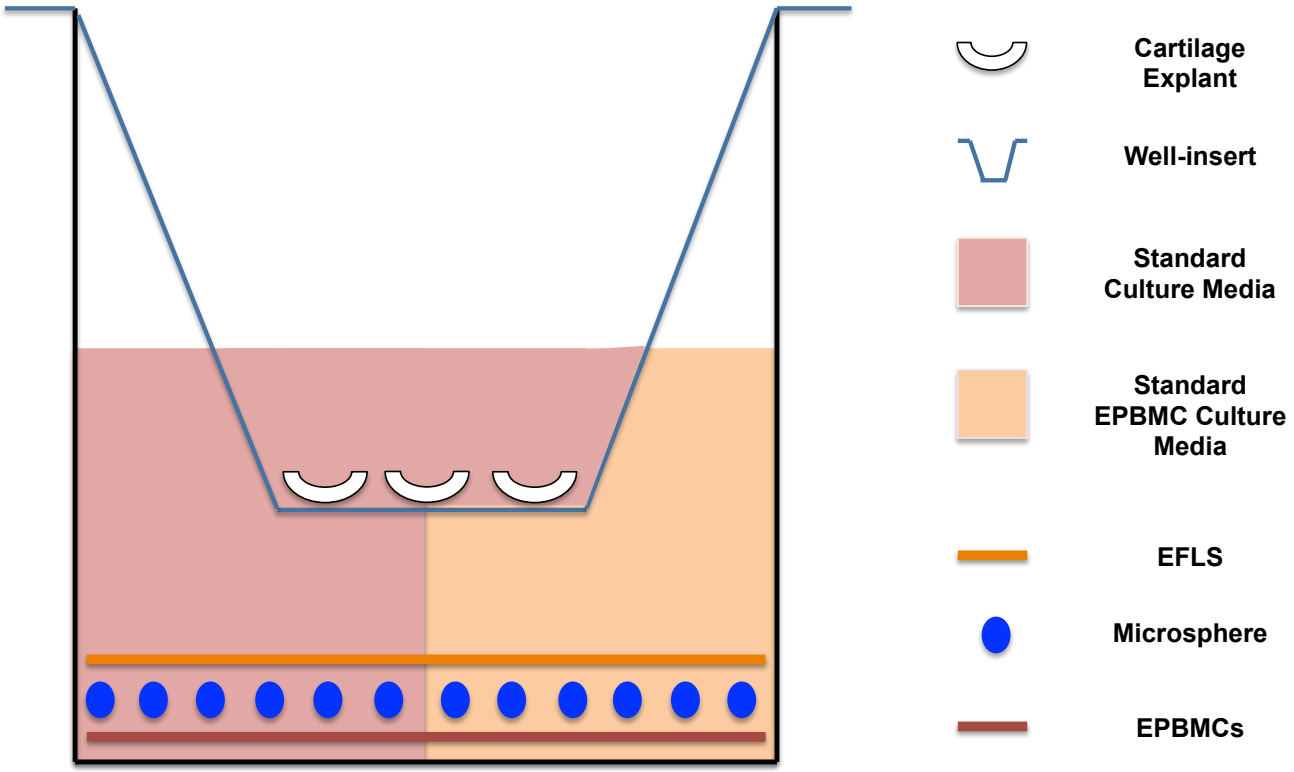

Figure 5.2 Synoviocyte and cartilage co-culture. EPBMCs were cultured with either control or anti-IL-1β siRNA loaded microspheres, and EFLS. Cartilage explants in a well-insert were placed into the main well. Cells were cultured in media containing 10μg/ml LPS.

5.2.1.9 Cell and Tissue Harvesting

Synoviocytes, media and cartilage explants were harvested at days 1, 8 and 28 of the experiment. Media was removed and cell layers were harvested either in 0.5ml tri-reagent (Sigma-Aldrich, Missouri, USA) and stored at -80°C, or were first washed with 1ml 1x PBS before being macerated using a cell scraper, in 45µl (1X) Novex tris-glycine SDS sample buffer 2X (Life Technologies, California, USA) and stored at -20°C. Media from the main well and well-insert were combined, and frozen at -20°C. Excess media was gently blotted from cartilage explants, which were then weighed. Cartilage wet weights were recorded before explants were either snap frozen in liquid nitrogen, or fixed in 4% PFA, and stored at -80°C.

5.2.2 Synoviocyte Gene Expression Analysis

As described in Chapter 2 Materials and Methods, section 2.7, synoviocyte samples harvested in tri-reagent underwent RNA extraction using the guanidinium-thiocyanate-phenol-chloroform technique with ethanol. Reverse transcription was carried out using 1µg RNA, random hexonucleotides and M-MLV reverse transcriptase (Promega, Wisconsin, USA). Quantitative RT-PCR was carried out using validated equine primers specific for GAPDH, IL-1β, IL-6, ADAMTS4, ADAMTS5, MMP3 and MMP13 (primers are listed in Chapter 2. Materials and Methods, section 2.7). The relative quantification of each gene normalised to the GAPDH reference gene, was calculated using the $2^{-\Delta Ct}$ method (Livak, Schmittgen et al. 2001).

5.2.3 Sulphated Glycosaminoglycan Assay

All media samples, including those stored when media was changed on days 4, 12, 17, 20 and 24, and those harvested at days 1, 8 and 28, were subjected to a sGAG assay, as described in Chapter 2 Materials and Methods, section 2.5. This 1-9 dimethylmethylene blue (DMMB) assay measures the concentration of sGAG within the cell media (Farndale, Buttle et al. 1986). This will reflect the quantity of sGAG released from cartilage explants, and to a lesser extent, secreted from EPBMCs and EFLS. A standard curve was created using known chondroitin sulphate (shark cartilage, C-4384, Sigma-Aldrich, Missouri, USA) concentrations ranging from 0 - 70µg/ml. Unknown sample sGAG concentrations were determined using the standard curve and linear equation. Absorbance was measured spectrophotometrically at a wavelength of 570nm. As the majority of sGAG will have originated from the cartilage explants, sGAG concentrations were normalized to total cartilage wet weight of the corresponding cartilage explants.

5.2.4 Analysis of Protein Within Culture Media

Western blot analysis was conducted using protein extracted from both cell media and cell lysate samples.

5.2.4.1 Pierce^{Tm} 660 Protein Assay

The protein concentrations of all samples were quantified using the Pierce^{Tm} 660 protein assay (Thermo-Fisher Scientific, Massachusetts, USA). A standard curve of absorbance, using a series of known bovine serum albumin (BSA) dilutions (0 - 2000µg/ml), was used to determine unknown protein concentrations. Absorbance was measured by a plate reader at a wavelength of 660nm.

5.2.4.2 Proteinase and Chondroitinase Treatment

Culture media samples harvested on day 1, 8 and 28 were treated with chondroitinase (0.001U/10µg sGAG) and proteinase inhibitors at 1 tablet/10ml media (Complete ULTRA tablets (EDTA-free), Roche, Basel, Switzerland) and incubated overnight.

5.2.4.3 Protein Extraction From Culture Media

Once protein concentrations of culture media samples were determined using the Pierce^{Tm} 660 protein assay, 10µl StrataClean^{Tm} Resin (Agilent, California, USA) was added to a known volume of culture media containing 80µg protein. Samples were processed as described in Chapter 2 Materials and Methods, section 2.6. Once the suspension had been thoroughly vortexed, the protein-bound resin was washed with DDH_2O and re-suspended in 15µl 1 x SDS-loading buffer to result in a total volume of 40µl containing 80µg protein per sample.

5.2.4.4 Western Blot Analysis

Sample were supplemented with 1µl mercaptoethanol (for reducing conditions) and incubated at 100°C for 5 minutes. Protein-bound resin samples were thoroughly mixed to re-suspend the resin in SDS-loading buffer. Samples of equal protein content (40µg) were loaded into a 4-12% Bis-Tris gel cassette. Proteins were separated by electrophoresis and transferred to a nitrocellulose membrane. The membrane was incubated in 1% non-fat milk blocking buffer to prevent non-specific antibody binding, before being exposed to the aggrecan interglobular doman (IGD) aggrecanase site-specific neoepitope monoclonal antibody (mAb) BC-3 1:200 (a kind gift from Professor Bruce Caterson, Cardiff

University). An anti-mouse IgG-peroxidase monoclonal antibody raised in the goat (Sigma-Aldrich, Missouri, USA) was used as a secondary antibody at 1:2000.

5.2.5 Cartilage Histology and Scoring

5.2.5.1 Sample Preparation

Each well-insert contained three cartilage explants; two explants were fixed in 4% neutral buffered PFA for 48 hours, before being immersed in 70% ethanol. Explants were embedded in paraffin wax, cut into 10μm sections and mounted onto glass slides. Control synovial membrane explants were processed using the same method.

Osteochondral wedge biopsies were fixed in 4% neutral buffered PFA for at least 24 hours. Samples were then de-calcified in 7.4% EDTA for one month. Water within the sample was first replaced with alcohol by dehydrating the samples; the tissue was passed through increasing concentrations of ethyl alcohol (0 to 100%). The alcohol was then replaced by xylene, which is miscible with paraffin wax, in the clearing step. Finally, the tissue was impregnated with, and embedded in, paraffin wax. Explants were cut into 10μm sections using a microtome, and mounted onto glass slides.

5.2.5.2 Histology Staining and Scoring

All histological cartilage, synovial membrane and osteochondral sections were stained with either H&E, or celestine blue, 0.5% fast green and 1% Safranin-O

stains. Sections were visualised using a Nikon Eclipse 80i microscope, and images were acquired using a Nikon DS-L2 standalone control unit. Cartilage explant sections were scored using a modified version of the cartilage histopathologic scoring system (McIlwraith, Frisbie et al. 2010). Osteochondral sections and synovial sections were scored using unmodified scoring systems (McIlwraith, Frisbie et al. 2010). Sections were scored twice by two users blinded to section identity. Inter- and intra- variability was assessed using the Cohen' kappa coefficient (Cohen 1960). Cartilage explant depth was measured at three different locations on each explant, using lines drawn perpendicular to the long axis of the explant.

5.3 Results

5.3.1 Synoviocyte Gene Expression

Synoviocyte gene expression levels of all cytokines, aggrecanases and MMPs on day 28 of the experiment, were dramatically lower than levels measured on day 1 (Figure 5.3). Gene expression levels of ADAMTS4, ADAMTS5 and MMP13 on day 8 were comparable to those measured on day 1. When comparing synoviocytes cultured with control microspheres to those cultured with anti-IL-1β siRNA loaded microspheres, gene expression levels of all cytokines, aggrecanases and MMPs were comparable between the two conditions at day 1, 8 and 28. However, synoviocytes cultured with anti-IL-1β siRNA loaded microspheres expressed a significantly higher amount of MMP3 mRNA on day 8 than synoviocytes cultured with control microspheres ($p<0.05$). The order of relative amount of synoviocyte gene expression from the most expressed to least expressed, was IL-6, ADAMTS5, MMP3, IL-1β, ADAMTS4 then MMP13, across the 28-day period.

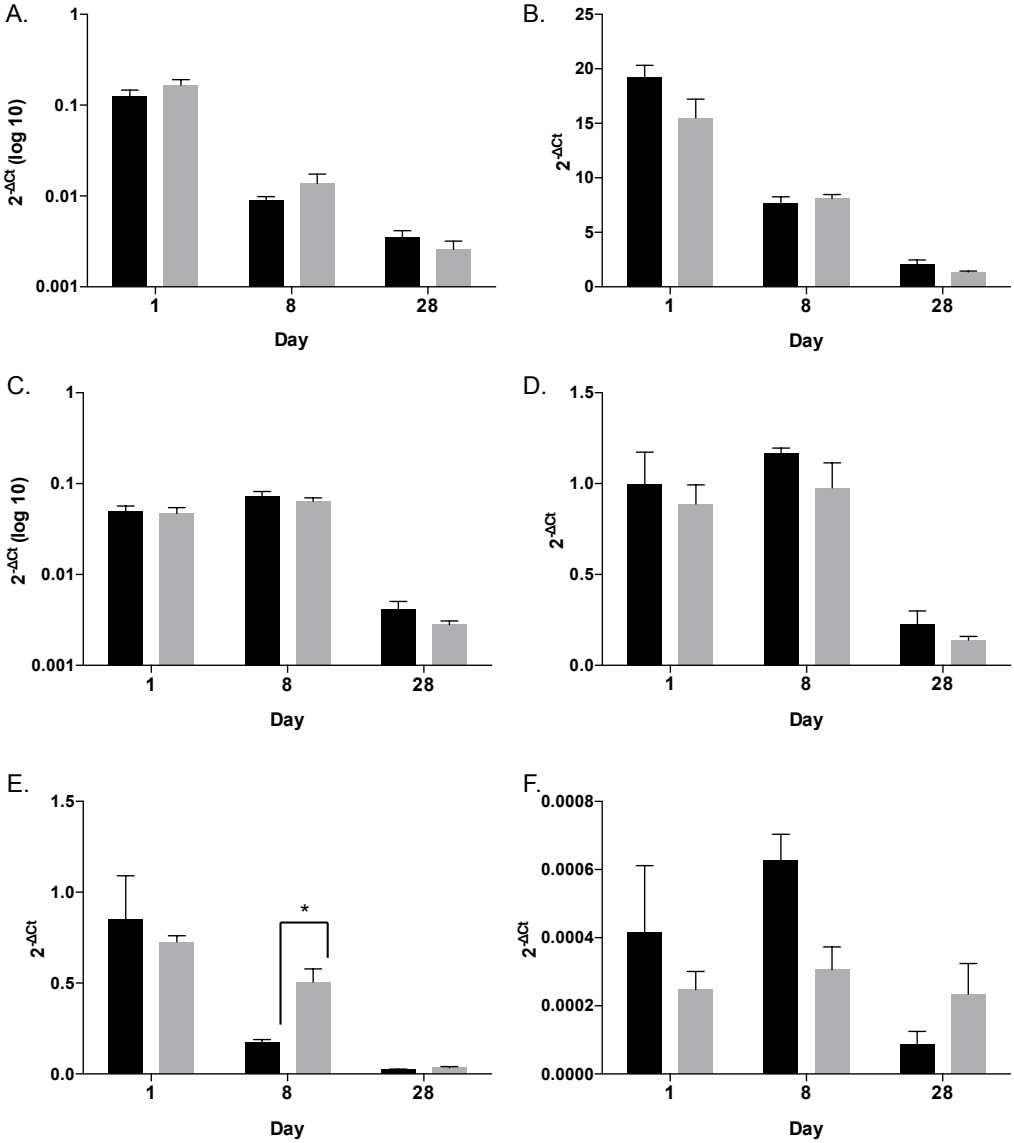

Figure 5.3 Synoviocyte gene expression when in co-culture. Synoviocyte (n=3) gene expression at day 1, 8 and 28 was analysed by qRT-PCR and normalised to GAPDH. Synoviocytes (EFLS and EPBMCs) were cultured with control microspheres (black bars) or anti-IL-1β siRNA loaded microspheres (grey bars). Genes investigated included (A) IL-1β, (B) IL-6, (C) ADAMTS4, (D) ADAMTS5, (E) MMP3, (F) MMP13. Standard error bars are shown. * = $p < 0.05$.

5.3.2 Sulphated Glycosaminoglycan Content

Sulphated glycosaminoglycan (sGAG) content within culture media was measured at day 1, 4, 8, 12, 17, 20, 24, and 28 of the experiment, and levels were normalised to cartilage wet weight. sGAG in culture media was evident within the first 24 hours of the experiment (Figure 5.4A). On day 1 of the experiment, media culturing control cartilage explants contained relatively more sGAG than media co-culturing synoviocytes and cartilage explants; this varied at each media change but the trend occurred again on days 12, 17, and 24 (Figure 5.4A). Individual assays of sGAG content measured at intervals, displayed a cyclic-like trend (Figure 5.4A). Sulphated GAG measurements at each media change were highly variable, however, sGAG content did decrease between day 1 and 28 in cartilage media but not in co-culture media (Figure 5.4A).

When analysing the cumulative sum of sGAG content within the media of each well over 28 days, significant increases were observed over the course of the experiment (Figure 5.4B). No significant difference in sGAG content of media containing synoviocytes treated with control microspheres compared to those treated with anti-IL-1β siRNA loaded microspheres was observed. When comparing media sGAG content of cartilage cultured with and without LPS, no significant difference was detected. However media co-culturing synoviocytes and cartilage, contained a significantly lower amount of sGAG, compared to media culturing solely cartilage ($p = 0.001$) (Figure 5.4C).

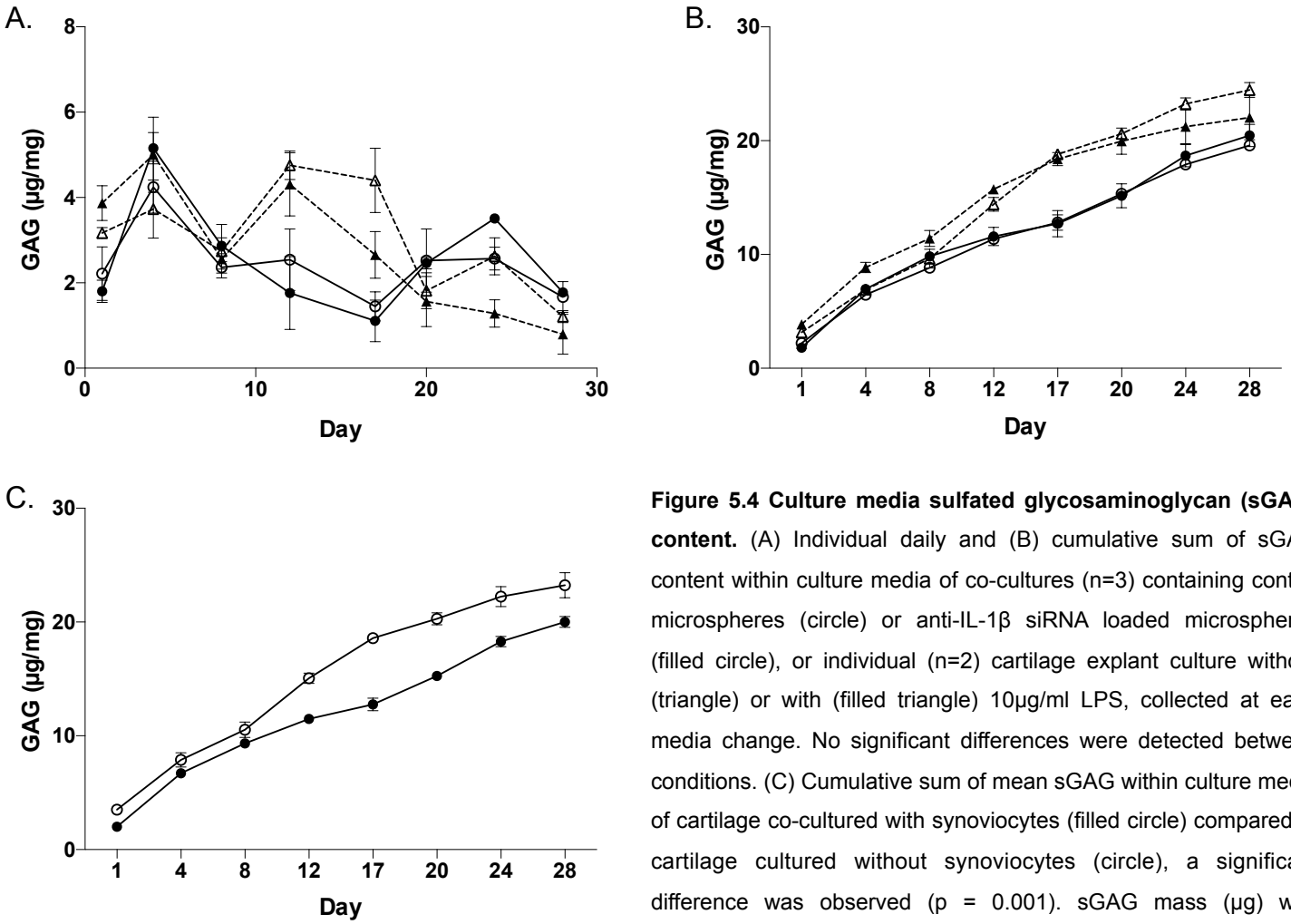

Figure 5.4 Culture media sulfated glycosaminoglycan (sGAG) content. (A) Individual daily and (B) cumulative sum of sGAG content within culture media of co-cultures (n=3) containing control microspheres (circle) or anti-IL-1β siRNA loaded microspheres (filled circle), or individual (n=2) cartilage explant culture without (triangle) or with (filled triangle) 10µg/ml LPS, collected at each media change. No significant differences were detected between conditions. (C) Cumulative sum of mean sGAG within culture media of cartilage co-cultured with synoviocytes (filled circle) compared to cartilage cultured without synoviocytes (circle), a significant difference was observed ($p = 0.001$). sGAG mass (µg) was normalised to cartilage wet weight (mg). Error bars represent SEM.

5.3.3 Western Blot Analysis

Proteins extracted from co-culture media of synoviocytes treated with control microspheres and anti-IL-1β siRNA loaded microspheres on days 1, 8, and 28 underwent western blotting. Proteins of 175kDa, 100kDa, 62-70kDa, 45kDa and 35kDa were detected using an aggrecan IGD aggrecanase site-specific neoepitope monoclonal antibody (mAb) BC-3 (Figure 5.5). The band at 62-70kDa is consistent with C-terminally truncated, ADAMTS-cleaved aggrecan (Busschers, Holt et al. 2010). Smaller fragments are consistent with smaller aggrecan breakdown products.

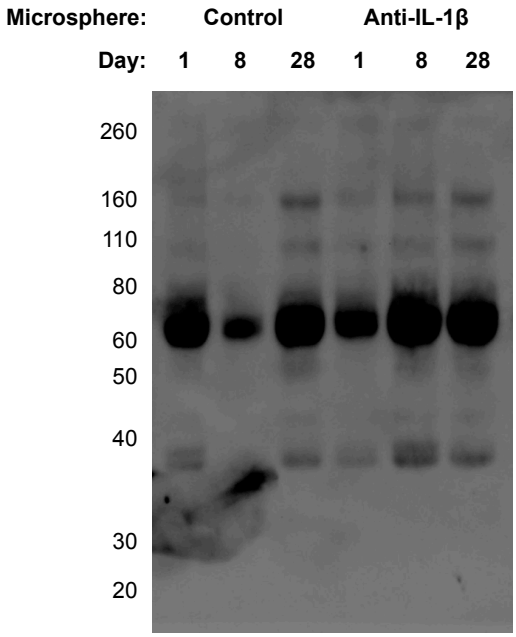

Figure 5.5 Detection of aggrecan breakdown products within the culture media of synoviocyte and cartilage co-cultures. Proteins within co-culture media of synoviocytes (n=3) treated with control microspheres and anti-IL-1β siRNA loaded microspheres on days 1, 8, and 28 were detected using an aggrecan interglobular doman (IGD) aggrecanase site-specific neoepitope monoclonal antibody (mAb) BC-3. Proteins of 175kDa, 100kDa, 62-70kDa, 45kDa, and 35kDa were detected.

5.3.4 Cartilage, Osteochondral and Synovial Histology Scores

Sections of the osteochondral wedge biopsies (Figure 5.6) and synovial explants, taken from joints which had scored 0 using the macroscopic cartilage scoring system, scored 0-2.67 out of 20 when using the cartilage and synovium histopathologic scoring systems. This supported the use of the macroscopic scoring system to detect joints free from orthopaedic disease. Inter- and intra-observer variability was moderate; 0.44 (95% CI: 0.2-0.67) and 0.6 (95% CI: 0.34-0.86) respectively.

When comparing histopathological scores of cartilage explants (Figure 5.7 & 5.8) co-cultured with synoviocytes that had either been treated with control microspheres (mean score: 4.75 out of 12, minimum-maximum score: 1 – 7, 95% CI: 0.57-8.94), or anti-IL-1β siRNA loaded microspheres (mean score: 3.8 out of 12, minimum – maximum score: 2 – 6, 95% CI: 2.29 – 5.38), scores were comparable. However, the scores of cartilage explants independently cultured (mean score: 1.19 out of 12, minimum – maximum score: 0.88-1.5, 95% CI: -2.78 – 5.38) were significantly lower than those co-cultured with synoviocytes ($p<0.05$).

Five of fourteen cartilage explants contained the most superficial aspect of the calcified cartilage layer. None of the explants contained subchondral bone. Cartilage explants that contained solely hyaline articular cartilage, or hyaline articular cartilage and the superficial aspect of the calcified cartilage layer, were approximately 0.04 - 0.41mm thick (mean: 0.2mm) and 0.09 - 0.24mm thick (mean: 0.16mm) respectively. Cartilage explants <0.1mm were

more difficult to correctly orientate for histopathological scoring than those that had a greater depth.

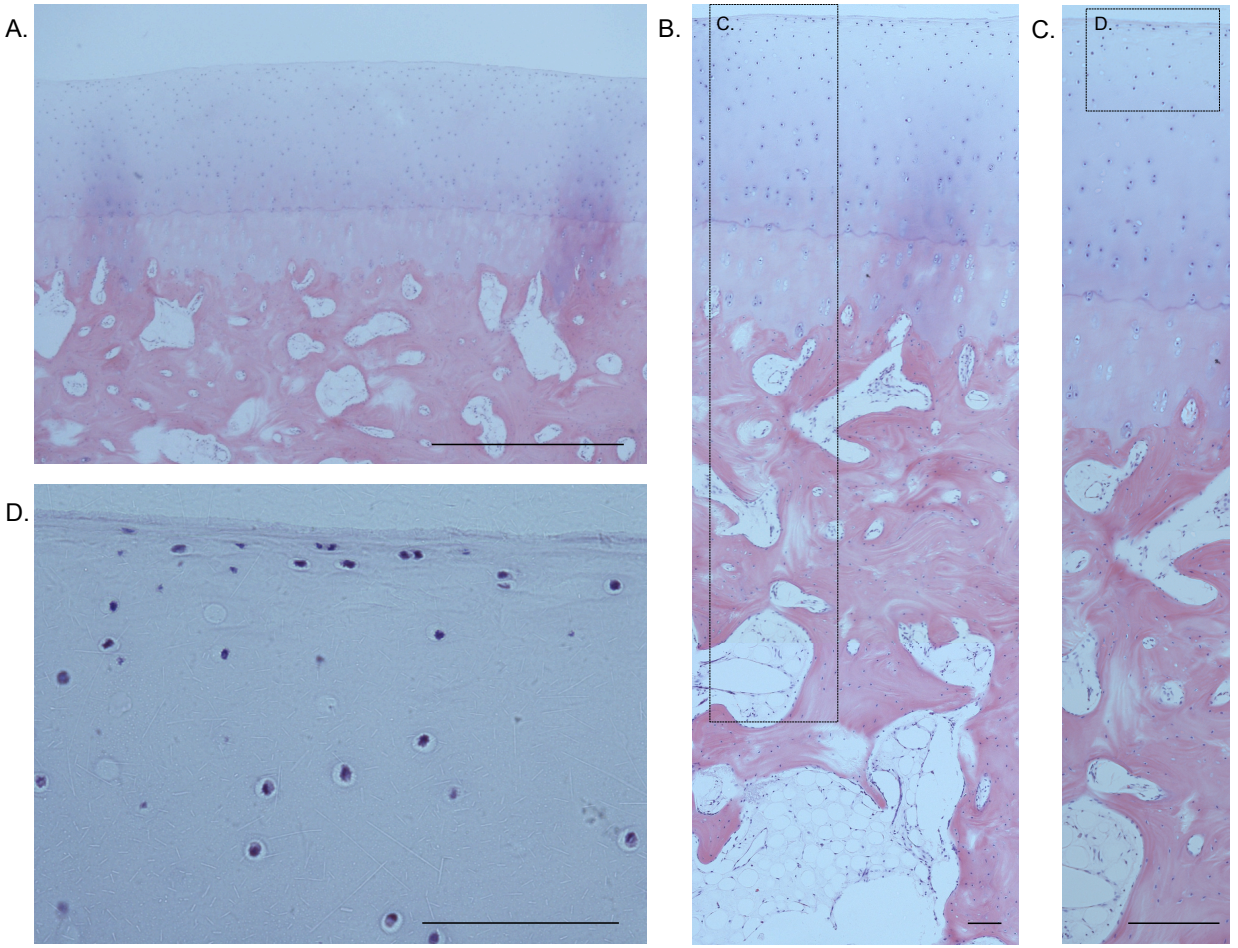

Figure 5.6 Healthy osteochondral wedge biopsy sections with no pathology. Osteochondral sections were scored using a histopathological cartilage scoring system, assessing focal cell loss, chondrocyte necrosis, fibrillation of the articular surface, and chondrocyte cluster (more than one chondrocyte within the same lacunae in the superficial zone). A. x4, scale bar = 1000μm. B. x10, C. x20, D. x40. B-D Scale bars = 100μm.

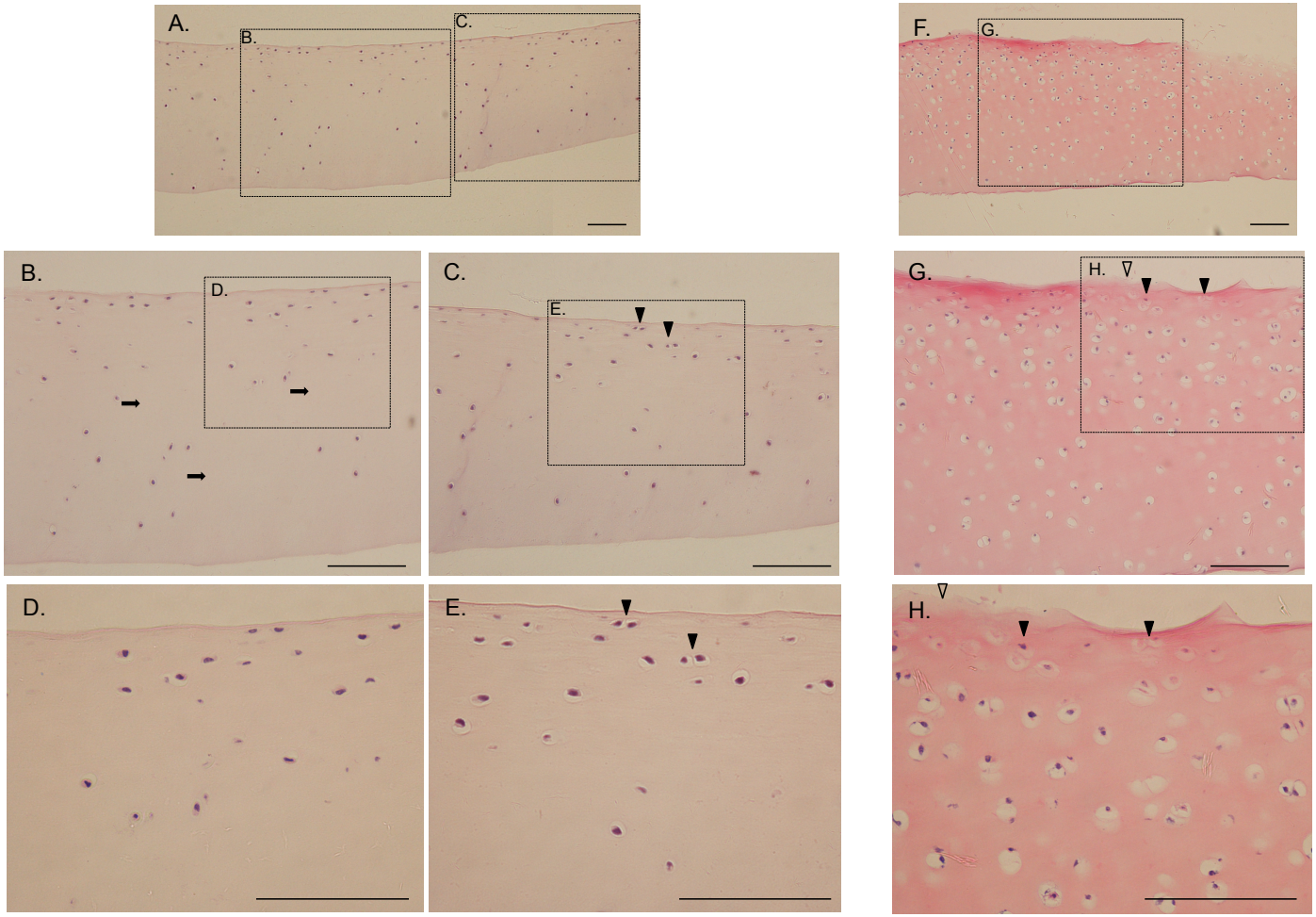

Figure 5.7 Cartilage explant sections graded. Sections were scored for focal cell loss (arrows), chondrocyte cluster formation (more than one chondrocyte within the same lacunae in the superficial zone of the explant) (arrowhead) and fibrillation of the articular surface (arrowhead outline). A. x4, B & C. x20, D & E. x40. All scale bars = 100µm. Sample A-E was graded 1.5, sample F-H was graded 6.5.

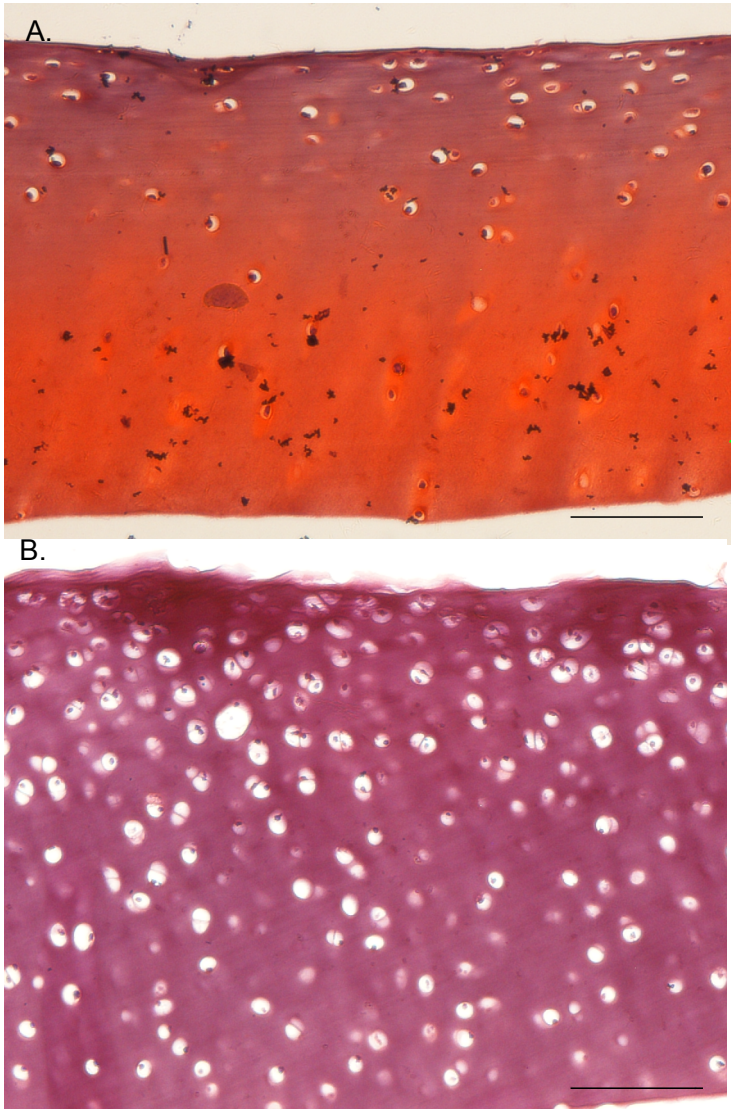

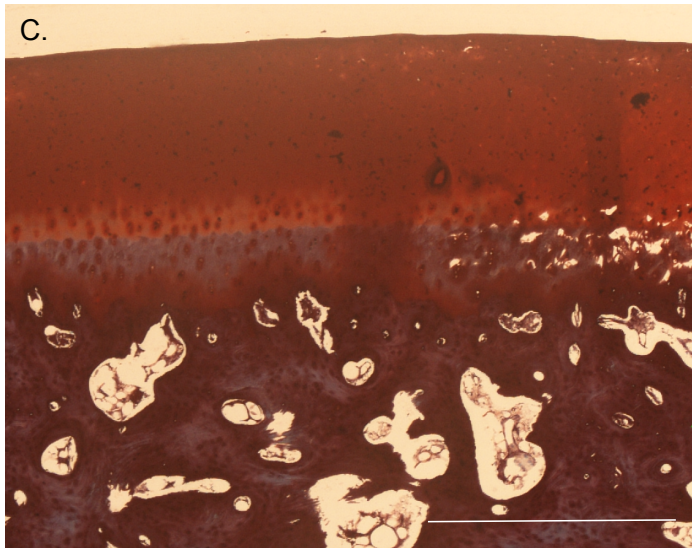

Figure 5.8 Cartilage explant (A & B) and osteochondral wedge biopsy (C) sections stained with Safranin-O to visualise the cartilage explant proteoglycan content. Sections were stained with celestine blue, 0.5% fast green then 1% safranin-O. Sections were scored for degree of normal staining; a loss of normal staining reflects a decrease in glycosaminoglycan content. (A) (same sample as Figure 5.7A-E) and (C) scored <1, and (B) (same sample as Figure 5.7F-H) scored 4 which indicates normal staining and >75% loss of staining characteristics, respectively. Scale bars = 100μm.

5.4 Discussion

5.4.1 Synoviocytes Reduce sGAG Loss from Cartilage Explants

The co-culture model designed in this study is based on an inflamed intra-articular environment. Direct co-culture of EFLS and EPBMCs reflect the close proximity of FLS and mononuclear cells within the synovium during synovitis. Indirect co-culture of synoviocytes and cartilage explants in a common culture media which provides a transport medium between the cells is synonymous to synovial fluid facilitating cellular signalling between intra-articular synovial membrane and cartilage.

Inflammation is one of the first events to occur in the pathogenesis of OA (Heinegård and Saxne 2011); severe synovitis has been detected early in the disease process and can aid in predicting cartilage breakdown (Sellam and Berenbaum 2010). Cytokine and aggrecanase release are both up-regulated during equine synovitis (Kamm, Nixon et al. 2010), therefore a true synovitis model should emulate these responses. An inflammatory response in this model, was induced by exposing synoviocytes and cartilage to LPS. Synoviocyte gene expression levels of all cytokines, aggrecanases and MMPs analysed were detectable from day 1, apart from TNF-α. The relative abundance of IL-6, ADAMTS5 and MMP3 mRNA transcripts were higher than IL-1β, ADAMTS4 and MMP13. Abundant IL-6 mRNA indicates a synovitis-like response. Synovial fluid (SF) IL-6 levels have been associated with the OA biomarker C-reactive protein, thought to be indicative of an increasing inflammatory cellular infiltrate in the synovial tissue (Pearle, Scanzello et al. 2007). The synoviocyte gene expression profiles produced in

this study reliably demonstrate a synovitis-like response within the co-culture model. A similar equine co-culture model failed to detect IL-1β and TNF-α mRNA expression, and found IL-6 expression unaffected in co-culture (Lee, Kisiday et al. 2013), however this model used a predominantly FLS culture. Co-culture models using bovine synovial explants, which may have retained a heterogeneous synoviocyte cell population more closely resembling that found during joint inflammation, observed an increase in IL-1β mRNA expression during co-culture but no detectable change in TNF-α mRNA expression (Lee, Fitzgerald et al. 2009).

Minor fibrillation of the cartilage surface and substantial release of aggrecan fragments from the cartilage define early OA pathology (Heinegård and Saxne 2011). This increase in aggrecan turnover has also been observed in early equine OA through the use of CA856 mAb and GAG assays, facilitating the measurement of aggrecan fragments within SF (Frisbie, Al-Sobayil et al. 2008, de Grauw, Van de Lest et al. 2009). Aggrecanases, which cleave the aggrecan core protein at four separate cleavage sites, have been inextricably linked to this early joint pathology (Glasson, Askew et al. 2004, Stanton, Rogerson et al. 2005). When analysing the amount of sGAG in this model, significantly lower total sGAG within the culture media of cartilage co-cultured with synoviocytes, compared to that of cartilage cultured independently ($p < 0.01$) was observed. This finding was also observed by Gregg *et al.* (2006) (Gregg, Fortier et al. 2006) who demonstrated a reduction in IL-1β-stimulated cartilage GAG loss when co-cultured with synoviocytes. However, this study also observed a reduction in IL-1β-induced suppression of chondrocyte aggrecan gene expression when in co-

culture with synoviocytes. Chondrocytes should increase the synthesis of these molecules to counteract the loss of aggrecan (Heinegård and Saxne 2011); whereas Lee *et al.* (2013) (Lee, Kisiday et al. 2013) observed less chondrocyte aggrecan gene expression when in co-culture with synovicoytes. It is therefore unknown whether this reduction of GAG loss is due to a protective synoviocyte mechanism encouraging anabolic metabolism, the inhibition of chondrocyte aggrecan synthesis, or suppression of aggrecanase production. The equal increase in sGAG content in culture media between conditions, throughout the first 8 days, may reflect early loss of aggrecan from cartilage ECM commonly observed in early stage OA. However after 8 days, sGAG content in co-culture media, is significantly lower than that of cartilage cultured independently.

Whether synoviocytes were treated with control or anti-IL-1β siRNA loaded microspheres made no difference to the amount of sGAG detected in culture media at day 1, 8 or 28. These results were consistent when using the DMMB assay, and through western blot analysis using the BC-3 mAb. The BC-3 antibody detects fragments of aggrecan that have been released after cleavage of aggrecan within the interglobular domain aggrecanase site (Ala-Glu) and therefore contain a new N-terminus (Busschers, Holt et al. 2010). The western blot analysis of culture media displayed a major band at 62-70kDa which is consistent with C-terminally truncated, ADAMTS-cleaved aggrecan. This indicates that GAG release in this system is driven, at least in part, by aggrecanase cleavage of the aggrecan core protein in the cartilage explants.

In vivo equine synoviocyte ADAMTS4 mRNA expression increases on exposure to LPS and recombinant human IL-1β (Ross, Kisiday et al. 2012). Synoviocyte aggrecanase mRNA expression was evident in this study, with relative abundance of ADATMS5 mRNA transcripts being approximately 10 x more than those of ADAMTS4 on day 1. However, it has also been shown that EFLS ADAMTS5 gene expression is moderated in response to external stimuli. In Chapter 4, it was established that EFLS ADAMTS5 gene expression is attenuated by macrophages, in an inflammatory environment. Other co-culture models have reported a decrease in synoviocyte aggrecanase gene expression in the presence of injured cartilage (Lee, Kisiday et al. 2013), however the model in this study did not incorporate macrophages. A similar negative feedback mechanism may be generated by macrophages and injured cartilage to suppress synoviocyte aggrecanase production, favouring an anabolic environment.

Cartilage explants cultured with synoviocytes had a significantly higher cartilage histopathological score than those cultured without synoviocytes ($p < 0.05$). Cartilage explant histopathological scores were based upon the degree of articular surface cartilage fibrillation, superficial zone chondrocyte cluster (chondrone formation) and safranin-O stain uptake observed. However, changes based upon these criteria may not be very sensitive for *in vitro* measurements of cartilage pathology. For example, fibrillation is dependent on mechanical wear, however the degree of fibrillation may change with loss of sGAG from the ECM. Chondrocyte necrosis and focal cell loss were removed from the modified scoring system as it was hypothesised that these changes are more likely to occur during *in vivo*

cartilage degradation. This significant difference in cartilage degradation when explants were cultured with and without synoviocytes, could be due to the abundant production of cytokines, aggrecanases and MMPs produced by the inflamed synoviocytes.

The method used in this study to dissect cartilage explants from the distal aspect of the condyles of the third metacarpal bone reliably ensured that subchondral bone was not incorporated in the sample. The inclusion of the tidemark and superficial aspect of the calcified cartilage layer, in samples up to 0.41mm thick, helped orientate the sample, allowing reliable deduction of articular surface location. This greatly aided the process of grading. Very thin explants (<0.1mm) were difficult to correctly orientate within paraffin wax, resulting in sections lacking an articular surface. This posed a problem with the histopathological grading system used in this study, as the scoring system demanded the inclusion of the superficial zone adjacent to the articular surface.

5.4.2 SiRNA-Loaded Microspheres Do Not Effect the Co-Culture

Treatment of synoviocytes with anti-IL-1β siRNA loaded microspheres compared to control microspheres, caused no significant differences in synoviocyte gene expression profiles, sGAG measurements within culture media, or cartilage histopathological scores. Previous work in Chapter 3, has verified post-transcriptional synoviocyte RNA interference through the use of equine anti-IL-1β siRNA, and successful EPBMC phagocytosis of small (2-6μm) PLGA-microspheres. However, in this co-culture model we were unable to reproduce these results when using the PLGA microspheres as

siRNA delivery vehicles. Many factors regarding the delivery of siRNA to target mRNA within the cell, need further investigation. These include the rate of EPBMC phagosome microsphere degradation and the subsequent rate of siRNA release, the route of siRNA translocation to the nucleus, and the dose of siRNA required to produce a therapeutic response at the determined rate of siRNA release.

EPBMCs were cultured with the microspheres for 48 hours before EFLS were introduced, allowing sufficient time for EPBMC phagocytosis of the microspheres. However, the rate of microsphere degradation and subsequent release of siRNA within the EPBMC phagosome is unknown. Previous work investigating siRNA-loaded PLGA microsphere phagocytosis with canine macrophage cells (DH82 cell line) (by John Hunt and colleagues) observed a controlled release of siRNA over 6 weeks, resulting in 30-40% siRNA remaining in the microsphere at week 6.

Subsequent to the release of siRNA from the PLGA microsphere, some reports suggest that it may become sequestered within the phagosome. To enable siRNA to move into the cell cytosol and target mRNA, a triggered colloid osmotic disruption of the phagosome may be required (Lee, Yang et al. 2009). As reported by Lee *et al.* (2009) (Lee, Yang et al. 2009) this was caused by hydrolysis of an acid-sensitive microparticle, and subsequent osmotic disruption of the phagosome. The exact mechanism of siRNA translocation out of the phagosome and into the cytosol requires further investigation. This could be achieved using fluorescent siRNA-loaded microspheres in culture with EPBMCs.

Synoviocyte mRNA was analysed via qRT-PCR on days 1, 8 and 28 of the experiment. IL-1β mRNA has a half life of 4-5 hours in monocytes and macrophages (Herzyk, Allen et al. 1992). siRNA release at the correct dose and cleavage of target mRNA would need to be simultaneous to detect an efficient reduction of IL-1β mRNA via qRT-PCR. The dose of siRNA used in this study was extrapolated from those used in the siRNA-lipofectamine transfection protocol in Chapter 3. However, in this study siRNA is encapsulated within microspheres, and only one microsphere can interact with one EPBMC. Therefore, the siRNA dose required to cause an overall therapeutic effect on synoviocyte gene expression, detectable via qRT-PCR, may have been underestimated. Secreted IL-1β protein measurement via an equine IL-1β ELISA kit is the preferred method to investigate RNA interference. However previous work demonstrated low concentrations of EPBMC secreted IL-1β protein that were undetectable by the ELISA assays used.

5.4.3 Conclusion

This study suggests that synoviocytes help moderate the inflammatory response during OA. They exert a protective mechanism over cartilage sGAG release during synovitis. However, they also drive the inflammatory response through production of pro-inflammatory cytokines, aggrecanases and MMPs. siRNA-loaded microspheres did not elicit an anti-inflammatory response from the synoviocytes, nor did they exert a positive effect on cartilage health. However, further investigation is warranted, to examine secreted IL-1β protein levels, and different siRNA doses.

Chapter 6. General Discussion

6.1 General Discussion

The inflamed synovial membrane is a significant source of pro-inflammatory cytokines and cartilage extracellular matrix degrading enzymes, which drive catabolic processes and contribute to the cartilage degradation observed during OA (Sellam and Berenbaum 2010). As synovitis has been directly linked to both bone (Blom, van Lent et al. 2004) and cartilage (Blom, van Lent et al. 2007) structural changes occurring in the joint during OA, the synovial membrane represents an important potential disease-modifying target. The experimental aims within this thesis were to design and test an anti-cytokine therapy using siRNA to decrease target catabolic cytokines produced by synoviocytes. An siRNA vehicle in the form of biodegradable polymer microspheres, designed to deliver siRNA to target cells, was also tested. *In vitro* co-culture systems were created to facilitate assessments of the therapy and therapy-delivery system on synoviocyte and cartilage health, and to examine interactions between the two predominant cell populations present during synovitis; synovial macrophages and FLS.

In Chapter 3, the gene expression profiles of both EFLS and EPBMCs were investigated in response to a range of LPS concentrations. It was decided that exposure to 10μg/ml LPS induced sufficient changes in cytokine gene expression and protein levels, to facilitate the testing of anti-cytokine siRNAs. A successful siRNA-mediated reduction of 65.7% of IL-1β transcripts was achieved when treating EFLS with a specific anti-IL-1β siRNA sequence.

EPBMCs also showed a moderate reduction in secreted IL-1β protein when transfected with the same anti-IL-1β siRNA sequence. Two factors appeared crucial in detecting siRNA-mediated changes in gene expression. (I) The length of LPS-exposure before analysing gene expression levels, as EFLS IL-1β mRNA levels peak 1-3 hours after inflammatory stimulation this is the most sensitive period in which to detect siRNA-mediated decreases in expression. (II) The relative siRNA and primer positions on the target mRNA sequence; 3' mRNA fragments may fail to undergo effective intracellular degradation and can subsequently be detected and amplified by primers designed to complement cDNA within this region, resulting in a false negative siRNA-mediated decrease in gene expression. These factors must be taken into consideration when measuring mRNA transcripts with regards to siRNA-mediated treatment. However, to produce an effective therapy, the reduction in mRNA transcripts must be translated to a reduction in protein levels. Therefore, the gold standard techniques to measure siRNA-mediated reductions in target gene expression are western blot analysis using an appropriate antibody, or ELISA kits. These techniques were used within this thesis; cell culture media IL-1β concentrations were measured using an equine IL-1β ELISA kit, however concentrations measured were below the lower concentration threshold of this assay making this data inconclusive. Protein concentration from cell culture media using Strataclean resin was undertaken to concentrate cell culture media proteins in an attempt to allow reliable IL-1β protein levels. However, the proteins extracted using protein-resin binding represented a subset of the range of proteins expected to be found in cell culture media, and it was hypothesised that a far greater

dispersity in protein size would be found. Protein concentrations measured before and after protein-resin binding reflected successful protein extraction from the cell culture media, however this was not reflected in the proteins identified through ponseau staining of the nitrocellulose membrane once proteins had been transferred after being processed by polyacrylamide gel electrophoresis. Why this process has extracted and concentrated proteins of a specific size, and not the entire range of proteins normally found in cell culture media, need further investigation. A lack of equine specific reactive reagents further impedes successful and thorough investigation into gene translation.

Having successfully designed and tested an equine anti-cytokine siRNA sequence, Chapter 3 also described evidence of highly efficient EPBMC phagocytosis of biodegradable polymer microspheres. A z-stack series of multichannel scanning confocal laser microscopy images allowed the entire volume of the cell to be visualised. Through these images, the phagocytosis of fluorescent microspheres was evident; multiple intracellular fluorescent phagosomes were present consistent with the phagocytic digestion. The phagocytic capabilities of synovial macrophages within synovial explants were also tested through co-culture with fluorescent microspheres. Fluorescent microspheres were clearly associated with the explants and had been degraded into smaller fluorescent particles. Although these particles appeared to be cell associated, it was not possible to definitively prove whether these particles were intracellular. Visualisation of synovial explant sections using confocal laser microscopy was inadequate to determine

whether microspheres had been internalised and phagocytosed, further work is required to achieve this.

In order to determine both the beneficial and disadvantageous effects of reducing target cytokine gene expression, we first needed to elucidate the cell-specific responses to inflammatory stimulation, of the two predominant cell populations present within the synovial membrane during synovitis; the FLS and synovial macrophages. This was achieved through the creation of a multi-species co-culture model, using equine FLS and a canine macrophage cell line (DH82), and through the design of species-specific primers for mRNA transcript quantification. It was interesting to note an increase in EFLS active ADAMTS5 protein secretion and mRNA expression upon exposure to LPS whereas mRNA expression was attenuated when EFLS were in co-culture with DH82 cells. This attenuation appeared to be caused by a thermally stable soluble factor produced by DH82 cells, which acted in an IL-1β independent manner. This moderation of the inflammatory response caused by macrophages, which are chiefly recognised as drivers of inflammation (Bondeson, Wainwright et al. 2006), has also been noted in other studies (Bailey 2014, Bailey 2015). Presence of macrophages in co-culture with EFLS also stimulated FLS mitosis, which may explain the synovial hyperplasia which occurs during synovitis and is recognised as a gross pathological change during OA.

Chapter 5 went on to further investigate the interactions between EFLS and EPBMC co-cultures, cultured with cartilage explants, to examine the effects

of synovitis on cartilage health, and to assess whether the anti-cytokine siRNA-mediated therapy delivered to cells via biodegradable polymer microspheres could help counteract the injurious effects of synovitis on cartilage. One of the most noteworthy results found in this chapter, was the significantly lower total sGAG measured within the culture media of cartilage co-cultured with synoviocytes, compared to that of cartilage cultured independently ($p < 0.01$). This finding indicates that synoviocytes reduce the GAG loss from cartilage, which has previously been reported (Gregg, Fortier et al. 2006) however, whether this is a protective synoviocyte mechanism encouraging anabolic metabolism, the inhibition of chondrocyte aggrecan synthesis, or suppression of aggrecanase production is unknown. In contrast to this finding, synoviocyte gene expression levels of pro-inflammatory cytokines and cartilage ECM degrading enzymes were abundant. No anti-inflammatory effects of siRNA loaded microspheres were observed on either synoviocyte gene expression levels or cartilage health.

To conclude, this thesis has successfully completed the initial design and testing of an anti-cytokine siRNA therapy, and delivery vehicle. It has also identified interesting and important interactions synovial like fibroblasts and inflammatory cells which may be involved in regulating pro-inflammatory and cartilage ECM degrading processes during synovitis. To successfully target the synovial membrane and produce a disease-modifying therapy, knowledge of these cellular responses, and how they are affected by the therapy, is critical when trying to re-create the intra-articular homeostatic balance that conserves cartilage health.

6.2 Further Work

There are several avenues of further investigation that could proceed from this thesis.

6.2.1 EFLS and EPBMC Co-Culture Experimental Work

Further investigation to determine how to extract and separate the full range of proteins present within EFLS and EPBMC cell culture media would allow analysis of changes in protein secretion.

To test the anti-equine IL-1β monoclonal antibody used in this thesis, for adequate cross-matching with recombinant equine IL-1β protein in western blot analysis.

Further investigate the influence macrophages have on joint cells by using single-species co-culture models. Canine models would include the canine macrophage cell line (DH82) with either primary canine fibroblast-like synoviocytes (CFLS) or primary canine chondrocytes. To produce the equine co-culture models, equine peripheral blood mononuclear cells (EPBMCs) isolated from equine blood using density cell separation would be co-cultured with EFLS or with primary equine chondrocytes. Differential fluorescent labeling of cell dyes within the co-cultures with cell tracker dyes could facilitate cell separation through FACS enabling the quantification of individual cell population gene expression of cytokines (IL-1β and IL-6), aggrecanases (ADAMTS4 and -5) and MMP-3 and -13. Flow cytometry analysis would also provide information about the proliferation of FLS whilst in co-culture with monocytes/macrophages of the same species.

6.2.2 Anti-cytokine siRNA-loaded Microsphere Experimental Work

To ensure siRNA-loaded onto microspheres can effectively translocate from the phagosome to the cell nucleus, fluorescent-siRNA-loaded microspheres should be cultured with synoviocytes. Through the use of fluorescently labelled dyes, the location of fluorescent-siRNA could be identified using multichannel laser scanning confocal microscopy.

When anti-IL-1β siRNA-loaded microspheres were cultured with synoviocytes in Chapter 5, a comparable reduction in synoviocyte IL-1β mRNA expression to that produced when transfecting EFLS with siRNA in Chapter 3, was not reproduced. As mentioned previously, this may have been due to the timing of synoviocyte mRNA analysis. A range of different time periods to include time of synoviocyte and siRNA-loaded microsphere culture, and time of exposure to LPS before cell harvesting, need to be trialled to ensure siRNA-mediated decrease in IL-1β mRNA is detected.

References

Alaaeddine, N., J. A. DiBattista, J. P. Pelletier, J. M. Cloutier, K. Kiansa, M. Dupuis and J. Martel-Pelletier (1997). "Osteoarthritic synovial fibroblasts possess an increased level of tumor necrosis factor-receptor 55 (TNF-R55) that mediates biological activation by TNF-alpha." Journal of Rheumatology **24**(10): 1985-1994.

Allen, J. B., C. L. Manthey, A. R. Hand, K. Ohura, L. Ellingsworth and S. M. Wahl (1990). "Rapid onset synovial inflammation and hyperplasia induced by transforming growth factor beta." Journal of Experimental Medicine **171**(1): 231-247.

Allen, K. D., S. B. Adams and L. A. Setton (2010). "Evaluating Intra-Articular Drug Delivery for the Treatment of Osteoarthritis in a Rat Model." Tissue Engineering. Part B, Reviews **16**(1): 81-92.

Alvaro-Gracia, J. M., N. J. Zvaifler and G. S. Firestein (1990). "Cytokines in chronic inflammatory arthritis. V. Mutual antagonism between interferon-gamma and tumor necrosis factor-alpha on HLA-DR expression, proliferation, collagenase production, and granulocyte macrophage colony-stimulating factor production by rheumatoid arthritis synoviocytes." Journal of Clinical Investigation **86**(6): 1790-1798.

Alwan, W. H., S. D. Carter, J. B. Dixon, D. Bennett, S. A. May and G. B. Edwards (1991). "Interleukin-1-like activity in synovial fluids and sera of horses with arthritis." Research in Veterinary Science **51**(1): 72.

Apparailly, F. and C. Jorgensen (2013). "siRNA-based therapeutic approaches for rheumatic diseases." Nature Reviews Rheumatology **9**(1): 56.

Attur, M., J. Samuels, S. Krasnokutsky and S. B. Abramson (2010). "Targeting the synovial tissue for treating osteoarthritis (OA): where is the evidence?" Best Practice & Research Clinical Rheumatology **24**(1): 71-79.

Bailey, K. N. (2014). "Pre-injury Depletion of Macrophages Results in Increased Acute Joint Inflammation Following Articular Fracture." Proceedings of the Orthopaedic Research Society 2015 Annual Meeting: 197-198.

Bailey, K. N. (2015). "Intra-articular Depletion of Macrophages following Articular Fracture Results in Bone Resorption and Altered Synovial Macrophage Polarity." Proceedings of the Orthopaedic Research Society 2015 Annual Meeting.

Bakali, J. E., H. Gras-Masse, L. Maingot, B. Deprez, J. Dumont, F. Leroux and R. Deprez-Poulain (2014). "Inhibition of aggrecanases as a therapeutic strategy in osteoarthritis." Future Medicinal Chemistry **6**(12): 1399-1412.

Bartok, B. and G. S. Firestein (2010). "Fibroblast-like synoviocytes: key effector cells in rheumatoid arthritis." Immunological Reviews **233**(1): 233.

Bau, B., P. M. Gebhard and J. Haag (2002). "Relative Messenger RNA Expression Profiling of Collagenases and Aggrecanases in Human Articular Chondrocytes In Vivo and In Vitro." Arthritis Rheum **46**: 2648.

Benito, M. J., D. J. Veale, O. FitzGerald, W. B. van den Berg and B. Bresnihan (2005). "Synovial tissue inflammation in early and late osteoarthritis." Annals of the Rheumatic Diseases **64**(9): 1263-1267.

Berenbaum, F. (2013). "Osteoarthritis as an inflammatory disease (osteoarthritis is not osteoarthrosis!)." Osteoarthritis Cartilage **21**(1): 16-21.

Bertone, A. L., J. L. Palmer and J. Jones (2001). "Synovial fluid cytokines and eicosanoids as markers of joint disease in horses." Veterinary Surgery **30**(6): 528-538.

Billinghurst, R. C., P. B. Fretz and J. R. Gordon (1995). "Induction of intra-articular tumour necrosis factor during acute inflammatory responses in equine arthritis." Equine Veterinary Journal **27**(3): 208.

Blom, A. B., P. L. van Lent, A. E. Holthuysen, P. M. van der Kraan, J. Roth, N. van Rooijen and W. B. van den Berg (2004). "Synovial lining macrophages mediate osteophyte formation during experimental osteoarthritis." Osteoarthritis Cartilage **12**(8): 627-635.

Blom, A. B., P. L. van Lent, S. Libregts, A. E. Holthuysen, P. M. van der Kraan, N. van Rooijen and W. B. van den Berg (2007). "Crucial role of macrophages in matrix metalloproteinase–mediated cartilage destruction during experimental osteoarthritis : Involvement of matrix metalloproteinase 3." Arthritis & Rheumatism **56**(1): 147-157.

Bobacz, K., I. G. Sunk, J. G. Hofstaetter, L. Amoyo, C. D. Toma, S. Akira, T. Weichhart, M. Saemann and J. S. Smolen (2007). "Toll-like receptors and

chondrocytes: the lipopolysaccharide-induced decrease in cartilage matrix synthesis is dependent on the presence of toll-like receptor 4 and antagonized by bone morphogenetic protein 7." Arthritis Rheum **56**(6): 1880-1893.

Bodick, N., J. Lufkin, C. Willwerth, J. Hauben, A. Kumar, P. Boen, J. Bolognese, C. Schoonmaker and M. Clayman (2015). "Prolonged joint residency of triamcinolone acetonide after an intra-articular injection of FX006, a sustained release formulation for the treatment of osteoarthritis." Osteoarthritis and Cartilage **23**(1, Number): A360.

Bondeson, J., S. Wainwright, B. Caterson and C. Hughes (2013). "Adamts5." Handbook of Proteolytic Enzymes, Vols 1 and 2, 3rd Edition: 1174-1180.

Bondeson, J., S. Wainwright, C. Hughes and B. Caterson (2015). "Can allosteric inhibitors of adamts4 and adamts5 prevent osteoarthritis disease progression." A Tenth of a Second: A History **10**(23): 5-14.

Bondeson, J., S. D. Wainwright, S. Lauder, N. Amos and C. E. Hughes (2006). "The role of synovial macrophages and macrophage-produced cytokines in driving aggrecanases, matrix metalloproteinases, and other destructive and inflammatory responses in osteoarthritis." Arthritis Res Ther **8**(6): R187.

Boulanger, M. J., D. C. Chow, E. E. Brevnova and K. C. Garcia (2003). "Hexameric structure and assembly of the interleukin-6/IL-6 alpha-receptor/gp130 complex." Science (Classic) **300**(5628): 2101-2104.

Bragdon, B., A. L. Bertone, J. Hardy, E. J. Simmons and S. E. Weisbrode (2001). "Use of an isolated joint model to detect early changes induced by intra-articular injection of paclitaxel-impregnated polymeric microspheres." Journal of Investigative Surgery **14**(3): 169-182.

Brew, C. J., P. D. Clegg, R. P. Boot-Handford, J. G. Andrew and T. Hardingham (2010). "Gene expression in human chondrocytes in late osteoarthritis is changed in both fibrillated and intact cartilage without evidence of generalised chondrocyte hypertrophy." Ann Rheum Dis **69**(1): 234-240.

Brunner, T., S. Cohen and A. Monsonego (2010). "Silencing of proinflammatory genes targeted to peritoneal-residing macrophages using

siRNA encapsulated in biodegradable microspheres." Biomaterials **31**(9): 2627-2636.

Buckwalter, J. A. and T. D. Brown (2004). "Joint Injury, Repair, and Remodeling." Clinical Orthopaedics and Related Research **423**: 7.

Busschers, E., J. P. Holt and D. W. Richardson (2010). "Effects of glucocorticoids and interleukin-1β on expression and activity of aggrecanases in equine chondrocytes." American Journal of Veterinary Research **71**(2): 176-185.

Butoescu, N., C. A. Seemayer, M. Foti, O. Jordan and E. Doelker (2009). "Dexamethasone-containing PLGA superparamagnetic microparticles as carriers for the local treatment of arthritis." Biomaterials **30**(9): 1772.

Caldorera-Moore, M., N. Guimard, L. Shi and K. Roy (2010). "Designer nanoparticles: incorporating size, shape and triggered release into nanoscale drug carriers." Expert opinion on drug delivery **7**(4): 479.

Caput, D., B. Beutler, K. Hartog, R. Thayer, S. Brown-Shimer and A. Cerami (1986). "Identification of a common nucleotide sequence in the 3'-untranslated region of mRNA molecules specifying inflammatory mediators." Proceedings of the National Academy of Sciences **83**(6): 1670-1674.

Carlson, E. R., A. A. Stewart, K. L. Carlson, S. S. Durgam and H. C. Pondenis (2013). "Effects of serum and autologous conditioned serum on equine articular chondrocytes treated with interleukin-1 β." American Journal of Veterinary Research **74**(5): 700-705.

Caron, J. P. (2011). Chapter 61 - Osteoarthritis. Diagnosis and Management of Lameness in the Horse (Second Edition). M. W. R. J. Dyson. Saint Louis, W.B. Saunders**:** 655-668.

Casal, M. and M. Haskins (2006). "Large animal models and gene therapy." European journal of human genetics **14**(3): 266-272

Caselli, G., R. Chiusaroli, M. Visintin, M. Lanza, F. Ferrari, D. Tremolada, B. Barbetta, G. Giacovelli, A. Bonazzi and L. C. Rovati (2015). "Effect size of the Anti-Aggrecanase-2 Monoclonal Antibody CRB0017 in Rodent Models of Osteoarthritis (abstract)." Arthritis & Rheumatology **67**((suppl 10)).

Chen, R., S. J. Curran, J. M. Curran and J. A. Hunt (2006). "The use of poly(l-lactide) and RGD modified microspheres as cell carriers in a flow

intermittency bioreactor for tissue engineering cartilage." Biomaterials **27**(25): 4453-4460.

Chevalier, X., P. Goupille, A. D. Beaulieu, F. X. Burch, W. G. Bensen, T. Conrozier, D. Loeuille, A. J. Kivitz, D. Silver and B. E. Appleton (2009). "Intraarticular injection of anakinra in osteoarthritis of the knee: a multicenter, randomized, double-blind, placebo-controlled study." Arthritis Rheum **61**(3): 344-352.

Chiusaroli, R., M. Visentini, C. Galimberti, C. Casseler, L. Mennuni, S. Covaceuszach, M. Lanza, G. Ugolini, G. Caselli, L. C. Rovati and M. Visintin (2013). "Targeting of ADAMTS5's ancillary domain with the recombinant mAb CRB0017 ameliorates disease progression in a spontaneous murine model of osteoarthritis." Osteoarthritis and Cartilage **21**(11): 1807-1810.

Chockalingam, P. S., W. Sun, M. A. Rivera-Bermudez, W. Zeng, D. R. Dufield, S. Larsson, L. S. Lohmander, C. R. Flannery, S. S. Glasson, K. E. Georgiadis and E. A. Morris (2011). "Elevated aggrecanase activity in a rat model of joint injury is attenuated by an aggrecanase specific inhibitor." Osteoarthritis and Cartilage **19**(3): 315.

Chomczynski, P. and N. Sacchi (1987). "Single-step method of RNA isolation by acid guanidinium thiocyanate-phenol-chloroform extraction." Analytical Biochemistry **162**(1): 156-159.

Clegg, P. D. and S. D. Carter (1999). "Matrix metalloproteinase-2 and -9 are activated in joint diseases." Equine Veterinary Journal **31**(4): 324.

Clements, K. M., J. S. Price, M. G. Chambers, D. M. Visco, A. R. Poole and R. M. Mason (2003). "Gene deletion of either interleukin-1beta, interleukin-1beta-converting enzyme, inducible nitric oxide synthase, or stromelysin 1 accelerates the development of knee osteoarthritis in mice after surgical transection of the medial collateral ligament and partial medial meniscectomy." Arthritis Rheum **48**(12): 3452-3463.

Cohen, J. (1960). "Kappa: Coefficient of concordance." Educ. Psych. Measurement **20**: 37.

Cohen, M., E. Klein, B. Geiger and L. Addadi (2003). "Organization and Adhesive Properties of the Hyaluronan Pericellular Coat of Chondrocytes and Epithelial Cells." Biophysical Journal **85**(3): 1996-2005.

Cook, J., K. Kuroki, D. Visco, J.-P. Pelletier, L. Schulz and F. Lafeber (2010). "The OARSI histopathology initiative–recommendations for histological assessments of osteoarthritis in the dog." Osteoarthritis and cartilage **18**: S66-S79.

Cun, D., D. K. Jensen, M. J. Maltesen, M. Bunker, P. Whiteside, D. Scurr, C. Foged and H. M. Nielsen (2011). "High loading efficiency and sustained release of siRNA encapsulated in PLGA nanoparticles: Quality by design optimization and characterization." European Journal of Pharmaceutics and Biopharmaceutics **77**(1): 26-35.

Cuzzocrea, S., P. K. Chatterjee, E. Mazzon, L. Dugo, I. Serraino, D. Britti, G. Mazzullo, A. P. Caputi and C. Thiemermann (2002). "Pyrrolidine dithiocarbamate attenuates the development of acute and chronic inflammation." British journal of pharmacology **135**(2): 496-510.

Dancevic, C. M. and D. R. McCulloch (2014). "Current and emerging therapeutic strategies for preventing inflammation and aggrecanase-mediated cartilage destruction in arthritis." Arthritis Research & Therapy **16**(5): 429.

David, F., J. Farley and H. Huang (2007). "Cytokine and Chemokine Gene Expression of IL-1b Stimulated Equine Articular Chondrocytes." Vet Surg **36**: 221.

Davidson, R. K., J. G. Waters, L. Kevorkian, C. Darrah, A. Cooper, S. T. Donell and I. M. Clark (2006). "Expression profiling of metalloproteinases and their inhibitors in synovium and cartilage." Arthritis Res Ther **8**(4): R124.

de Grauw, J. C., C. Van de Lest and P. R. van Weeren (2009). "Inflammatory mediators and cartilage biomarkers in synovial fluid after a single inflammatory insult: a longitudinal experimental study." Arthritis Res Ther **11**: R35.

de Hooge, A. S., F. A. van de Loo and M. B. Bennink (2005). "Male IL-6 gene knock out mice developed more advanced osteoarthritis upon aging." Osteoarthritis Cartilage **13**: 66.

Dechant, J. E., G. M. Baxter, D. D. Frisbie, G. W. Trotter and C. W. McIlwraith (2003). "Effects of dosage titration of methylprednisolone acetate and triamcinolone acetonide on interleukin-1-conditioned equine articular cartilage explants in vitro." Equine Vet J **35**(5): 444-450.

Deleavey, Glen F. and Masad J. Damha (2012). "Designing Chemically Modified Oligonucleotides for Targeted Gene Silencing." Chemistry & Biology **19**(8): 937-954.

Deuel, T. F., R. M. Senior, J. Huang and G. Griffin (1982). "Chemotaxis of monocytes and neutrophils to platelet-derived growth factor." Journal of Clinical Investigation **69**(4): 1046.

Dinarello, C. A. (1988). "Biology of interleukin 1." The FASEB Journal **2**(2): 108-115.

Dinarello, C. A. (1996). "Biologic basis for interleukin-1 in disease." Blood **87**(6): 2095-2147.

Dominska, M. and D. M. Dykxhoorn (2010). "Breaking down the barriers: siRNA delivery and endosome escape." Journal of Cell Science **123**(8): 1183-1189.

Donlin, L. T., A. Jayatilleke, E. G. Giannopoulou, G. D. Kalliolias and L. B. Ivashkiv (2014). "Modulation of TNF-induced macrophage polarization by synovial fibroblasts." J Immunol **193**(5): 2373-2383.

Dower, S. K., S. R. Kronheim, T. P. Hopp, M. Cantrell, M. Deeley, S. Gillis, C. S. Henney and D. L. Urdal (1986). "The cell surface receptors for interleukin-1[alpha] and interleukin-1[beta] are identical." Nature **324**(6094): 266-268.

Dripps, D. J., B. J. Brandhuber, R. C. Thompson and S. P. Eisenberg (1991). "Interleukin-1 (IL-1) receptor antagonist binds to the 80-kDa IL-1 receptor but does not initiate IL-1 signal transduction." The Journal of Biological Chemistry **266**(16): 10331-10336.

Durigova, M., H. Nagase, J. S. Mort and P. J. Roughley (2011). "MMPs are less efficient than ADAMTS5 in cleaving aggrecan core protein." Matrix Biol **30**(2): 145-153.

East, C. J., H. Stanton, S. B. Golub, F. M. Rogerson and A. J. Fosang (2007). "ADAMTS-5 Deficiency Does Not Block Aggrecanolysis at Preferred Cleavage Sites in the Chondroitin Sulfate-rich Region of Aggrecan." J Biol Chem **282**: 8632.

Edwards, J. C. (1994). "The nature and origins of synovium: experimental approaches to the study of synoviocyte differentiation." Journal of Anatomy (Blackwell) **184 (Pt 3)**: 493-501.

Edwards, S. H. R. (2011). "Intra-articular drug delivery: The challenge to extend drug residence time within the joint." The Veterinary Journal **190**(1): 15-21.

Ehrle, A., C. J. Lischer, J. Lasarzik, R. Einspanier and A. Bondzio (2015). "Synovial Fluid and Serum Concentrations of Interleukin-1 Receptor Antagonist and Interleukin-1ß in Naturally Occurring Equine Osteoarthritis and Septic Arthritis." Journal of Equine Veterinary Science **35**(10): 815-822.

Elbashir, S. M., J. Harborth, W. Lendeckel, A. Yalcin and et al. (2001). "Duplexes of 21-nucleotide RNAs mediate RNA interference in cultured mammalian cells." Nature **411**(6836): 494-498.

Farndale, R. W., D. J. Buttle and A. J. Barrett (1986). "Improved quantitation and discrimination of sulphated glycosaminoglycans by use of dimethylmethylene blue." Biochimica et Biophysica Acta (BBA) - General Subjects **883**(2): 173-177.

Felson, D. T. and R. Hodgson (2014). "Identifying and Treating Preclinical and Early Osteoarthritis." Rheumatic Disease Clinics of North America **40**(4): 699-710.

Fernandes, J. C., J. Martel-Pelletier and J.-P. Pelletier (2002). "The role of cytokines in osteoarthritis pathophysiology." Biorheology **39**(1): 237-246.

Filer, A., G. Parsonage, E. Smith, C. Osborne, A. M. Thomas, S. J. Curnow, G. E. Rainger, K. Raza, G. B. Nash, J. Lord, M. Salmon and C. D. Buckley (2006). "Differential survival of leukocyte subsets mediated by synovial, bone marrow, and skin fibroblasts: site-specific versus activation-dependent survival of T cells and neutrophils." Arthritis Rheum **54**(7): 2096-2108.

Fioravanti, A., M. Fabbroni, A. Cerase and M. Galeazzi (2009). "Treatment of erosive osteoarthritis of the hands by intra-articular infliximab injections: a pilot study." Rheumatology International **29**(8): 961-965.

Fjordbakk, C. T., G. M. Johansen, A. C. Løvås, K. L. Oppegård and A. K. Storset (2015). "Surgical stress influences cytokine content in autologous conditioned serum." Equine Veterinary Journal **47**(2): 212-217.

Flannery, C. R., C. B. Little, B. Caterson and C. E. Hughes (1999). "Effects of culture conditions and exposure to catabolic stimulators (IL-1 and retinoic acid) on the expression of matrix metalloproteinases (MMPs) and disintegrin

metalloproteinases (ADAMs) by articular cartilage chondrocytes." Matrix Biology **18**(3): 225.

Flannery, C. R., C. B. Little, C. E. Hughes and B. Caterson (1999). "Expression of ADAMTS Homologues in Articular Cartilage." Biochemical and Biophysical Research Communications **260**(2): 318-322.

Flannery, C. R., C. B. Little, C. E. Hughes, C. L. Curtis, B. Caterson and S. A. Jones (2000). "IL-6 and its soluble receptor augment aggrecanase-mediated proteoglycan catabolism in articular cartilage." Matrix Biology **19**(6): 549-553.

Fosang, A., K. Last, H. Stanton, S. Golub, C. Little, L. Brown and D. Jackson (2010). Neoepitope Antibodies Against MMP-Cleaved and Aggrecanase-Cleaved Aggrecan. Matrix Metalloproteinase Protocols. I. M. Clark, Humana Press. **622:** 305-340.

Fosang, A. J., F. M. Rogerson, C. J. East and H. Stanton (2008). "ADAMTS-5: the story so far." Eur Cell Mater **15**(1): 11-26.

Frisbie, D. D. (2012). Chapter 78 - Synovial Joint Biology and Pathobiology. Equine Surgery (Fourth Edition). J. A. Stick, Auer, John A. Saint Louis, W.B. Saunders**:** 1096-1114.

Frisbie, D. D., F. Al-Sobayil, R. C. Billinghurst, C. E. Kawcak and C. W. McIlwraith (2008). "Changes in synovial fluid and serum biomarkers with exercise and early osteoarthritis in horses." Osteoarthritis and Cartilage **16**(10): 1196-1204.

Frisbie, D. D., S. C. Ghivizzani, P. D. Robbins, C. H. Evans and C. W. McIllwraith (2002). "Treatment of experimental equine osteoarthritis by in vivo delivery of the equine interleukin-1 receptor antagonist gene." Gene Therapy **9**(1): 12.

Frisbie, D. D., C. E. Kawcak, N. M. Werpy, R. D. Park and C. W. McIlwraith (2007). "Clinical, biochemical, and histologic effects of intra-articular administration of autologous conditioned serum in horses with experimentally induced osteoarthritis." American Journal of Veterinary Research **68**(3): 290.

Frisbie, D. D. and C. W. McIlwraith (2000). "Evaluation of Gene Therapy as a Treatment for Equine Traumatic Arthritis and Osteoarthritis." Clinical Orthopaedics and Related Research **379**: S273-S287.

Fushimi, K., L. Troeberg, H. Nakamura, N. H. Lim and H. Nagase (2008). "Functional Differences of the Catalytic and Non-catalytic Domains in Human ADAMTS-4 and ADAMTS-5 in Aggrecanolytic Activity." Journal of Biological Chemistry **283**(11): 6706-6716.

Gendron, C., M. Kashiwagi, N. H. Lim, J. J. Enghild, I. B. Thøgersen, C. Hughes, B. Caterson and H. Nagase (2007). "Proteolytic activities of human ADAMTS-5: comparative studies with ADAMTS-4." The Journal of Biological Chemistry **282**(25): 18294-18306.

Ghadially, F. N. (1983). Fine structure of synovial joints: a text and atlas of the ultrastructure of normal and pathological articular tissues, Butterworth-Heinemann.

Glasson, S. S., R. Askew, B. Sheppard, B. Carito, T. Blanchet, H. Ma, C. R. Flannery, D. Peluso, K. Kanki, Z. Yang, M. K. Majumdar and E. A. Morris (2005). "Deletion of active ADAMTS5 prevents cartilage degradation in a murine model of osteoarthritis." Nature **434**(7033): 640-644.

Glasson, S. S., R. Askew, B. Sheppard, B. A. Carito, T. Blanchet, H. Ma, Ling, C. R. Flannery, K. Kanki, E. Wang, D. Peluso, Z. Yang, M. K. Majumdar and E. A. Morris (2004). "Characterization of and osteoarthritis susceptibility in ADAMTS-4-knockout mice." Arthritis & Rheumatism **50**(8): 2547.

Goldring, M. and K. Marcu (2009). "Cartilage homeostasis in health and rheumatic diseases." Arthritis Research & Therapy **11**(3): 224.

Goldring, M. B. and M. Otero (2011). "Inflammation in osteoarthritis." Current opinion in rheumatology **23**(5): 471-478.

Goldring, M. B., M. Otero, D. A. Plumb, C. Dragomir, M. Favero, K. El Hachem, K. Hashimoto, H. I. Roach, E. Olivotto, R. M. Borzì and K. B. Marcu (2011). "Roles of inflammatory and anabolic cytokines in cartilage metabolism: signals and multiple effectors converge upon MMP-13 regulation in osteoarthritis." European Cells and Materials **21**: 202-220.

Goodrich, L. R., V. W. Choi, B. A. D. Carbone, C. W. McIlwraith and R. J. Samulski (2009). "Ex Vivo Serotype-Specific Transduction of Equine Joint Tissue by Self-Complementary Adeno-Associated Viral Vectors." Human Gene Therapy **20**(12): 1697.

Goodrich, L. R., J. N. Phillips, C. W. McIlwraith, S. B. Foti, J. C. Grieger, S. J. Gray and R. J. Samulski (2013). "Optimization of scAAVIL-1ra In Vitro and In

Vivo to Deliver High Levels of Therapeutic Protein for Treatment of Osteoarthritis." Mol Ther Nucleic Acids **2**: e70.

Gregg, A. J., L. A. Fortier, H. O. Mohammed, K. G. Mayr, B. J. Miller and J. L. Haupt (2006). "Assessment of the catabolic effects of interleukin-1β on proteoglycan metabolism in equine cartilage cocultured with synoviocytes." American Journal of Veterinary Research **67**(6): 957.

Gregg, A. J., L. A. Fortier, H. O. Mohammed, K. G. Mayr, B. J. Miller and J. L. Haupt (2006). "Assessment of the catabolic effects of interleukin-1β on proteoglycan metabolism in equine cartilage cocultured with synoviocytes." American Journal of Veterinary Research **67**(6): 957-962.

Griffin, D. J., K. F. Ortved, A. J. Nixon and L. J. Bonassar (2015). "Mechanical properties and structure–function relationships in articular cartilage repaired using IGF-I gene-enhanced chondrocytes." Journal of Orthopaedic Research.

Guerne, P. A., D. A. Carson and M. Lotz (1990). "IL-6 production by human articular chondrocytes." J Immunol **144**: 499.

Guerne, P. A., A. Desgeorges, J. M. Jaspar, B. Relic, R. Peter, P. Hoffmeyer and J. M. Dayer (1999). "Effects of IL-6 and its soluble receptor on proteoglycan synthesis and NO release by human articular chondrocytes: comparison with IL-1. Modulation by dexamethasone." Matrix Biology **18**(3): 253.

Hardingham, T. E. and A. J. Fosang (1992). "Proteoglycans: many forms and many functions." The FASEB journal : Official Publication of the Federation of American Societies for Experimental Biology **6**(3): 861-870.

Haringman, J. J., T. J. Smeets, P. Reinders-Blankert and P. P. Tak (2006). "Chemokine and chemokine receptor expression in paired peripheral blood mononuclear cells and synovial tissue of patients with rheumatoid arthritis, osteoarthritis, and reactive arthritis." Annals of the Rheumatic Diseases **65**(3): 294-300.

Haseeb, A. and T. M. Haqqi (2013). "Immunopathogenesis of osteoarthritis." Clin Immunol **146**(3): 185-196.

Hauptmann, B., J. Van Damme and J. M. Dayer (1991). "Modulation of IL-1 inflammatory and immunomodulatory properties by IL-6." European Cytokine Network **2**(1): 39-46.

Hawkins, D. L., R. J. MacKay, G. G. Gum, P. T. Colahan and J. C. Meyer (1993). "Effects of intra-articularly administered endotoxin on clinical signs of disease and synovial fluid tumor necrosis factor, interleukin 6, and prostaglandin E2 values in horses." American journal of veterinary research **54**(3): 379-386.

Haywood, L., D. F. McWilliams, C. I. Pearson, S. E. Gill, A. Ganesan, D. Wilson and D. A. Walsh (2003). "Inflammation and angiogenesis in osteoarthritis." Arthritis Rheum **48**(8): 2173-2177.

Heinegård, D. and T. Saxne (2011). "The role of the cartilage matrix in osteoarthritis." Nature Reviews Rheumatology **7**(1): 50-56.

Hemphill, D. D., C. W. McIlwraith, R. J. Samulski and L. R. Goodrich (2014). "Adeno-associated viral vectors show serotype specific transduction of equine joint tissue explants and cultured monolayers." Sci Rep **4**: 5861.

Herzyk, D. J., J. N. Allen, C. B. Marsh and M. D. Wewers (1992). "Macrophage and monocyte IL-1 beta regulation differs at multiple sites. Messenger RNA expression, translation, and post-translational processing." The journal of immunology **149**(9): 3052-3058.

Holmes, K., C. M. Williams, E. A. Chapman and M. J. Cross (2010). "Detection of siRNA induced mRNA silencing by RT-qPCR: considerations for experimental design." BMC research notes **3**: 53.

Hoshi, H., T. Sasho, R. Akagi, Y. Muramatsu, S. Mukoyama, Y. Akatsu, T. Fukawa, J. Katsuragi, J. Endo and Y. Yamamoto (2014). "Effective knock down of MMP13 and ADAMTS5 by intra-articular injection of small interference RNA (siRNA) in a surgically induced osteoarthritis model of mice." Osteoarthritis and Cartilage **22**: S372-S373.

Houard, X., M. B. Goldring and F. Berenbaum (2013). "Homeostatic Mechanisms in Articular Cartilage and Role of Inflammation in Osteoarthritis." Current rheumatology reports **15**(11): 375-375.

Hraha, T. H., K. M. Doremus, C. W. McIlwraith and D. D. Frisbie (2011). "Autologous conditioned serum: the comparative cytokine profiles of two commercial methods (IRAP and IRAP II) using equine blood." Equine Vet J **43**(5): 516-521.

Hynes, R. O. and A. Naba (2012). "Overview of the matrisome—an inventory of extracellular matrix constituents and functions." Cold Spring Harbor perspectives in biology **4**(1): a004903.

Inoue, A., K. A. Takahashi, O. Mazda, Y. Arai, M. Saito, T. Kishida, M. Shin-Ya, T. Morihara, H. Tonomura, K. Sakao, J. Imanishi and T. Kubo (2009). "Comparison of anti-rheumatic effects of local RNAi-based therapy in collagen induced arthritis rats using various cytokine genes as molecular targets." Mod Rheumatol **19**(2): 125-133.

Inoue, A., K. A. Takahashi, O. Mazda, R. Terauchi, Y. Arai, T. Kishida, M. Shin-Ya, H. Asada, T. Morihara, H. Tonomura, S. Ohashi, Y. Kajikawa, Y. Kawahito, J. Imanishi, M. Kawata and T. Kubo (2005). "Electro-transfer of small interfering RNA ameliorated arthritis in rats." Biochemical and biophysical research communications **336**(3): 903.

Ishihara, A., J. S. Bartlett and A. L. Bertone (2012). "Inflammation and immune response of intra-articular serotype 2 adeno-associated virus or adenovirus vectors in a large animal model." Arthritis **2012**: 735472.

Ishimi, Y., C. Miyaura, C. H. Jin, T. Akatsu, E. Abe, Y. Nakamura, A. Yamaguchi, S. Yoshiki, T. Matsuda and T. Hirano (1990). "IL-6 is produced by osteoblasts and induces bone resorption." The journal of immunology **145**(10): 3297-3303.

Janssen, M., G. Mihov, T. Welting, J. Thies and P. Emans (2014). "Drugs and Polymers for Delivery Systems in OA Joints: Clinical Needs and Opportunities." Polymers **6**(3): 799-819.

Janssen, M., G. Mihov, T. Welting, J. Thies and P. Emans (2014). "Drugs and Polymers for Delivery Systems in OA Joints: Clinical Needs and Opportunities." Polymers **6**(3): 799.

Janssens, S. and R. Beyaert (2003). "Functional Diversity and Regulation of Different Interleukin-1 Receptor-Associated Kinase (IRAK) Family Members." Molecular Cell **11**(2): 293.

Jay, G. D., D. E. Britt and C. J. Cha (2000). "Lubricin is a product of megakaryocyte stimulating factor gene expression by human synovial fibroblasts." The Journal of rheumatology **27**(3): 594-600.

Jeffcott, L. B., P. D. Rossdale, J. Freestone, C. J. Frank and P. F. Towers-Clark (1982). "An assessment of wastage in Thoroughbred racing from conception to 4 years of age." Equine Veterinary Journal **14**(3): 185-198.

Jensen, D. M. K., D. Cun, M. J. Maltesen, S. Frokjaer, H. M. Nielsen and C. Foged (2010). "Spray drying of siRNA-containing PLGA nanoparticles intended for inhalation." Journal of Controlled Release **142**(1): 138-145.

Jensen, L. B., J. Griger, B. Naeye, A. K. Varkouhi, K. Raemdonck, R. Schiffelers, T. Lammers, G. Storm, S. C. de Smedt, B. S. Sproat, H. M. Nielsen and C. Foged (2012). "Comparison of Polymeric siRNA Nanocarriers in a Murine LPS-Activated Macrophage Cell Line: Gene Silencing, Toxicity and Off-Target Gene Expression." Pharmaceutical research **29**(3): 669.

Jotanovic, Z., R. Mihelic, B. Sestan and Z. Dembic (2012). "Role of Interleukin-1 Inhibitors in Osteoarthritis." Drugs & Aging **29**(5): 343-358.

Jouglin, M., C. Robert, J. Valette, F. Gavard, F. Quintin-Colonna and J. Denoix (2000). "Metalloproteinases and tumor necrosis factor-alpha activities in synovial fluids of horses: correlation with articular cartilage alterations." Veterinary Research (EDP Sciences) **31**(5): 507.

Kamm, J. L., A. J. Nixon and T. H. Witte (2010). "Cytokine and catabolic enzyme expression in synovium, synovial fluid and articular cartilage of naturally osteoarthritic equine carpi." Equine Vet J **42**(8): 693-699.

Kanasty, R. L., K. A. Whitehead, A. J. Vegas, D. G. Anderson, R. L. Kanasty, K. A. Whitehead, A. J. Vegas and D. G. Anderson (2012). "Action and Reaction: The Biological Response to siRNA and Its Delivery Vehicles." Molecular therapy (Elsevier) **20**(3): 513.

Kapoor, M., J. Martel-Pelletier, D. Lajeunesse, J. P. Pelletier and H. Fahmi (2011). "Role of proinflammatory cytokines in the pathophysiology of osteoarthritis." Nat Rev Rheumatol **7**(1): 33-42.

Kataoka, Y., W. Ariyoshi, T. Okinaga, T. Kaneuji, S. Mitsugi, T. Takahashi and T. Nishihara (2013). "Mechanisms involved in suppression of ADAMTS4 expression in synoviocytes by high molecular weight hyaluronic acid." Biochem Biophys Res Commun **432**(4): 580-585.

Kato, H., T. Ohashi, H. Matsushiro, T. Watari, R. Goitsuka, H. Tsujimoto and A. Hasegawa (1997). "Molecular cloning and functional expression of equine

interleukin-1 receptor antagonist." Veterinary Immunology and Immunopathology **56**(3–4): 221-231.

Kato, H., H. Y. Youn, T. Ohashi, T. Watari, R. Goitsuka, H. Tsujimoto and A. Hasegawa (1996). "Identification of an alternatively spliced transcript of equine interleukin-1 beta." Gene **177**(1-2): 11.

Kavanaugh, T. E., T. A. Werfel, H. Cho, K. A. Hasty and C. L. Duvall (2015). "Particle-based technologies for osteoarthritis detection and therapy." Drug delivery and translational research: 1-16

Kawai, T. and S. Akira (2008). "Toll-like Receptor and RIG-1-like Receptor Signaling." Annals of the New York Academy of Sciences **1143**(1): 1.

Kay, J. D., E. Gouze, T. J. Oligino, J.-N. Gouze, R. S. Watson, P. P. Levings, M. L. Bush, A. Dacanay, D. M. Nickerson, P. D. Robbins, C. H. Evans and S. C. Ghivizzani (2009). "Intra-articular gene delivery and expression of interleukin-1Ra mediated by self-complementary adeno-associated virus." Journal of Gene Medicine **11**(7): 605.

Khanna, D., P. Balgir and K. Gurlovleen (2007). "RNA interference: An Ancient Mechanism for Novel Therapeutics." The Internet Journal of Genomics and Proteomics **2**: 1540-2630.

Kidd, J. A., C. Fuller and A. R. S. Barr (2001). "Osteoarthritis in the horse." Equine Veterinary Education **13**(3): 160.

Kobayashi, H., M. Hirata, T. Saito, S. Ito, U. i. Chung and H. Kawaguchi (2013). "Transcriptional induction of ADAMTS5 by an NF-κB family member RelA/p65 in chondrocytes during osteoarthritis development." Osteoarthritis and Cartilage **21**: S122.

Kudo, S., K. Mizuno, Y. Hirai and T. Shimizu (1990). "Clearance and tissue distribution of recombinant human interleukin 1 beta in rats." Cancer Research **50**(18): 5751-5755.

Kumar, A., A. M. Bendele, R. C. Blanks and N. Bodick (2012). "Sustained efficacy of intra-articular FX006 in a rat model of osteoarthritis." Osteoarthritis and Cartilage **20**(4): S289.

Kumar, S., J. Boehm, J. C. Lee, S. Kumar, J. Boehm and J. C. Lee (2003). "p38 MAP kinases: key signalling molecules as therapeutic targets for inflammatory diseases." Nature Reviews Drug Discovery **2**(9): 717.

Kwon, S., M. L. Vandenplas, M. D. Figueiredo, C. E. Salter, A. L. Andrietti, T. P. Robertson, J. N. Moore and D. J. Hurley (2010). "Differential induction of Toll-like receptor gene expression in equine monocytes activated by Toll-like receptor ligands or TNF-alpha." Veterinary immunology and immunopathology **138**(3): 213.

Lacey, D., A. Sampey, R. Mitchell, R. Bucala, L. Santos, M. Leech and E. Morand (2003). "Control of fibroblast-like synoviocyte proliferation by macrophage migration inhibitory factor." Arthritis Rheum **48**(1): 103-109.

Larkin, J., T. Lohr, L. Elefante, J. Shearin, R. Matico, J. L. Su, Y. Xue, F. Liu, E. I. Rossman, J. Renninger, X. Wu, L. Abberley, R. E. Miller, S. Foulcer, K. W. Chaudhary, C. Genell, D. Murphy, P. B. Tran, S. Apte, A. M. Malfait, C. C. Maier and C. J. Matheny (2014). "The highs and lows of translational drug development: antibody-mediated inhibition of ADAMTS-5 for osteoarthritis disease modification." Osteoarthritis and Cartilage **22**: S483-S484.

Larsen, C., J. Ostergaard, S. W. Larsen, H. Jensen, S. Jacobsen, C. Lindegaard and P. H. Andersen (2008). "Intra-articular depot formulation principles: Role in the management of postoperative pain and arthritic disorders." Journal of Pharmaceutical Sciences **97**(11): 4622.

Lee, C. M., J. D. Kisiday, C. W. McIlwraith, A. J. Grodzinsky and D. D. Frisbie (2013). "Synoviocytes protect cartilage from the effects of injury in vitro." BMC Musculoskeletal Disorders 2013, 14:54 **14**: 54.

Lee, D. M., H. P. Kiener, S. K. Agarwal, E. H. Noss, G. F. Watts, O. Chisaka, M. Takeichi and M. B. Brenner (2007). "Cadherin-11 in synovial lining formation and pathology in arthritis." Science (Classic) **315**(5814): 1006-1010.

Lee, H.-M., J.-M. Yuk, K.-H. Kim, J. Jang, G. Kang, J. B. Park, J.-W. Son and E.-K. Jo (2012). "Mycobacterium abscessus activates the NLRP3 inflammasome via Dectin-1–Syk and p62/SQSTM1." Immunology and cell biology **90**(6): 601-610.

Lee, J. H., J. B. Fitzgerald, M. A. DiMicco, D. M. Cheng, C. R. Flannery, J. D. Sandy, A. H. Plaas and A. J. Grodzinsky (2009). "Co-culture of mechanically injured cartilage with joint capsule tissue alters chondrocyte expression patterns and increases ADAMTS5 production." Arch Biochem Biophys **489**(1-2): 118-126.

Lee, S., S. C. Yang, C. Y. Kao, R. H. Pierce and N. Murthy (2009). "Solid polymeric microparticles enhance the delivery of siRNA to macrophages in vivo." Nucleic Acids Research **37**(22): e145.

Lee, S., S. C. Yang, C. Y. Kao, R. H. Pierce and N. Murthy (2009). "Solid polymeric microparticles enhance the delivery of siRNA to macrophages in vivo." Nucleic Acids Res **37**(22): e145.

Lefebvre, V., C. Peeters-Joris and G. Vaes (1990). "Modulation by interleukin 1 and tumor necrosis factor alpha of production of collagenase, tissue inhibitor of metalloproteinases and collagen types in differentiated and dedifferentiated articular chondrocytes." Biochimica et Biophysica Acta (BBA) - Molecular Cell Research **1052**(3): 366.

Ley, C., S. Ekman, A. Elmén, G. Nilsson and M. L. Eloranta (2007). "Interleukin-6 and Tumour Necrosis Factor in Synovial Fluid from Horses with Carpal Joint Pathology." Journal of Veterinary Medicine Series A **54**(7): 346-351.

Ley, C., S. Ekman, B. Roneus and M. L. Eloranta (2009). "Interleukin-6 and high mobility group box protein-1 in synovial membranes and osteochondral fragments in equine osteoarthritis." Res Vet Sci **86**(3): 490-497.

Ley, C., E. Svala, A. Nilton, A. Lindahl, M. L. Eloranta, S. Ekman and E. Skioldebrand (2011). "Effects of high mobility group box protein-1, interleukin-1beta, and interleukin-6 on cartilage matrix metabolism in three-dimensional equine chondrocyte cultures." Connect Tissue Res **52**(4): 290-300.

Li, N. G., Z. H. Shi, Y. P. Tang, Z. J. Wang, S. L. Song, L. H. Qian, D. W. Qian and J. A. Duan (2011). "New hope for the treatment of osteoarthritis through selective inhibition of MMP-13." Current Medicinal Chemistry **18**(7): 977-1001.

Little, C. B., M. M. Smith, M. A. Cake, R. A. Read, M. J. Murphy and F. P. Barry (2010). "The OARSI histopathology initiative – recommendations for histological assessments of osteoarthritis in sheep and goats." Osteoarthritis and Cartilage **18, Supplement 3**: S80-S92.

Liu-Bryan, R. (2013). "Synovium and the Innate Inflammatory Network in Osteoarthritis Progression." Current Rheumatology Reports **15**(5).

Livak, K. J. and T. D. Schmittgen (2001). "Analysis of Relative Gene Expression Data Using Real Time Quantitative PCR and the 2^dCT Method." Methods **25**: 402.

Livak, K. J., T. D. Schmittgen, K. J. Livak and T. D. Schmittgen (2001). "Analysis of Relative Gene Expression Data Using Real-Time Quantitative PCR and the 2-ddCT Method." Methods **25**(4): 402.

Loeser, R. F., S. R. Goldring, C. R. Scanzello and M. B. Goldring (2012). "Osteoarthritis: A disease of the joint as an organ." Arthritis & Rheumatism **64**(6): 1697-1707.

Lopez-Castejon, G., D. Brough, G. Lopez-Castejon and D. Brough (2011). "Understanding the mechanism of IL-1β secretion." Cytokine & growth factor reviews **22**(4): 189.

Lotz, M. and P. Guerne (1991). "Interleukin-6 induces the synthesis of tissue inhibitor of metalloproteinases-1/erythroid potentiating activity (TIMP-1/EPA)." Journal of Biological Chemistry **266**(4): 2017-2020.

Lotz, M., R. Terkeltaub and P. M. Villiger (1992). "Regulation of IL-8 expression by human articular chondrocytes." J Immunol **148**: 466.

Martel-Pelletier, J., C. Boileau, J.-P. Pelletier and P. J. Roughley (2008). "Cartilage in normal and osteoarthritis conditions." Best Practice & Research Clinical Rheumatology **22**(2): 351-384.

Mason, R. M., J. H. Kimura and V. C. Hascall (1982). "Biosynthesis of hyaluronic acid in cultures of chondrocytes from the Swarm rat chondrosarcoma." Journal of Biological Chemistry **257**(5): 2236-2245.

May, S. A., R. E. Hooke and P. Lees (1990). "The characterisation of equine interleukin-1." Veterinary immunology and immunopathology **24**(2): 169.

May, S. A., R. E. Hooke and P. Lees (1992). "Inhibition of interleukin-1 activity by equine synovial fluid." Equine Veterinary Journal **24**(2): 99.

May, S. A., R. E. Hooke and P. Lees (1992). "Interleukin-1 stimulation of equine articular cells." Research in Veterinary Science **52**(3): 342.

McIlwraith, C. W. (2005). "Use of synovial fluid and serum biomarkers in equine bone and joint disease: a review." Equine Veterinary Journal **37**(5): 473.

McIlwraith, C. W. (2011). "Principles and Practices of Joint Disease Treatment." ROSS, MW; DYSON, SJ Diagnosis and management of lameness in the horse. Philadelphia: Elsevier: 840-852.

McIlwraith, C. W., D. D. Frisbie and C. E. Kawcak (2012). "The horse as a model of naturally occurring osteoarthritis." Bone & Joint Research **1**(11): 297-309.

McIlwraith, C. W., D. D. Frisbie, C. E. Kawcak, C. J. Fuller, M. Hurtig and A. Cruz (2010). "The OARSI histopathology initiative - recommendations for histological assessments of osteoarthritis in the horse." Osteoarthritis Cartilage **18 Suppl 3**: S93-105.

McIlwraith, C. W. and A. Vachon (1988). "Review of pathogenesis and treatment of degenerative joint disease." Equine Veterinary Journal **20**(s6): 3.

McIlwraith, C. W. and D. C. Van Sickle (1981). "Experimentally induced arthritis of the equine carpus: histologic and histochemical changes in the articular cartilage." American journal of veterinary research **42**(2): 209-217.

Meijer, H., J. Reinecke, C. Becker, G. Tholen and P. Wehling (2003). "The production of anti-inflammatory cytokines in whole blood by physico-chemical induction." Inflammation Research **52**(10): 404.

Miller, R. E., P. B. Tran, S. Ishihara, J. Larkin and A. M. Malfait (2014). "Therapeutic Efficacy of Anti-Adamts5 Antibody in the Dmm Model." Osteoarthritis and Cartilage **22**: S35-S36.

Mitragotri, S., P. A. Burke, R. Langer, S. Mitragotri, P. A. Burke and R. Langer (2014). "Overcoming the challenges in administering biopharmaceuticals: formulation and delivery strategies." Nature Reviews Drug Discovery **13**(9): 655.

Moors, M. A. and S. B. Mizel (2000). "Proteasome-mediated regulation of interleukin-1β turnover and export in human monocytes." Journal of leukocyte biology **68**(1): 131-136.

Moreira, J. J., A. P. L. Moraes, P. M. Brossi, T. S. L. Machado, Y. M. Michelacci, C. O. Massoco and R. Y. A. Baccarin (2015). "Autologous processed plasma: cytokine profile and effects upon injection into healthy equine joints." J Vet Sci **16**(1): 47-55.

Morris, E. A., B. S. McDonald, A. C. Webb and L. J. Rosenwasser (1990). "Identification of interleukin-1 in equine osteoarthritic joint effusions." American journal of veterinary research **51**(1): 59-64

Moskalewski, S., A. Osiecka-Iwan, E. Jankowska-Steifer and A. Hyc (2014). "Synovial membrane asks for independence." Folia Morphologica **73**(4): 395.

Mosser, D. M. (2003). "The many faces of macrophage activation." Journal of Leukocyte Biology **73**(2): 209-212.

Mountziaris, P. M., D. C. Sing, S. A. Chew, S. N. Tzouanas, E. D. Lehman, F. K. Kasper and A. G. Mikos (2011). "Controlled Release of Anti-inflammatory siRNA from Biodegradable Polymeric Microparticles Intended for Intra-articular Delivery to the Temporomandibular Joint." Pharmaceutical research **28**(6): 1370.

Murata, N., Y. Takashima, K. Toyoshima, M. Yamamoto and H. Okada (2008). "Anti-tumor effects of anti-VEGF siRNA encapsulated with PLGA microspheres in mice." Journal of Controlled Release **126**(3): 246-254.

Murray, K. N., A. R. Parry-Jones and S. M. Allan (2015). "Interleukin-1 and acute brain injury." Frontiers in Cellular Neuroscience **9**.

Nagai, T., M. Sato, M. Kobayashi, M. Yokoyama, Y. Tani and J. Mochida (2014). "Bevacizumab, an anti-vascular endothelial growth factor antibody, inhibits osteoarthritis." Arthritis Research & Therapy **16**(5): 427.

Nair, A., V. Kanda, C. Bush-Joseph, N. Verma, S. Chubinskaya, K. Mikecz, T. T. Glant, A. M. Malfait, M. K. Crow, G. T. Spear, A. Finnegan and C. R. Scanzello (2012). "Synovial fluid from patients with early osteoarthritis modulates fibroblast-like synoviocyte responses to toll-like receptor 4 and toll-like receptor 2 ligands via soluble CD14." Arthritis Rheum **64**(7): 2268-2277.

Naito, S., T. Shiomi, A. Okada, T. Kimura, M. Chijiiwa, Y. Fujita, T. Yatabe, K. Komiya, H. Enomoto, K. Fujikawa and Y. Okada (2007). "Expression of ADAMTS4 (aggrecanase-1) in human osteoarthritic cartilage." Pathology International **57**(11): 703.

Narazaki, M., K. Yasukawa, T. Saito, Y. Ohsugi, H. Fukui, Y. Koishihara, G. D. Yancopoulos, T. Taga and T. Kishimoto (1993). "Soluble forms of the interleukin-6 signal-transducing receptor component gp130 in human serum

possessing a potential to inhibit signals through membrane-anchored gp130." Blood **82**(4): 1120-1126.

Nixon, A. and L. Strassheim (2006). "1039. Targeted Catabolic Gene Knockdown Using RNA Interference in Chondrocytes Abrogates the IL-1β Response for Arthritis Control." Molecular Therapy : The Journal of the American Society of Gene Therapy **13**: S398.

Nixon, A. J., L. R. Goodrich, M. S. Scimeca, T. H. Witte, L. V. Schnabel, A. E. Watts and P. D. Robbins (2007). "Gene Therapy in Musculoskeletal Repair." Annals of the New York Academy of Sciences **1117**(1): 310.

Nixon, A. J., M. L. Strassheim, M. S. Scimeca, N. Khadem and T. H. Witte (2007). "Plasmid based RNA interference controls Interleukin-1 Expression in Osteoarthritis " Osteoarthritis and Cartilage **15**: C113.

Nophar, Y., O. Kemper, C. Brakebusch, H. Englemann, R. Zwang, D. Aderka, H. Holtmann and D. Wallach (1990). "Soluble forms of tumor necrosis factor receptors (TNF-Rs). The cDNA for the type I TNF-R, cloned using amino acid sequence data of its soluble form, encodes both the cell surface and a soluble form of the receptor." EMBO Journal **9**(10): 3269-3278.

Ortved, K., B. Wagner, R. Calcedo, J. Wilson, D. Schaefer and A. J. Nixon (2015). "Humoral and Cell-Mediated Immune Response, and Growth Factor Synthesis After Direct Intraarticular Injection of rAAV2-IGF-I and rAAV5-IGF-I in the Equine Middle Carpal Joint." Human Gene Therapy **26**(3): 161.

Ortved, K. F., L. Begum, H. O. Mohammed and A. J. Nixon (2014). "Implantation of rAAV5-IGF-I transduced autologous chondrocytes improves cartilage repair in full-thickness defects in the equine model." Molecular Therapy.

Palmer, J. L. and A. L. Bertone (1994). "Experimentally-induced synovitis as a model for acute synovitis in the horse." Equine Veterinary Journal **26**(6): 492-495.

Palmer, J. L. and A. L. Bertone (1994). "Joint structure, biochemistry and biochemical disequilibrium in synovitis and equine joint disease." Equine Veterinary Journal **26**(4): 263.

Panova, E. and G. Jones (2015). "Benefit–Risk Assessment of Diacerein in the Treatment of Osteoarthritis." Drug Safety **38**(3): 245-252.

Patil, Y., J. Panyam, Y. Patil and J. Panyam (2009). "Polymeric nanoparticles for siRNA delivery and gene silencing." International journal of pharmaceutics **367**(1-2): 195.

Patwari, P., G. Gao and J. H. Lee (2005). "Analysis of ADAMTS4 and MT4-MMP indicates that both are involved in aggrecanolysis in interleukin-1-treated bovine cartilage." Osteoarthritis Cartilage **13**: 269.

Pearle, A. D., C. R. Scanzello, S. George, L. A. Mandl, E. F. DiCarlo, M. Peterson, T. P. Sculco and M. K. Crow (2007). "Elevated high-sensitivity C-reactive protein levels are associated with local inflammatory findings in patients with osteoarthritis." Osteoarthritis and Cartilage **15**(5): 516.

Peffers, M. J., D. J. Thornton and P. D. Clegg (2015). "Characterization of neopeptides in equine articular cartilage degradation." Journal of Orthopaedic Research.

Pelletier, J.-P., J. Martel-Pelletier and S. B. Abramson (2001). "Osteoarthritis, an inflammatory disease: Potential implication for the selection of new therapeutic targets." Arthritis & Rheumatism **44**(6): 1237-1247.

Pettipher, E. R., G. A. Higgs and B. Henderson (1986). "Interleukin 1 induces leukocyte infiltration and cartilage proteoglycan degradation in the synovial joint." Proceedings of the National Academy of Sciences of the United States of America (PNAS) **83**(22): 8749-8753.

Poole, A. R., M. Kobayashi, T. Yasuda, S. Laverty, F. Mwale, T. Kojima, T. Sakai, C. Wahl, S. El-Maadawy, G. Webb, E. Tchetina and W. Wu (2002). "Type II collagen degradation and its regulation in articular cartilage in osteoarthritis." Annals of the Rheumatic Diseases **61**(suppl 2): 78-81.

Poole, K. M., C. E. Nelson, R. V. Joshi, J. R. Martin, M. K. Gupta, S. C. Haws, T. E. Kavanaugh, M. C. Skala and C. L. Duvall (2015). "ROS-responsive microspheres for on demand antioxidant therapy in a model of diabetic peripheral arterial disease." Biomaterials **41**: 166-175

Pratta, M. A., P. A. Scherle and G. Yang (2003). "Induction of Aggrecanase 1 (ADAM-TS4) by Interleukin-1 Occurs Through Activation of Constitutively Produced Protein." Arthritis Rheum **48**: 119.

Présumey, J., G. Salzano, G. Courties, M. Shires, F. Ponchel, C. Jorgensen, F. Apparailly and G. De Rosa (2012). "PLGA microspheres encapsulating

siRNA anti-TNFalpha: Efficient RNAi-mediated treatment of arthritic joints." European Journal of Pharmaceutics and Biopharmaceutics **82**(3): 457-464.

Rechenberg, B., C. Leutenegger, K. Zlinsky, C. W. McIlwraith, M. K. Akens and J. A. Auer (2001). "Upregulation of mRNA of interleukin-1 and -6 in subchondral cystic lesions of four horses." Equine Veterinary Journal **33**(2): 143.

Rehli, M. (2002). "Of mice and men: Species variations of Toll-like receptor expression." Trends in Immunology **23**(8): 375-378.

Reynolds, A., D. Leake, Q. Boese, S. Scaringe, W. S. Marshall and A. Khvorova (2004). "Rational siRNA design for RNA interference." Nature biotechnology **22**(3): 326.

Rickey, E. J., A. M. Cruz, D. R. Trout, B. J. McEwen and M. B. Hurtig (2012). "Evaluation of experimental impact injury for inducing post-traumatic osteoarthritis in the metacarpophalangeal joints of horses." American Journal of Veterinary Research **73**(10): 1540.

Ritter, S. Y., R. Subbaiah, G. Bebek, J. Crish, C. R. Scanzello, B. Krastins, D. Sarracino, M. F. Lopez, M. K. Crow, T. Aigner, M. B. Goldring, S. R. Goldring, D. M. Lee, R. Gobezie and A. O. Aliprantis (2013). "Proteomic analysis of synovial fluid from the osteoarthritic knee: comparison with transcriptome analyses of joint tissues." Arthritis Rheum **65**(4): 981-992.

Robbins, P. D., C. H. Evans and Y. Chernajovsky (2003). "Gene therapy for arthritis." Gene Therapy **10**(10): 902.

Rogerson, F. M., Y. M. Chung, M. E. Deutscher, K. Last and A. J. Fosang (2010). "Cytokine-induced increases in ADAMTS-4 messenger RNA expression do not lead to increased aggrecanase activity in ADAMTS-5-deficient mice." Arthritis Rheum **62**(11): 3365-3373.

Rose-John, S., J. Scheller, G. Elson and S. A. Jones (2006). "Interleukin-6 biology is coordinated by membrane-bound and soluble receptors: role in inflammation and cancer." Journal of leukocyte biology **80**(2): 227-236.

Rosengren, S., D. L. Boyle and G. S. Firestein (2007). Acquisition, culture, and phenotyping of synovial fibroblasts. Arthritis Research, Springer**:** 365-375.

Ross, T. N., J. D. Kisiday, T. Hess and C. W. McIlwraith (2012). "Evaluation of the inflammatory response in experimentally induced synovitis in the

horse: a comparison of recombinant equine interleukin 1 beta and lipopolysaccharide." Osteoarthritis Cartilage **20**(12): 1583-1590.

Rossdale, P. D., R. Hopes and N. J. Digby (1985). "Epidemiological study of wastage among racehorses 1982 and 1983." The Veterinary Record **116**(3): 66-69

Rothenfluh, D. A., H. Bermudez, C. P. O'Neil and J. A. Hubbell (2008). "Biofunctional polymer nanoparticles for intra-articular targeting and retention in cartilage." Nature materials **7**(3): 248-254

Russo, C. and R. Polosa (2005). "TNF-α as a promising therapeutic target in chronic asthma: a lesson from rheumatoid arthritis." Clinical Science **109**(2): 135-142.

Saklatvala, J. (1986). "Tumour necrosis factor α stimulates resorption and inhibits synthesis of proteoglycan in cartilage." Nature **322**(6079): 547.

Saklatvala, J., W. Davis, F. Guesdon, M. Karin and C. J. Marshall (1996). "Interleukin 1 (IL1) and Tumour Necrosis Factor (TNF) Signal Transduction [and Discussion]." Philosophical Transactions of the Royal Society of London B: Biological Sciences **351**(1336): 151-157.

Sandy, J. D., C. R. Flannery, P. J. Neame and L. S. Lohmander (1992). "The structure of aggrecan fragments in human synovial fluid. Evidence for the involvement in osteoarthritis of a novel proteinase which cleaves the Glu 373-Ala 374 bond of the interglobular domain." Journal of Clinical Investigation **89**(5): 1512.

Scaife, S., R. Brown, S. Kellie, A. Filer, S. Martin, A. M. C. Thomas, P. F. Bradfield, N. Amft, M. Salmon and C. D. Buckley (2004). "Detection of differentially expressed genes in synovial fibroblasts by restriction fragment differential display." Rheumatology **43**(11): 1346-1352.

Scanzello, C. R. and S. R. Goldring (2012). "The role of synovitis in osteoarthritis pathogenesis." Bone **51**(2): 249-257.

Sellam, J. and F. Berenbaum (2010). "The role of synovitis in pathophysiology and clinical symptoms of osteoarthritis." Nat Rev Rheumatol **6**(11): 625-635.

Sharifi, A. M., F. E. Hoda and A. M. Noor (2010). "Studying the effect of LPS on cytotoxicity and apoptosis in PC12 neuronal cells: role of Bax, Bcl-2, and Caspase-3 protein expression." Toxicol Mech Methods **20**(6): 316-320.

Simmons, E. J., A. L. Bertone, J. Hardy and S. E. Weisbrode (1999). "Nitric oxide synthase activity in healthy and interleukin 1beta-exposed equine synovial membrane." American journal of veterinary research **60**(6): 714-716.

Smith, D. E., R. Hanna, F. Della, H. Moore, H. Chen, A. M. Farese, T. J. MacVittie, G. D. Virca and J. E. Sims (2003). "The Soluble Form of IL-1 Receptor Accessory Protein Enhances the Ability of Soluble Type II IL-1 Receptor to Inhibit IL-1 Action." Immunity **18**(1): 87.

Sokolove, J. and C. M. Lepus (2013). "Role of inflammation in the pathogenesis of osteoarthritis: latest findings and interpretations." Therapeutic Advances in Musculoskeletal Disease **5**(2): 77-94.

Song, R., Hua, M. D. Tortorella, A. Malfait, Marie, J. T. Alston, Z. Yang, E. C. Arner and D. W. Griggs (2007). "Aggrecan degradation in human articular cartilage explants is mediated by both ADAMTS-4 and ADAMTS-5." Arthritis & Rheumatism **56**(2): 575.

Stanton, H., S. B. Golub, F. M. Rogerson, K. Last, C. B. Little and A. J. Fosang (2011). "Investigating ADAMTS-mediated aggrecanolysis in mouse cartilage." Nat. Protocols **6**(3): 388-404.

Stanton, H., J. Melrose, C. B. Little and A. J. Fosang (2011). "Proteoglycan degradation by the ADAMTS family of proteinases." Biochimica et Biophysica Acta (BBA) - Molecular Basis of Disease **1812**(12): 1616-1629.

Stanton, H., F. M. Rogerson, C. J. East, S. B. Golub, K. E. Lawlor, C. T. Meeker, C. B. Little, K. Last, P. J. Farmer and I. K. Campbell (2005). "ADAMTS5 is the major aggrecanase in mouse cartilage in vivo and in vitro." Nature **434**(7033): 648-652

Stockwell, R. A. (1971). "The interrelationship of cell density and cartilage thickness in mammalian articular cartilage." Journal of Anatomy **109**(Pt 3): 411-421.

Sung, S. and J. Walters (1991). "Increased cyclic AMP levels enhance IL-1 alpha and IL-1 beta mRNA expression and protein production in human myelomonocytic cell lines and monocytes." Journal of Clinical Investigation **88**(6): 1915.

Sutton, S., A. Clutterbuck, P. Harris, T. Gent, S. Freeman, N. Foster, R. Barrett-Jolley and A. Mobasheri (2009). "The contribution of the synovium,

synovial derived inflammatory cytokines and neuropeptides to the pathogenesis of osteoarthritis." Vet J **179**(1): 10-24.

Svenson, M., M. B. Hansen, P. Heegaard, K. Abell and K. Bendtzen (1993). "Specific binding of interleukin 1 (IL-1)β and IL-1 receptor antagonist (IL-1ra) to human serum. High-affinity binding of IL-1ra to soluble IL-1 receptor type I." Cytokine **5**(5): 427.

te Boekhorst, B. C. M., L. B. Jensen, S. Colombo, A. K. Varkouhi, R. M. Schiffelers, T. Lammers, G. Storm, H. M. Nielsen, G. J. Strijkers, C. Foged and K. Nicolay (2012). "MRI-assessed therapeutic effects of locally administered PLGA nanoparticles loaded with anti-inflammatory siRNA in a murine arthritis model." Journal of Controlled Release **161**(3): 772.

Textor, J. (2011). "Autologous Biologic Treatment for Equine Musculoskeletal Injuries: Platelet-Rich Plasma and IL-1 Receptor Antagonist Protein." Veterinary Clinics of North America: Equine Practice **27**(2): 275-298.

Tice, T. R., D. H. Lewis, D. R. Cowsar and L. R. Beck (1985). Antiinflammatory microparticles in suspension, Google Patents.

Tice, T. R., D. H. Lewis, D. R. Cowsar and L. R. Beck (1985). Injectable, long-acting microparticle formulation for the delivery of anti-inflammatory agents, Google Patents.

Todhunter, P. G., S. A. Kincaid, R. J. Todhunter, J. R. Kammermann, B. Johnstone, A. N. Baird, R. R. Hanson, J. M. Wright, H. C. Lin and R. C. Purohit (1996). "Immunohistochemical analysis of an equine model of synovitis-induced arthritis." American journal of veterinary research **57**(7): 1080-1093.

Tortorella, M. D., A. M. Malfait, C. Deccico and E. Arner (2001). "The role of ADAM-TS4 (aggrecanase-1) and ADAM-TS5 (aggrecanase-2) in a model of cartilage degradation." Osteoarthritis and Cartilage **9**(6): 539-552.

Trumble, T. N., G. W. Trotter, J. R. T. Oxford, C. W. McIlwraith, S. Cammarata, J. L. Goodnight, R. C. Billinghurst and D. D. Frisbie (2001). "Synovial fluid gelatinase concentrations and matrix metalloproteinase and cytokine expression in naturally occurring joint disease in horses." American Journal of Veterinary Research **62**(9): 1467-1477.

Urech, D. M., U. Feige, S. Ewert, V. Schlosser, M. Ottiger, K. Polzer, G. Schett and P. Lichtlen (2010). "Anti-inflammatory and cartilage-protecting

effects of an intra-articularly injected anti-TNF{alpha} single-chain Fv antibody (ESBA105) designed for local therapeutic use." Annals of the Rheumatic Diseases **69**(2): 443-449.

Vachon, A., F. Keeley, C. McIlwraith and P. Chapman (1990). "Biochemical analysis of normal articular cartilage in horses." American journal of veterinary research **51**(12): 1905-1911.

Valencia-Sanchez, M. A., J. Liu, G. J. Hannon and R. Parker (2006). "Control of translation and mRNA degradation by miRNAs and siRNAs." Genes & development **20**(5): 515-524.

van Lent, P. L., A. B. Blom, P. van der Kraan, A. E. Holthuysen, E. Vitters, N. van Rooijen, R. L. Smeets, K. C. Nabbe and W. B. van den Berg (2004). "Crucial role of synovial lining macrophages in the promotion of transforming growth factor beta-mediated osteophyte formation." Arthritis Rheum **50**(1): 103-111.

van Meurs, J. B. J., P. L. E. M. van Lent, I. I. Singer, E. K. Bayne, F. A. J. van de Loo and W. B. van den Berg (1998). "Interleukin-1 receptor antagonist prevents expression of the metalloproteinase-generated neoepitope VDIPEN in antigen-induced arthritis." Arthritis & Rheumatism **41**(4): 647-656.

Vankemmelbeke, M. N., I. Holen, A. G. Wilson, M. Z. Ilic, C. J. Handley, G. S. Kelner, M. Clark, C. Liu, R. A. Maki, D. Burnett and D. J. Buttle (2001). "Expression and activity of ADAMTS-5 in synovium : ADAMTS-5 in synovium." European Journal of Biochemistry **268**(5): 1259.

Verbruggen, G., R. Wittoek, B. V. Cruyssen and D. Elewaut (2012). "Tumour necrosis factor blockade for the treatment of erosive osteoarthritis of the interphalangeal finger joints: a double blind, randomised trial on structure modification." Annals of the Rheumatic Diseases **71**(6): 891-898.

Villiger, P. M., R. Terkeltaub and M. Lotz (1992). "Production of monocyte chemoattractant protein-1 by inflamed synovial tissue and cultured synoviocytes." The journal of immunology **149**(2): 722-727.

Vincenti, M. P. and C. E. Brinckerhoff (2002). "Transcriptional regulation of collagenase (MMP-1, MMP-13) genes in arthritis: integration of complex signaling pathways for the recruitment of gene-specific transcription factors." Arthritis research **4**(3): 157-164.

Wainwright, S. D., J. Bondeson, B. Caterson and C. E. Hughes (2013). "ADAMTS-4_v1 Is a Splice Variant of ADAMTS-4 That Is Expressed as a Protein in Human Synovium and Cleaves Aggrecan at the Interglobular Domain." Arthritis & Rheumatism **65**(11): 2866-2875.

Wang, C. X., J. A. Olschowka and J. R. Wrathall (1997). "Increase of interleukin-1β mRNA and protein in the spinal cord following experimental traumatic injury in the rat." Brain Research **759**(2): 190-196.

Wasserman, J., L. Diese, Z. VanGundy, C. London, W. Carson and T. Papenfuss (2012). "Suppression of canine myeloid cells by soluble factors from cultured canine tumor cells." Veterinary immunology and immunopathology **145**(1): 420-430.

Watson, R. S., T. Broome, A. Smith, P. Colahan and S. Ghivizzani (2014). Exploring the Capacity of Local Self-Complimentary AAV Mediated Delivery of Equine IL-1Ra to Block the Symptoms and Progression of Osteoarthritis in an Equine Model. Molecular Therapy, Nature Publishing Group, 75 Varick Street, 9th Flr, New York, NY 10013-1917, USA. .

Watson, R. S., T. A. Broome, P. P. Levings, B. L. Rice, J. D. Kay, A. D. Smith, E. Gouze, J. N. Gouze, E. A. Dacanay, W. W. Hauswirth, D. M. Nickerson, M. J. Dark, P. T. Colahan and S. C. Ghivizzani (2013). "scAAV-mediated gene transfer of interleukin-1-receptor antagonist to synovium and articular cartilage in large mammalian joints." Gene Ther **20**(6): 670-677.

Wehling, P., C. Moser, D. Frisbie, C. Wayne McIlwraith, C. Kawcak, R. Krauspe and J. Reinecke (2007). "Autologous Conditioned Serum in the Treatment of Orthopedic Diseases." BioDrugs **21**(5): 323.

Westacott, C. I., R. M. Atkins, P. A. Dieppe and C. J. Elson (1994). "Tumor necrosis factor-alpha receptor expression on chondrocytes isolated from human articular cartilage." Journal of Rheumatology **21**(9): 1710-1715.

Whitmire, R. E., D. S. Wilson, A. Singh, M. E. Levenston, N. Murthy and A. J. García (2012). "Self-assembling nanoparticles for intra-articular delivery of anti-inflammatory proteins." Biomaterials **33**(30): 7665-7675

Wylie, J. D., J. C. Ho, S. Singh, D. R. McCulloch and S. S. Apte (2012). "Adamts5 (aggrecanase-2) is widely expressed in the mouse musculoskeletal system and is induced in specific regions of knee joint

explants by inflammatory cytokines." Journal of Orthopaedic Research **30**(2): 226-233.

Yamamoto, K., L. Troeberg, S. D. Scilabra, M. Pelosi, C. L. Murphy, D. K. Strickland and H. Nagase (2013). "LRP-1-mediated endocytosis regulates extracellular activity of ADAMTS-5 in articular cartilage." FASEB J **27**(2): 511-521.

Yamanishi, Y., D. L. Boyle, M. Clark, R. A. Maki, M. D. Tortorella, E. C. Arner and G. S. Firestein (2002). "Expression and Regulation of Aggrecanase in Arthritis: The Role of TGF-β." The Journal of Immunology **168**(3): 1405-1412.

Yielding, K. L., G. M. Tomkins and J. J. Bunim (1957). "Synthesis of hyaluronic acid by human synovial tissue slices." Science (Classic) **125**(3261): 1300.

Yu, S. P.-C. and D. J. Hunter (2015). "Emerging drugs for the treatment of knee osteoarthritis." Expert Opinion on Emerging Drugs **20**(3): 361-378.

Zhang, E., X. Yan, M. Zhang, X. Chang, Z. Bai, Y. He and Z. Yuan (2013). "Aggrecanases in the human synovial fluid at different stages of osteoarthritis." Clinical Rheumatology **32**(6): 797-803.

Zhang, J.-j., Z.-m. Xu, C.-m. Zhang, H.-y. Dai, X.-q. Ji, X.-f. Wang and C. Li (2011). "Pyrrolidine dithiocarbamate inhibits nuclear factor-κB pathway activation, and regulates adhesion, migration, invasion and apoptosis of endometriotic stromal cells." Molecular human reproduction **17**(3): 175-181.

Zhang, Z. and G. Huang (2012). "Micro- and Nano-Carrier Mediated Intra-Articular Drug Delivery Systems for the Treatment of Osteoarthritis." Journal of Nanotechnology **2012**: 1-11.

Ziegler-Heitbrock, H., T. Sternsdorf, J. Liese, B. Belohradsky, C. Weber, A. Wedel, R. Schreck, P. Bäuerle and M. Ströbel (1993). "Pyrrolidine dithiocarbamate inhibits NF-kappa B mobilization and TNF production in human monocytes." The Journal of Immunology **151**(12): 6986-6993.